



Targeted activation of dendritic cells via the CD40 receptor

Brittany Jade Wingham

A thesis submitted for the Degree of Doctor of Philosophy in Biomedical Sciences

University of Hull

Supervised by

Dr Elena Rosca

Dr Charlotte Dyer

Professor John Greenman

April 2018

Abstract

Dendritic cell (DC) activation underpins the patient immune response in multiple cancers, including ovarian cancer. While DCs are detected within the margins of ovarian tumours, DC populations are maintained in an immature state, displaying low levels of co-stimulatory receptor expression and cytokine production, with impaired antigen presentation capacity.

Engagement of the DC surface receptor CD40 (CD40R) is required for efficient immune activation. This thesis investigated the potential of a Monovalent Targeted Peptide targeting CD40R (MTP40) to bind the CD40R of a murine DC cell line (tsDC), and whether the interaction could be enhanced by multivalent presentation.

This work aimed to demonstrate the suitability of two potential scaffolds for multivalent presentation. The first system investigated the activity of MTP40 presented on streptavidin as a tetramer (Tet40), which improved the binding kinetics of MTP40 (K_D 1.32 μ M) when presented as Tet40 (K_D 0.072 μ M). Binding capacity was confirmed as MTP40 conjugated to streptavidin Dynabeads successfully isolated the CD40R by pull down assay. The second system explored MTP40 attached to the surface of gold nanoparticles through thiol-Au bonds, to produce targeted polyvalent gold nanoparticles (TPN40) presenting up to 2000 peptide units per molecule, which demonstrated binding to CD40R by coomassie stain.

Changes in outputs associated with tsDC activation were observed in response to CD40R targeted treatments. Surface expression of CD40R was upregulated in response to Tet40 or TPN40, while TPN40 induced increased expression of activating receptors CD86 and CD54. tsDC upregulated expression of IL-2 and IL-12, with a corresponding down-regulation of IL-10, in response to Tet40 or TPN40. TPN40 treatments also stimulated uptake of the model antigen FITC-Ova by tsDC.

After confirming the tsDC cell line induced functional changes in response to CD40R targeted activation, second goal was to determine whether the “activated” tsDCs were able to induce priming of effector T cells in an antigen specific manner. T cell lines significantly upregulated production of IL-2 and IL-12 in response to TPN40, while the cytotoxic T cell line specifically upregulated IFN- γ . T cell induced cytotoxicity and proliferation were not significantly affected by the addition of ID8 tumour cell lysates, suggesting further optimizations are needed to produce an antigen-specific response.

This study provided evidence that multivalent engagement of CD40R is required to induce effective tsDC maturation, highlighting the importance of ligand presentation in immunity. The work also provides a multistep model of immune activation as stimulated tsDCs were capable of inducing changes in T cell lines. This demonstrates proof-of-principle that multivalent activation at the DC level is sufficient to prime an effector T cell response.

These conclusions have wider significance in the field of immunology, where they suggest multivalent interactions can produce optimised immune responses. Gold nanoparticles provided a stable, well-tolerated platform for multivalent drug delivery. Future work should investigate the bimodal application of gold nanoparticles for targeted drug delivery with tumour imaging.

Poster presentations

Wingham, B., Greenman, J & Rosca, E.V., Nanoparticle activated DC sparking T cells as tumour cytotoxic mediators, *British Association for Cancer Research & Experimental Cancer Medicine Centre Joint Conference: Therapeutic interventions for cancer prevention: the way forward*, Bristol UK (July 2016)

Wingham, B., Greenman, J & Rosca, E.V., Nanoparticle activated DC sparking T cells as tumour cytotoxic mediators *European Association for Cancer Research 24th Biennial Congress*, Manchester UK (June 2016)

Wingham, B., Greenman, J & Rosca, E.V., DC Immunomodulatory nanoparticles: investigating the effects of multivalency and rigidity *Keystone Symposia Conference, Cancer Immunotherapy: Immunity and Immunosuppression Meet Targeted Therapies* Vancouver BC, Canada (January 2016)

Wingham, B., Greenman, J & Rosca, E.V., Releasing the immunosuppressing brakes: Calling to arms of dendritic cells *British Society for Immunology: Summer School for Young Researchers* York, UK (July 2015)

Wingham, B., Greenman, J & Rosca, E.V., Releasing the immunosuppressing brakes: Calling to arms of dendritic cells *Association for Cancer Immunotherapy 16th Annual Meeting: Immunotherapy: the right treatment for the right patient* Mainz, Germany (May 2015)

Bursaries & Funding bodies

PhD Research Scholarship, the University of Hull, 2013-2016

The James Reckitt Academic Achievement Bursary, 2016

The Robert's Fund Travel Grant, The University of Hull Graduate School, 2016

Travel Award – The European Association for Cancer Research (EACR), 2016

Travel Award – The Experimental Cancer Medicine Centre (ECMC), 2016

Authors Declaration

I confirm that the work presented in this publication is original and my own. If any passage(s) or diagram(s) have been copied from academic papers, books, the internet or any other sources, the original sources are clearly identified by the use of quotation marks, and the relevant reference is fully cited. I certify that, other than where indicated, the work is my own and does not breach the University of Hull regulations regarding plagiarism or academic conduct in examinations.

“No ray of sunlight is ever lost”

List of abbreviations

ACT	Adoptive cell transfer
APC	Antigen presenting cell
APS	Ammonium persulphate
ASR	Age standardised rate
BCA	Bicinchoninic acid assay
BIOT-MTP40	Biotinylated MTP40
BSA	Bovine serum albumin
CAF	Cancer associated fibroblast
CART	Chimeric antigen receptor T cell
CCL	Chemokine ligand
CD	Cluster of differentiation
CD40L	T cell surface expressed CD40 ligand (CD40L)
CD40R	CD40 transmembrane receptor
cDC	Conventional myeloid derived dendritic cell
CIITA	Class II major histocompatibility complex trans-activator
CLL	Chronic lymphocytic leukaemia
Con-a	Concanavalin A
CRD	Cysteine rich domain
CRS	Cytokine release syndrome
CTL	Cytotoxic T lymphocyte
CTLA4	Cytotoxic T lymphocyte associated antigen 4
CTLL-2	Murine CD8 ⁺ cytotoxic T cell line (IL-2 dependent)
D10 4NM	Murine CD4 ⁺ helper T cell line (Th2 type)
DCs	Dendritic cells; generic term used as per the literature
DMEM	Dulbecco's modified eagle medium
DMSO	Dimethyl sulfoxide
ECL	Enhanced chemiluminescence
ECM	Extracellular matrix
EDTA	Ethylenediaminetetraacetic acid
ELISA	Enzyme-linked immunosorbent assay
EPR	Enhanced permeability and retention effect
ER	Endoplasmic reticulum

ERAAP	Endoplasmic reticulum aminopeptidase associated with antigen
ϵ	Extinction coefficient
Fas-L	First apoptosis signal ligand
Fas-R	First apoptosis signal receptor
FBS	Fetal bovine serum
Fc	Fragment crystallizable
FcR	Fc Receptor
FDA	Food and drug association
FITC	Fluorescein
GM-CSF	Granulocyte-macrophage colony-stimulating factor
H ₂ O	Milli-Q ultrapure water
HCl	Hydrochloric acid
HEPES	4-(2-hydroxyethyl)-1-piperazineethanesulfonic acid
HER2	Human epidermal growth factor receptor 2
HIF	Hypoxia inducible factor
HLA	Human leukocyte antigen
HRP	Horseradish peroxidase
IARC	International agency for research on cancer
IBD	Inflammatory bowel disease
IFN	Interferon
Ig	Immunoglobulin
IHC	Immunohistochemistry
IL	Interleukin
IL-12	Interleukin-12p70
IMDM	Iscove's modified Dulbecco's medium
JAK	Janus Kinase
JNK	C-Jun N-terminal kinase
K _D	Dissociation coefficient
KSHV	Karposes sarcoma associated herpes virus
LFA-1	Lymphocyte function associated antigen-1
LPS	Lipopolysaccharide
MAPK	Mitogen associated pathway kinase
MFI	Mean fluorescence intensity

MHCI	Major histocompatibility complex class I
MHCII	Major histocompatibility complex class II
MMP	Matrix metalloproteinase
moDC	Monocyte derived dendritic cell
MTP40	Monovalent CD40R targeted peptide
MTS	3-(4,5-dimethyliazol-2-yl)-5-(3-carboxymethoxyphenyl)-2-(4-sulfophenyl)-2 H-tetrazolium inner salt
MTT	3-(4,5-dimethylthiazol-2-yl)-2, 5-diphenyltetrazolium inner salt
MW	Molecular weight
MWCO	Molecular weight cut off
NCI	National cancer institute
NFκB	Nuclear factor kappa-light-chain-enhancer of activated B cells
NHS-ester	N-hydroxysuccinamide ester
NIH	National institute of health
NK cell	Natural killer cell
NO	Nitric oxide
NP	Nanoparticle
NSCLC	Non-small cell lung cancer
OC	Ovarian Cancer
OVA	Ovalbumin
PAP	Prostatic acid phosphatase
PBS	Phosphate buffered saline
PBST	Phosphate buffered saline + 0.05% Tween-20
PDAC	Pancreatic ductal adenocarcinoma
pDC	Plasmacytoid derived dendritic cell
PD-1	Programmed cell death receptor 1
PD-L1	Programmed cell death receptor 1 ligand
PE	Phycoerythrin
PGLA	Peptidyl-glycine-leucine-carboxamide
PHA	Phytohaemagglutinin P
PMA	Phorbol-12-myristate-13-acetate
PVDF	Polyvinylidene fluoride
RAS	RAS oncogene family protein

Res	Reticuloendothelial system
RMA	Murine CD4 ⁺ helper T cell line (Th1 type)
ROS	Reactive oxygen species
RPMI	Roswell park memorial institute medium
SCFV	Single chain variable fragment
SCLC	Small cell lung cancer
SDS-PAGE	Sodium dodecyl sulphate polyacrylamide gel electrophoresis
STAT	Signal transducer and activator of transcription
STREP	Pierce recombinant streptavidin
TAA	Tumour associated antigen
TAP	Transported associated with antigen processing
TBS	Tris-buffered saline
TBST	Tris-buffered saline + 0.05% Tween-20
TCEP	Tris(2-carboxyethyl)phosphine
TEMED	Tetramethylethylenediamine
TET40	STREP conjugated MTP40
TGF	Transforming growth factor
Th	Helper T cell subset
TIFF	Tagged image file format
TIL	Tumour infiltrating lymphocyte
TIM	Tumour infiltrating macrophage
TLR	Toll like receptor
TMB	3,3',5,5'-Tetramethylbenzidine
TNF	Tumour necrosis factor
TPN40	UPN conjugated MTP-40
TRAF	TNF receptor associated factor
Treg	Regulatory T cell subset
Tris	Trisaminomethane
tsDC	Immortalised murine dendritic cell line; specifically referring to the model cell line used throughout this work
UK	United Kingdom
UPN	Untargeted polyvalent nanoparticle
VEGF	Vascular endothelial growth factor
WHO	World health organisation

Table of Contents

Table of Tables	xv
Table of Equations	xv
1 Chapter 1: General introduction.....	1
1.1 Changing cancer demographics in the United Kingdom	1
1.2 Cellular biology of the tumour	6
1.2.1 Tumour vasculature and cancer associated fibroblasts.....	7
1.2.2 Immune cell subsets and functions in the tumour	8
1.2.2.1 Macrophages, NK cells and B lymphocytes in the tumour	11
1.2.2.2 DCs in the tumour	12
1.2.2.3 T Lymphocytes	15
1.2.2.4 Regulatory immune cell subsets	17
1.2.2.5 The influence of cytokines on immune cell development.....	18
1.2.3 IL-2	19
1.2.4 IL-10.....	20
1.2.5 IL-12.....	21
1.2.6 IFN- γ	22
1.2.7 Cytokine interactions in immune function	23
1.3 Mechanisms of evading cellular immunity.....	25
1.3.1 Defective antigen presentation <i>via</i> MHC I.....	26
1.3.2 Induction of immune checkpoints	30
1.4 Current immunotherapies	31
1.4.1 Immune checkpoint blockade.....	32
1.4.1.1 CD28/cytotoxic T lymphocyte antigen-4.....	34
1.4.1.2 Programmed cell death 1 receptor.....	34
1.4.1.3 Checkpoint blockade combination therapies.....	35
1.4.2 Adoptive cell transfer.....	38
1.4.3 Chimeric Antigen Receptor T cell therapy.....	39
1.4.4 DCs as immunotherapeutic agents	42
1.5 CD40R anatomy and physiology.....	45
1.5.1 Receptor structure and ligand interaction	45
1.5.2 Downstream responses of CD40R binding.....	46
1.5.3 Current immunotherapies targeting CD40R in the clinic	50
1.5.4 Agonistic antibodies for CD40R	50
1.5.5 CD40R targeted therapies in adjuvant and combination therapies.....	52
1.6 Parameters influencing CD40R stimulation	54
1.7 Limitations of antibody therapies for CD40 stimulation	59
1.8 Advantages and limitations of peptide based immunotherapies	61
1.9 Drug delivery <i>via</i> nanoparticles.....	65
1.9.1 Nanoparticulate therapies targeting CD40R on DCs.....	66
1.10 Gold nanoparticles for targeted immunotherapy	67
1.11 Aims of the current study.....	69
2 Chapter 2: Methods and materials	71
2.1 List of suppliers.....	71

2.2	General suppliers.....	72
2.3	Glassware and consumables	72
2.4	Reagents.....	72
2.5	Generating a CD40-targeting peptide.....	74
2.5.1	MTP40 Characterisation by Peptide Synthetics	74
2.5.2	Mass spectrometry analysis of MTP40.....	75
2.5.3	MTP40 re-solubilisation	76
2.5.3.1	MTP40 solubilisation (Method A).....	76
2.5.3.2	Biotinylated MTP40 solubilisation (Method B).....	76
2.5.4	Peptide concentration measurements	77
2.5.5	MTP40 labelling with NHS DyLight for saturation assay.....	77
2.6	Development of a flexible multivalent construct.....	78
2.6.1	Unlabelled Tet40 synthesis	78
2.6.2	Fluorescent tetramer synthesis for saturation assay.....	79
2.7	Development of the rigid targeting construct.....	80
2.7.1	MTP40 conjugation to gold nanoparticles.....	80
2.8	Cell culture	83
2.8.1	tsDC cell line	85
2.8.2	CTLL-2 cell line.....	85
2.8.2.1	Preparation of IL-2 growth factor in-house.....	85
2.8.3	RMA cell line.....	86
2.8.4	D10-N4M cell line	86
2.8.5	ID8 cell line.....	86
2.9	Characterising tsDC response to LPS as a positive control for DC activation..	86
2.10	Scaffold backbones as negative control treatments	88
2.11	tsDC activation by CD40R targeted treatments.....	88
2.12	DC co-culture with T cell lines.....	89
2.13	Fluorescence activated cell sorting.....	90
2.13.1	Surface receptor analysis <i>via</i> FACS.....	92
2.13.2	tsDC preparation for FACS saturation assay.....	93
2.13.3	FACS Analysis.....	93
2.14	Fluorescent microscopy of CD40R binding.....	95
2.15	CD40R isolation by pull down assay.....	95
2.16	Western Blot.....	98
2.16.1	Gel casting and recipes.....	98
2.16.2	Lysate preparation.....	99
2.16.3	Preparing heat-shocked ID8 cultures lysates	99
2.16.4	Protein quantification and gel loading	100
2.16.5	Antibody probing.....	100
2.17	MTP40 peptide imaging by Coomassie Stain	101
2.18	Enzyme -linked immunosorbent assay.....	101
2.19	Cytokine analysis by ELISA assay	102
2.20	Nanoparticle imaging by Transmission Electron Microscopy.....	104
2.21	Assessing antigen uptake using FITC-OVA model antigen.....	105
2.21.1	Antigen uptake image analysis.....	105
2.22	Cell viability	106

3.1	Theoretical sequence of MTP40	108
3.2	Chemical analysis of MTP40 <i>via</i> mass spectrometry	109
3.3	MTP40 specificity for the CD40R determined by <i>in vitro</i> pull down assay	110
3.4	Characterising MTP40 bound to flexible multivalent scaffolds	113
3.4.1	Quantifying MTP40 conjugation to streptavidin.....	113
3.4.2	Characterising the binding affinity of MTP40 presented as monomer <i>versus</i> tetramer to CD40R.....	116
3.4.3	Visualisation of Tet40 binding to tsDC by fluorescent microscopy	124
3.5	Characterising MTP40 bound to rigid multivalent scaffolds.....	125
3.5.1	Quantification of MTP40 conjugation to gold nanoparticles by optical properties.....	125
3.5.2	Visualisation of MTP40 conjugation to gold nanoparticles by coomassie stain	127
3.6	General Discussion.....	128
4	Chapter 4: Analysis of tsDC outputs in response to CD40R Activation <i>via</i> a flexible multivalent construct	131
4.1	Establishing a baseline for tsDC activation by activation using the known stimulator LPS	133
4.2	Characterising the effect of CD40R targeted peptide on tsDC surface receptor expression when presented as a tetrameric conjugate.....	139
4.3	Cytokine profile changes in response to Tet40, analysed by ELISA.....	143
4.4	Analysis of streptavidin construct toxicity by MTS assay	147
4.5	General Discussion.....	148
5	Chapter 5: Analysis of tsDC outputs in response to CD40R Activation <i>via</i> a rigid multivalent construct.....	150
5.1	tsDC receptor changes in response to nanoparticle platform	151
5.2	Cytokine profile changes in response to TPN40, analysed by ELISA.....	157
5.3	Analysis of nanoparticle construct toxicity by MTS assay	159
5.4	Antigen uptake by tsDC.....	160
5.5	Conclusions.....	163
6	Chapter 6: Monitoring T cell effector outputs following incubation with TPN40-activated tsDCs.....	165
6.1	Cytokine production induced by three T cell lines, following co-culture with TPN40 treated tsDC.....	166
6.1.1	CTLL-2 cell line induced IL-12 and IFN- γ production in response to TPN40-DCs.....	172
6.1.2	D10 cell line induced IL-12 production in response to TPN40-DCs...	173
6.1.3	RMA cell line induced IL-2 and IL-12 production in response to TPN40- DCs	173
6.2	T cell viability following treatment with TPN40-DC co-culture.....	174
	Summary of T cell viability following activation treatments	178
6.3	Determining the cytotoxic function of CTLL-2 cells in response to DC activation.....	179
6.4	Conclusions.....	182

7	Chapter 7: General discussion & limitations of the study	183
7.1	General Discussion.....	183
7.2	Limitations of the study.....	187
7.3	Experiments requiring further optimisation.....	187
7.3.1	Collection and enrichment of DC precursors from human blood	187
7.3.2	Alternative outputs of DC activation.....	187
7.3.3	Protocol for T cell activation.....	188
7.4	Future directions.....	189
7.4.1	Alternative methods to assess T cell response	189
7.4.2	Investigating efficacy of TPN40 in 3d models and <i>in vivo</i>	189
7.4.3	Prospects for <i>in vivo</i> delivery and imaging of TPN40.....	192
7.4.4	Combination prospects for TPN40 with other immunotherapies.....	194
7.4.5	A role for FcYR studies in optimising TPN40 delivery.....	195
7.5	Concluding remarks	195
8	Chapter 8: Reference list	197
8.1	Online Resources:.....	246

Table of Figures:

Figure 1-1: Trends in UK cancer mortality rates from 1983 to present.....	2
Figure 1-2: Comparison of the most common cancers in the U.K. by gender between 2004 and 2014.....	3
Figure 1-3: Causal pathogens associated with common preventable cancers.....	4
Figure 1-4: Annual reported cancer incidences in the UK for all disease sites.....	6
Figure 1-5: Cellular components of the tumour microenvironment.....	7
Figure 1-6: Differentiation and function of immune cell subsets under physiological conditions.....	10
Figure 1-7: Receptors of interest involved in cell-cell interactions at the immunological synapse between DC and T cells.....	15
Figure 1-8: Stages of early T cell development and selection in the thymus.....	16
Figure 1-9: Polarisation of naïve CD4 T cells into differentiated effector subsets.....	19
Figure 1-10: Infiltrating immune cell interactions with the tumour <i>via</i> soluble factors. Authors own.....	24
Figure 1-11: The hallmarks of cancer, from Hanahan & Weinberg, 2011.....	26
Figure 1-12: MHC I subunit assembly required for antigen presentation.....	27
Figure 1-13: Dynamics of immune checkpoint proteins PD-1 and CTLA-4 with examples of FDA approved checkpoint blockade antibodies.....	33
Figure 1-14: Clinical efficacy of various immune stimulating therapies when used in combination with CTLA-4 blockade.....	37
Figure 1-15: Evolution of CART structural components across four generations.....	41
Figure 1-16: Downstream signalling pathways induced upon CD40R stimulation at the DC surface by CD40L expressed on CD4 ⁺ T cells.....	48
Figure 2-1: Modifications to the original CD40R targeting peptide sequence adapted from Yu et al., 2013 (NP31).....	75
Figure 2-2: Evolution 300 UV-Visible Spectrophotometer settings used for the characterisation of gold nanoparticles.....	81
Figure 2-3: A schematic diagram of multivalent construct formation.....	82
Figure 3-1: Hypothetical structure of MTP40 generated using the Tulane University Peptide Characterisation Tool.....	108
Figure 3-2: API-ES analysis of the peptide sample using a 130A 4.6x50mm column on 10-90% acetonitrile gradient for 8 minutes at 80°C.....	109
Figure 3-3: Low-resolution MALDI-MS chromatogram of biotinylated MTP40.....	111
Figure 3-4: Pull down assay of the CD40R probed with Abcam anti-CD40R.....	112
Figure 3-5: Excel file format for calculations determining the concentration of Tet40 reactions based on absorbance.....	115
Figure 3-6: Histogram overlay of fluorescently labelled MTP40 titrations to CD40R on the tsDC surface.....	118

Figure 3-7: Histogram overlay of fluorescently labelled Tet40 titrations to CD40R on the tsDC surface.....	119
Figure 3-8: Comparison of MTP40 versus Tet40 binding patterns acquired by flow cytometry	121
Figure 3-9 Kinetics of CD40R binding specificity of MTP40 and Tet40 analysed by flow cytometry	123
Figure 3-10: Fluorescent binding images of FITC-MTP40 and FITC-Tetramer to CD40R at the tsDC surface	124
Figure 3-11: Characteristics of gold nanoparticles determined by absorbance.....	126
Figure 3-12: UPN and TPN40 incubated with Coomassie Brilliant Blue dye for visualisation on SDS-PAGE gels	127
Figure 4-1: Morphology of tsDC following 24 hour activation with 10ug/ml LPS	133
Figure 4-2: Percent activation of tsDC in response to LPS activation.....	134
Figure 4-3: tsDC Expression of CD40R in response to time point activations with LPS	135
Figure 4-4: Histogram overlay of tsDC activation receptor changes in response to LPS activation. expression on DCs following 24 hour incubation period with 10µg/ml LPS at 37°C.....	136
Figure 4-5: Expression changes in c-SMAC receptors at the tsDC surface in response to 24 hour treatment with 10µg/ml LPS.....	137
Figure 4-6: Expression changes in integrin receptors at the tsDC surface in response to treatment with 10µg/ml LPS for 24 hours	138
Figure 4-7: Expression of cSMAC associated proteins at the tsDC surface following 24-hour incubation with streptavidin-based activating treatments	140
Figure 4-8 Expression of receptors not associated with activation at the tsDC surface following 24-hour incubation with streptavidin-based activating treatments.....	142
Figure 4-9: Cytokine changes observed by ELISA following 24-hour incubation with MTP40 presented on flexible multivalent scaffolds	145
Figure 4-10: tsDC Viability assessed by MTS assay following activation with flexible multivalent scaffolds.....	147
Figure 5-1 Expression of cSMAC associated proteins at the tsDC surface following 24-hour incubation with nanoparticle based activating treatments.....	152
Figure 5-2: Expression of generic receptors not associated with activation at the tsDC surface following 24-hour incubation with nanoparticle-based activating treatments	154
Figure 5-3: tsDC cytokine expression profile detected by ELISA following 24-hour incubation with MTP40 presented on rigid multivalent scaffolds.	158
Figure 5-4: tsDC Viability assessed by MTS assay following activation with rigid multivalent scaffolds.....	159
Figure 5-5: tsDC capacity for antigen uptake determined by phagocytosis of FITC-OVA post-activation.	161
Figure 6-1: IL-2 production by three T cell lines following co-culture with TPN-40 stimulated tsDCs.....	167

Figure 6-2: IL-12 production by three T cell lines following co-culture with TPN-40 stimulated tsDCs.....	168
Figure 6-3: IFN- γ production by three T cell lines following co-culture with TPN-40 stimulated tsDCs.....	170
Figure 6-4: IL-10 production by three T cell lines following co-culture with TPN-40 stimulated tsDCs.....	171
Figure 6-5: Cellular viability of the CD8 ⁺ T cell line CTLL2 following culture with TPN40-activated tsDC.....	175
Figure 6-6: Cellular viability of the CD4 ⁺ Th2 cell line D10 following culture with TPN40-activated tsDC.....	176
Figure 6-7: Cellular viability of the CD8 ⁺ T cell line CTLL2 following culture with TPN40-activated tsDC.....	177
Figure 6-8: CTLL-2 induced cytotoxicity of ID8 murine tumour cells following incubation with TPN40 activated tsDCs.....	179
Figure 6-9: CTLL-2 induced cytotoxicity of ID8 murine tumour cells following incubation with TPN-40 activated tsDCs in the presence of the Th1 cell line RMA.....	181

Table of Tables

Table 1-1: Prognostic indications of cancer subsets with demonstrable MHCI down-regulation.....	29
Table 1-2: Monoclonal antibody therapies targeting the CD40 pathway in cancer immunotherapy in clinical trials.....	51
Table 1-3: Limitations of peptide based therapies.....	63
Table 2-1: Summary of cell lines investigated in this study.....	84
Table 2-2: tsDC activation treatments.....	89
Table 2-3: Co-culture activation experiment treatments.....	90
Table 2-4: SDS gel recipes for 10% and 15% acrylamide gels.....	99
Table 6-1: Summary of the data from figures 6.1-6.3.....	172
Table 6-2: Summary of changes in T cell line viability in response to activation treatments.....	178

Table of Equations

Equation 1: Beer's Law.....	77
Equation 2: Peptide extinction coefficient.....	77
Equation 3: Molar concentration of tetramer.....	79

Acknowledgements and Thanks

Over the last few months, I have thought many times what I could write on this page to describe my gratitude for the people who have helped and supported me over the last five years. Now that it's time, I'm not sure I have words to explain it.

First and foremost, I would like to thank my supervisor, Dr Elena Rosca, for being an incredible mentor on many levels. As my supervisor, I am grateful for her endless time, patience and dedication to both science and teaching. Thank you for excellent scientific guidance and for providing expertise in statistical analysis. As a friend, Elena's wisdom and advice has helped me to be the best scientist that I can be, but also to develop and grow outside of the lab. It has been an honour to work for her.

I would also like to thank my second supervisor, Professor John Greenman, for providing a fountain of knowledge and guidance throughout this project, particularly in the final weeks before completion. Your time and positivity has been invaluable.

I would like to thank the members of my PhD panel, Dr Jenny Waby, Dr Stephen Maher and Dr Charlotte Dyer, for their guidance and diverse expertise in the fields of Cancer Research and Immunology. Also to Dr Leigh Madden for sharing his experience and technical skill. Additional thanks to The University of Hull for funding this project, and the opportunities it has presented.

It is difficult to list the number of people who have provided invaluable contributions during my time here at Hull – to the people in this department who feel like family - and I hope they know who they are. To the coffee girls; Beeb, Cordula, Anne, Jennie, Sage and James. Were it not for this group, I don't think I'd have made it to the end. You are my dear friends, who make dark days that bit brighter. Thank you also to Debbie, for being a wild spirit, for always being there and for helping me regroup, and to Miffy and Guy, for things I can't write in an official document! Last but by no means least, thank you to Stuart. You were the first person I ever met in the walls of the Hardy Building, and I can honestly say I would not be where I am today without you! Thank you for years of kindness and care.

Thank you all for making Hull a really difficult place to leave.

To my mum – thank you for teaching me every truly important lesson in life, and for shaping me into a person I am proud to be. I am so grateful to have you in my life, I could never put it onto a piece of paper. Your unbreakable strength inspires me so much – I am incredibly proud to be your daughter. To my brother Ryan – thank you for helping me escape whenever I need it. I'm so proud of the person you're becoming. Thanks to my dad, for instilling me with the determination to study cancer research – I wish I had better words to explain.

David, you have been there through so much. You encourage, console and support me, and still put up with me when I am a foot from the edge. There have been times when this PhD has been just as difficult for you as it has been for me, and I am so thankful for you every day.

Chapter 1: General introduction

The present chapter provides an overview to the changing demographics of cancer prevalence, the established treatment methods and recent developments in the field of immunotherapy. Reviewing this background information aims to highlight the need for improved treatment modalities, and thus introduce the potential for nanoparticle based dendritic cell (DC) therapies to improve the existing therapeutic landscape.

1.1 Changing cancer demographics in the United Kingdom

The growth rate of the United Kingdom (UK) population continues to rise as a result of increased life expectancy (Office for National Statistics [ONS], 2017). Cancer accounts for 39% of the annual preventable deaths across England and Wales (Laudicella et al., 2016) and cancer patients now live 10 times longer following diagnosis compared to the 1970's, meaning an estimated 2.5 million patients are living with a cancer diagnosis in the UK today (Siegel et al., 2012).

In the field of cancer research, it is relevant to point out that the age bracket showing the greatest increase is in citizens aged 85 years and older (Kaur & Poole., 2017); in 1982, only 1% of the population fell in this age bracket, which now accounts for 2.6% of the population (Kaur & Poole., 2017). An increasingly aged population correlates with cancer diagnosis since for the majority of new cases occur in the 70+ age group, with 50% of all new diagnoses being made in this population (Kaur & Poole., 2017). In the last decade alone, total incidence rates of all cancers in the UK have increased by 7% (Kaur & Poole., 2017). If current trends in population aging and cancer development continue, cancer prevalence in the UK is expected to increase by approximately 1 million survivors per decade from 2010 to 2040 (Maddams et al., 2012).

In a pioneering quantitative analysis, Doll & Peto proposed that 75% of all preventable cancers in western populations could be attributed to three primary factors: tobacco smoking, diet and obesity, and infectious agents (Doll & Peto, 1981). This figure has recently been amended, and recent publications suggest these three risk factor categories now account for approximately only 23% of western cancers (Okada, 2014; Brown et al., 2018), indicating the changing demographics of malignant disease. Improved scientific understanding and public awareness of risk

factors associated with cancer development is likely to influence prevalence and disease prognosis and as such, figure 1.1 outlines the changing mortality rates of common cancers in the UK to date (WHO Mortality Database, 2017).

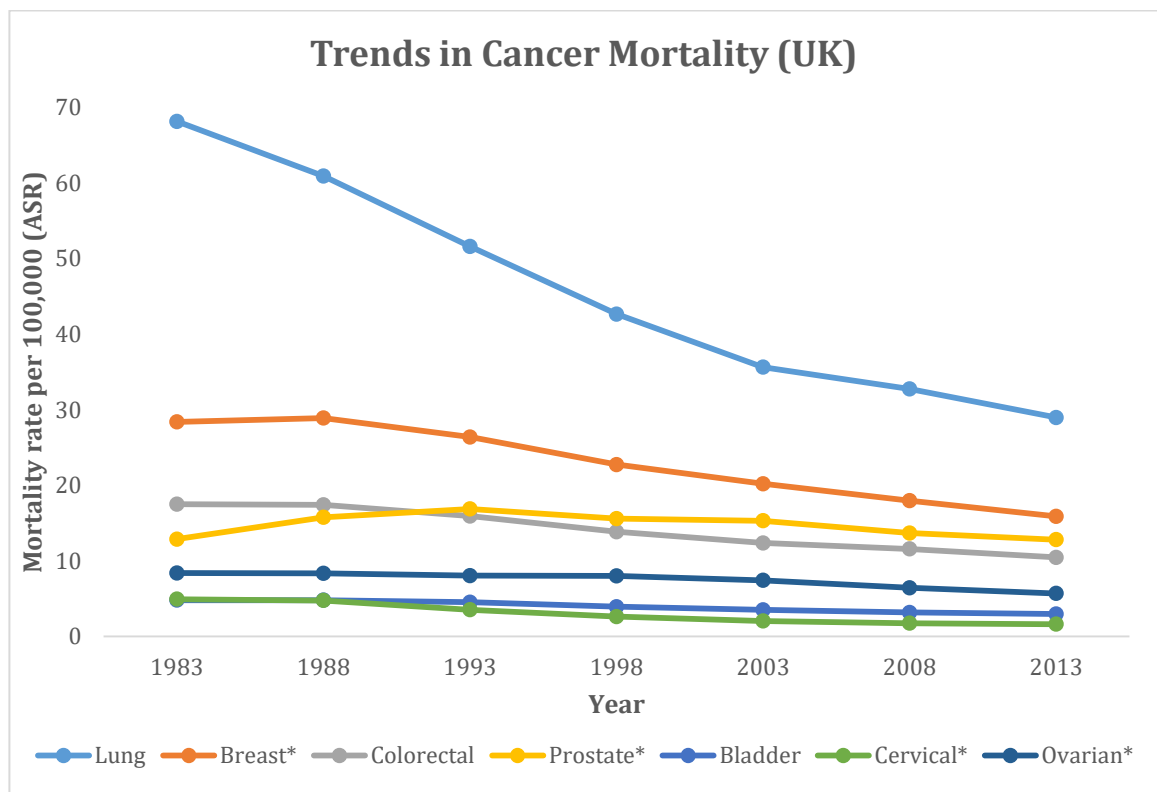


Figure 1-1: Trends in UK cancer mortality rates from 1983 to present

Trends in cancer mortality rates for 6 of the most common cancers observed in the UK between 1983 and 2013. Data sets marked (*) refer to cancers primarily affecting one gender only. Data represent the age-standardised rate (ASR) per 100,000 individuals. Data compiled from the WHO Cancer Mortality Database (most recent data available in online database 2013, next publication update due 2018). Authors own.

The most striking observation from this data is the decrease in mortality from lung cancers. The causal relationship between smoking and lung cancer was identified following the lung cancer epidemic in the 1940's and 1950's (Berenblum., 1944; Levin et al., 1950), and it is presently accepted that accumulated somatic mutations induced by cigarette smoking results in cancer development (CDC General Surgeon's Report, 2010).

Since public awareness of the risks of smoking increased and populations began to reduce their tobacco intake, the mortality rates resulting from lung cancer in the UK has continued to fall since the 1970's (figure 1.1), while incidence rates have also decreased from 63 to 39 new diagnoses per 100,000 between 2004 and 2014 alone (figure 1.2). Notably, these figures correlate with a decline in the number of UK smokers. When UK smoking statistics were first recorded in 1974, 46% of the population identified as active smokers. By 2016, this statistic had decreased to 15.8% of the UK population, highlighting the correlation between smoking and lung cancer incidences.

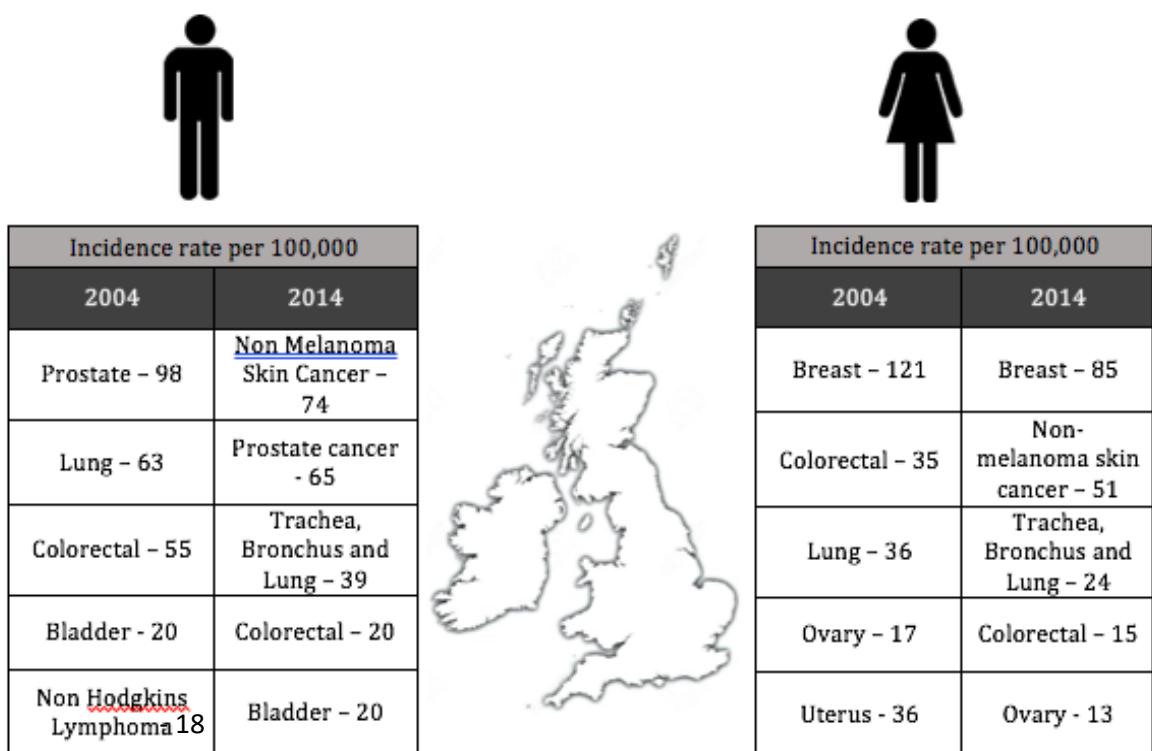


Figure 1-2: Comparison of the most common cancers in the U.K. by gender between 2004 and 2014

The pictograph compares the 5 most common cancers in males and females in the UK between 2004 and 2014 (2004 data adapted from the Office of National Statistics, 2014 data adapted from the International Association of Cancer Registries). Data represent ASR per 100,000 individuals. Authors own figure.

The body of evidence for causal relationships between lifestyle and environment and cancer risk continues to grow. Most recently, the role of meat consumption in cancer development has been investigated following a meta-analysis suggesting that consuming 100g of red meat daily, and 50g of processed meats daily increases an individual's risk of developing colorectal cancer by 17% and 18%, respectively (Bouvard et al., 2015). In 2015, the International Agency for Research on Cancer

(IARC) published a monograph evaluating this data among 800 other epidemiological studies. The report concluded that red meats are to be categorised as a Class 2A carcinogen—'probably carcinogenic to humans'—and processed meats as a Class 1 carcinogen—'carcinogenic to humans'.

The third most prevalent, preventable risk factor for cancer development is infection and related inflammation. It is currently estimated that approximately 20% of global cancers result from one of seven infectious agents; *Helicobacter pylori*, Hepatitis B or C, Human Papilloma Virus (HPV) strains 16 or 18, Human Immunodeficiency Virus (HIV), or Kaposi's Sarcoma-Associated Herpesvirus (KSHV) (figure 1.3). While acute inflammatory responses promote healing of injured or infected tissue, chronic inflammation causes DNA damage through production of mutagenic factors including reactive oxygen species (ROS) and nitric oxide (NO) which cause mutations such as deamination of DNA bases and oxidative modifications. Repeated damage and repair of DNA in the presence of highly mutagenic species results in genomic alterations which accumulate over time; for example, p53 gene mutations occur at similar frequencies in inflammatory diseases as is seen in the tumour environment (Coussens & Werb., 2002).

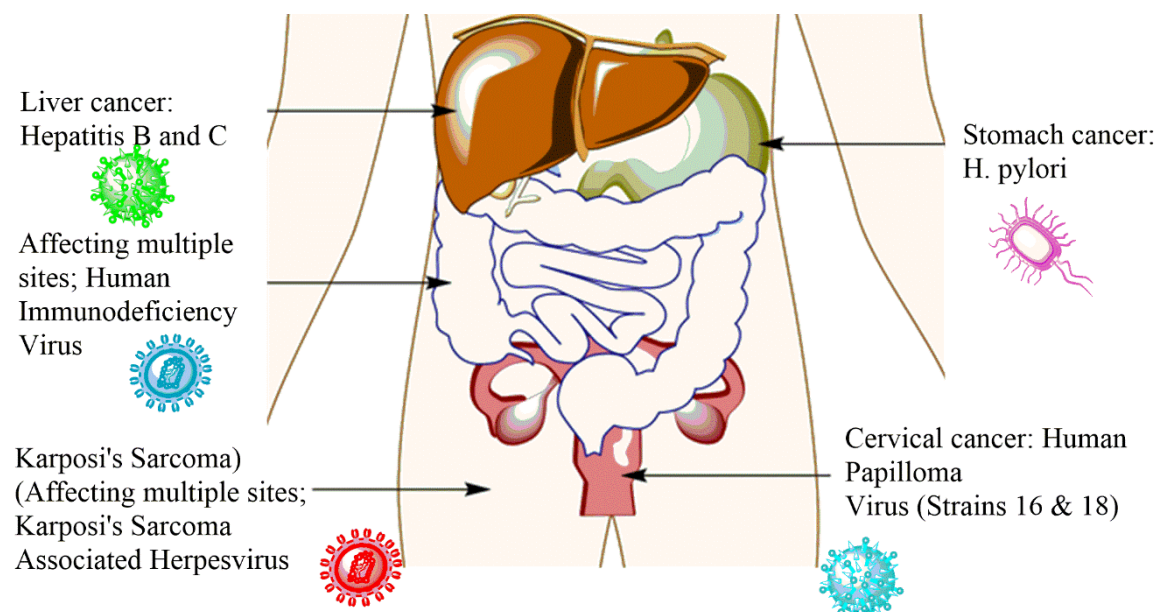


Figure 1-3: Causal pathogens associated with common preventable cancers

Infection and inflammation result in chronic immune stimulation and damage to host tissues. Specific have been identified as causal factors in various cancer types. Two strains of HPV virus, types 16 and 18, are responsible for 70% of all cervical cancer cases, while chronic hepatitis B and C infections are causal factors in 60-70% of hepatocellular carcinomas worldwide. Authors own figure adapted from multiple primary sources (Coussens & Werb., 2002; De Flora & Bonanni., 2011; Oh & Weiderpass., 2014).

A recent study investigating the impact of high doses (600mg/day) aspirin in patients genetically predisposed to developing Lynch Syndrome correlated with a 63% reduction in the relative risk of cancer development after two years, compared to placebo treatment (Beck et al., 2012). Cohort studies since have supported these data, correlating long-term aspirin use with a 19% reduction in colorectal cancer and a 15% reduction in all gastrointestinal cancers (Chao et al., 2016; Huang et al., 2017).

Despite encouraging successes in some cancer types, others disease sites show much more limited treatment options. Ovarian cancer is one of the most common cancers in females (figure 1.2), which has particularly poor prognostic outcomes. This occurs as a result of asymptomatic progression contributing to late stage diagnosis, and the standard of care consists of invasive surgery required to de-bulk the tumour mass, followed by aggressive chemotherapy regimens derived from platinum based therapies (Vergote et al., 2011). The prognosis of ovarian cancer patients deteriorates as a result of the frequent re-occurrence rate of the disease, expected to occur in 70% of patients. In light of such poor statistics, the landscape of ovarian tumours clearly demonstrates the need for new modalities in cancer treatments (Armstrong., 2002). Most recently, studies have identified increased levels of vascular endothelial growth factor α (VEGF- α) and IL-6 in the ascitic fluid of patients with epithelial ovarian cancer, which correlated with significantly shorter progression free survival (Dalal et al., 2018). This presents the potential for VEGF- α and IL-6 to be developed as a much needed biomarker for diagnosis. Despite improved understanding of cancer risk factors, the total number of cancer incidences across all sites has continued to increase sharply over consecutive years, summarised in figure 1.4.

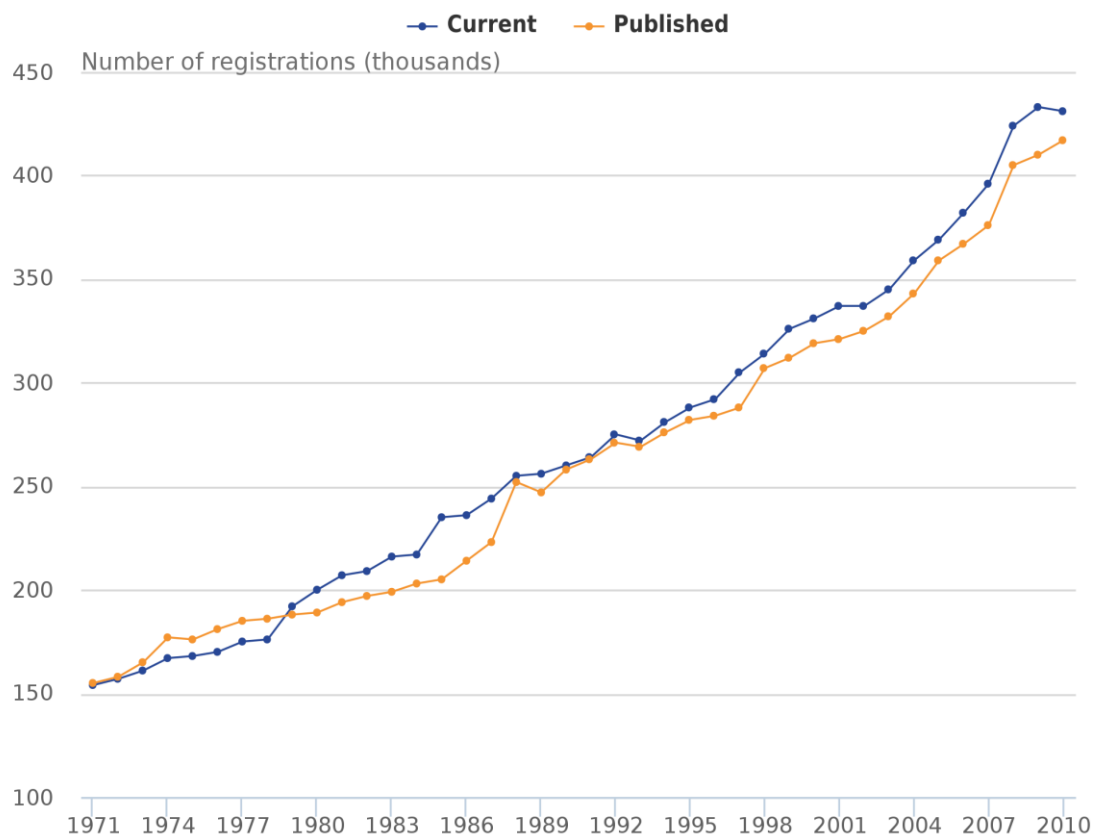


Figure 1-4: Annual reported cancer incidences in the UK for all disease sites

The data in figure 1.4 illustrates the number of cancer cases registered annually. Figure taken from Kaur & Poole., 2015, Cancer Statistics Bulletin showing data for 2013, the most recent data publication all neoplasms combined. Data is shown as ASR in thousands. While surgery, radiotherapy and chemotherapy have traditionally been considered the pillars of cancer therapy, the continued rise in cancer prevalence presents need for new and improved treatments. In the past decade, immunotherapy has entered the arena of cancer research to bridge this niche.

1.2 Cellular biology of the tumour

In order to develop novel treatments capable of effectively priming an immune response against neoplastic cells, it is useful to provide a brief overview of cellular components within the tumour. Metastatic growths are composed of two basic components, the parenchyma of transformed cells, which largely determine the characteristic behaviour of the tumour, and the surrounding stromal cells of the host which alter how the neoplasm develops (Fukumura et al., 2007). As the tumour continues to grow and disturb local homeostasis, host cells are recruited to the area where they develop dysfunctional roles. Immune cells, connective tissues, vasculature, and the lymphatic system all demonstrate unique characteristics in the tumour. This section will present a summary of the cell components relevant to immunotherapy (as summarised in figure 1.5). As the tumour microenvironment as a whole has been extensively studied, the reader is directed to read the

comprehensive review by Balkwill and colleagues for further information (Balkwill et al., 2012).

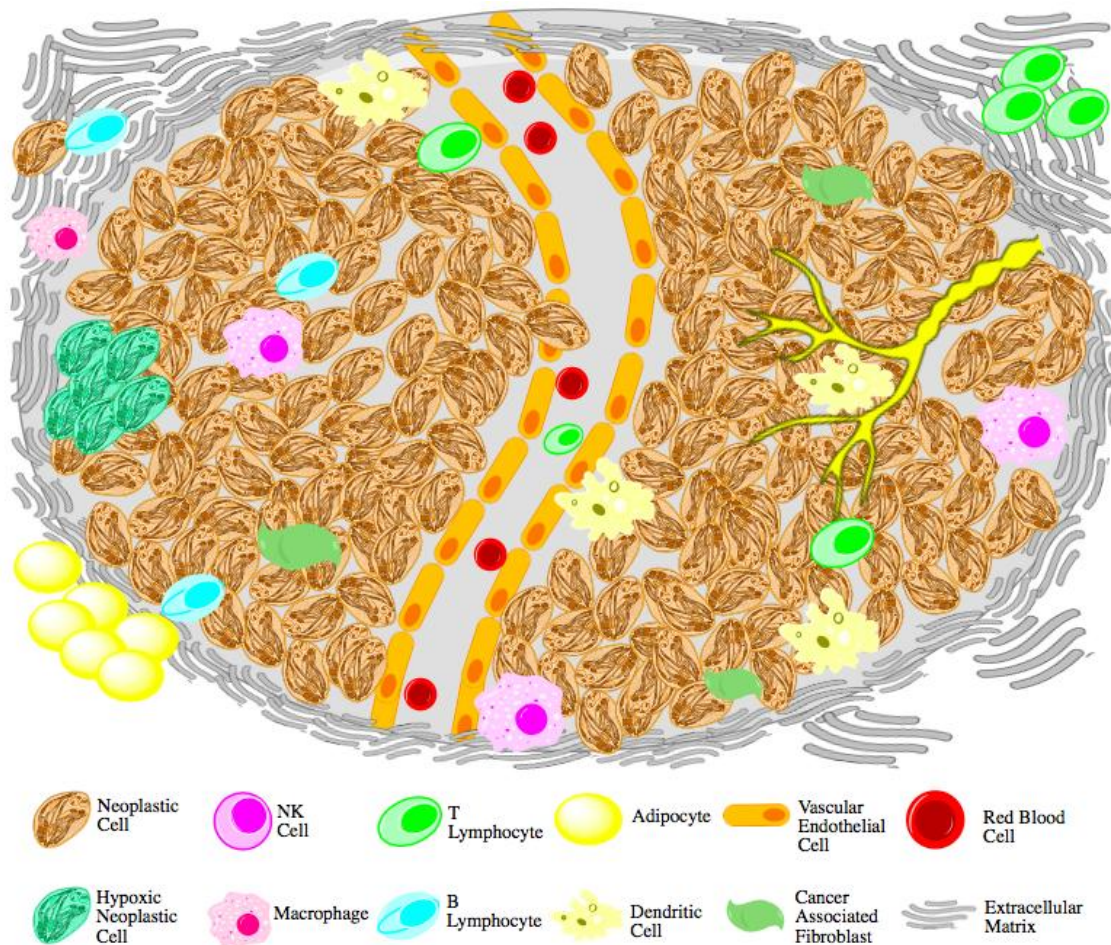


Figure 1-5: Cellular components of the tumour microenvironment

Alongside transformed cells, supporting tissues from the host are also sequestered to the tumour microenvironment where they promote tumour growth and metastasis. The above diagram indicates the cell subsets most relevant to the field of immunotherapy (adapted from Kerkar & Restifo, 2012; Goubran et al., 2014).

1.2.1 Tumour vasculature and cancer associated fibroblasts

In the initial stages of tumour development, mutated cells can sequester enough oxygen and nutrients to sustain growth of a mass up to 2mm in diameter (Muthukkaruppan et al., 1982). As neoplastic cells continue to divide at an uncontrolled rate, cells furthest from the tumour vasculature receive inadequate oxygen and nutrients from the blood, at which point angiogenesis is induced to promote development of new blood vessels to meet such requirements (Yadav et al., 2015). To this end, nutrient deprived hypoxic cells in the tumour secrete hypoxia-inducible-factors (HIFs) to regulate gene expression involved in angiogenesis and extracellular matrix (ECM) remodelling to facilitate invasion and metastasis of the tumour (Potente et al., 2011). One factor produced in response to HIF secretion is

VEGF, which induces differentiation and proliferation of vascular endothelial cells lining blood vessels of the tumour, allowing more effective delivery of nutrients (Bernatchez et al., 1999). In addition, tumour cells may synchronously express VEGF-receptors (VEGF-R) which enables the neoplastic cells to respond directly to autocrine and paracrine signalling, thus allowing tumours greater potential to control their own development (Goel & Mercurio., 2014). The induction of HIF associated proteins demonstrates how adaptations in tumour vasculature aid tumour progression by stimulating angiogenesis outside of normal physiological requirements. Therapies targeting neo-angiogenesis in the tumour have continued to develop since the approval of Bevacizumab (a monoclonal antibody targeting VEGF- α) by the Food and Drug Administration (FDA) in 2004 and many show clinical benefit. The primary limitation of anti-angiogenic therapies is that resistance mechanisms can develop as a result of the hypoxic conditions they induce (Dey et al., 2015), which has been correlated with tumour metastasis and relapse (de Groot et al., 2010).

Fibroblasts in the tumour environment switch to an activated phenotype during cancer progression, at which point they are defined as cancer associated fibroblasts (CAFs) which make up the most abundant stromal cells in the tumour, responsible for synthesis of collagen and other proteins of the ECM (Madar, 2013). Established roles of CAFs in the tumour include upregulation of matrix metalloproteinases (MMPs) which degrade the local ECM to allow tumour invasion and metastasis (Karagiannis et al., 2012), and production of HIFs, VEGF and other factors (Ostman & Augsten., 2009). During tumour progression, CAFs also induce gene expression changes which promote the recruitment of specific immune cell subsets to pre-metastatic environments. For example, VEGF produced by dysregulated signal transducer and activator of transcription 3 (STAT3) dependent signalling attracts immune subsets expressing cluster of differentiation 11b (CD11b) (Servais & Erez., 2013). Fibronectin and integrin $\alpha v \beta 3$ have recently been associated with tumour invasion; conversely, it has been shown that the invasive capacity of tumours is diminished in the absence of fibronectin, illustrating the bi-modal function of soluble factors in tumour development (Attieh et al., 2017).

1.2.2 Immune cell subsets and functions in the tumour

The host immune system actively shapes tumour development and outcome, during the three-phase process known as immuno-editing (Dunn et al., 2002). During the initial phase of elimination, the competent immune system can eliminate spontaneously occurring transformed cells. If a small number of the neoplastic cells do not encounter the immune system, the surviving cells may enter the equilibrium phase in which immuno-editing takes place (Schreiber et al., 2011). During equilibrium, the number of tumour cells displaying a non-immunogenic phenotype increases due to selective pressure applied by the immune system. Variants with beneficial mutations increase in number and confer additional resistance to immune detection. During the final phase of immuno-editing, mutated variants are no longer controlled by the immune system and escape, allowing tumour cells to grow in an uncontrolled manner and resulting in established malignancies (Mittal et al., 2014).

Cellular immunity is a protective process that involves the activation of multiple cell subsets including phagocytes, lymphocytes and antigen presenting cells (APCs). B and T lymphocytes are the functional effectors of cellular immunity responsible for eliminating pathogens, the functions of which are strongly influenced by DCs. The role of DCs in T cell development has been intensively studied since pioneering work by Banchereau & Steinman in 1998 (reviewed more recently by Benvenuti in 2016). More recently, the role for DCs in determining the functional outputs of other immune subsets such as B cell response to microbial infection (Sprokholt et al., 2017) and natural killer (NK) subsets function have been established, showing the diverse role of DCs in controlling immunity (Bottcher et al., 2018). Differentiation pathways of immune cells which are commonly observed within tumour margins are outlined in figure 1.6, and their role in tumour immunity will be discussed in this chapter.

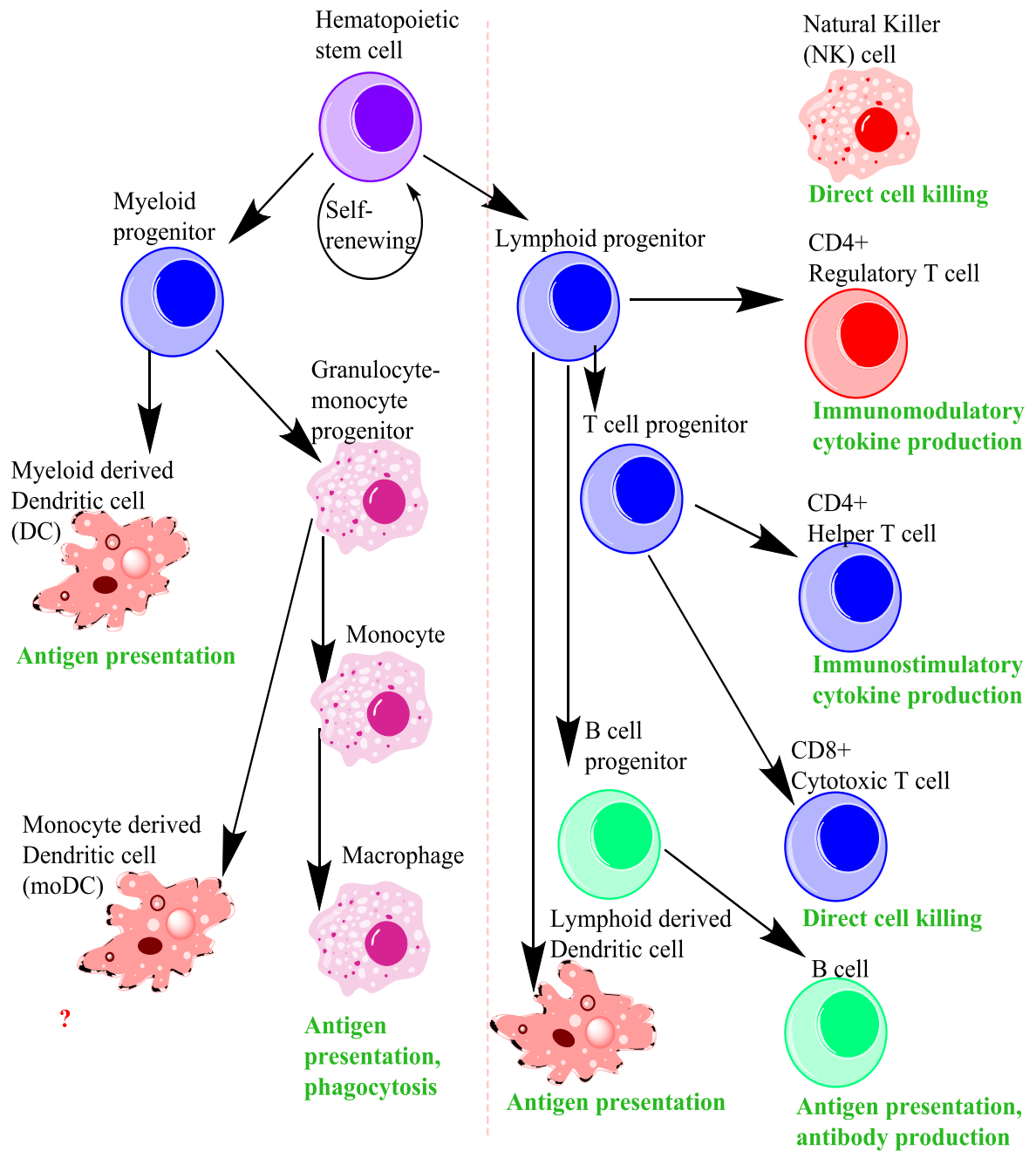


Figure 1-6: Differentiation and function of immune cell subsets under physiological conditions

Haematopoietic stem cells may follow one of two progenitor pathways. Myeloid progenitors generate cells of the innate immune system (left of dashed line) while lymphoid progenitors generate cells involved in adaptive immunity (right of dashed line). The primary function of cell subsets during physiological conditions is annotated below each subset in green (representing immunostimulatory function) or red (representing immunosuppressive function. Authors own, adapted from various sources (Murphy et al., 2012; Abbas & Lichtman., 2017).

1.2.2.1 Macrophages, NK cells and B lymphocytes in the tumour

Several innate immune subsets can be identified within tumour margins. Macrophages differentiate within peripheral tissues and are primarily responsible for phagocytosis of compromised cells. Macrophage populations within growing tumours are divided into two distinct subsets; those which modulate tumour development, primarily through abundant production of ROS and NO (Mills., 2016), and those which promote tumour growth, primarily through dysregulated production of VEGF and EGF (Li et al., 2016). Macrophage secreted factors in the established tumour are therefore associated with tumour angiogenesis and increased mutagenesis.

NK cells identify target cells based on the absence of major histocompatibility complex (MHC) ligands at the cell surface including MHCI, MHC class-1 like, and co-recognition proteins, which induces secretion of interferon gamma (IFN- γ) and direct killing of tumour cells (Cauwels et al., 2018). NK cell infiltrates are associated with good prognosis in early stage cancers (Palucka and Coussens, 2016), although NK function appears to be downregulated in advanced tumours since resident NK cells are detected within tumour margins, but fail to eliminate most tumours (Bottcher et al., 2018). Advanced tumours demonstrate abnormal signalling and expression of c-kit/SCF, c-myc, and STAT3 which have been suggested to drive tumour progression, (Zakiryanova et al., 2017). Recent data investigating murine melanoma demonstrated that depletion of NK cells correlates with decreased peripheral and intra-tumoural helper T cells and increased tumour growth (Paul & Lal., 2018).

B lymphocyte functions include antibody production, presentation of pathogen-derived antigens to T cells, and cytokine production. While the majority of immunotherapy research has focused on tumour infiltrating T cells, recent work suggests a modest increase in B cell numbers within the tumour compared to healthy surrounding tissues (Deng et al., 2016), while separate research groups have proposed a role for tumour infiltrating B cells as immune suppressors in the tumour (Xiao et al., 2016). Tumour infiltrating B cells have been categorised into three phenotypes; activated, antigen-associated, or non-responsive (Bruno et al., 2017), of which the activated and antigen-associated cells have been linked to effector T cell development *in vitro*, while exhausted B cell subsets are associated with regulatory T cell development (Bruno et al., 2017).

1.2.2.2 DCs in the tumour

The central role of DCs is to endocytose foreign antigens, process to the required format within the DC cytoplasm and express the antigenic peptides produced at the cell surface in the context of MHC I or MHC II receptors, for presentation to CD8⁺ or CD4⁺ T cells, respectively (Murphy et al., 2012). Within this role, DCs are the only APC subset able to stimulate naïve T cells to produce an antigen directed immune response. DCs are a desirable candidate for immunotherapies, since stimulating adaptive cellular immunity could allow the host immune system to determine the extent of an immune response, and maintain effector functions for extended periods after a tumour has been eliminated. Despite these attractive characteristics, tumour associated DCs are often suppressed in an immature state, displaying low levels of MHC and the co-stimulatory molecules which should be upregulated during normal maturation (Tan & O'Neill., 2005). Studies have demonstrated functional impairment of DC populations within multiple tumour types, including multiple myeloma (Brimnes et al., 2006), oral squamous cell carcinoma (Han et al., 2017), ovarian cancer (Krempski et al., 2011), and melanoma (Lopez et al., 2009), amongst others.

As illustrated in figure 1.6, DCs differentiate in the bone marrow *via* sequential progression through myeloid or lymphoid derived pathways. In steady state conditions, DC populations are composed primarily of myeloid derived subsets (Fogg et al., 2006), while dysregulated transcription factor (TF) production in cancer pathogenesis drives differentiation of monocyte derived DCs (Segura & Amigorena., 2013). Although the exact mechanisms remain poorly defined; studies have demonstrated tumour induced dysregulation of TFs including Id2, IRF8 and Batf3 (Satpathy et al., 2011). More recent studies suggest IRF8 is dispensable for survival of differentiated monocytic DCs, but plays a role in survival of conventional and plasmacytoid subsets (cDC and pDC, respectively) (Sichien et al., 2016). Only a small fraction of DCs localised at the tumour lymph node are characterised as pDC, which are much more prevalent in peripheral tissues (Swiecki & Colonna., 2015), and recent data has suggested that infiltration of this particular DC subset may correlate with poor prognostic outcomes in some tumours (Han et al., 2017).

Mouse models lacking lymph nodes demonstrated that cDCs were still capable of activating T cells, suggesting this takes place despite the presence of immunosuppressive mechanisms (Thompson et al., 2010). Separate groups have

shown cDCs are capable of infiltrating tumour lesions and directly presenting tumour associated antigen (TAAs) to T cells in the local environment, without prior migration to the draining lymph node (Liu & Cao., 2015), and that priming within the tumour is particularly associated with cross presentation by Batf3/IRF8 cDCs (Sanchez-Paulete et al., 2017). As such, DC subsets in the tumour microenvironment can directly influence the functions of effector T cell subsets to initiate tumour cytotoxicity (Sluiter et al., 2015), which may explain why higher DC numbers in the tumour correlate with positive outcomes in some cancer types. The myeloid DC subset will be referred to as DCs throughout the current review.

As a result of the heterogeneous differentiation of the DC lineage, not all DC subsets produce the same outputs in response to activating stimuli; for example mature DCs generated from peripheral blood monocytes using granulocyte-macrophage colony stimulating factor (GM-CSF) and IL-4 are capable of inducing IL-12 in response to CD40R activation, while pDCs generated by culture with IL-3 are not (Gilliet et al., 2002). Other groups have identified a cDC subset which expresses high levels of co-stimulatory receptors (CD40R, CD80, CD86 and MHCII) in response to stimulation with CD40R antibodies or lipopolysaccharide (LPS) and demonstrates successful antigen presentation capacity but is unable to induce IL-12 production even after antigen activation with co-stimulatory factors (Lutz., 2012). While specific DC subsets hold potential to control tumour development, such studies illustrate that their functions remain inhibited in the local microenvironment.

The production of immunosuppressive factors such as IL-10, IL-6, and transforming growth factor- β (TGF- β) also affect DC development in a tumour-specific manner, resulting in decreased expression of co-stimulatory receptors (Michielsen et al., 2011). DC maturation and function is also tumour-type specific; for instance, high numbers of DCs are detected in ovarian cancer, however abundant production of VEGF- α in this environment induces transformation in arriving DCs to pro-angiogenic and pro-inflammatory phenotypes, enabling tumour expansion (Conejogarcia et al., 2004). This situation is in direct contrast with colorectal cancers where infiltration of mature DCs is inhibited, and ranges between three and six times lower in primary or metastatic tumours *versus* the normal colonic mucosa, respectively (Schwaab et al., 2001; Pryczynicz et al., 2016). Recent studies have also demonstrated that DC conditioning by lactate, which is produced by many tumours, correlates with impaired cross-presentation and increased rate of antigen

degradation at the APC surface, impairing antigen presentation efficacy in lung cancers (Caronni et al., 2018). Such data highlight a range of factors which contribute to ineffective DC maturation and function in the tumour microenvironment.

In other cancers, DC numbers within tumour margins are limited as a result of poor infiltration and reduced survival times (Mullins & Engelhard., 2017), and in many cases increased DC numbers have been associated with improved patient survival (Nagorsen et al., 2007; Tran-Janco et al., 2015). The potency of DC-T cell interaction has been correlated with expression of CD80/CD86 on the DC surface, and abrogating this signal by blocking antibodies results in weakened intercellular interactions and decreased T cell activation (Dilioglou et al., 2003). CD80/86 binding interaction with CD28 on the T cell surface induces signal transduction in DC, responsible for DC production of T cell activating cytokines IFN- γ and IL-6 associated with complete T cell priming (Koorella et al., 2014).

The dampened expression of surface receptors on immature DCs in the tumour also influences the DC ability to produce cytokines. In the tumour, DC cytokine production is insufficient to produce optimal T cell priming, resulting in anergic T cell clones (Benencia et al., 2012). In particular, immature DC populations in tumour margins show a shift toward inhibitory cytokine profiles, including increased secretion and sensitivity to IL-10 and reduced production of IL-2 (Ma et al., 2015). This shift occurred alongside progressive upregulation of programmed cell death receptor 1 ligand (PD-L1) at the DC surface (Ma et al., 2015), which correlates with reduced capacity for CD8⁺ stimulation (Lim et al., 2015).

During APC-T cell encounters, a specific molecular complex is assembled at the immunological synapse between the APC and T cell surfaces (Monks et al., 1998). In the central supramolecular activation cluster (c-SMAC), APC:T cell interactions predominantly occur through interactions between MHC and TCR molecules, assisted by co-stimulatory molecules CD28 and CD80/86 and stabilised by the adhesion molecule CD54 in the periphery as shown in figure 1.7 (Friedl et al., 2005). Increased surface expression of c-SMAC receptors improves the chances of interaction with the cognate receptor on interacting T cells, leading to more efficient T cell priming and reciprocal DC licensing. Seminal work by Caux et al in 1994 identified the role of CD40R activation in upregulating MHCII at the DC surface,

along with accessory molecules CD80 and CD86 (Caux et al., 1994). Subsequent ligation of CD80/86 to CD28 on the T cell surface initiates effective T cell priming, while alternate binding to cytotoxic T-lymphocyte-associated protein 4 (CTLA-4) dampens the T cell response (Tivol et al., 1995). Expression of the surface molecule CD70 is particularly associated with DCs in the licenced state, and it has been suggested that inhibition of this receptor enables tumour escape from immune detection (Summers DeLuca & Gommerman., 2012).

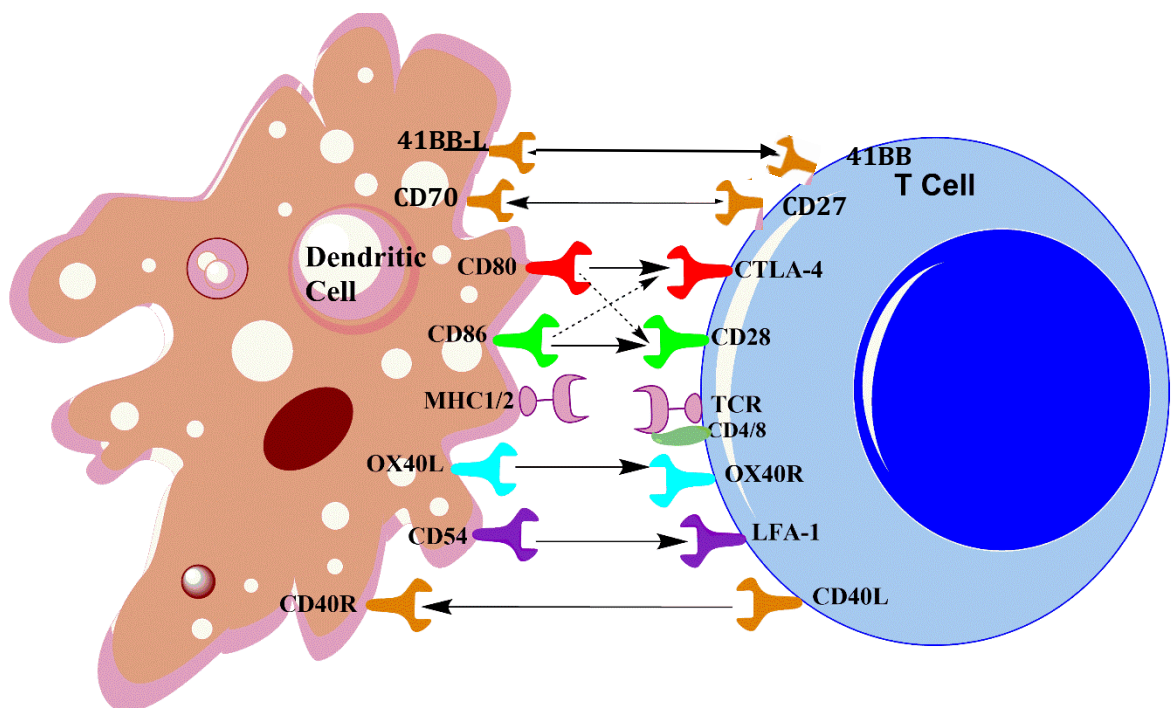


Figure 1-7: Receptors of interest involved in cell-cell interactions at the immunological synapse between DC and T cells

The process of T cell activation can be simplified as a two-signal process. Signal 1 is delivered through the TCR in response to MHC-peptide complex engagement whereas signal 2 provides co-stimulation generated by multiple surface receptors binding to their complementary partners. Authors own, adapted from Caux et al., 1994., Dustin et al., 2010 & de Luca & Gommerman, 2012.

1.2.2.3 T Lymphocytes

T lymphocytes are the primary effector cell type associated with tumour immunity. Immature T lymphocytes develop and proliferate in the thymus to create a repertoire of T cell receptor (TCR) proteins through gene recombination. The resulting cells can be further divided into two categories based on the expression of surface molecules CD4 or CD8 (figure 1.8). CD4⁺ T lymphocytes optimise antigen presentation by APC subsets through receptor interactions at the cell surface, and steer cytotoxic effector cell activity through the secretion of cytokines (Murphy et al.,

2012). CD8⁺ T lymphocytes induce direct cytotoxicity of infected cells through the release of perforin and granzyme proteins from cytotoxic granules which disturb the membrane integrity of target cells to induce apoptosis in response to interaction

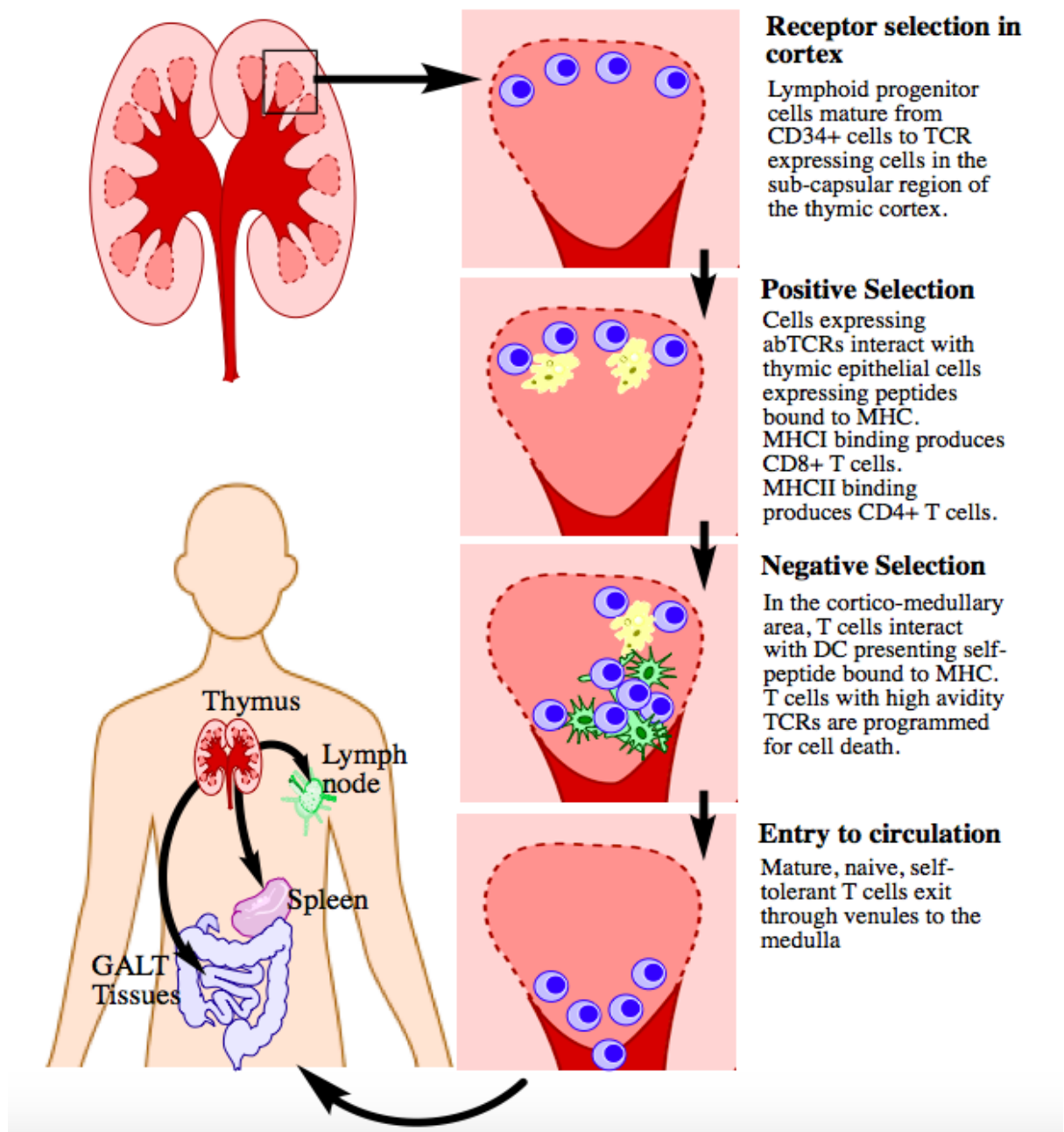


Figure 1-8: Stages of early T cell development and selection in the thymus

with antigenic peptide at the APC surface.

T cells undergo a rigorous process of positive and negative selection during development in the thymus. Immune checkpoints aim to prevent T cell reactivity to host tissues by dampening the immune response to self-proteins and chronic infections. The same mechanisms also prevent detection of transformed cells, which express a similar array of surface receptors and thus potential antigen to the

progenitor cell (Korman et al., 2006). Image adapted from Korman et al., 2006 and Murphy et al., 2012.

Considering that the primary role of CTLs is to directly eliminate foreign or compromised host cells through antigen recognition and that tumours express specific forms of TAA, various factors must modulate the function of CD8⁺ cells in the tumour environment to allow neoplastic cells to divide unregulated. The failure of CTLs to eliminate tumours can be explained as patient tumour infiltrating lymphocytes (TILs) are deficient in several outputs, including proliferation, cytokine production, and cytotoxicity, (Vazquez-Cintron et al., 2010) and are unable to induce tumour cell lysis *in situ*. As such, the factors mediating T cell function in the tumour have been extensively studied, and are outlined below.

1.2.2.4 Regulatory immune cell subsets

Regulatory cells affect the development of effector subsets in the tumour, including myeloid derived suppressor cells (MDSCs) which expand in pathological conditions into a heterogeneous cell population. MDSCs appear to suppress T cell function due to their aberrant production of inflammatory mediators IL-10 and TGF- β , and complete loss of CD28 on the T cell surface has been identified in tumours expressing MDSCs in high numbers (Spaulding et al., 1999). Alternatively activated MDSC and macrophages appear to accumulate at the tumour periphery in response to dysfunctional cytokine signalling in the tumour, particularly VEGF, GM-CSF, HIF-1 α and IL-10, amongst others (Nagaraj et al., 2013; Shojaei et al., 2008). This phenomenon is particularly evident in melanoma lesions, suggesting that these subtypes are recruited to the site by immunosuppressive factors produced by the tumour, rather than developing as a result of conversion of existing immune subsets within the tumour (Umansky & Sevko, 2013). At the tumor site, MDSCs undergo activation (via TNF- α , IL-10, IL-1 β , IL-6, IFN- γ , COX-2 and HIF-1 α , amongst others) and strongly inhibit anti-tumor reactivity of DC, T and NK cells. Elimination of the immunosuppressive cytokine TNF- α in murine models correlated with drastically reduced accumulation of MDSCs, suggesting TNFR signalling promotes MDSC survival and therefore tumour evasion (Zhao et al., 2012).

The differentiation of effector T cells depends on the nature of the activation signal received, which produces distinct subsets of T helper or T regulatory (Treg) cells characterised by their surface markers and cytokine profiles (figure 1.9). Treg cells are required to dampen the immune response once a pathogen has been eliminated,

but in cancers these subtypes can suppress the anti-tumour response, aiding immune evasion and escape.

In the tumour microenvironment, effector T cell production is skewed toward an immunosuppressive effector phenotype (Shevach., 2009). It is well documented that Tregs inhibit the cytokine production and cytotoxic outputs of effector T cells in the tumour, and several groups have shown that this dynamic remains unaltered following stimulation by *ex vivo* peptide pulsed DCs (Celluzzi et al., 1996; Curiel et al., 2004), although DCs have shown success in relieving Treg induced immunosuppression in model systems (Dissanayake et al., 2014). High ratios of Treg cells (particularly those with the CD4⁺CD25⁺FoxP3⁺ phenotype) compared to helper T effector cells are associated with poor prognosis in many cancers (Lee et al., 2005). Treg accumulation is particularly prevalent in ovarian cancer, due to dysregulated chemokine production in this tumour type. The chemokine ligand (CCL) CCL22 involved in lymphocyte trafficking is upregulated by macrophages in the tumour microenvironment, which induces Treg infiltration (Curiel et al., 2004). In addition to recruitment of new Treg cells, CD4⁺ cells also undergo conversion into Treg subsets as a result of aberrant IL-10, TGF- β , and adenosine production in the microenvironment, which appear to adopt similar profiles of cytokine production (Liu & Cao, 2005; Zarek et al., 2008). Treg cells expressing this regulatory cytokine profile appear to exert enhanced suppressive functions in the tumour compared to normal homeostasis (Gasparoto et al., 2010; Facciabene et al., 2011).

1.2.2.5 The influence of cytokines on immune cell development

Immune cell populations secrete and respond to different cytokines, which are largely responsible for inducing different subpopulations with stimulatory or suppressive phenotypes. The current understanding of which cytokines determine the differentiation of T cell subsets is outlined in figure 1.9 below.

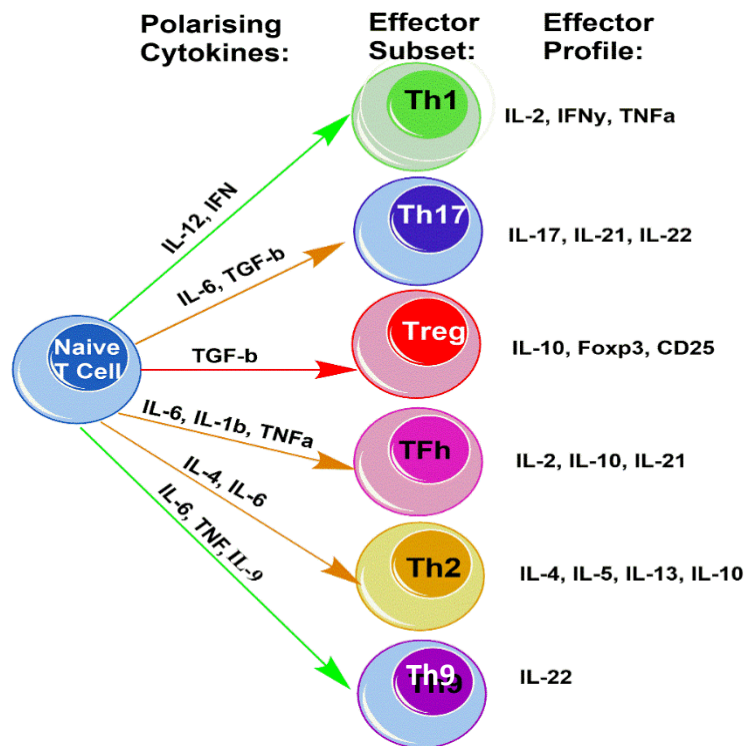


Figure1-9: Polarisation of naïve CD4⁺ T cells into differentiated effector subsets

Naïve CD4⁺ T cells may differentiate into one of several subsets depending on the mechanism of TCR activation and local cytokine milieu. This figure uses a “traffic light” colour coding method to indicate immunostimulatory (green), immunosuppressive (red) or intermediate (or poorly defined) (amber) cytokine profiles. Compiled from the current literature regarding immunomodulatory cytokines. Authors own.

Of the cytokines outlined in this diagram, IL-2, IL-12, IL-10 and IFN- γ are particularly well recognised for their role in DC and T cell interaction, as DC priming in normal homeostasis induces increased calcium mobilisation and production of cytokines IL-2 and IFN- γ (Lim et al., 2012). These cytokines will now be discussed in more detail.

1.2.3 IL-2

The first interleukin (IL) deemed essential for T cell growth *in vitro* was IL-2, over 30 years ago (Morgan et al., 1976). IL-2 has remained one of the most intensively studied cytokines due to its extensive role in regulating immune activation and homeostasis. IL-2 is a 15.5kDa cytokine predominately secreted by antigen stimulated CD4⁺ cells, but also by activated DC, NK, and CD8⁺ cells (Zelante et al., 2012). DCs produce IL-2 in response to various activation stimuli, the most effective being microbial products which induce activation through calcineurin/NFAT signalling (Granucci et al., 2001). Secretion by DC is marginal compared to the levels

produced by primed T cells, which suggests a role of maintaining T cell expansion rather than initiating the process (D'Souza & Lefrancois, 2003). IL-2 signalling occurs rapidly after TCR activation, inducing antigen-specific effector T cells and promoting long-term lymphocyte survival *via* proto-oncogenic and anti-apoptotic signalling (Boyman & Sprent, 2012).

IL-2 is predominantly produced by T cells in response to mitogenic stimuli (Theze., 1998). Over the past two decades, the production of IL-2 by DC subsets has been identified and appears to be induced by activation of the calcineurin/NFAT pathway in response to microbe exposure including treatment with LPS (Granucci et al., 2003; Zelante et al., 2012). Although DC are therefore capable of IL-2 production, other research groups have suggested that this feature is dispensable for T cell stimulation and abolishing IL-2 production by DCs does not negate the ability to induce effector and memory T cell responses or NK cell proliferation in lymph nodes (Schartz et al., 2005). While microbial cell components including LPS can trigger IL-2 induction to variable extents, DC stimulation by cytokines failed to induce any changes, illustrating that the activation output is largely dependent on the type of activating stimulus.

The value of IL-2 as an immunotherapeutic agent is illustrated by the case study of a 33-year-old female patient who presented with metastatic melanoma in November 1984. Following multiple alternative prior treatments, the patient was the first to receive aggressive recombinant IL-2 (rIL-2) infusion. This patient remained disease free for the following three decades (Rosenberg, 2014). Complete remissions have also been seen in cutaneous metastatic melanoma patients treated with IL-2 in combination with topical retinoid treatment. For example, combination therapy has induced 100% complete local response rates in all 11 patients involved in the trial (Shi et al., 2015). Conclusions are limited by the small number of patients involved in this trial but indicate promising prospects for IL-2 therapies, which can produce objective and durable responses in metastatic melanoma.

1.2.4 IL-10

IL-10 is produced by Treg and T helper CD4⁺ subsets, B cells, and macrophages to down-regulate the Th1 response once an infection is resolved. Knockout mice unable to produce IL-10 experience collateral damage to the surrounding tissues through uncontrolled activity of effector Th1 cells and their cytokines, including

inflammatory bowel disease (IBD) driven by unrestricted reactivity of effector CD4⁺ T cells (Sellon et al., 1998).

However, circulating IL-10 has been correlated with poor patient prognosis in multiple cancers in which upregulation of this cytokine inhibits production of pro-inflammatory cytokines IL-12, IFN- γ , and TNF- α (Mannino et al., 2015; Sato et al., 2011). IL-10 dampens the antigen-presenting function of DC through suppression of PI3K and Akt pathways (Bhattacharyya et al., 2004) and thereby reducing expression of MHC and co-stimulatory molecules required for maturation (Sato et al., 2011). Despite the abundance of literature defining the role of IL-10 as an immune-dampening cytokine, recent data also indicate an anti-tumour effect of IL-10. In a recent study of pegylated IL-10 administration in patients with advanced solid tumours, serum levels of pro-inflammatory cytokines increased, which correlated with an overall response rate of 21%, suggesting a potential opportunity for IL-10 administration in tumour immunotherapy (Naing et al., 2016).

Research using a murine model of ovarian cancer demonstrated that DCs extracted from the established tumour showed poor response to danger signals and were insufficient at inducing T cell priming *ex vivo*. Recovered DC populations retained expression of CD11c and CD11b at the cell surface, however loss of function was associated with aberrant IL-10 production, which increased from less than 250pg/ml to more than 750pg/ml (Krempski et al., 2011), showing the direct inhibitory effects of IL-10 on DC maturation and function.

1.2.5 IL-12

IL-12 is produced as a heterodimeric mature protein (IL-12p70) consisting of two covalently linked subunits (p35 and p40). The IL-12p40 homodimer competitively suppresses activity of IL-12p70. Production of the active p70 heterodimer is increased in response to danger signals received *via* the toll like receptor (TLR) and CD40R-CD40L interactions (Lasek et al., 2014). IL-12 acts as an orchestrating agent determining the Th1-type immune response against tumours and promotes T cells to induce IFN- γ in response to priming (Pegram et al., 2012), and as such has come into focus as an adjuvant therapy to guide primary immunotherapies. Early work demonstrated that ligation of CD40R on the DC surface by T helper cell ligand was sufficient to induce biologically active levels of IL-12 in the range of 260-4000pg/ml, while other groups have suggested that production in response to CD40R is

dependent on the presence of microbial stimuli (Koch et al., 1996, Schulz et al., 2000). More recent research has shown that CD40R antibodies conjugated to the surface of peptidyl-glycine-leucine-carboxamide (PGLA) NPs induces dramatic IL-12 production by CD8⁺ T cells on a nanomolar scale (Rosalia et al., 2015), providing encouraging data to support the potential for multivalent drug therapies to induce T cell activation *via* CD40R.

The key challenge for current research is to develop novel methods of inducing and delivering cytokines directly to the tumour environment where effector lymphocytes are likely to encounter TAAs. Pre-clinical trials of intra-tumoural injections with plasmid vectors containing the IL-12 gene have resulted in systemic anti-tumour immunity and regression. However, these results did not translate to the clinic due to low gene transfer efficacy (Heinzerling et al., 2005). In addition, long-term treatment with IL-12 may have detrimental effects on anti-tumour responses, as observed in follicular B cell non-Hodgkin's lymphoma. In this setting, long-term IL-12 administration correlates with upregulation of checkpoint inhibitor TIM-3, leading to T cell exhaustion (Yang et al., 2012).

Production of IL-12 by DCs drives T cells toward a Th1 response (Kelsall et al., 1996), and simultaneously supports DC survival post-activation (Koch et al., 1996). Furthermore, IL-12 production by DCs is significantly repressed in the tumour environment, and has been correlated with impaired DC maturation and poor antigen presentation capacity (Scarlett et al., 2009).

1.2.6 IFN- γ

IFNs are broadly categorised as soluble factors capable of protecting the host cell from viral infection, while the IFN- γ form is only produced by lymphocytes (Boehm et al., 1997). Secretion of IFNs inhibits the proliferation of infected cells and recruits inflammatory mediators including NK cells and cytotoxic T cells to the site of inflammation.

In cancer cells, the alterations in gene expression that are attributed to IFN- γ are associated with increased immunogenicity, which thereby induces immune stimulation, primarily by upregulation of MHC class I molecules on the cell surface (Martini et al., 2010). IFN- γ induced MHC class I expression has been shown to activate a tumour-specific immune response in a mouse model of prostate cancer, while sarcoma cells engineered to secrete IFN- γ acquire sensitization to cytotoxic

killing by CTLs. Furthermore, retrovirally mediated gene transfer of human IFN- γ upregulates MHC antigen expression in human breast cancer and leukaemia cell lines (Zimmerman et al., 2010), and the inclusion of IFN- γ in combination with platinum based therapies for the first-line treatment of ovarian cancer has resulted in an improvement in progression-free survival (Marth et al., 2006). Importantly, significant increases in T-helper cells, T-cytotoxic cells, NK cells, and total leukocytes have been observed following IFN- γ treatment (Giannopoulos et al., 2003), demonstrating the potential to stimulate immune effector cells. IFN- γ has also shown potential to directly recover DC function following tumour induced suppression. DC extracted from peripheral blood and ascites of ovarian cancer patients presented an immature phenotype (characterised by low expression of CD40R and co-stimulatory receptors). Recovered cells were cultured for 5-7 days *in vitro* with IFN- γ and GM-CSF, which was sufficient to recover expression of CD40R and CD80 at the cell surface, demonstrating that these cells retained the capacity for maturation once the immunosuppressive stimulus was removed (Marth et al., 2006). Re-stimulated cells were investigated for the capacity to induce a mixed lymphocyte reaction, and found that IFN- γ recovered DCs from ovarian tumours induced immunosuppression and increased production of IL-12 by allogeneic T (Zavadova., 2001).

1.2.7 Cytokine interactions in immune function

Although select cytokines influence the effector function of immune cells, these factors do not act in isolation, but form a complex soluble network between immune cells. Within the CD4⁺ T cell lineage, Tregs express IL-2R, and require IL-2 in the local environment to survive (Seddiki et al., 2006). IFN- γ is primarily secreted by activated T, NK and NKT cells, and plays a fundamental role in systemic and local immunity. IFN- γ secretion by NK cells and DCs in response to tissue injury and antigen exposure induces production of IL-12 and IFN- γ by effector cells, and thereby induces a Th1 response (Zhou et al., 2009). Th1 cytokines including IL-2, IFN- γ , and the functionally active heterodimer IL-12p70 (IL-12) help prime T cells to cytotoxic effector cells expressing IFN- γ and cytolytic molecules such as perforin and granzymes, able to initiate apoptosis of cellular targets including malignant tumours (Ebert., 2004; Pintaric et al., 2008). Repeated exposure of naïve CD4⁺ T cells to IL-10 in the presence of antigen induces APC to develop immunosuppressive phenotypes characterised by production of IL-10 and TGF- β which prevent APC

activation (Groux., 2003; Shachar & Karin., 2013). IFN- γ with IL-12 activates macrophages to more efficiently produce tumour necrosis factor- α (TNF- α) and NO (Hall et al., 1984), outlining how cytokines form a complex network of pleiotropic signals in the tumour environment illustrated in figure 1.10.

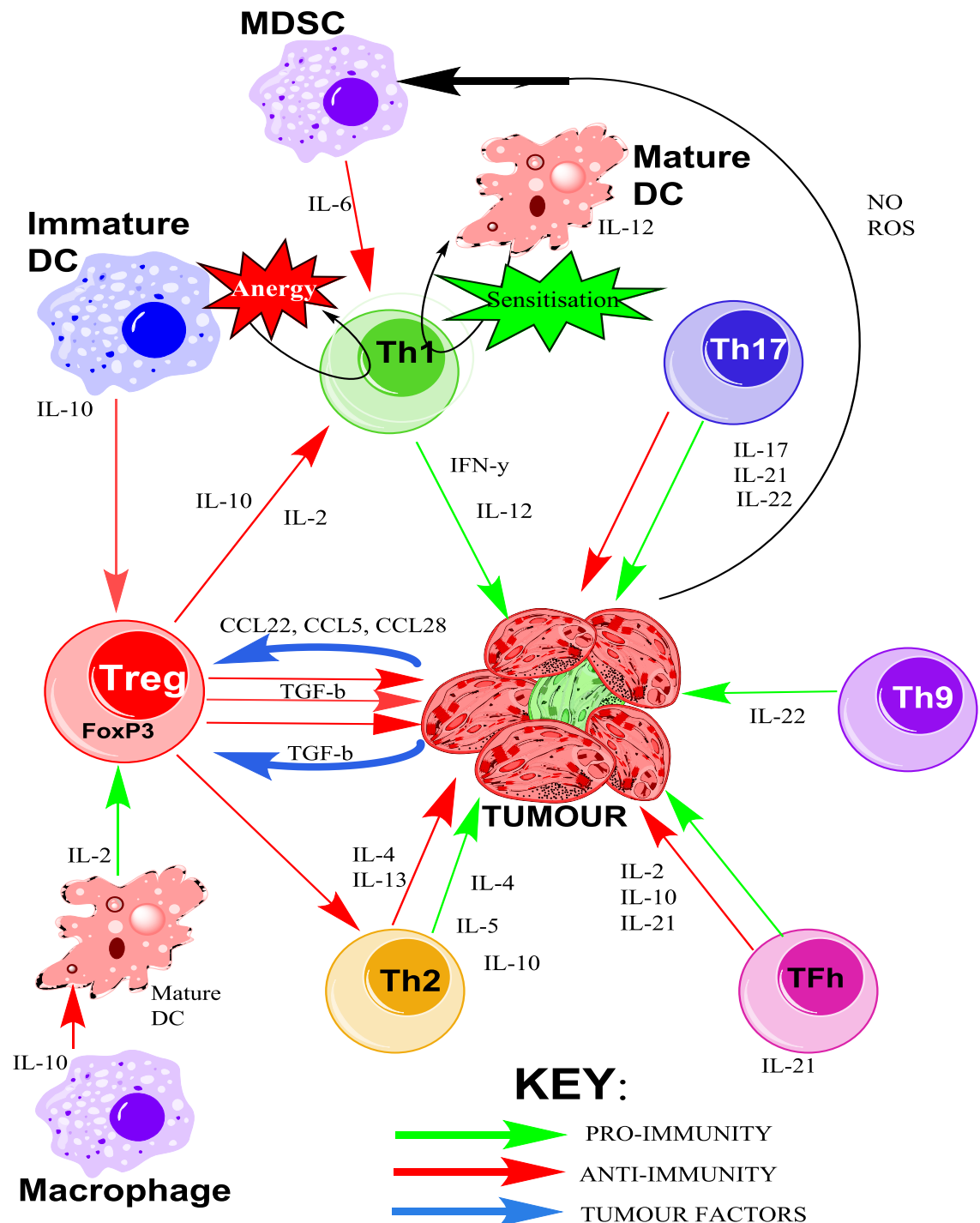


Figure 1-10: Infiltrating immune cell interactions with the tumour via soluble factors. Authors own, adapted from Hall et al., 1984; Ebert., 2004 & Pintaric et al., 2008

As cancers become established over time, immune cells contribute to the tumour stroma where they form a complex network enabling tumour growth. Many

immune cells display dual roles in tumour development depending on the cytokine profile in the tumour. Additionally, tumour-induced factors such as CCL22, CCL5, and CCL28 promote Treg recruitment and expansion.

1.3 Mechanisms of evading cellular immunity

Section 1.2 highlights the diverse roles of immune cell types in the tumour, and their association with DC based immunity to varying degrees. CTL priming requires synergistic signalling from both MHC and co-stimulatory molecules to induce activation and clonal expansion. First, an antigen specific signal is received as a short TAA peptide presented in the context of MHCI on the tumour cell. This signal is accompanied by co-stimulatory signals induced by interaction of CD80/86 with their cognate receptor (CD28). Finally, a T cell response requires further stimulation by the presence of immunostimulatory polarizing cytokines.

Since pioneering work by Boon et al. uncovered genes encoding antigens by screening transfected tumour DNA libraries (Boon et al., 1994), antigenic peptides are predicted to be expressed by most, if not all, tumours. As such, tumour cells expressing high mutational loads are associated with stronger immunogenicity and a more potent immune response (Blankenstein et al., 2012). Considering the discovery of TAAs and the increased risk of cancer incidence in immune-compromised populations (as described in section 1.1), tumours must demonstrate innate or acquired capacity to manipulate immune responses to avoid immune elimination during the initial phases of tumour development.

The Hallmarks of Cancer by Hanahan & Weinberg provides an organised framework in which to categorise the acquired characteristics of neoplastic diseases, illustrated in figure 1.11. Acquisition of these characteristics provides a selective advantage over the normal cell population, enabling tumour cells to become dominant in the microenvironment. As normal cells progressively evolve into the neoplastic state, abnormal activity in critical functions such as DNA repair and replication lead to increased frequency of somatic mutations; for example mutations in DNA polymerase genes can result in high tumour mutational load because the efficacy of DNA proof-reading is decreased. In another example, mutations affecting the DNA damage checkpoint P53 through somatic mutation, copy number loss, or epigenetic silencing increase cell tolerance to DNA damage, which also results in increased frequency of mutations (Palucka & Coussens., 2016).

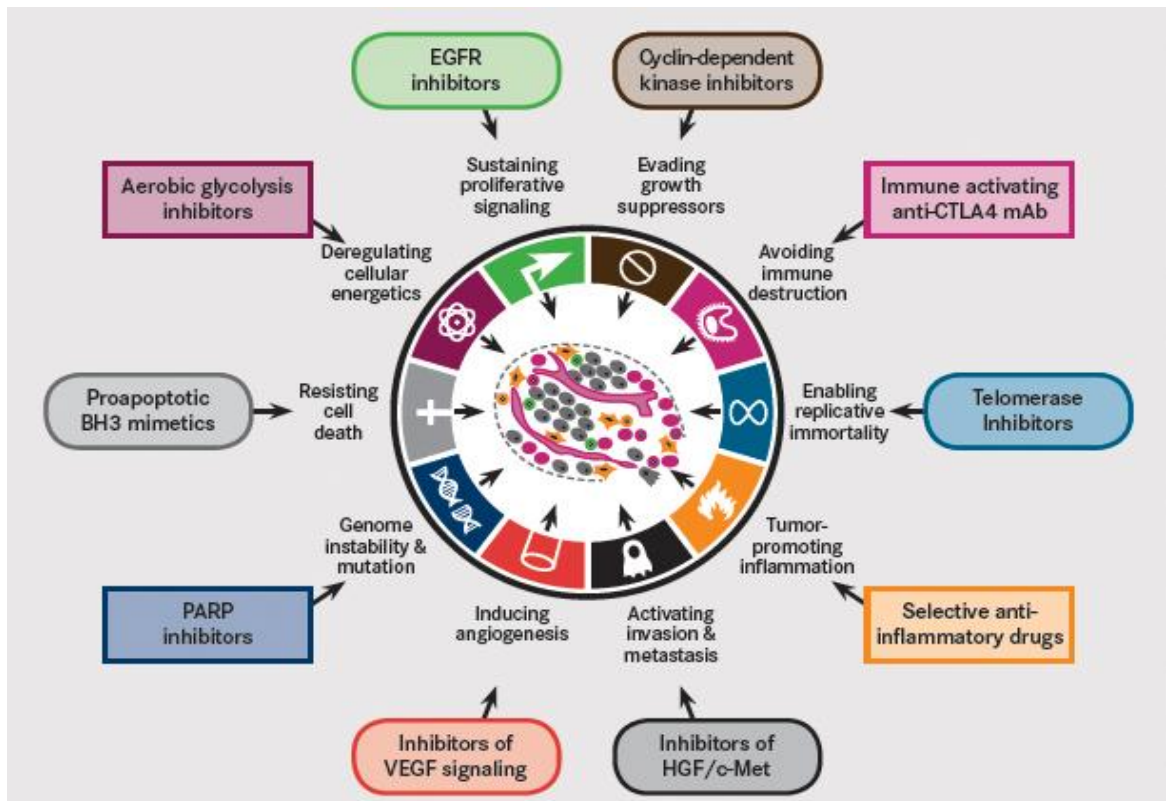


Figure 1-11: The hallmarks of cancer, from Hanahan & Weinberg, 2011

Over the past decade, the Hallmarks of Cancer framework has been updated to include the acquired capacity of tumour cells to evade immune detection and elimination (Hanahan & Weinberg, 2011).

The most recent addition to the Hallmarks of Cancer is the ability of tumour cells to avoid immune destruction, influenced by the activation profile of infiltrating immune cells (Hanahan & Coussens, 2012). The ability of tumours to escape immune recognition will be discussed here.

1.3.1 Defective antigen presentation *via* MHC I

As discussed in chapter 1.2.2.3 the TCR, unlike antibody, does not directly bind to unprocessed antigen. Instead, recognition of antigen by effector T cells requires presentation at the APC surface in the context of MHC molecules, making this protein an essential component in the initiation of an immune response. Some of the most common mutations identified in tumour populations affect the structure and function of MHC associated proteins, illustrated in figure 1.12.

Prior to their presentation on the APC surface, cytosolic and nuclear proteins are degraded by the proteasome in the cell cytoplasm into peptide subunits. The heavy chain of MHC class I is stabilised by $\beta 2$ microglobulin, initiating the peptide loading complex with transporter associated with antigen processing (TAP) proteins,

calreticulin and tapasin. Peptide delivery through TAP1/2 proteins forms the mature MHC molecule, which dissociates from the peptide loading complex and is exported to the plasma membrane to present a short peptide of 8-10 amino acids to the immune system (Murphy et al., 2012).

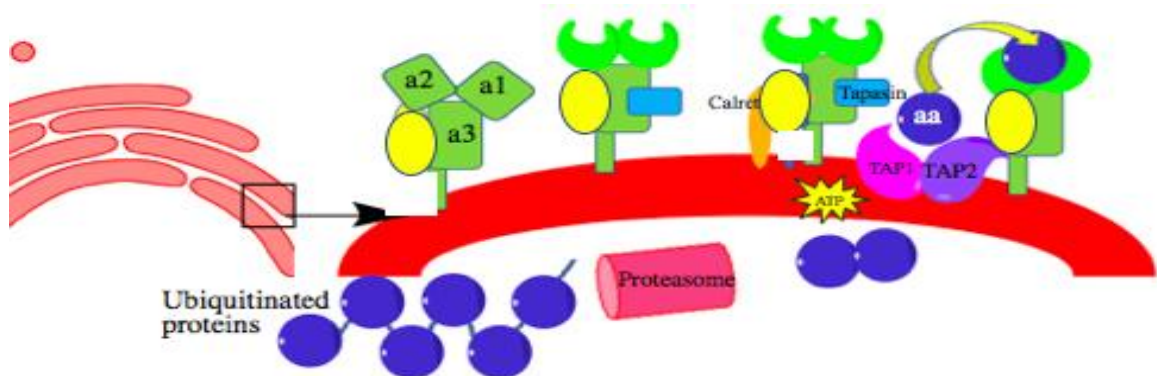


Figure 1-12: MHC I subunit assembly required for antigen presentation

TAP proteins are responsible for translocation of peptides into the lumen of the endoplasmic reticulum (ER), where they induce specific folding of MHC I. Image adapted from Murphy et al., 2012.

Mutations in the $\beta 2$ microglobulin gene are associated with loss of heterozygosity and ultimately failure to express MHC I at the tumour cell surface. Gene mutations in $\beta 2$ are observed in melanoma, colorectal carcinoma, prostate adenocarcinoma, and breast carcinoma (Algarra et al., 1997). MHC downregulation can occur from defects in other MHC genes primarily involved in synthesis of TAP1/2 proteins. TAP genes function as tumour suppressors, and mutations in this family correlate with significantly reduced subcutaneous tumour growth and pulmonary metastasis in B16 mouse models (Agrawal et al., 2004). Immunosuppression resulting from mutations in TAP1/2 genes has shown potential to be counteracted using treatment with IFN- γ and TNF- α (Seliger et al., 2001), which upregulate TAP1/2 at the transcriptional level.

Disruptions to the proteins and enzymes involved in effective MHC assembly and loading affect tumour recognition. Another enzyme which shows dysregulated function in tumours is the endoplasmic reticulum aminopeptidase associated with antigen processing (ERAP1/2) (Stratikos., 2014). ERAP1 is induced in response to IFN- γ and modifies the peptide repertoire available for T cell recognition by trimming peptides received from the proteasome to the antigenic peptides presented by MHC I (Murphy et al., 2012). Interestingly, downregulation of this enzyme appears to act differentially depending on the cancer type. For example,

downregulation of ERAP1 has shown potential to induce cytotoxic activity of NK cells against murine lymphoma, which may result from lack of MHC expressed at the cell surface (Nagarajan et al., 2012). This finding was followed by additional studies demonstrating that ERAP1 downregulation is also capable of inducing CTL responses to TAAs in colorectal cancer which are normally eliminated by ERAP processing (James et al., 2013).

Defective antigen presentation in the tumour prevents cytotoxic T cells from recognising TAAs presented in the context of appropriate MHC molecules. Secondary analysis of human tumours derived from tissues which were identified as MHC^I⁺ at primary testing has demonstrated that between 40-90% are subsequently identified as MHC^I⁻ upon re-testing, illustrating the evolving dynamic of the tumour (Haworth et al., 2015). A summary of MHC expression profiles in various tumours is provided in table 1.1.

Table 1-1: Prognostic indications of cancer subsets with demonstrable MHCI down-regulation

Adult tumour type	Prognostic indications	References
Endometrial carcinoma	Downregulation associates with poor survival	Bijen et al., 2010
Lung carcinoma		Hanagiri et al., 2013
Tonsillar squamous cell carcinoma		Nilsman et al., 2013
Melanoma	High expression predicts positive response to immunotherapy <i>in vitro</i>	Lechner et al., 2013
Merkel cell carcinoma		Paulson et al., 2014
Renal cortical adenocarcinoma		Lechner et al., 2013
Head and neck carcinomas	Downregulation correlates with increased regional lymph node metastasis	Duray et al., 2010
Prostate carcinoma	Downregulation associates with high Gleason grade and early reoccurrence	Bubenik., 2004
Bladder carcinoma	Downregulation associates with relapse in BCG associated cases	Carretero et al., 2016
Breast adenocarcinoma	Expression inversely correlates with human epidermal growth receptor (HER2) expression; Expression predicts immunotherapy response <i>in vitro</i>	Inoue et al., 2012 ; Lechner et al. ,2013
Colorectal carcinoma	High expression correlates with improved survival; Expression predicts immunotherapy response <i>in vitro</i>	Simpson et al., 2010; Lechner et al., 2013
Cervical carcinoma	Low expression correlates with improved prognosis in HPV+ cases; Normal expression correlates with improved prognosis in HPV- cases	Bubenik., 2004; Ashrafi et al., 2015
Ovarian carcinoma	Low expression characterises high risk serous carcinoma	Yoshihara et al., 2012.

MHC associated proteins control peptide generation, trimming, and editing prior to MHCI loading. Altered expression of processing machinery molecules affects MHC expression in the tumour and correlates with poor prognosis in various tumour. Original table, data compiled from primary publications (cited).

1.3.2 Induction of immune checkpoints

Throughout the lifetime of an activated T cell, these effectors of immunity also express multiple co-inhibitory receptors known as immune checkpoints. Checkpoint receptors monitor the immune landscape and prevent overt or uncontrolled immune responses to pathogens or self-antigens, which could cause inflammation or autoimmune type reactions (Korman et al., 2014). Proteins responsible for this function include lymphocyte-activation gene 3 (LAG-3), Programmed cell death receptor 1 (PD-1) and CTLA-4 (Nirschl & Drake 2013), which also modulate T cell responses to self-proteins, including TAA (Topalian 2012).

In resting naive T cells CTLA-4 is located primarily in the intracellular compartment and is upregulated at the cell surface in response to complimentary TCR and CD28 signalling (Linsley., 1996). Oppositely, Tregs constitutively express CTLA-4, and this is thought to be important for their suppressive functions (Takahashi., 2000). CTLA-4 binds the B7 family with higher avidity than stimulatory CD28, demonstrating 500-fold binding affinity to CD83 and 2500-fold to CD86 (Parry et al., 2005). CD28 provides one of the key activating signals for T cell activation, which displaces CD28 as a result of its greater affinity, to dampen the immune response once an inflammatory stimulus has been dealt with. In CTLA-4 knockout mice, extensive lymphoproliferative disease resulted in death by age 3-4 weeks from unrestrained CD28-induced T cell activation (Pentcheva-Hoang et al., 2004). Susceptibility of CTLA-4 knockout mice to fatal unregulated immune responses illustrates the importance of the CTLA-4 pathway in maintaining normal homeostasis at the end of an immune reaction. CTLA-4 is the first of several immune checkpoints encountered by T cells during development, and is responsible for eliminating potentially autoreactive T cells at the first stage of naïve T cell activation in lymph nodes. Ligand-receptor interaction of CTLA-4 dampens effector T cell proliferation and IL-2 production, applying a physiologic brake to immune system activation (Egen & Allison., 2002).

A second well-defined immune checkpoint is the PD-1 pathway, an inhibitory receptor also present on the activated T cell surface, which is generally expressed by T cell populations within tumours as opposed to in lymphoid organs (Topalian et al., 2012). PD-1 suppresses T cells later in the immune response than CTLA-4, primarily in peripheral tissues, and binds two cognate ligands: PD-L1 and PD-L2.

PD-L2 is expressed on APC populations, suggesting a role in regulating T cell priming. PD-L1 displays more homogenous expression and is detected on immune subsets and by some tumours. PD-1 expression is a hallmark of “exhausted” T cells – seemingly incapable of initiating effector functions – which are induced by exposure to suboptimal antigen presentation or reduced CD4⁺ T-cell help (Wherry., 2011). A final example of altered immune checkpoint expression is LAG-3; a homolog of CD4 which binds MHCII on the APC surface, providing an alternative pathway for T cell inhibition. LAG-3 specifically inhibits CD8⁺ effector T cell functions by enhancing the suppressive activity of Tregs (Grosso et al., 2007). Under inflammatory conditions, the receptor is expressed *in vivo* on the surface of activated CD4⁺, CD8⁺ and NK cells and is also upregulated on anergic T cells (Topalian et al., 2012). Recent studies in murine ovarian cancer models have investigated the potential for LAG3 as combination therapy with PD1, where the synergistic activity of these pathways has shown encouraging results in dampening anti-tumour immunity (Huang et al., 2015).

1.4 Current immunotherapies

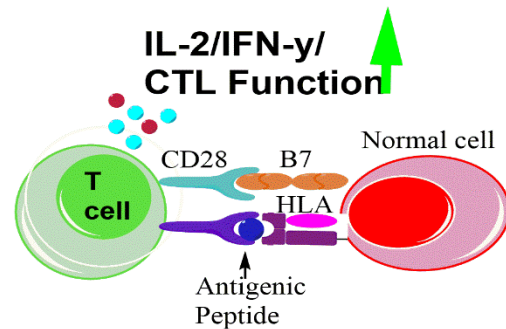
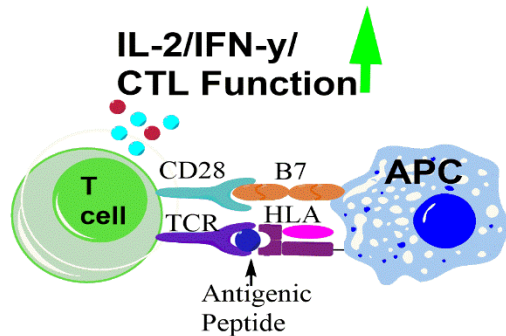
Immunotherapies aim to harness the patient’s immune system to specifically target malignant cells. The goal is to utilise the unique attributes of the immune system for cellular memory and unmatched specificity to induce complete and durable remissions with few or no side effects compared to traditional therapies. As a result of these desirable traits, immunotherapies have been hailed by Cancer Research UK as “the most promising new cancer treatment approach since the first chemotherapies” (Stanculeanu et al., 2016). In particular, cellular immunotherapies present the opportunity to induce extraordinarily long-term responses. In some cases, patient responses to immunotherapy have been detected for more than 10 years after treatment, as has been observed in melanoma patients treated with Ipilimumab. One study recorded patient survival for over 10 years following therapy, including some patients who were no longer receiving treatment, indicating that treatment free survival is possible in some cancers (McDermott et al., 2014). Unfortunately, the persistence and durability of the cellular response also extends the timeline over which potential toxicities can result far beyond that seen using conventional chemotherapies (Weber et al., 2016). The consistent need for improvement in the field of immunotherapy drives continued research for new

treatments with higher specificity and lower toxicities. This section details the most relevant advances in immunotherapies currently under investigation.

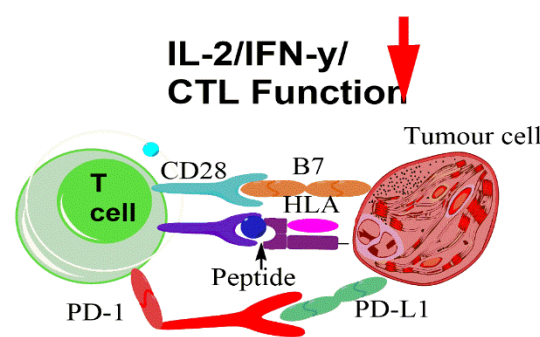
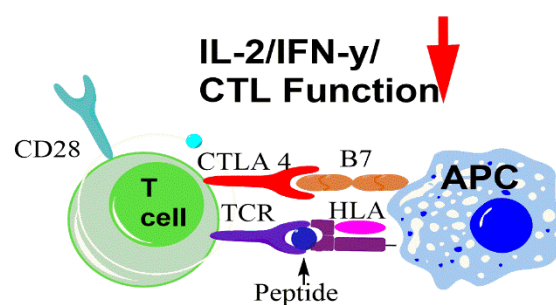
1.4.1 Immune checkpoint blockade

Targeting immune checkpoint pathways in the tumour has demonstrated promising potential to re-stimulate the suppressed local immune system driven largely by two key pathways: CTLA-4 and PD-1 (figure 1.13).

NORMAL IMMUNE FUNCTIONING



CHECK-POINT SUPPRESSION



CHECK-POINT INHIBITOR

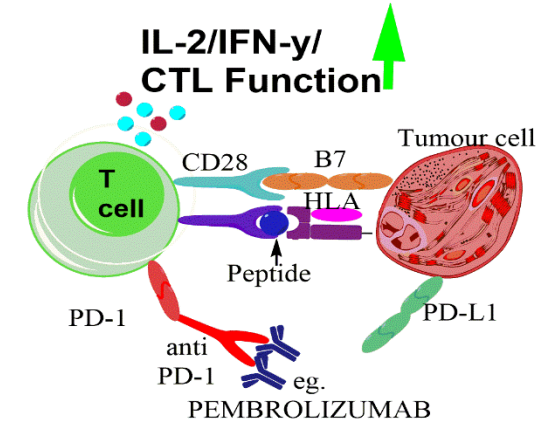
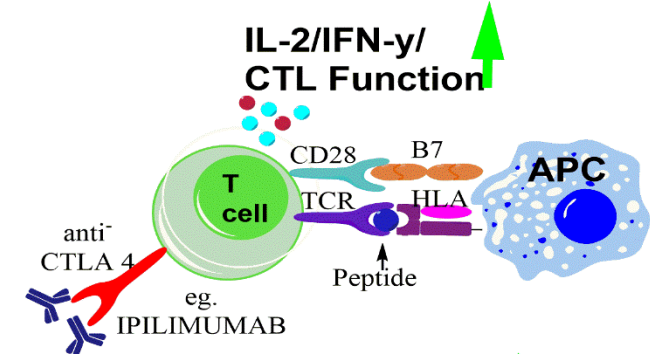


Figure 1-13: Dynamics of immune checkpoint proteins PD-1 and CTLA-4 with examples of FDA approved checkpoint blockade antibodies

The CD28/CTLA-4 receptor family of immune checkpoints are expressed on T lymphocytes at the end of an immune response and competitively bind to conjugate ligands of the B7 family at the APC surface to dampen activation. The PD-1 receptor family is expressed on T lymphocytes under normal conditions, while tumour cells induce expression of PD-L1 to induce T cell death. Authors own, adapted from multiple primary references (Das et al., 2015; Parry et al., 2005; Peggs et al., 2006).

1.4.1.1 CD28/cytotoxic T lymphocyte antigen-4

Anti-CTLA-4 therapy is one of the first treatments to demonstrate definite clinical benefit through direct T-cell activation, and is currently in clinical use for treatment of stage IV melanoma (Weber, 2007). Although CTLA-4 therapy has demonstrated significant success in melanoma, this response has not yet been reproducible in the wider context of cancer treatment, potentially due to the specific immunogenicity of tumours. Tissue studies suggest that melanoma samples display a particularly high number of somatic mutations (Snyder et al., 2014), which may result in a more accessible source of TAA to utilise as immune stimulators alongside checkpoint inhibitor immunotherapies. Pigment differentiation proteins for example are expressed by most melanoma samples throughout all stages of disease development and display incomplete immune-tolerance (Snyder et al., 2014), providing a uniquely accessible target for immunotherapies.

The ability of CTLA-4 to inhibit T cell activation is dependent upon a number of factors, including the strength of the TCR signal and the activation state of the APC. CTLA-4 inhibits both CD4⁺ and CD8⁺ T-cell responses and CTLA-4 localization at the immunological synapse is favored under conditions of stronger TCR signalling (Egen & Allison., 2002). Clinical trials evaluating anti-CTLA-4 monotherapy were based on preclinical data that showed that, when used alone, this treatment regimen induced rejection of several tumor types, including colon carcinoma, fibrosarcoma, prostatic carcinoma, lymphoma, and renal carcinoma (Peggs et al., 2006). However, anti-CTLA-4 monoclonal antibody monotherapy failed in less immunogenic tumors such as B16 melanoma, which may result from the ability of CTLA-4 blockade to induce general immunity sufficient to eliminate highly immunogenic tumours, rather than initiating a highly selective tumor-specific response (Tivol et al., 1995).

1.4.1.2 Programmed cell death 1 receptor

The pro-inflammatory tumour environment upregulates PD-L1 expression at the tumour surface in response to pro-inflammatory molecules TNF- α , LPS, GM-CSF, VEGF, and IL-10 (Sznol & Chen, 2013). In this system, although T cells in the tumour may receive the necessary interactions *via* CD28 and MHC-bound peptide, PD-1/PD-L1 binding down-modulates the ability of the activated T cells to produce an effective immune response by forming a barrier between the cancer cells and the immune system (Philips & Atkins, 2015). Exhausted TIL populations have shown a

correlation with PD-1 expression on tumour cells, suggesting that PD-1 interaction not only prevents T cells from recognising the tumour, but that these immune cells are prevented from launching a subsequent immune reaction.

In clinical trials, antibodies Nivolumab and Pembrolizumab directed against PD-1 and its ligand have demonstrated potential to restore or augment anti-tumour immunity. Clinical activity has now been demonstrated in several cancers, including melanoma, lung cancer, and renal cell carcinoma (Carbognin et al., 2015). The efficacy of anti-PD1 monoclonal antibodies has also been investigated in combination with adjuvant therapies GVAX and FVAX, cell lines modified to produce either granulocyte macrophage GM-CSF or FMS like tyrosine kinase 3 ligand (FLT3), respectively (Duraiswamy et al., 2013). When combined with GVAX vaccination therapies, antibody mediated PD-1 or PD-L1 blockades have triggered rejection of ID8 tumours in 75% of mouse subjects. Rejection was associated with increased proliferation and function of tumour specific effector CD8⁺ T cells, resulting in enhanced cancer control (Duraiswamy et al., 2013).

While robust and significant regressions have been reported in selected tumours following immunotherapy treatment, the overall rate of patient responders requires further improvements. As recently as 2017, it has been recorded that 20% of Hodgkin's lymphoma patients and 60% of melanoma patients failed to show any response to PD-1 therapies (Ott et al., 2017).

1.4.1.3 Checkpoint blockade combination therapies

Hoping to improve the percentage of patient responders to checkpoint inhibitor therapies, the number of clinical trials investigating a combination of PD-1 or PL-L1 alongside at least one additional therapy has risen annually over the past six years, from just 13 trials in 2011 to 467 trials in 2017, with the majority of the latter focusing on combination therapies with CTLA-4 (Tang., 2018). Checkpoint blockade of either CTLA-4 or PD-1 display separate mechanisms of action. Blocking CTLA-4 binding to enhance T cell priming cannot be fully effective if tumour cells can avoid recognition by primed immune cells through PD-L1 interaction (Das et al., 2015), therefore combinations therapies have primarily targeted the PD-1 and CTLA-4 pathways, since the two follow distinct mechanisms of action by acting at different points in the immune response. PD-1 is thought to predominantly regulate effector

T-cell activity at the antigen recognition stage within tissue and tumours, whereas CTLA-4 regulates T-cell activation in the priming phase in the lymph node.

As of September 2017, 251 trials investigating combination therapies of CTLA-4 with PD-1 were underway according to the CRI Annual Review. Overall, combinations of anti-CTLA-4 therapies with treatments targeting other aspects of tumour immunity demonstrated higher clinical efficacies than CTLA-4 monotherapies alone. Of the areas investigated, combination treatments simultaneously targeting antigen presentation and tumour killing have revealed the greatest improvement (Swart et al., 2016).

The combination of CTLA-4 and PD1 blocking antibodies have demonstrated a higher level of anti-cancer activity than either treatment in monotherapy. Figure 1.14, taken from Swart, Verbrugge & Beltman., 2016, succinctly illustrates the efficacy of CTLA-4 immune blockade in combination with various other immunotherapies affecting separate stages in the cancer-immune cycle, and shows that with PD-1/PD-L1 have shown the most robust response, demonstrating an increased clinical efficacy of 60% in the overall survival of melanoma patients. Recently, combination therapy of low-dose antibodies against CD137, OX40, and CTLA4 have demonstrated clinical efficacy which was able to induce systemic tumour regressions in murine models of colon cancer and B cell lymphoma (Hebb et al., 2018). In other cancers such as non-small cell lung cancer (NSCLC), PD-L1 membranous expression appears to serve as a potential marker for the patients who are potentially most sensitive to anti-PD-1 therapies (Reck et al., 2016). However this indication is not absolute, as not all patients whose tumours express membranous PD-L1 respond to anti-PD-1 or anti-PD-L1 therapy, and other immune parameters such as the infiltration of CD8 cells also appear to be important for the sensitivity to immune checkpoint inhibitors (Taube et al., 2014).

The interaction of secondary immune parameters alongside checkpoint blockade therapies has been demonstrated in murine models of pancreatic cancer. Pancreatic ductal adenocarcinoma (PDAC) typically shows a low response rate to immunotherapy, with a 5 year survival rate of only 6% (Zheng, 2017). Murine studies have shown antibodies for CD40R improves responses to PD-L1 blockade in patients with pancreatic cancer (Luheshi et al., 2016), providing encouraging prospects for combination immunotherapies in difficult to treat cancer types.

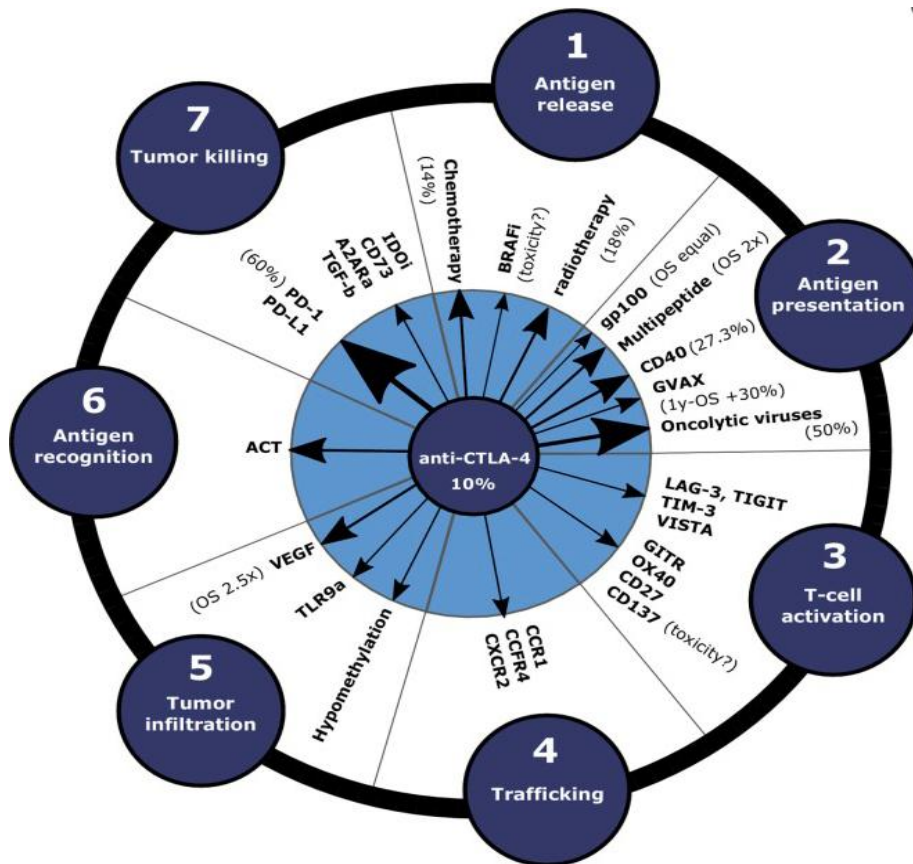


Figure 1-14: Clinical efficacy of various immune stimulating therapies when used in combination with CTLA-4 blockade

The efficacy of anti-CTLA-4 therapies has been tested in combination with primary therapies targeting different categories of cancer-immune interactions. Arrow size indicates the increase in immune response compared to anti-CTLA-4 monotherapy. Image taken from Swart et al., 2016.

Application of combined immunotherapies are primarily limited by the increased risk of adverse events. Grade 4 (life threatening) adverse events have been reported in 54% of patients receiving more than one immunotherapy treatment in combination, while only 20% of monotherapy patients experienced similar reactions (Weber et al., 2016). Although progress continues to be made in understanding of disease pathology and resultantly immunotherapy, these figures illustrate the need for improvement in treatment specificity. Recent studies investigating the efficacy of Ipilimumab treatment in metastatic melanoma following primary treatment with anti-PD1 therapy induced responses in patients who previously failed monotherapy. However, addition of Ipilimumab was also

associated with high-grade, immune-related adverse events in this cohort, with three patients (7%) developing severe pneumonitis, which resulted in the death of one patient (Zhang et al., 2017). In this case, the immunological profile induced by PD-1 pre-treatment was hypothesised to promote T cells with increased autoimmune potential, reacting aggressively against non-target host cells (Swart et al., 2016).

Encouragingly, complete regression and long-term survival has been observed in patients treated with checkpoint blockade combinations, particularly in melanoma. However, there is still a large proportion of patients who remain non-responsive to checkpoint blockade. This field has developed rapidly since Ipilimumab was approved as the first checkpoint inhibitor by the FDA for treatment of melanoma in 2011. Considering the infancy of this field, many of the mechanisms of tumour resistance to checkpoint blockade therapies have yet to be elucidated.

1.4.2 Adoptive cell transfer

Adoptive cell transfer (ACT) involves engineering cells from individual patients to recognise and attack tumours, particularly in late-stage cancers with limited alternative treatments. ACT currently involves a complex procedure in which patients undergo lymphodepletion by chemotherapy or whole-body radiation prior to ACT infusion. This phase is followed by a high dose IL-2 infusion (which is associated with high toxicity) to aid survival of the transplanted T cells, before re-introducing the patient's lymphocytes (Muranski & Restifo., 2009).

Pioneering work in ACT by Dr Steven Rosenberg at the National Cancer Institute (NCI) involving three small cohort clinical trials in melanoma clearly demonstrated efficacy of ACT-modified TILs. Infused cells were able to induce anti-tumour effects when infused as a single-dose treatment alongside adjuvant IL-2 therapy to support T cell survival post infusion. The first trial investigated the half-life and immunologic effects of IL-2 derived from Jurkat cells in a 12-patient cohort (Lotze et al., 1985). Further studies by the same group showed objective remissions in 3 of 6 patients lasting up to several months without additional treatments, establishing that IL-2 therapy could mediate the regression of established cancer in select patients (Lotze et al., 1986). Of the 93 melanoma patients participating in the initial three trials, 20 demonstrated complete response. A further 19 subjects demonstrated tumour-free survival five years after treatment; this result is

especially encouraging as this cohort had previously been non-responsive to alternative immunotherapies. Therefore, ACT therapy has been deemed one of the most important treatments in melanoma prior to checkpoint blockade. However, it is crucial to reiterate the unique context of the immune environment in melanoma, which may not provide a representative model for the general tumour response to this treatment.

Infusion of an exponential number of T cells in the manner required for ACT has demonstrated a risk of inducing severe immune responses, including cytokine storm, with potentially fatal outcomes. As a result, clinical trials have investigated the efficacy of ACT using lower doses of enriched T cells, and reduced lymphodepletion (Hunder et al., 2008). Recent clinical trials investigating low dose IFN- α for pre-treatment sensitisation combined with low dose IL-2 post treatment resulted in persistence of infused T cells with substantially diminished toxicity (Khammari et al., 2009). Considering the lifetime of the TIL and potential for clonal expansion, as well as the individual clone's recognition of allogeneic or autologous tumour cells, has optimised cell selection for ACT. As such, it is now recognised that TIL populations with longer telomeres persist in circulation for an extended duration and therefore, require lower initial infusion numbers, reducing associated side effects (Zhou et al., 2005). Continued continued developments in the field alongside improved understanding of molecular mechanisms in immunology continues to enhance specificity of ACT treatments.

1.4.3 Chimeric Antigen Receptor T cell therapy

One form of ACT, Chimeric Antigen Receptor T cell technology (CART), was first investigated in the 1980's by Zelig Eshhar's group at the Weizmann Institute of Science in Israel (Gross et al., 1989). This research group replaced the TCR variable region with variable regions derived from monoclonal antibodies, providing a mechanism to induce tumour specificity into ACT. In this procedure, target cells are removed from the donor, genetically engineered to express specific targeting moieties, expanded *ex vivo*, and then re-introduced into the patient. Re-infused cells contain the extracellular, transmembrane, and cytoplasmic domains of normal TCRs with binding specificity of engineered antibodies. These cells also produced functional activation of T cells including proliferation, interleukin production, and target cell lysis (Gross et al., 1989).

CART is now in clinical practise and CART therapies have specific advantages over transgenic expression of the T cell receptor. For example, CARs recognise antigen independently of human leukocyte antigen (HLA) and typically interact with larger epitopes than the small peptides recognised by transgenic methods, thereby reducing the risk of cross reactivity. CAR-T cells overcome some of the limitations of conventional T cell therapies, which may be rendered ineffective by resistance mechanisms of the tumour, and have demonstrated benefits in tumours where downregulation of MHC is induced to evade immune detection.

The structural components of CART receptors are outlined in figure 1.15, adapted from Dotti et al., 2014. Since initial design in the 1980s (Gross et al., 1989), CART structures have been modified to improve specificity by attaching co-stimulatory signalling domains required for effective activation. The function and specificity of CART therapies is defined by the affinity of the single chain variable fragment (scFv) and location of the target epitope on the antigen; for example, CART therapies which bound an epitope on CD22 at the B cell plasma membrane have demonstrated greater efficacy in leukaemia than CAR-T therapies targeted against an epitope located deep in the cell membrane (Fry et al., 2018). The hinge region connects the antigen binding ectodomain to the transmembrane domain and changes in length and flexibility of the hinge also affect CART function (Dotti et al., 2014). The transmembrane domain is commonly derived from CD3, CD4, CD8, or CD28; the choice of protein for the base of a CART affects stability at the cell surface while the endodomains communicate activating and co-stimulatory signals to the T cells (Dotti et al., 2014). Proteins including CD28 and LFA-1 have been incorporated into the receptor endodomain, helping to initiate robust T cell priming with specificity to avoid T cell anergy through incomplete activation signalling.

Most recently, the fourth generation of CART therapies have incorporated transgenic gene vectors for inducible cytokine production, referred to as T cell redirected universal cytokine killing “TRUCK” CARTs. Synchronous delivery of cytokine therapy alongside targeted CART therapy provides a bimodal attack, with potential for therapeutic benefit since not all cells within a tumour may express the target epitope for CART therapy due to phenotypic heterogeneity in an established tumour. Inducible expression of stimulatory cytokines such as IL-2 and IL-12 could potentiate the benefit of CART efficacy in this patient cohort by inducing non-

specific immune activation in the microenvironment. To date, CART trials incorporating TRUCK moieties have demonstrated the most effective increase in tumour immunity, as IL-12 exerts direct pleiotropic effects on stromal and infiltrating immune cells, as well as recruiting additional immune cells to the area (Pegram et al., 2012; Klingemann, 2014).

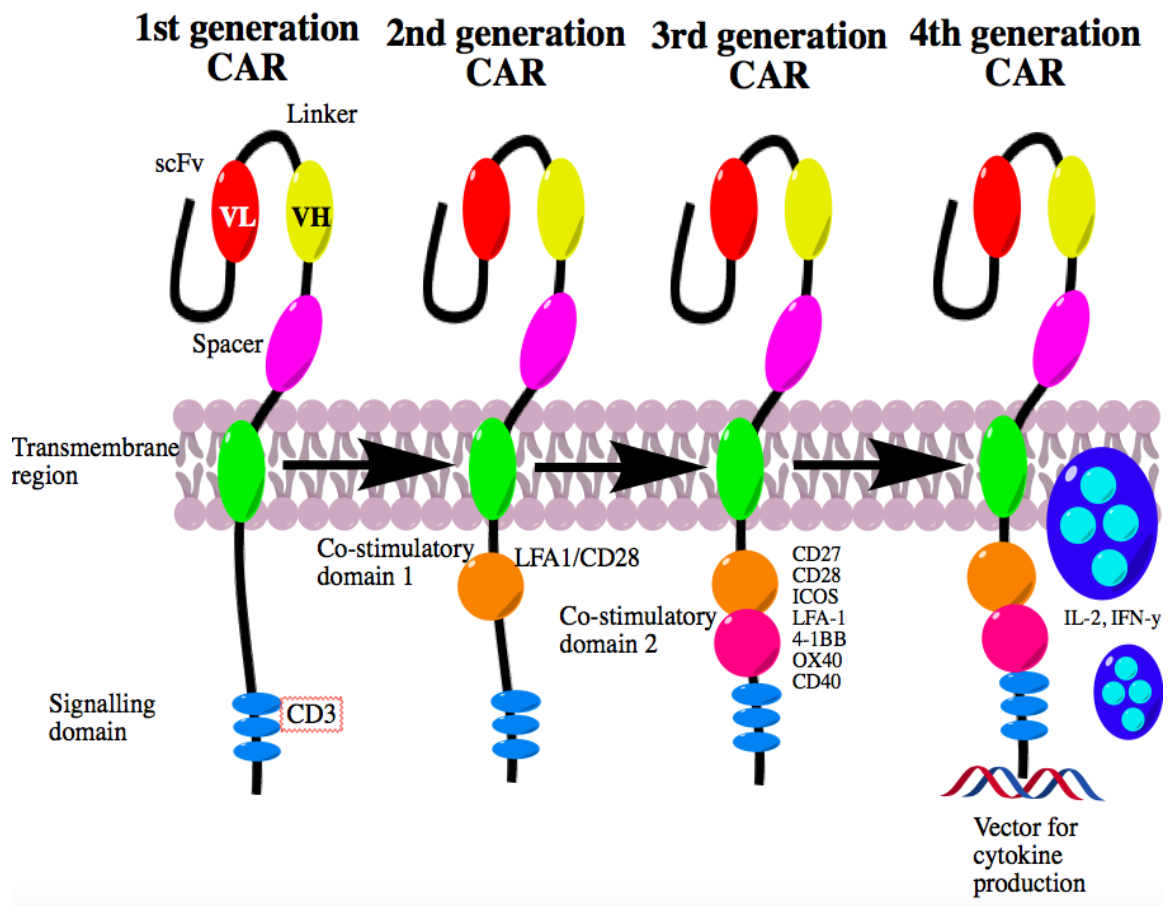


Figure 1-15: Evolution of CART structural components across four generations

CART therapy efficacy depends on a suitable epitope location, scFv affinity, hinge and transmembrane domains, and a number of signalling domains. Novel CART engineering has continued to optimise therapies by incorporating new elements to enhance efficacy. Authors own, adapted from Dotti et al., 2014 & Hartmann et al., 2017.

CART therapy has demonstrated potential for treatment of haematological malignancies including Non-Hodgkin Lymphoma (NHL), Chronic Lymphocytic Leukaemia (CLL), and, with notable success, Acute Lymphoblastic Leukemia (ALL). As the B cell lineage marker CD19 is expressed throughout development, targeting this protein allows targeting of nearly all B cell malignancies including those present in CLL, ALL, and NHL (Rosenberg et al., 2008). Encouraging early trial results have demonstrated high *in vivo* expansion of CD19-targeted T cells,

designated CTL019 in relapsed or refractory ALL. One notable trial yielded six-month survival rates of 67% and continued remissions up to 24 months in some cases (Maude et al., 2015). More recent studies have shown a 90% treatment success rate in childhood ALL (Maude et al., 2015), which highlights the continued progress in this area. While childhood survival now demonstrates encouraging trends, survival for adult ALL remains between 30-40%, while relapse in ALL still presents a challenging target in both age groups. As of 2017, Kymriah by Novartis (Tisagenlecleucel) became the first FDA approved CART therapy, targeting CD19 in young patients (under 25 years) with refractory or relapsed B cell precursor ALL (Novartis Press Release, 2017). At time of writing, an additional 76 active clinical trials related to CART therapies are ongoing (ClinicalTrials.gov, 2018).

The success of CD19 targeted CART therapies is hampered by cell-mediated adverse events which continue to pose a concern in CART therapy, the most common of which is cytokine release syndrome (CRS) (Breslin, 2007). A phase 1 clinical trial of TGN1412 (an anti-CD28 monoclonal antibody) tested on six healthy male volunteers reported severe induction of CRS within 90 minutes of a single intravenous dose of the drug. All six volunteers experienced symptoms of a systemic inflammatory response, which progressed within twelve hours post infusion, by which point all patients became critically ill. After 24 hours, severe depletion of lymphocytes and monocytes occurred, requiring patients to be transferred to intensive care for cardiopulmonary support (Suntharalingam et al., 2006). While no fatalities occurred, this incident led to two patients requiring intensive care for 8 and 18 days, respectively. Severity of CRS in response to CART depends on the therapeutic agents used for lymphodepletion and is more severe in patients with high tumour burdens (Lee et al., 2014), and is a key consideration in new treatment developments.

1.4.4 DCs as immunotherapeutic agents

Targeting DCs provides an attractive route for immunotherapy since DCs are highly efficient at generating robust immune responses, demonstrating the unique ability to prime naive T cells into functional effectors (Banchereau & Steinman., 1998; Palucka & Banchereau., 2012). Stimulating DCs to produce an antigen-specific immune response holds the potential to produce novel therapies with high specificity, reducing the toxicities observed in several of the immunotherapies

discussed in earlier sections (see chapters 1.4.1-1.4.3), which result from off-target activation. Despite this unique potential, DCs are maintained in the immature state by immunosuppressive factors in the tumour microenvironment, where tolerogenic populations with reduced antigen capture and presentation capacities are observed (Pinzon-Charry et al., 2005). Re-stimulating suppressed DCs in the tumour holds the potential to initiate a robust immune response.

DCs drew rapid attention as potential immunotherapy agents following the FDA approval of the autologous cellular immunotherapy Sipuleucel-T for the treatment of asymptomatic or minimally symptomatic metastatic castration-resistant prostate cancer in 2010 (Kantoff et al., 2010). Sipuleucel-T is a personalised, targeted therapy in which DCs are incubated with a recombinant fusion protein containing prostatic acid phosphatase (PAP) antigen to target cells to the tumour, alongside GM-CSF that aids DC maturation. Late-stage randomised trials observed an overall extended survival of at least 4.1 months and reduced risk of death by 22.5% compared to the control group. These trials demonstrated the potential of DC immunotherapies, and were closely followed by the approval of the monoclonal antibody Ipilimumab (targeted against CTLA-4) for melanoma the following year in 2011. Interestingly, the mechanism of action of Sipuleucel-T is still presently not clearly defined, and to date, a consensus has not been agreed on the most appropriate maturation stimulus to generate DCs with strong immunostimulatory capacities.

Early work investigating the role of the CD54 receptor in immunity demonstrated a complimentary role between CD54 and CD40R in B cell activation. Cross-linking of CD54 receptors on Th1 cells induced upregulation of MHCII and CD54 on target B cells, which was abolished in the presence of blocking antibodies for CD54 (Poudier & Owens, 1994). Recent research investigating the mechanism of action of Sipuleucel T identified that antigen presentation and T cell priming induced by this cellular agent was exclusively attributed to APC subsets expressing CD54, indicating that the receptor could represent a “surrogate” marker for DC activation (Sheikh & Jones., 2008). As such, the receptor is currently being investigated as a potential target for antibody based treatment of metastatic melanoma, after Fc-engineered human CD54 antibodies recently demonstrated the ability to inhibit tumour growth in animal models (Klausz et al., 2017).

Multiple combinations of maturation stimuli have been tested, including cytokine stimulation and treatments engaging TLR agonists (Sabado & Bhardwaj, 2010). Maturation of DCs is required to initiate an effective anti-tumour response since mature DCs show enhanced expression of costimulatory molecules and increased production of cytokines and chemokines, while immature DCs fail to prime antigen specific T cells (Scarlett et al., 2009). Distinct DC vaccine loading approaches have been tested in clinical trials including loading of DCs with peptides, proteins, and tumour lysates; mRNA transfection, delivery of DNA and the use of viral vectors, which have translated to clinical trials at various stages.

During the last decade, novel methods have been developed for loading DCs with TAAs aimed to generate tumour specific anti-cancer vaccines. DCs loaded with cell lysates from various tumour types have been investigated in phase I/II trials and have shown encouraging results regarding safety, while a select few also demonstrated efficacy against target cells (Galluzzi et al., 2012). One case which particularly emphasises the potential of DC in immunotherapy vaccinated melanoma patients with allogeneic cell lysates derived from melanoma cell lines, which induced a hypersensitivity type reaction in 50% of patients and correlated with increased survival and reduced disease progression (Lopez., 2009). TAAs presented either as full-length proteins or short peptides have induced protective and therapeutic anti-cancer immune responses in other pilot studies, where three of four follicular B cell lymphoma patients showed improved clinical outcomes (Baskar et al., 2004). In this case, two patients showed complete regression while the third responder showed partial regression (Hsu et al., 2013). The accumulation of successful early trials such as these demonstrates the potential for DC targeted cancer therapies.

Upon detection of foreign antigen, DCs require secondary activation stimuli in the form of CD40 ligand (CD40L) expressed by CD4⁺ T cells to prime effector CD8⁺ T cells. CD40L interacts with CD40R expressed by DCs, which in turn upregulate CD40R at the DC surface (Murphy et al., 2012). The binding and upregulation of CD40R signals DCs to enhance surface expression of co-stimulatory receptors and cytokines involved in T cell priming, leading to subsequent activation of CD8⁺ T cells (van Kooten & Banchereau., 2000). The interaction between CD40R and CD40L can also increase antigenic cross-presentation mediated by DCs (Elgueta et al., 2009). The importance of this interaction has been demonstrated as blocking CD40R-

CD40L interactions prevents primary and memory T cell responses in either CD4⁺ or CD8⁺ subsets. This process results in a subdued immune response to allogenic peptides in which clonal proliferation is aborted and replaced by induction of regulatory T cell functions (Quezada et al., 2008).

1.5 CD40R anatomy and physiology

The CD40R/CD40L system plays an important role in the pathophysiology of diseases such as respiratory diseases, autoimmune disorders, atherothrombosis, and cancers. Efficient immunotherapies are likely to benefit from the ability to stimulate both the innate and adaptive arms of the immune system. A key molecule involved in bridging innate and adaptive immunity is CD40R, which is expressed on APCs including subsets of monocytes, macrophages, and DCs. CD40R is also expressed by B cells and platelets in addition to some non-haematopoietic cell types including fibroblasts, endothelial cells, and smooth muscle cells. Further, ligation of CD40R *in vivo* has the potential to elicit an array of outcomes from activation of APCs to induction of tumour cell death (Ridge et al., 1998). CD40R is therefore of particular interest in tumour immunotherapy due to its ability to form a central link between both arms of immunity.

A member of the tumour necrosis factor receptor (TNFR) superfamily, CD40R has diverse functions in mammalian biology, including the maintenance and survival of leukocytes. CD40R mediated signalling is essential to induce the priming environment required for effective T cell-DC crosstalk. The CD40L has similar widespread expression but is primarily detected on the surface of antigen-primed T helper cells. CD40R binding to its natural ligand induces DC activation and enhances immune response.

1.5.1 Receptor structure and ligand interaction

The CD40R is a 48-kDa type1 transmembrane protein of 193 amino acid residues which are highly conserved between species. CD40R is widely expressed among immune cell subsets with an extracellular domain containing 22 cysteine residues that are conserved between members of the TNFR family. The CD40L is a 30.6kDa transmembrane receptor on the surface of CD4⁺ helper cells. Crystallographic studies of the CD40R-CD40L interaction determined the extracellular structure and binding of CD40R using the pre-existing crystallographic structure of CD40L as a

search probe (An et al., 2011; Karpusas et al., 1995). These works revealed that the CD40L trimer is bound by two CD40R receptor molecules, while the third interaction site remains empty in both crystallographic and molar ratio studies (An et al., 2011), suggesting that at least bivalent binding is required for physiological interactions between CD40R and CD40L.

The TNF family of receptors are known to contain several cysteine rich domains (CRD) forming elongated ladder structures, including CD40R which displays three CRD in the extracellular domain. This structure has been determined by sequence alignment, which revealed that each CRD is composed of two structural molecules critically stabilised by 1-3 disulphide bridges (Naismith & Sprang, 1998). The extracellular domain of CD40R binds in a crevice between CD40L subunit pairs, interacting with both in an asymmetric manner determined by unequal binding of CRD to CD40L subunits. Binding is strongly influenced by hydrophilic and charge interactions, with only one third of interaction interfaces occurring at nonpolar amino acids. The charge interaction between CD40R and CD40L displays complementarity as CD40R contains predominantly negatively charged residues, while CD40L is oppositely positive. Mutations at charged residues lead to inhibited binding and activity; individual residue substitutions can prevent receptor-ligand interactions, illustrating that CD40R-CD40L complementarity is predominantly influenced by charge interactions (Singh et al., 1998).

Mutagenesis experiments investigating the essential structure sequences in CD40R binding and activation have identified a critical loop structure required for DC activation *via* CD40R. Mutations affecting CD40L binding occur in residues involved in direct contact with the CD40R, including E129G and T134W, while mutations in non-contact residues such as S132W do not affect the binding affinity in comparison to wild-type mice (An et al., 2011).

1.5.2 Downstream responses of CD40R binding

Upon ligand binding, the CD40R can initiate downstream signalling *via* TNF Receptor Associated Factor (TRAF) pathways or through Janus Kinase/Signal Transducers and Activators of Transcription (JAK/STAT) pathways, as outlined in figure 1.16. JAK/STAT in mammals is the principle signalling pathway for cytokine and growth factor stimulation. Activation of the TRAF and JAK/STAT pathways *via* CD40R engagement results in proliferation, differentiation, migration, and

apoptosis, which contributes to the critical regulation of homeostasis of immune functioning (Hanissian & Geha., 1997).

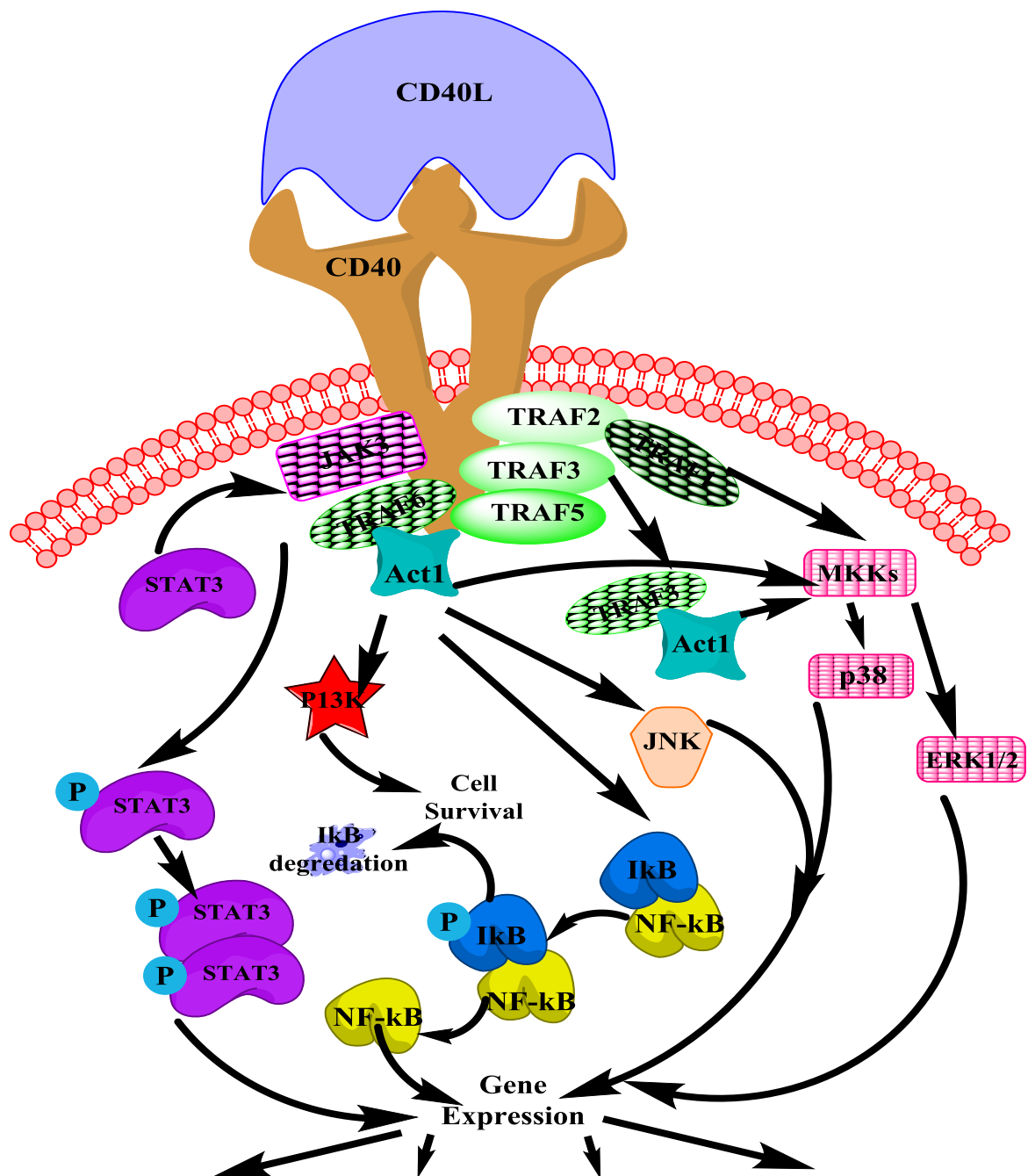


Figure 1-16: Downstream signalling pathways induced upon CD40R stimulation at the DC surface by CD40L expressed on CD4⁺ T cells

A schematic diagram illustrating the key signalling pathways stimulated by CD40R-ligand binding. Ligand binding to CD40R induces receptor dimerisation and the recruitment of adapter molecules that couple the CD40R to downstream mediators.

It has been suggested that JAK3 and STAT3/5 are activated in response to CD40R signalling as activation of JAK3 is observed following CD40R ligation. This relationship is indicated by immunoprecipitation of phosphorylated proteins from cell lysates following cross-linked CD40R activation treatments, which were

observed early in activation and peaked at 10 minutes post-activation. STAT5 undergoes dimerisation upon phosphorylation to begin translocation to the nucleus where it initiates transcription through promoters. This cycle all occurs within 15 minutes of treatment with CD40R targeted antibodies (Hanissian & Geha., 1997).

The cytoplasmic domain of CD40R also contains binding sites for TRAFs, consisting of six structurally similar proteins initially identified as adaptor proteins, coupling the TNF family to signalling pathways. The TRAF family of receptors function as a signalling cascade which, upon binding the cytoplasmic domain of cellular receptors, recruit secondary TRAF proteins (Bradley & Pober., 2001). TRAF1, 2, 3, 5, and 6 have been demonstrated to mediate induction of intracellular signalling pathways including nuclear factor kappa-light-chain-enhancer of activated B cells (NF- κ B), the mitogen associated pathway kinase (MAPK) p38, and C-Jun N-terminal kinase (JNK) (Bradley & Pober., 2001). Ligand binding to CD40R induces conformational changes in receptor structure, which exposes the cytoplasmic docking site for TRAF2 at the canonical motif, driving rapid signalling through adapter and kinase proteins. Induction of TRAF2 signalling induces degradation of TRAF3, initiating downstream pathways.

The independent roles of TRAF proteins in DC maturation and signalling have been identified through mutation of distinct binding sites for TRAF2, 3, 5, and 6 in the cytoplasmic domain of CD40R. TRAF6 functions as a key inducer of CD80/86 expression (Kobayashi et al., 2004), and blockade of CD40R interaction with TRAF2, 3, and 6 showed that TRAF6 blockade alone was sufficient to inhibit pro-inflammatory responses including IL12-p40 production in non-haematopoietic cells (Portillo et al., 2015), while a separate study suggested disruption of TRAF6 uniquely decreased p39/JNK signalling and abrogated IL-12 production in response to CD40L stimulation (Mackey et al., 2003). In the latter study, disruptions in TRAF2, 3, and 5 did not affect downstream signalling pathways to the same extent, suggesting a predominant role of TRAF6 in the production of DC activation following CD40R ligation. Induction of p38 leads to transcription of pro-inflammatory cytokine synthesis, while JNK signalling promotes transcription of genes promoting apoptosis. Signalling by these MAPK pathways is affected by environmental stimuli to integrate signals involved in proliferation, differentiation, survival, and migration.

The impact of CD40R signalling in DC maturation has been extensively studied in the past two decades. Early work confirmed that CD40R ligation was essential for complete DC maturation inducing functional IL-12 secretion (Kelsall et al., 1996), while later groups have suggested that CD40R signalling plays a role in desensitising DC to antigen; populations stimulated by CD40R produced much higher levels of IL-10 compared to those stimulated by cytokine exposure, which resulted in reduced INF- γ production in corresponding CD8⁺ T cells (Tuettenberg et al., 2010).

1.5.3 Current immunotherapies targeting CD40R in the clinic

CD40R signalling can induce primary and memory cytotoxic T cells in conditions which are otherwise tolerogenic. This finding was reported following observations that the adoptive transfer of FITC-OVA specific T cells promoted lytic activity and clonal expansion in the presence of agonistic CD40R antibodies in an adoptive T cell transfer system, which was abolished in the presence of CD40R blocking antibodies. FITC-OVA is a poorly immunogenic, soluble antigen which alone does not elicit cytotoxicity and the induction of memory T cells. This illustrates the significance of CD40R signalling, which induced a response to an otherwise tolerogenic stimulus (Lefrancois et al., 2000). Many approaches aiming to activate the CD40R pathway have been investigated in the current literature, including recombinant CD40L, CD40L gene therapy, and agonistic antibodies.

1.5.4 Agonistic antibodies for CD40R

Pre-clinical models investigating CD40R targeted antibodies have produced exceptional therapeutic success in murine models of CD40⁺ B cell lymphoma showing 80-100% eradication and immunity to subsequent re-challenge in a CD8⁺-dependent manner (French et al., 1999). The encouraging early success of targeting the CD40R pathway for immune stimulation *in vitro* and in animal models prompted high anticipation for the efficacy of therapies targeting the CD40R pathway in the clinic. An outline of monoclonal antibodies targeted towards CD40R which have been investigated in cancer immunotherapy clinical trials is provided in table 1.2.

Table 1-2: Monoclonal antibody therapies targeting the CD40 pathway in cancer immunotherapy in clinical trials

Antibody Name	Binding Affinity	Particulars	Development Phase	Primary Reference
ADC-1013	High; 1x10 ⁻¹¹ M	Binding is stable under acidic conditions to pH5.4, activity is dependent on FcR binding and cross linking	Phase I: Solid tumours (various)	Mangsbo et al., 2015
APX005M	High; 1x10 ⁻¹¹ M	Activity is enhanced in response to CD40R cross linking	Phase II trials: Gastric, oesophageal, NSCLC, pancreatic cancer Phase I trials: Malignant melanoma, NSCLC, pancreatic cancer, brain cancer, glioma	Zhang et al., 2014
CDX-1140	Moderate; 8.13x10 ⁰ M	Reduces but does not block CD40L binding, potential for CD40L synergy at local level.	Phase 1; Advanced solid tumours (various); lymphoma.	He et al., 2016.
CP-870,893	Low; 4x10 ⁻¹⁰ M	Humanised IgG2 agnostic antibody, mediates CD40L binding in the absence of cross linking	Discontinued treatment: Mesothelioma, pancreatic cancer, solid tumours (various)	Bedian et al., 2008
Chi/Lob 7/4	Moderate 2x10 ⁻¹⁰ M	Chimeric IgG1 antibody, requires CD40R cross linking for CD40R stimulation in APCs	Phase I: Solid tumours (various)	Johnson et al., 2010
Dacetuzumab	Low; 1x10 ⁻⁹ M	Weak stimulator of B cell proliferation; potent anti-proliferative and pro-apoptotic properties against B cell lymphoma; enhances CD40L binding	Phase I: Solid tumours (various)	Burington et al., 2011; Francisco et al., 2000
Lucatumumab	Low; 5x10 ⁻⁵ M	Does not display agonistic activity; induces tumour cell death <i>via</i> antibody dependent opsonisation and cell-mediated cytotoxicity	Discontinued treatment: Follicular lymphoma, lipoma, multiple myeloma	Chowdhury et al., 2013
SEA-CD40	Low; 5x10 ⁻⁹ M	Derived from dacetuzumab with improved KD resulting from enhanced FcγRIIIa binding	Phase I: Lipoma, solid tumours (various)	Gardai et al., 2015
Selicrelumab	Moderate; 2x10 ⁻¹⁰ M	Human IgG2 agnostic antibody, development in combination with combination therapies (Tecentriq).	Phase 1: Pancreatic cancer (USA only); various advanced local/metastatic tumours adverse to standard therapy.	Mompo & Gonzalez-Fernandez, 2018.

Table of CD40 antibody therapies currently in clinical trials. Antibodies listed are universally humanised IgG1 structure unless otherwise stated. Data sourced from ClinicalTrials.gov website (December 2017), details compiled from primary references (cited in table). Authors own.

The antibody therapies targeting the CD40 pathway listed in table 1.2 display distinctly separate mechanisms of action that vary from strong agonistic antibodies such as CP-870,893 which induces T cell immunity in highly aggressive, immunosuppressive cancers such as pancreatic ductal adenocarcinoma (Vonderheide et al., 2013) to antagonistic therapies including lucatumumab, the mechanism of action of which is poorly characterised. The examples presented illustrate the diverse potential of CD40R therapies in various pathological contexts. The reason for such a broad spectrum of responses is still not satisfactorily characterised and it is therefore critical that understanding of the mechanisms by which CD40R therapies induce their effects is investigated further.

The administration of CD40R agonists as cancer immunotherapies has largely been limited in the clinic by toxicities associated with antibody therapies. For example, treatment with CP-870,893 induces CRS in the majority of patients, a condition characterized by fever, rigors, and chills, in addition to thromboembolic events in some patients. Separate research groups have also reported infusion reactions, non-infectious inflammatory eye disorders and immune mediated liver damage, anaemia, thrombocytopenia, and pleural effusion (Medina-Echeverz et al., 2014; Remer et al., 2017).

1.5.5 CD40R targeted therapies in adjuvant and combination therapies

Therapies targeting CD40R present potential for synergistic effects when delivered with chemotherapeutic agents, which has demonstrated effective tumour regressions in clinical trials. This complementarity occurs as the destruction of tumour cells by chemotherapies releases TAAs, while CD40R agonists prime DCs to process the newly available antigen (Boon et al., 1994; Bruno et al., 2017). The amount of antigenic constituents released from the tumour cell by chemotherapy has been suggested to be akin to that produced by conventional viral vaccinations, providing readily available tumour derived targets for DCs primed by co-stimulation *via* CD40R exposure.

In pre-clinical studies, co-administration of CD40R antibodies with gemcitabine in the Pdx1-Cre; K-Ras⁺/LSLG12D; p53R172H/⁺ (KPC) mouse model has induced rapid regression in tumours, mediated by T cell-independent infiltration of macrophages (Beatty et al., 2011). Administration of CP-870,893 in combination with gemcitabine in pancreatic cancer has demonstrated objective tumour regressions in

approximately 20% of patients (Vonderheide et al., 2013). These findings demonstrate significant improvement considering the standard response rate with gemcitabine alone as standard of care therapy for pancreatic cancer is only 5%. CD-870,893 combination with gemcitabine also demonstrated lower toxicity levels than immune checkpoint inhibitor therapies or CD-870,893 delivered as monotherapy (Beatty et al., 2011), providing rationale for the delivery of CD40R agonists as adjuvants in cancer therapy. The existing literature therefore demonstrates the diverse roles of CD40R interaction in immune function, which is likely to be affected by the sequence and duration of exposure to antigen and effector cells.

Combinations of CD40R antibodies with TLR3 agonists have also induced maturation in tumour infiltrating DCs and stimulated resultant DC-antigen complexes to migrate to the lymph node in ovarian cancer models (Scarlett et al., 2009). One study concluded that tumour regressions following CD40R activation of DCs occurred from macrophage stimulation, suggesting a more prevalent role for innate immune components in CD40R adjuvant therapies than was previously expected (Beatty et al., 2011).

The existing literature surrounding therapeutic agents targeting CD40R therefore shows clear potential for these agents in the setting of immunotherapy, but has also demonstrated a niche for improved antibody specificity in order to reduce toxicity and obtain optimal clinical benefits. As such, strategies to ameliorate toxicity associated with CD40R agonists are under investigation. One approach involves direct administration in the tumour, and peritumoural injection of an agonistic CD40R antibody in an immunogenic model of bladder cancer was found to effectively elicit a tumour-specific T cell response at reduced doses compared to interleukin injection (Sandin et al., 2014). In addition, the group demonstrated that bio-distribution of CD40R antibodies to the liver was decreased following local administration compared to systemic injection (Sandin et al., 2014).

As interest in CD40-based immunotherapies continues to grow, many outstanding questions remain regarding the delivery of CD40R therapies, including dose, route of administration, formulation, and whether they should be used alone or as adjuvant therapies.

1.6 Parameters influencing CD40R stimulation

Multivalent interactions are common in the context of immunity, as it is often necessary to engage multiple receptors to reach an activation threshold, including antibody mediated activation of the complement system (Xu and Shaw; 2016; Skehej & Wiley., 2000). This activation requires clustering of cell surface immunoglobulin G (IgG) molecules to activate C1 through increased binding affinity, functioning as a regulatory mechanism against non-specific immunity (Burton., 1985). Other examples of multivalent interactions in immunity include transmigration of immunological cells to sites of inflammation (Luster et al., 2005) and T cell priming (Stone & Stern., 2006), where multivalent interactions improve the strength and specificity of cellular interactions. Multivalent interactions play a role in the induction of effective T cell stimulation, where antigen binding to TCR can either activate or inhibit T cells depending on the avidity of antigen and ligand interactions (Schneck et al., 2001).

A defining characteristic of the antibody response is its polyclonality; antibodies have the capacity to target an array of antigens through almost unlimited diversification of their fragment antigen-binding (F(ab)) domains by somatic recombination and mutation. However, it is becoming increasingly clear that polyclonality of the antibody response also applies to the effector molecules engaged by the antibody-antigen complex (Stuart et al., 2005). Specific interactions of the IgG fragment constant (Fc) domain with receptors expressed by leukocyte cell types result in pleiotropic effector functions for IgG, including the clearance of pathogens and toxins, lysis and removal of infected or malignant cells and modulation of the innate and adaptive branches of immunity to shape an immune response (Bournazos et al., 2009). It has been suggested that CD40R signalling *via* targeting antibodies requires presentation by fragment crystallisable gamma receptor (FcγR)-expressing cells to present a sufficient number of ligands capable of inducing CD40R clustering, resulting in effective signal transduction (Banchereau et al., 1998). As such, interactions between FcR and TFNR stimulation has been studied intensely over the past decade.

FcRs for IgG were identified over 35 years ago, in early studies which determined the properties of cells binding IgG antibodies was independent of the F(ab) region of the antibody and required only Fc interactions (Berken & Benacerraf, 1966).

Activation of CTLs by APCs which did not directly express the antigen was coined cross-priming by M. Bevan in the 1970s, and the process of APCs internalizing and presenting antigens to CD8⁺ T cells *via* MHCI rather than MHCII was coined cross-presentation (Bevan, 1976). Considering that DCs cross present antigen more effectively than any other APC (Théry & Amigorena, 2001), antigen internalization by DCs presents a critical step in cross-priming. On the basis of the two dominant conformational states that the Fc domain can adopt, two structurally distinct classes of FcRs which bind IgG are now recognized. Type I FcRs belong to the immunoglobulin receptor superfamily and comprise canonical Fcγ receptors, including the activating receptors FcγRI, FcγRIIa, FcγRIIc, FcγRIIIa and FcγRIIIb and the inhibitory receptor FcγRIIb. Each of these receptors binds Fc domains in the open conformation near the hinge-proximal region⁶ in a complex with a stoichiometry of 1:1 (receptor/antibody) (Bournazos et al., 2009). On the other hand, type II FcRs, represented by the family of C-type lectin receptors (including CD209 and CD23) specifically bind Fc domains in the closed conformation at the interface of the constant domains of the immunoglobulin heavy chains in a complex with a stoichiometry of 2:1 (receptor/antibody) (Sondermann et al., 2013).

Engagement of activating type I FcRs results in uptake of immune complexes by endocytosis or phagocytosis (Stuart et al., 2005). DCs internalize immune complexes through type I FcR-mediated pathways, and DCs and subsequent T cell priming are substantially enhanced when antigen is internalized as an immune complex through activating type I FcR compared to lectin or mannose receptor induced activation pathways (Yin et al., 2016). The process of cross-presentation to CD8⁺ T cells is significantly increased by targeting *in vitro* antigens to FcγR receptors of IgG molecules, a reaction which is specific to multivalent antigen interactions (Théry & Amigorena, 2001). Within this receptor class, FcγRII (CD32) and FcγRIII (CD16) bind monomeric IgG inefficiently, but demonstrate high affinity binding for immune complexes. FcγRI (CD64), in contrast, binds monomeric IgG with high affinity, but does not signal unless IgGs are cross-linked by their specific polymeric ligands (Amigorena, 2002). Given the ability of individual receptor types to initiate distinct effector and immunomodulatory pathways, the conformational diversity of the IgG Fc domain serves as a general strategy for shifting receptor specificity to actively effect different immunological outcomes.

FcγRIIb is involved in abrogating the signalling and function delivered from other receptors; archetypally those initiated by activatory FcγR and the B cell receptor (BCR) for antigen. Engagement of these receptors on DCs negatively regulates antigen presentation, and DCs derived from FcγRIIb-deficient mice are more potent inducers of T cell activation both *in vitro* and *in vivo* (Kalergis & Ravetch., 2002). The activation of type I FcγR pathways on other immune subsets including granulocytes, monocytes and macrophages triggers degradation of antigens in lysosomal compartments and production of proinflammatory chemokines and cytokines (Mantovani et al., 2004). This activity, as with DCs, is in turn moderated by FcγRIIb. Controlling the ability of antibodies to engage activating *versus* inhibitory type I FcRs on effector cells (either through genetic deletion of the inhibitory FcγRIIb or engineering of the IgG Fc to selectively engage activating type I FcRs) modulates the cytotoxic potential of antitumour antibodies for enhanced ADCC and tumour clearance (Smith et al., 2012). A striking example of antitumour antibody therapies engaging type I FcRs is Obinutuzumab, an FDA approved monoclonal antibody to CD20. Obinutuzumab demonstrates enhanced binding of FcγRIIIa, and in trials has extended CLL patient survival by one year, relative to the survival afforded by Rituximab, an unmodified CD20-specific antibody (Goede et al., 2014). Immunomodulatory mAb directed against various members of the TNFR superfamily show the ability of FcγRIIb to regulate immune responses and immunotherapy (White et al., 2014). In summary, numerous agonistic and antitumour antibodies require interactions with activating type I FcRs on innate effector cells to effectively mediate their therapeutic effects on malignant cells. Several Fc engineering approaches discovered recently can augment the anti-tumour or immunostimulatory activities of TNFR antibodies by enhancing their agonistic activities and/or effector functions. In a study investigating the impact of FcR binding on OX40 activation, mutations facilitated enhanced binding to FcγRIIb and thus increased FcγRIIb cross-linking mediated agonist activity (Zhang et al., 2016). However, both mutations abrogated the binding to FcγRIIIa and thus decreased the antibody-dependent cellular cytotoxicity. In contrast, mutations which promote antibody multimerization upon receptor binding facilitated anti-OX40 antibody agonism by promoting the clustering of OX40 receptors without the dependence on FcγRIIb cross-linking (White et al., 2014; Zhang et al., 2016). The antibody-dependent cellular cytotoxicity and complement-dependent cytotoxicity

of the mutated anti-OX40 antibody were affected by the choice of IgG subtypes, suggesting Fc engineering can guide the design of engineered antibodies to OX40 and other TNFR members (Zhang et al., 2016).

Studies in mice have shown that anti-CD40R antibodies require engagement of FcR to activate antitumour immunity (Wilson et al., 2011). Crosslinking of the activation receptor FcγRIIa domain results in tyrosine phosphorylation of ITAM containing receptors including the TCR (Weiss & Littman, 1994), and targeting antigens to FcγR promotes cross-presentation by several orders of magnitude in mouse bone marrow-derived DCs (Amigorena, 2002). This holds relevance to the current study, as analysis of a number of immunomodulatory antibodies have revealed a critical yet variable role for Fcγ receptors. It has generally been accepted that agonistic anti-CD40R mAbs require cross-linking by FcγRIIb, which has been shown in treatment of systematic treatment of lymphoma, where therapeutic efficacy is lost when using murine IgG2a mAbs without FcγRIIb crosslinking (White et al., 2014).

However, further data showed that co-administration of anti-CD40R antibodies with TLR3 agonists recovered activation outputs through FcR cross linking (White et al., 2014). Clinical trials investigating CP-870,893, a fully human IgG2 molecule, have shown the antibody does not require FcR crosslinking for potency (Richman & Vonderheide, 2014). CP-870,893 is a fully human CD40 selective agonist mAb that was designed with minimal Fc receptor binding activity based on its IgG2 isotype (Vonderheide et al., 2007), which demonstrated the first-in-human study of a CD40 agonist in patients with advanced cancer. The most common adverse event with CP-870,893 treatment was grade 1-2 cytokine release syndrome manifested by chills, fever and rigors within minutes to hours after infusion, although overall the antibody demonstrated relative safety as well as promising clinical activity with a response rate of 14% (Beatty et al., 2016). IgG2 has a low affinity for Fc receptors, and is presumably minimally crosslinked *via* FcR-Fc interactions *in vivo* (Vonderheide & Glennie, 2013). APC activation by CP-870,893 occurs independently of FcR crosslinking *in vitro*, as no statistically significant difference was observed in the ability of F(ab)² CP-870,893 vs. intact CP-870,893 to stimulate B cells in culture. Artificial crosslinking by an FcγRII expressing cell line or anti-Fc antibodies did not enhance B cell activation (Richman & Vonderheide., 2014). In contrast, an anti-mouse CD40 agonist mAb, FGK45 (rat IgG2a), does require FcR crosslinking, a

necessary component both *in vitro* and *in vivo* to induce APC activation (White et al., 2013). It has thus been suggested that the requirement for Fc engagement is specific to murine models of CD40R engagement.

Since the first clinical report of an anti-CD40R agonist, several other agonists have now been developed and are under active investigation in patients with advanced malignancies. These second generation CD40R agonists have been engineered with an IgG1 Fc domain to facilitate enhanced Fc γ R interactions based on findings that increased Fc binding affinity to Fc γ RIIB enhances the potency of a CD40R agonist in murine models through crosslinking (White et al., 2011). These agonists contrast CP-870,893, which has an IgG2 Fc domain, and thus a low binding affinity to human Fc γ Rs. Recently, antibodies with an IgG2 Fc domain have been found to mediate Fc γ R-independent agonistic activity that is conferred by the unique hinge properties of this isotype (Beatty et al., 2016). However, for CP-870,893, the Fc domain of the antibody and FcR crosslinking are not required for CD40R stimulation (Richman & Vonderheide, 2014). The conflicting mechanisms shown here are demonstrated by three crosslinking-dependent anti-CD40R mAbs (FGK45, 1C10, 3/23), which all compete with CD40L for binding to CD40R on the surface of murine B cells. In contrast, CP-870,893, recognizes an epitope independent of the human CD40L binding site (Richman & Vonderheide., 2014). These results suggest that the fine specificity of epitope binding is key in dictating the agonist potency of CD40R mAb, and that targeting the right epitope can bypass the need for FcR-mediated crosslinking.

Using a mouse model humanized for its Fc γ Rs and CD40R, Dahan et al (2016) demonstrated that Fc γ RIIB engagement is essential for the activity of human anti-CD40R therapies, but that engagement of the activating Fc γ RIIA inhibits this activity. By engineering Fc variants with selective enhanced binding to Fc γ RIIB, but not to Fc γ RIIA, the group showed significantly improved antitumor immunity, supporting the suggestion that IgG1 is more potent for CD40R stimulation than IgG2, and that this activity is Fc γ R dependent (Dahan et al., 2016). These findings highlight the need to optimise the Fc domain for this class of therapeutic antibodies by using appropriate preclinical models that accurately reflect the affinities and cellular expression of human Fc γ R. Alternative strategies beyond Fc engineering for enhancing anti-CD40R efficacy, such as chemical crosslinking of CD40R antibodies,

have also shown Fc-independent activity in murine models, as can be found in the recent review by Beatty et al (2016).

Other parameters influencing crosslinking include the valency of stimulating molecules; monovalent constructs have proven insufficient to reach the threshold for activation and cross priming, and appear to prevent the immune system from forming a durable anti-tumour response (Wilson et al., 2011). This is supported by studies which demonstrated that although presentation of a single CD40L was not able to stimulate activation outputs in B cells, molecules expressing trimeric CD40L exhibited significantly greater stimulatory capacity (Haswell et al., 2001).

This observation was supported by data which showed presentation of hexameric soluble CD40L effectively reinstated IL-12 and TNF- α production in Sézary syndrome, an advanced form of T cell lymphoma characterised by impaired cellular immunity and deficiency in the production of these cytokines resulting from defective CD40L expression (French et al., 2005). Other groups have demonstrated that NF κ B signalling in the cytosol requires engagement of dimeric CD40L, while monomeric CD40L alone is not sufficient to generate a signal through CD40R (Werneburg et al., 2001). Taken together, these observations show optimised CD40R signalling can be induced by multivalent stimulation, suggesting multivalent interactions induce functionally robust CD40R-based immunotherapies. Understanding the fundamental nature of multivalent interactions in stimulating immunity is therefore likely to be valuable in designing effective platforms with improved specificity and stimulation of CD40R for effective DC activation.

1.7 Limitations of antibody therapies for CD40 stimulation

Toxicities associated with CD40R-antibodies for cancer immunotherapy have been a major limitation in the progression of this field, as is eluded to in the discussion of the role of FcRs in mediating antibody toxicity. Anti-CD40R therapies are commonly accompanied by increased thrombocytopenia and transaminitis, which are the primary drivers of the dose limiting toxicities. Such adverse events are observed as a result of non-specific antibody induced activation of CD40R expressed on platelets, a result of off-target activation (Knorr et al., 2018). Enhancing the Fc binding capacities of anti-CD40R antibodies showed improved *in vivo* activity compared to equivalent antibodies without Fc modulation which are currently under clinical observation (Dahan et al., 2016). Toxicity tests dosing a murine model expressing

humanised CD40R and FcγRs with increasing concentrations of Fc-enhanced antibody showed that transaminitis and hepatotoxicity continued to produce dose-limiting adverse reactions when delivered at doses greater than 0.125mg/kg, despite Fc-enhancement. This was attributed to the high levels of FcγRIIB expression on liver sinusoids, considering the liver acts as a primary site of immune complex clearance (Stegner et al., 2016). In summary, this demonstrated that although Fc enhancement improved antitumour activity of agonistic anti-CD40R, this negatively affected mechanism-based liver toxicities. This finding supports the rational design of immune modulating antibodies and the prospect for antibody engineering to improve tumour specificity, however does not yet provide a solution for the obstacle of off-target receptor binding. Monotherapy treatment with anti-CD40R antibodies alone have shown success in select mouse models such as MC38, where tumours show enhanced activation of T cells in the local microenvironment and draining lymph nodes. In comparison, B16 melanoma models are less immunogenic and failed to respond to single-agent therapy, potentially because of the increased expression of PD-L1 in this tumour (Juneja et al., 2017), meaning combination therapy may be required to overcome immunosuppression in this case. In order to overcome issues with toxicity, recent research has focused on optimising the dose and delivery regimen to minimise toxicity and optimise antitumour efficacy, for example through intra-tumoural injection of antibody therapies in accessible tumours (Knorr et al., 2018).

The work described by Knorr et al. was conducted using a macaque model of nonhuman primate immune activation. Despite this being the preferred preclinical toxicology model for immunological studies, previous research of agonistic antibodies has shown human Fc receptors show suboptimal crosslinking of Fc receptors in this model, resulting in underestimation of toxicity and efficacy of Fc-engineered antibodies (Hussain et al., 2015). Unaffiliated research groups have further established an alternative method of CD40R activation independent of Fc interaction. The human IgG2 antibody CDX-1140 was recently described to induce activation through F(ab')₂ fragment binding, and interacts at a distinct epitope away from the CD40L binding site, which when used in combination with CD40L at low-doses (below the threshold capable of producing a clinical response individually) produced potent effects on B cell proliferation and IL-12 production by DCs, as well as activation markers on the cell surface, with no indication of

cytokine storm events (Vitale et al., 2018). Such data demonstrates the potential for CD40 targeted therapies to induce specific immune stimulation, focusing on unique binding characteristics and rational antibody design.

Recent data describing the injection of an ECM-binding variant of anti-CD40R also showed higher anti-tumour activity compared to the unmodified form, with lower adverse events. Improved tolerance was achieved by conjugating the antibody to a placenta growth factor derived peptide, which allowed interaction with the tumour stroma and acted as a depot for antibody retention, which improved efficacy and safety profiles upon intra-tumoural injection. Pre-clinical results from this work showed lower levels of anti-CD40R were detected in systemic circulation, while cytokine release syndrome and liver toxicity were also reduced, alongside improved T cell infiltration and prolonged survival overall (Ishihara et al., 2018). Cumulatively, work by groups such as Ishihara, Vitale, and Knorre amongst others demonstrate the ongoing efforts to optimise CD40 Rantibody therapies, in order to overcome the dose limiting adverse events of antibody therapies, and provide more effective treatment modalities.

1.8 Advantages and limitations of peptide based immunotherapies

Immuno-oncology commonly utilises monoclonal antibodies or protein-based scaffolds that bind with high affinity to cancer cells and can generate an immune response. Peptides are recognized for being highly selective and efficacious and, at the same time, relatively safe and well tolerated. Consequently, there is an increased interest in peptides in pharmaceutical research and development. Peptides can bind with high affinity to cancer cells, with an intermediate size range between antibodies and small molecules. Peptides have received attention as defined-antigen cancer vaccines, as small peptides specific for antigenic epitopes of the tumour provide one of the most immunogenic vaccine treatments. This approach has shown particular success in melanoma, where CTL responses have been observed with a large number of peptide epitopes (Novellino et al., 2005). They are also synthetically accessible and therefore easily modified to optimize their stability, binding affinity and selectivity, however existing peptide vaccines have had limited success at inducing clinical tumor regressions, despite reliable induction of T cell responses in the majority of patients (Slingluff et al., 2007). A summary of the advantages and limitations of peptide vaccines against TAAs is

provided in table 1.3 below, adapted from Slingluff, 2011 and Fosgerau & Hoffmann, 2015.

Table 1-3: Limitations of peptide based therapies

Advantages	Limitations
<ul style="list-style-type: none">• Readily synthesized and purified at low cost	<ul style="list-style-type: none">• Class I MHC restriction limits relevance of individual peptides to certain HLA types.
<ul style="list-style-type: none">• Stable in many storage conditions; allows off-the-shelf reagent composition	<ul style="list-style-type: none">• Short peptides may bind directly to MHC on non-professional APC*, which may induce tolerance
<ul style="list-style-type: none">• Predictable metabolism means shorter time to market	<ul style="list-style-type: none">• Rapidly degraded by serum/tissue peptidases
<ul style="list-style-type: none">• High selectivity and potency	<ul style="list-style-type: none">• Low membrane permeability
<ul style="list-style-type: none">• Very effective at inducing CD8⁺ or CD4⁺ T cell responses <i>in vivo</i> in humans	<ul style="list-style-type: none">• Patients have variable repertoires for melanoma antigens: a peptide vaccine may have to include a large number of peptides to be useful across a wide range of patients.
<ul style="list-style-type: none">• Enables direct monitoring of T cell responses induced by the vaccine.	<ul style="list-style-type: none">• Immune responses may be transient and/or of low magnitude
<ul style="list-style-type: none">• Safety in many studies, good efficacy and tolerability	<ul style="list-style-type: none">• Limited effectiveness as monotherapies due to narrow spectrum of immune response
<ul style="list-style-type: none">• Using defined epitopes avoids use of uncharacterized antigens that may have nontherapeutic autoimmune activity	<ul style="list-style-type: none">• Chemically and physically unstable; prone to hydrolysis and oxidation
<ul style="list-style-type: none">• Repeated booster vaccines feasible	<ul style="list-style-type: none">• Tendency for aggregation
	<ul style="list-style-type: none">• Short half-life with fast elimination

Table 1.3 summarises the advantages and limitations of peptide treatments in immunotherapy. Combined data from reviews by Slingluff, 2011 and Fosgerau & Hoffmann, 2015.

Currently, most peptide drugs are administered by the parenteral route and approximately 75% are given as injectable doses. However, alternative

administration forms are gaining increasing traction, including oral, intranasal, and transdermal delivery routes, according to the respective technology developments (Transparency Market Research., 2012). One example of an alternative administration route evaluated for application in peptide delivery is the transbuccal delivery *via* the conjugation of peptides to gold nanoparticles (Midatech). Although peptide therapies can provide highly potent signal transduction molecules with potent physiological effects, they are generally characterised by a relatively short circulating plasma half-life. Rational peptide design methods including alanine scan analysis and amino acid substitution aim to overcome these limitations (Manning et al., 2010). Rational design can start with a known crystal structure of the peptide giving the secondary and tertiary structure. Then, input from various analyses, such as alanine substitutions (Ala-scan) followed by small focused libraries determines the structure-activity relationship of a given peptide. A second important aspect in peptide design is to improve the physicochemical properties of peptides, for example by reducing the tendency to form aggregates through disulphide bridge formations or to improve water solubility (Hamley., 2007).

In general, natural peptides have a relatively short circulating plasma half-life; the vast majority are cleared in under 10 hours (Mathur et al., 2016; PEPLife database), compared to antibody therapies which can persist in circulation for up to 20 days with modification (Mathur et al., 2016). Thus, several techniques have been investigated to extend half-life of peptide therapies to a comparable duration. The first line approach is to limit the enzymatic degradation of the peptide through identification of possible molecular cleavage sites followed by substitution of the relevant amino acids (Manning et al., 2010). Alternative methods include binding peptides to the circulating protein albumin as a vehicle, which has in some cases obtained half-life extensions which require treatment to be made less frequent, in some cases up to once weekly (Knudsen, 2010). The leuprolide acetate implant (Viadur™) for the palliative treatment of advanced prostate cancer allows automatic dose regulation of 120 micrograms of leuprolide acetate per day over 12 months (Fowler et al., 2000), demonstrating the new and innovative approaches being developed to optimise the delivery of peptides as medicines.

A popular direction for peptide therapies over the past decade has been to directly target components of the immune system for activation, rather than targeting

epitopes on the tumour cell surface. DCs have been deemed nature's adjuvant because of their high potency to initiate and support innate and adaptive immune responses (Banchereau & Steinman, 1998). DCs have been investigated as cancer vaccines by two means; by directly targeting antigens to DC receptors *in vivo* and by *ex vivo* generation of antigen-loaded DCs, with particular interest in *ex vivo* methods of DC maturation *via* utilisation of co-stimulatory receptor engagement (Palucka & Banchereau, 2012).

DCs are easily manipulated before administration, can be loaded with any tumor antigen and are optimally activated with a plethora of adjuvants. Nevertheless, *ex vivo* production of DCs is labor intensive and costly, and limited numbers thereof are often available. Thus, an attractive alternative is to specifically target DCs *in vivo*, i.e., load them with the appropriate tumor antigens and activate them to produce pro-inflammatory cytokines. Although in this case, less control over quality and magnitude of induced responses is offered, proof of efficacy was robustly demonstrated when Sipuleucel-T became the first DC based anti-cancer vaccine achieving FDA approval for prostate cancer in 2010 (Anassi & Ndefo, 2011). More recent work in the arena of DC vaccinations in phase II/III trials has demonstrated improved clinical outcomes in patients with melanoma, glioma and glioblastoma, ovarian cancer, renal cell carcinoma and multiple myeloma (Ophir et al., 2016).

1.9 Drug delivery *via* nanoparticles

Based on studies outlining the importance of multivalent interactions in immunity, novel scaffolds continue to be investigated. Nanoparticles present a potential scaffold for multivalent therapies, and offer potential to optimise delivery of peptide therapies, overcoming traditional shortcomings by improving receptor affinity and providing a stable scaffold. The use of nanoparticles is one of the most novel and rapidly progressing strategies for delivering therapeutic molecules in cancer therapy. Nanoparticles provide a particularly attractive system for drug delivery due to the plasticity of their characteristics. Namely, surface charge and size can be manipulated to optimise circulation time in the blood stream and uptake or evasion of local immune components (Moghimi et al., 2001). Research is currently focused on implementing nanoparticle therapy to address several common limitations in conventional chemotherapeutic delivery systems, including nonspecific bio-

distribution, lack of water solubility, poor oral bioavailability, and low therapeutic treatment indices (Yeshchenko et al., 2013).

Non-specific bio-distribution of traditional chemotherapeutic agents leads to undesirable effects on non-cancerous cells and limits the dose obtainable within the tumour, which results in sub-optimal treatments and excessive toxicities (Larsen et al., 2000). Molecularly targeted therapies are emerging as an approach to overcome this lack of specificity, which could potentially be overcome through the attachment of targeting molecules to nanoparticles as multivalent scaffolds.

1.9.1 Nanoparticulate therapies targeting CD40R on DCs

Recent studies have also investigated the potential of nanoparticle therapies in the activation of DC. One notable study investigated PGLA-based nanoparticles carrying model antigen and TLR3 molecules. PGLA nanoparticles were targeted to either CD40R, CD11c, or the DC marker DC-205 *via* monoclonal antibodies conjugated to the nanoparticle surface. Results indicated that nanoparticle binding and internalisation lead to similar induction of DC maturation *in vitro*; however, CD40R targeting resulted in slightly more efficient CD8⁺ T cell responses *in vivo* (Cruz et al., 2014). DCs incubated with PGLA nanoparticles for 72 hours and analysed by MTS display average viability of 80%, while activation with LPS over the same period shows much lower cell survival (20% after 72 hours), which declined sharply after 24-hour incubation (Song et al., 2015; Schwiebs et al., 2016). This suggests nanoparticle therapies may be particularly well tolerated by DCs *in vivo* compared to alternative activating treatments. Related work using a CD40R-targeted adenoviral tumour vaccine induced stronger anti-tumour responses when compared with non-targeted vectors, lending support to the theory that DC-expressed CD40R is a suitable target for the delivery of various particulate vaccines (Hangalapura et al., 2011).

Current research investigating the combined use of monoclonal CD40R antibodies with nanoparticle therapy has produced mixed results. As highlighted previously, CD40R therapies alone may have significant potential for tumour therapeutics, if the limitations in antibody associated toxicity can be overcome. Therefore, a logical hypothesis could be that coupling monoclonal antibodies to nanoparticles could improve cross-linking of CD40R on the DC surface and thereby enhancing the therapeutic effects of targeting agents. However, recent data have not supported

this claim. For example, a recent study demonstrated no enhancement in DC activation when monoclonal antibodies were coupled to PGLA nanoparticles compared to the free-circulating antibody, although specific DC targeting *in vivo* following subcutaneous injection was greatly improved by CD40R targeting (Rosalia et al., 2015). Earlier research had demonstrated that CD40R antibodies immobilised on the surface of 4.5µm carboxylated polystyrene particles induced upregulation of CD86 and CD83 (Kempf et al., 2003), an alternative marker of functional DC maturation which plays a role in antigen presentation which is able to directly bind T cells, inducing activation (Ju et al., 2016). Small CD40R coated particles also demonstrated detectable but low-level, production of IL-12 (Kempf et al., 2003). Recent studies investigating the influence of multivalent presentation of a CD40R-targeting antibody on the surface of silicon nanoparticles demonstrated that multivalent presentation induced activation of B cells characterised by upregulation of surface receptors CD86 and MHCII, while equivalent doses of free peptide fail to demonstrate an activation response (Gu et al., 2012). Inconsistent outputs demonstrated by CD40R-targeted antibody coupled nanoparticles illustrates potential for DC targeting which requires further optimisation. Delivery of CD40R targeted therapies stand to benefit significantly from delivery platforms based on nanoparticle conjugation, as these systems could help avoid some of the treatment limiting side effects induced by traditional CD40L delivery systems, which have been highlighted in section 1.5.4.

1.10 Gold nanoparticles for targeted immunotherapy

Merging well-established principles of immunology with novel approaches in biotechnology such as nanoparticle development could enable more effective and safer immunotherapies. Within this arena, gold nanoparticles are attracting interest as potential biological adjuvants as a result of several unique characteristics. Initially, gold nanoparticles provide an attractive scaffold for small molecule conjugation as biological molecules can be attached to the particles by more than one method. The most well-utilised method is to conjugate the functional groups of biological molecules (such as thiols, common in peptides and proteins) to the surface of the gold nanoparticle, as the molecules can take the place of stabilizer molecules when they are added directly to gold nanoparticles in solution and bind

to the surface by formation of gold–sulphur bonds. Thiol-modified ligands are frequently used for this purpose (Kim et al., 2018).

Although gold nanoparticles are composed of an inert material, biocompatibility issues have to be considered as cells exposed to gold nanoparticles will incorporate the particles (similar to nanoparticles of other materials). Gold nanoparticles are regarded as biocompatible, and initial studies have shown positive biocompatibility assessments so far, in direct opposition to treatments involving cadmium-based nanoparticles which show much lower tolerance (Kumar et al., 2017). In immunological studies, human monocyte-derived DC samples displayed no change in morphology, viability, or cytokine profile, along with a low level increase in surface receptor expression following treatment with gold nanoparticles 6nm in diameter for 6 and 24 hours (Bastus et al., 2009). More recent research investigated the impact of 10nm gold nanoparticles on murine-derived DC cultures *via* apoptosis, activation markers, and cytokine secretion over periods ranging from 4 hours to 48 hours, and showed no detrimental cell responses, supporting the biocompatibility for DC targeting (Bastus et al., 2011).

As well as presenting improved biocompatibility profiles compared to existing methods, the metallic properties of gold nanoparticles also make them a very effective contrast agent which can be visualized through various different techniques (Kim et al., 2018). The most prominent detection techniques are based on the interaction between the nanoparticles and light, whereby gold strongly absorbs and scatter visible light to produce the so-called surface plasmon (Yeshchenko et al., 2013). Besides the interaction with visible light, interaction with both electron waves and X-rays can also be used for visualization of gold nanoparticles, particularly in medical applications. The high atomic weight of gold provides excellent contrast in transmission electron microscopy (TEM), and scatters X-rays efficiently, providing effective contrast agents for X-ray imaging (Huang et al., 2010).

Gold nanoparticles are also being actively investigated in combination with radiotherapy regimens due to their high atomic number (high-Z), which has been shown to increase the dose deposited during photon irradiation (Letchman et al., 2013). One of the first studies demonstrating this effect was carried out using gold nanoparticles in mice, where a one-year survival rate of 86% was demonstrated in

the cohort treated with a combination of radiotherapy and 1.9nm nanoparticles, *versus* only 20% survival radiotherapy alone (Hainfield et al., 2004). Similarly dramatic results corroborated this work as administration of larger (11nm) gold nanoparticles were administered to mice with imminently lethal intracerebral gliomas; animals receiving gold nanoparticle injection 15 hours prior to irradiation demonstrated 50% survival after 1 year, whereas all mice receiving radiotherapy alone died within 5 months (Hainfield et al., 2013). Such work succinctly illustrates the potential for incorporating gold nanoparticles to improve the efficacy of existing cancer therapies.

In summary, this means that in addition to their potential as imaging contrast agents and proven efficacy as adjuvants in radiotherapy, gold nanoparticles provide the added appeal that they can be readily modified due to their surface plasticity, presenting an ideal platform for bimodal cancer therapeutics.

1.11 Aims of the current study

DCs are a key initiator of the cellular immune response and CD40R has a prominent role in optimising activation of these cells in response to antigen exposure. Activation stimulates priming of T cells, determining the adaptive cellular immune response toward a tumour. Because effector lymphocyte functions requires DC activation, and considering DC activation is suboptimal in the immature phenotype of DCs in the tumour, DC based immunotherapies aim to relieve immunosuppression by providing activating stimuli to induce antigen specific T cell priming. The ultimate goal therein is to stimulate a tumour specific cytotoxic T cell response from the DC activation level.

Previous work has developed a synthetic peptide ligand for the CD40R, isolated *via* selective phage display (Yu et al., 2013). This ligand specifically targets the CD40R and has the potential to regulate DC activation and signalling. This research aims to produce an optimised sequence of the CD40R-targeting peptide which could be conjugated to multivalent scaffolds to induce DC activation through CD40R binding.

The first step is to modify the original cyclical peptide sequence (NP31) to ensure linear presentation, and to then confirm specific binding capacity for the linear sequence to the CD40R. The next goal is to determine whether presentation of the

linear peptide on different multivalent scaffolds enhances binding avidity toward CD40R and whether enhanced binding could affect DC activation parameters. To investigate the efficacy of multivalent presentation, two platforms for multivalent presentation are investigated. The first platform uses streptavidin as a semi-flexible scaffold to present ~4 peptides per molecule. The second platform investigates gold nanoparticles as a rigid support with the potential to present ~2000 peptides per targeting molecule.

The pivotal role of DCs in immunotherapy is the ability to prime naïve T cells into functional effector types. The secondary aim of this work is therefore to assess the capacity of CD40R stimulated DCs to induce T cell priming following a period of co-culture incubation. To this end, T cell lines will be grown alongside DCs in a single dish, with additional activating treatments. In the current work, T cell priming is detected through changes in T cell cytokine signalling profiles, while also determining the biocompatibility of CD40R targeting constructs. These “Primed” T cells are introduced to allogenic tumour cells in culture to investigate whether primed cells can induce cytotoxicity. Ultimately, this two-step method of analysis aims to demonstrate a proof of principle concept that robust immune activation can be induced by targeting the CD40R on immature DCs, capable of stimulating effector cell outputs.

Chapter 2: Methods and materials

2.1 List of suppliers

Unless stated otherwise, general chemicals were supplied by Thermo Fisher Scientific and cell culture reagents were supplied by Sarstedt.

Becton Dickinson, New Jersey, USA

Beckman Coulter, High Wycombe, United Kingdom

Bio-Rad, Hercules, California, USA

Dako, Glostrup, Denmark

ECACC, Porton Down, Salisbury, UK

Ilford Imaging UK Limited, Cheshire, UK

Invitrogen, Paisley, UK

Millipore, Watford, Hertfordshire, UK

New England Biolabs, Hertfordshire, UK

Peptide Synthetics (Peptide Protein Research) Hampshire, UK

Pierce Biotechnology, Cramlington, UK

Sigma, Sigma-Aldrich Company Ltd, Poole, Dorset, UK

Statagene, Amsterdam, the Netherlands

2.2 General suppliers

Unless specified otherwise, reagents used for this research were analytical grade and solutes were dissolved in H₂O (MilliQ Type 1 UltraPure water).

2.3 Glassware and consumables

Unless specified otherwise, glassware was purchased from Fisher Scientific and cell culture pipettes, and plastics were purchased from Sarstedt. All pipettes were manufactured by Gilson.

2.4 Reagents

β-mercaptoethanol, Fisher Scientific

30% w/w Acrylamide/bis-acrylamide solution, Sigma Aldrich

4-(2-hydroxyethyl)-1-piperazineethanesulfonic acid (HEPES) salt, Thermo Fisher Scientific

Bovine serum albumin (Fraction V, Heat shock treated), Sigma Aldrich

Ammonium persulfate (APS), Sigma Aldrich

Bicinchoninic acid assay kit, Thermo Fisher Scientific

Biotinylated 200kDa protein ladder detection pack, Cell Signalling

Bromophenol blue, Sigma Aldrich

Calcium chloride (CaCl₂), Sigma Aldrich

Cyanine (Cy5) Labelled Streptavidin, AbD

Cytofix 1% Paraformaldehyde (PFA) Solution, BD

Coomassie Brilliant Blue (R-250) Stain, Thermo Fisher Scientific

Concanavalin A, Sigma Aldrich

Dimethyl sulfoxide (DMSO), Sigma Aldrich

Dulbecco's Modified Eagle's Medium (DMEM), Gibco

Dylight 488 Amine Reactive Dyes, Thermo Fisher Scientific Scientific

Dylight 488 Labelled Streptavidin, Thermo Fisher Scientific Scientific

ChemiLuminescence Enhancer and Peroxide Solutions, Thermo Fisher Scientific

Ethylenediaminetetraacetic acid (EDTA), Thermo Fisher Scientific

Foetal Calf Serum, Gibco Invitrogen

Glycerol, Sigma Aldrich

Glucose, Sigma Aldrich

Goat Anti-CD40 Horseradish Peroxidase Conjugated Antibody, Cell Signalling

Interleukin 2 (IL-2) ELISA Murine Antibodies, R&D Systems
Interleukin 10 (IL-10) ELISA Murine Antibodies, R&D Systems
Interleukin 12p70 (IL-12) ELISA Murine Antibodies, R&D Systems
Iscove's Modified Dulbecco's Medium (IMDM), Gibco
L-glutamine, Fisher Scientific
Lipopolysaccharide (LPS), Sigma Aldrich
Magnesium Chloride (MgCl₂), Sigma Aldrich
Novex Sharp Pre-Stained Protein Ladder, Invitrogen
N,N,N',N'- Tetramethylethylenediamine (TEMED), Sigma Aldrich
Penicillin Streptomycin, Lonza
Phosphate Buffered Saline, Fisher Scientific
Phycoerythrin (PE) labelled Antibodies for FACS, BioLegend
Pierce Protease and Phosphatase Inhibitor Mini Tablets, Thermo Fisher Scientific
Polyvinylidene fluoride (PVDF) transfer membrane, GE Healthcare
Rabbit Anti-Goat Biotinylated IgG Antibody, R&D Systems
Rabbit Anti-HSP Biotinylated IgG Antibody, Cell Signalling
Sodium Chloride (NaCl), Sigma Aldrich
Sodium Dodecyl Sulfate (SDS), Thermo Fisher Scientific
Sodium pyruvate, Thermo Fisher Scientific
Streptavidin Dynabeads M270, Invitrogen
Tris(2-carboxyethyl)phosphine (TCEP), Sigma Aldrich
Tris base, Sigma Aldrich
Tris HCl, Sigma Aldrich
Triton X-100, Thermo Fisher Scientific
Tris Base, Thermo Fisher Scientific
Trypan Blue, Gibco
TrypLE Express, Gibco
Tween-20, Thermo Fisher Scientific

2.5 Generating a CD40-targeting peptide

2.5.1 MTP40 Characterisation by Peptide Synthetics

The linear CD40R-targeting peptide (MTP40) used in this research was developed based on original work by Yu et al., 2013, who investigated the binding affinity of the NP31 peptide to target inflamed joints based on specificity for CD40R in a murine model for rheumatoid arthritis. The original peptide sequence (CMSYEGSWRKWVMWGGCG) was identified by selective phage display.

The original CD40R-targeting peptide sequence was modified as illustrated in figure 2.1. The primary cysteine residue in the sequence was replaced by alanine to prevent intra-peptide disulphide bond formation between the two cysteine residues, which could result in a cyclic structure of the peptide sequence. This decision was made considering that linear MTP40 structures would protrude more prominently from the multivalent scaffold in a flexible manner, increasing the likelihood of target interactions and simultaneous binding of multiple target receptors. The lysine residue was also substituted from the original sequence for alanine, which allowed for MTP40 labelling with NHS esters at a 1:1 ratio. In summary, the particle used in the current work was based on an existing sequence which had been shown to effectively bind CD40R. Modifications to this sequence were intended to improve the affinity and avidity of the peptide for receptor binding.

The MTP40 was synthesised externally by Peptide Protein Research (Hampshire, UK). This modified version of the targeting sequence was designated as a **Monomeric-Targeting Peptide for the CD40R of DCs (MTP40)**. During synthesis, MTP40 was purified and eluted in acetonitrile and H₂O containing 0.1% ammonium hydroxide. MTP40 was supplied as 1mg lyophilised aliquots, while analysis was conducted by the supplier using high pressure liquid chromatography (HPLC) with an injection volume of 20µl into a 100Å 4.6 x 50mm column using a flow rate of 1.5ml/min over a 10%-90% acetonitrile gradient in 8 minutes at 60°C.

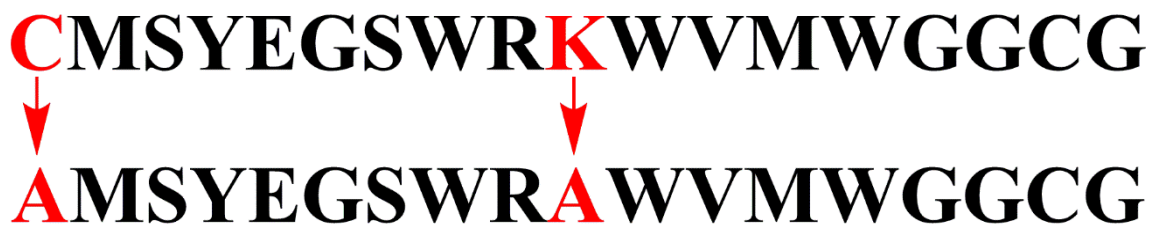


Figure 2-1: Modifications to the original CD40R targeting peptide sequence (NP31) produced by Yu et al., 2013

The original sequence by Yu et al was modified to produce **Monomeric Targeted Peptide for CD40R (MTP40)** by substituting cysteine and lysine residues at positions 1 and 10, respectively (theoretical pI 6.04).

2.5.2 Mass spectrometry analysis of MTP40

API electrospray (API-ES) is useful for analysing samples which may acquire multiple charges, such as proteins, peptides, and oligonucleotides. API-ES is commonly used for rapid confirmation of the molecular weight (MW) of synthetic peptides. The process involves three basic phases. First, the liquid sample is passed through a nebulizing needle at ground potential. The sample then passes through a cylindrical electrode at high potential, resulting in a strong electrical field from the difference in potential. This phase charges the surface of the liquid to form a spray of charged droplets. Next, the charged droplets are attracted toward the capillary sampling orifice; here, the counter flow of heated nitrogen gas dries and shrinks the droplets and removes uncharged materials. As the droplets reduce, they approach a point where the electrostatic forces exceed the cohesive forces until the analyte ions become desorbed into the gas phase. The gas-phase ions can pass through the capillary sampling orifice into the low-pressure region of the ion source and the mass analyser. Mass spectrometry data for MTP40 samples were provided by the manufacturer.

2.5.3 MTP40 re-solubilisation

Two batches of MTP40 peptide were purchased to investigate the impact of multivalent presentation on different scaffold backbones. The first was the unmodified sequence as described in 2.5.1 above. This sequence was additionally purchased with a biotin molecule attached to the amine terminus. Solubilisation of the lyophilised MTP40 was conducted as described in the following sections (2.5.3.1 and 2.5.3.2).

2.5.3.1 MTP40 solubilisation (Method A)

Lyophilised MTP40 1mg aliquots were solubilised directly in H₂O to produce a working concentration of 1mg/ml. The addition of H₂O produced a cloudy solution so 1M sodium hydroxide (NaOH) was added in 1µl increments to gradually adjust the solution to pH11 and remove protein precipitates. Once the solution cleared, Trisaminomethane (Tris)(2-carboxyethyl)phosphine (TCEP) solution (0.5M in H₂O) was added in 0.2µl increments to return the solution to pH8 while simultaneously reducing intermolecular disulphide bonds.

2.5.3.2 Biotinylated MTP40 solubilisation (Method B)

Lyophilised 1mg aliquots of biotinylated MTP40 were solubilised directly into 200µl dimethyl sulphoxide (DMSO) and diluted to a working concentration of 1mg/ml with phosphate buffered saline (PBS). NaOH 1M solution was added in 1µl increments until pH11 was reached to remove MTP40 precipitates. TCEP solution (0.5M in PBS) was then added in 0.2µl increments until the solution returned to pH8.

2.5.4 Peptide concentration measurements

The concentration of MTP40 and BiotMTP40 in solution were determined based on absorbance values at 280nm and calculated based on Beer's Law (Equation 1). This calculation relies on the molar absorption coefficient of a peptide or protein resulting from the composition of aromatic amino acids tryptophan (W), tyrosine (Y), and cysteine (C) (Equation 2). Absorbance at 280nm was measured by spectrophotometer (Evo300 UV Vis, Thermo Fisher Scientific) blanked with the corresponding solvent used for peptide solubilisation. Absorbance values were based on the average of three measurements per run multiplied by the dilution factor of the sample and divided by the molar extinction coefficient (ϵ 18470) of the peptide.

$$A_{\lambda} = \epsilon c L$$

Equation 1: Beer's Law

A_{λ} = absorbance at specified wavelength; ϵ = the extinction coefficient of the protein of interest; c = concentration; L = length of light path.

$$\epsilon = (nW \times 5500) + (nY \times 1490) + (nC \times 125)$$

Equation 2: Peptide extinction coefficient

The calculation of the extinction coefficient of a protein or peptide based on amino acid aromatic side chain composition.

2.5.5 MTP40 labelling with NHS DyLight for saturation assay

For receptor saturation analysis, MTP40 was conjugated to fluorescently labelled DyLight 488 NHS Ester reagent as per the manufacturer's guidelines (Thermo Fisher Scientific). The dye molecule contained an *N*-hydroxysuccinimide (NHS) ester moiety which reacts with primary amines of proteins (in this case, the *N*-terminal α -amino group of MTP40) to form a stable, covalent amide bond and releasing the NHS group.

DyLight aliquots were equilibrated to room temperature for 30 minutes before use to avoid condensation. For MTP40 labelling with Dylight NHS, 1mg of lyophilised MTP40 (MW 2034) solubilised directly in 200 μ l DMSO was added to 1mg of lyophilised NHS-DyLight (MW 1011) to provide a 2x molar excess, as per the manufacturer's recommendations (Thermo Fisher Scientific). NHS Ester Dylight

was left to solubilise in the MTP40-DMSO solution for 5 minutes before adjusting to a final working concentration of 20% DMSO with 0.1M sodium bicarbonate buffer.

The MTP40 NHS reaction was incubated for 1 hour at room temperature with agitation. The NHS-labelled MTP40 product was purified using dialysis by adding 100µl of the reacted sample to a 0.1ml Slide-A-Lyzer Mini Dialysis cassette with a molecular weight cut-off (MWCO) of 2kDa (Thermo Fisher Scientific). Dialysis was performed against 1L of PBS as the dialysis exchange buffer with agitation at 4°C. The dialysis buffer was changed after 30 and 120 minute intervals before being left to dialyse overnight at 4°C with agitation to remove unreacted MTP40 from the solution and exchange buffer.

After dialysis, samples were concentrated in a Millipore Centricon filter unit (MWCO 3kDa) by centrifugation at 10,000xg for 5 minutes. The solution containing the labelled MTP40 was transferred into a glass vial for storage. Absorbance of the DyLight-labelled MTP40 was read in a UV cuvette at wavelengths of 280nm and 493nm, respectively. The concentration of the fluorescent product was calculated based on the observed absorbance of the product at 280nm corrected for the absorbance at 493nm produced by the NHS dylight label as per the manufacturer's recommendations (outlined in equation 3 below).

$$\text{Protein concentration(M)} = \frac{[A_{280} - (A_{493} \times CF)]}{\epsilon(\text{peptide})} \times \text{dilution factor}$$

Equation 3: Molar concentration of NHS-labelled MTP40 peptide

2.6 Development of a flexible multivalent construct

2.6.1 Unlabelled Tet40 synthesis

Biotinylated MTP40 (Biot-MTP40) was purchased pre-conjugated from the manufacturer (Peptide Synthetics). The BiotMTP40 was reacted in solution with streptavidin to produce the **Tetrameric** peptide construct targeting CD40R (Tet40). Reaction volumes were calculated based on molar ratios; 1mg/ml stock solution of unlabelled streptavidin (Sigma) provided a stock solution with a theoretical molar concentration of 19µM (based on the published MW for streptavidin of 53kDa). To produce a tetrameric construct, streptavidin and MTP40 were reacted at a molar ratio of 1:4, respectively, for 45 minutes at room temperature with agitation. Following incubation, light absorbance was measured at 280nm wavelength (A_{280})

and the obtained value was converted into molar concentration to confirm the theoretical values (equation 4). As exact molar ratios of streptavidin:MTP40 were used, purification was not required.

$$\frac{A_{280}}{(\text{MW Streptavidin} + [\text{MW MTP40} \times 4 \text{ binding sites per tetramer]})} := \text{Concentration of Tetramer (M)}$$

Equation 4: Molar concentration of tetramer

Calculation of the molar concentration of Tet40 based on the absorbance of solution at 280nm.

2.6.2 Fluorescent tetramer synthesis for saturation assay

Alexa-Fluor 488-labelled streptavidin was purchased from Thermo Fisher Scientific in solution at a concentration of 1mg/ml (19 μ M). Solubilised BiotMTP40 was added to streptavidin at a molar ratio of 1:4 (streptavidin:BiotMTP40) and incubated at room temperature for 1 hour. Dialysis and concentration were carried out as described in section 2.5.5. Post-dialysis, fluorescent Tet40 concentration was calculated based on absorbance values at 493nm wavelength. Unbound DyLight (MW 1011) and Biot-MTP40 (MW 2034) were removed using 3kDa MWCO filters.

MTP40 binding to the streptavidin scaffold was quantified based on absorbance produced by streptavidin labelled with FITC fluorophore at 280nm and 493nm. Absorbance measurements were recorded in triplicate from both the stock streptavidin substrate and Tet40 product. FITC-labelled streptavidin was provided as a 19 μ M stock solution by Thermo Fisher Scientific. MTP40 was solubilised as described in section 3.4.3 to 1mg/ml and incubated with FITC-labelled streptavidin to produce a Tet40 as detailed in section 2.6.1. Fresh Tet40 was synthesised prior to each experiment.

Following substrate reaction and purification, the absorbance of the Tet40 product was recorded at 280nm and 493nm. The concentration of streptavidin in the Tet40 product was calculated based on the observed absorbance of the product at 493nm. This approach provided a logical method to calculate streptavidin concentration in the reacted product because absorbance at 493nm could only result from the FITC-labelled streptavidin as no absorbance was observed from MTP40. Once the concentration of streptavidin molecules was determined for the sample, this value was then divided by four, to account for the four Biot-MTP40 molecules bound to each streptavidin scaffold.

2.7 Development of the rigid targeting construct

2.7.1 MTP40 conjugation to gold nanoparticles

Untargeted Polyvalent gold Nanoparticles (UPN) with an average diameter of 25nm suspended in PBS were purchased from Sigma Aldrich. Nanoparticle concentration and diameter were provided by Sigma and used to characterise MTP40 binding by gold nanoparticles.

The MTP40 was solubilised at 4mg/ml and molar concentration was calculated based by absorbance at 280nm. The concentration of UPN in 500 μ l (provided by the manufacturer) was 3×10^{11} . Based on the surface area volume of UPN, this value was multiplied by 2000 to calculate the final number of MTP40 molecules required to saturate the surface of 500 μ l of UPN.

Solubilised MTP40 and UPN were added to 1.5ml centrifuge microtubes and incubated at 4°C with rotation for 48 hours to allow the MTP40 to assemble on the gold surface *via* the available cysteine-producing disulphide bonds. An additional 1.5ml centrifuge microtube was set to rotate containing UPN and TCEP only as controls. After the reaction period, both samples were removed and transferred to 10,000 MWCO Pall Centricon Units (VWR). This step allowed purification based on separation of reactants and products by size. Samples were concentrated by centrifugation at 12,000xg for 5 minutes at room temperature to reduce the final volume of sample retained by approximately 40%.

Following incubation, successful conjugation of MTP40 with UPN to produce Targeted Polyvalent Nanoparticles against CD40R (TPN-40) was characterised by absorbance characteristics of the resultant particles. A Thermo Evo300 UV Vis Spectrophotometer was first blanked using PBS and wavelength absorption scanning of UPN from 400-600nm provided a baseline for nanoparticle absorption peak. Calibration of the spectrophotometer for nanoparticle characterisations is outlined in figure 2.2. MTP40 conjugation to the UPN surface was indicated by a slight but significant shift in absorption peak, resulting from modification of the nanoparticle surface.

The resulting TPN40 were characterised by spectrophotometry using a Thermo Scientific Evolution 300 UV-Visible Spectrophotometer and analysed with VISION-

pro software. The machine was first blanked with 100 μ l PBS followed by running of a 100 μ l sample in quartz micro cuvette (Fisher Scientific).

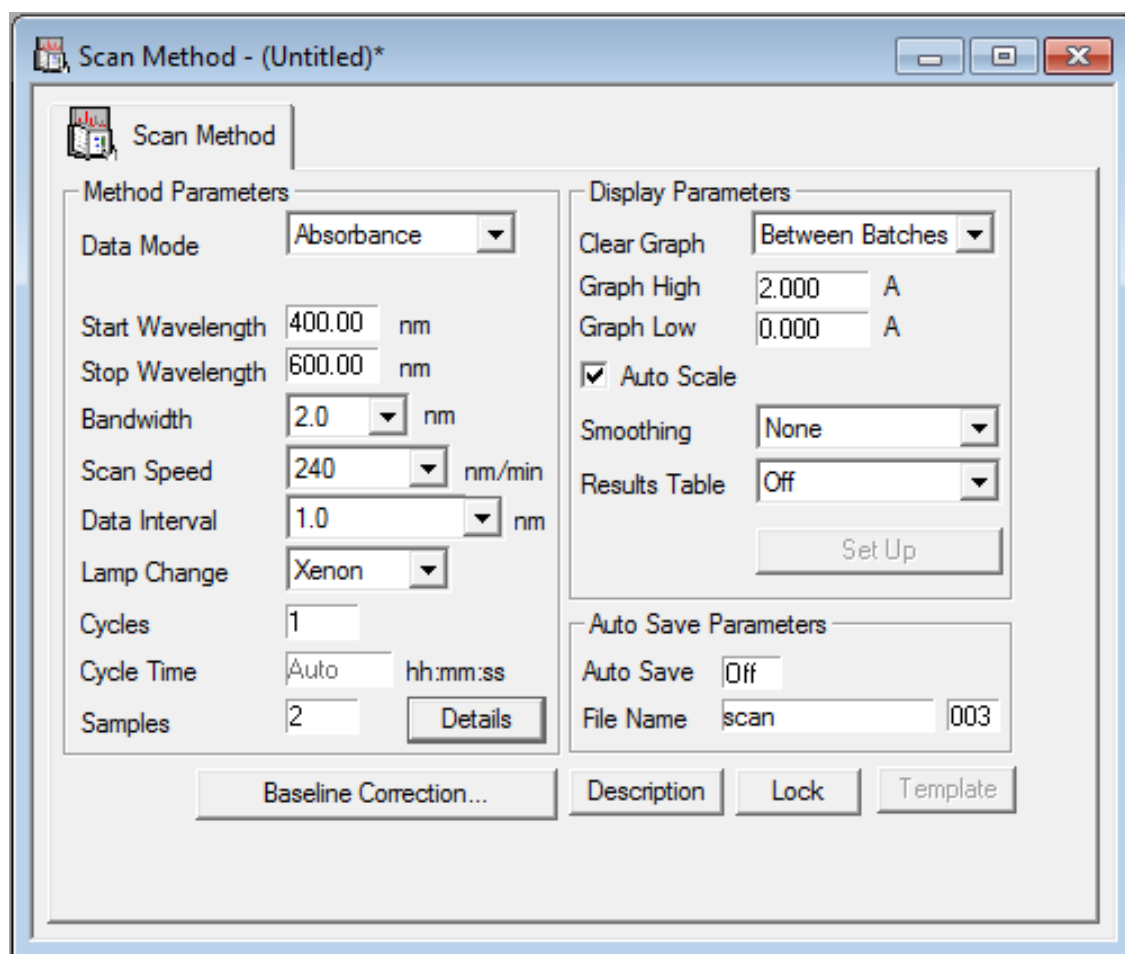


Figure 2-2: Evolution 300 UV-Visible Spectrophotometer settings used for the characterisation of gold nanoparticles

To characterise the shift in absorbance peak, the software was programmed to acquire the absorbance spectra of samples over a defined interval of 200nm with bandwidth measurements of 2nm and standard speed and data intervals of 240nm/min and 1.0nm (figure 2.2). To quantify the amount of MTP40 bound to TPN40, the software was set to acquire the absorbance value at 280nm.

The concentration of TPN40 was calculated based on absorbance at 280nm by subtracting the absorbance of UPN from total absorbance of TPN40, assuming that remaining absorbance occurred from bound MTP40. The resulting absorbance was divided by the MW of the MTP40 to calculate concentration. A schematic diagram summarising the formation of the two multivalent scaffolds is illustrated in figure 2.3. UPN were used as the negative control for comparison against TPN40.

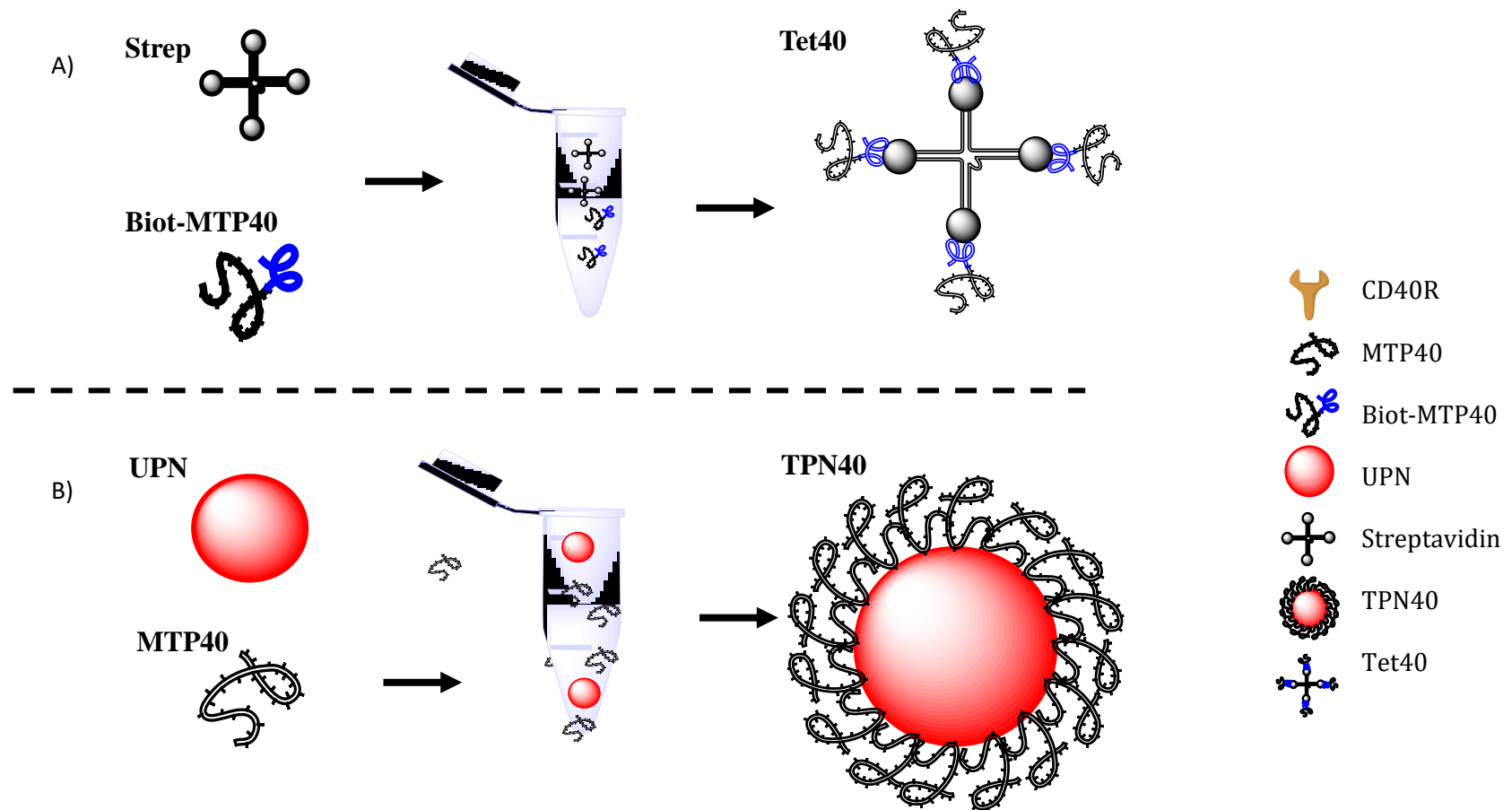


Figure 2-3: A schematic diagram of multivalent construct formation

Panel A) Streptavidin backbone was incubated with BiotMPT40 at a molar ratio of 1:4 for 1 hour at room temperature to allow biotinylated MTP40 to bind with streptavidin backbone. As the exact concentration of MTP40 was added to saturate the biotin binding sites of streptavidin, no purification step was carried out. **Panel B)** UPN were incubated with an excess ratio of MTP40 at 5,000:1 for 48 hours at 4°C to ensure saturation of the UPN surface. Resulting TPN40 product was concentrated by centrifugation at 12,000xg for 5 minutes in 10,000 MWCO filter units (Pall) to remove excess unbound MTP40.

2.8 Cell culture

For routine subculture, adherent cells cultured in T75 flasks were washed three times with 10ml PBS and incubated at 37°C with TrypLE dissociation enzyme. Cells were aspirated and transferred into a 50ml falcon tube before washing the base of the flask with an additional 10ml PBS by 10ml sterile pipette transferred into the same tube.

For suspension cultures, 10ml of cells in suspension were aspirated from the culture vessel, collected by centrifugation at 200xg for 5 minutes to form a pellet, and then gently re-suspended in 1ml media by p1000. Cells were collected by centrifugation at 200xg for 5 minutes and re-seeded at the densities specified for individual cell lines (sections 2.8.1-2.8.5) after cell counting by haemocytometer.

For cell counts, a 100µl aliquot was taken from each culture sample and diluted 1:1 with Trypan Blue live cell exclusion dye to determine cell viability. All seeding densities specified are for the T75 flask for general culture maintenance. All cultures were incubated at 37°C in a humidified atmosphere with 5% CO₂ in an ESCO AirstreamClass II BSC and routinely tested for mycoplasma contamination at three-month intervals. A summary of characteristics for the cell lines investigated in this study are outlined in table 2.1 below.

Table 2-1: Summary of cell lines investigated in this study

Cell Line	Origin & Type	Morphology	Culture medium	Function & Primary Reference
tsDC ECACC	CBA (H-2k) mice Dendritic cell	Semi-adherent	IMDM	Constitutive MHCII expressing, Differentiates in contact with T cells & their cytokines; Volkmann et al., 1996
CTLL-2 ECACC	C57b1/6 mice Cytotoxic T cell	Suspension line	RPMI	Long term culture of tumour-specific cytotoxic T cells, IL-2 dependent; Gillis & Smith, 1977
D10-N4M ATCC	AKR/J mice Helper T cell Th2	Suspension line	DMEM	Antigen responsive helper T cells, IL-1 responsive; Watson, 1979
RMA	C57BL/6 mice Cytotoxic T cell	Suspension line	DMEM	Co-stimulatory lymphoma derived T cell line; Nieland & Kruisbeek 1995, Gays et al., 2000
ID8	C57BL/6 mice Ovarian tumour	Adherent cell line	IMDM	Syngeneic mouse model for human ovarian cancer; Roby et al., 2000

Summary of the five cell lines used in this project, including primary references.

2.8.1 tsDC cell line

The murine bone marrow derived dendritic cell line tsDC was purchased from the European Collection of Cell Cultures (ECACC) and cultured in complete Iscove's Modified Dulbecco's Media (IMDM) containing 10% v/v fetal bovine serum (FBS) + 1% v/v penicillin/streptomycin. tsDC were seeded at 2.5×10^4 cells per cm^2 for maintenance and sub-cultured at 80% flask confluence at approximately seven-day intervals. For receptor analysis experiments, PBS containing 15mM EDTA was substituted in place of TrypLE enzyme to minimise disruption to cell surface receptor expression.

2.8.2 CTLL-2 cell line

Cells of the murine cell line cytotoxic T lymphocyte-IL-2 dependent (CTLL2) were seeded at 1×10^4 cells/ml in complete Roswell park memorial institute medium (RPMI) media supplemented with the following reagents: 2mM L-glutamine, 1mM sodium pyruvate, 10mM HEPES (4-(2-hydroxyethyl)-1-piperazineethanesulfonic acid) buffer solution, 2000 μ M glucose, 5% growth factor supplement (prepared in-house; described in section 2.8.3), in addition to standard supplementation with 10% FBS v/v and 1% penicillin streptomycin v/v. Cells were seeded at 1×10^4 and sub-cultured at 5×10^5 cells/ml approximately every 4 days.

2.8.2.1 Preparation of IL-2 growth factor in-house

To prepare rat growth factor, spleens were removed from female Sprague-Dawley rats weighing 200g. Spleens from two rats were coarsely minced before being passed through a No. 60 sieve (Sigma). Cells were washed three times with RPMI 1640 medium by centrifugation for 10 minutes at 1000xg and gently re-suspending the pellet in fresh RPMI by pipetting. Cells were re-suspended at $1-1.5 \times 10^6$ viable cells/ml in 150 cm^2 flasks containing 100ml RPMI 1640 supplemented with 1% heat-inactivated FBS, 0.05mM β -mercaptoethanol, 15mM HEPES, 100units/mL penicillin, 100mg/mL streptomycin, and 1.0 μ g/mL Concanavalin A (Con-A). Cells were incubated at 37°C in a CO₂ incubator for 48 hours for IL-2 enrichment of media. Supernatant was harvested following centrifugation at 4,000xg for 20 minutes. Media was sterilised by filtration through a 0.22 μ M membrane and stored at -80°C until use.

2.8.3 RMA cell line

The RMA T cell line was kindly donated by Dr Frances Davison from the University of Newcastle. Cells were cultured in Dulbecco's modified eagle medium (DMEM) media, supplemented with 10% FBS and 1% penicillin/streptomycin with an addition of 1% pre-prepared MEM non-essential amino acids (Sigma). Cells were seeded in T75 suspension flasks at 1×10^3 cells/ml and sub-cultured approximately every three days.

2.8.4 D10-N4M cell line

The D10-N4M T cell line (D10) was also kindly donated by Frances Davison from the University of Newcastle. Cells were cultured in complete DMEM media supplemented with 10% FBS, 1% penicillin/streptomycin, 2% MEM non-essential amino acid supplement (Sigma), and $5 \mu\text{M}$ β -mercaptoethanol. Cells were seeded at 1×10^5 cells/ml and sub-cultured at seven-day intervals.

2.8.5 ID8 cell line

The murine ovarian cancer cell line ID8 was generously provided by Dr Kathryn Roby, University of Kansas Medical Centre. The ID8 cell line was investigated as a representative cancer line since ovarian cancer currently has poor response rates to existing chemotherapy regimens and also represents a unique setting whereby the tumour is contained within the intraperitoneal cavity in the early stages (see section 1.1), presenting the opportunity for direct intra-tumoural delivery and potential for imaging agents, such as gold nanoparticles (see section 1.9 and 1.10). ID8 cells were seeded at 1×10^5 cells/ml for two days in IMDM supplemented with 4% v/v FBS and $5 \mu\text{g/ml}$ insulin, $5 \mu\text{g/ml}$ transferrin, and 5ng/ml sodium selenite (Invitrogen). Suspension cells were re-suspended using a 10ml sterile pipette before centrifugation and counting. T75 flasks were seeded with 1×10^4 cells/ml. Cells were routinely sub-cultured at five-day intervals and showed approximately 80% confluence.

2.9 Characterising tsDC response to LPS as a positive control for DC activation

LPS was used as a stimulating factor to confirm that the tsDC population used for this work demonstrated activation outputs in a similar manner to DC populations described in current literature. LPS induces an innate immune response in a broad

range of cell types through interaction with TLR4 at the cell surface, and has been well characterised in scientific literature (Dunzendorfer et al., 2004; Wang et al., 2008). The primary objective here was to demonstrate that the immature tsDC population being investigated was able to undergo functional changes associated with immune activation in a time and cost effective manner. LPS provided a reliable means of cell activation as this was commercially available as a quality controlled product, with an extensive shelf life at a more economical price than CD40R antibodies. Although LPS acts by binding a distinct receptor to CD40R binding (LPS binds Toll-like receptors as opposed to members of the TNF family), there is overlap in the down-stream signalling of the two pathways, which ultimately both result in the activation of transcription factors NF- κ B, p38 MPAK and JNK, unlike other activating factors such as IFN which do not result in NF- κ B signalling (Abdi et al., 2012; Castiello et al., 2011). Furthermore, current literature suggests that exposure to either LPS or CD40L induce DC maturation over a similar time scale of 24-48 hours (Baltathakis et al., 2001; Matsunaga et al., 2002). This is compared to alternative DC activators such as TNF- α which requires up to 7 days incubation to induce maturation (Le-Naur et al., 2001), *versus* culture with IFN for DC maturation which is recommended to be incubated for less than 24 hours, with various groups suggesting 8 hour incubation is optimal (Schlaak et al., 2002).

To provide a baseline for tsDC maturation, tsDC were seeded at 2×10^4 per well in a 96 well flask and incubated with varying concentrations of LPS for 24 hours to establish whether the established changes in morphology and phenotype associated with activation *via* LPS binding were observed. Changes in cell morphology observed by light microscopy can be used as an initial indicator of cell maturation status before proceeding with further analysis (including FACS and western blott), as this provided an immediate indicator of successful maturation, as established by Granucci et al., 1999. This therefore provided a primary indicator of tsDC response to activating treatments. Because LPS only provides an indirect positive control and does not target the CD40R pathway, LPS activation was supported by conducting a pull down assay (method described in section 2.15; results in section 3.3) to confirm that functional changes induced by MTP40 resulted from specific binding between MTP40 and the CD40R. This was visualised by anti-CD40R antibody binding using western blot.

2.10 Scaffold backbones as negative control treatments

To confirm that any changes observed throughout this project occurred as a result of successful multivalent presentation of MTP40, control samples treated with either PBS buffer (used for treatment solubilisation), MTP40, streptavidin backbone or UPN were included where appropriate, illustrated in tables 2.2 and 2.3. This confirmed whether any changes in phenotype or effector function were specific to the multivalent treatment, or whether this resulted from non-specific binding and interaction with other components.

2.11 tsDC activation by CD40R targeted treatments

For tsDC activations, cells were cultured to 80% confluence and media were changed immediately before treatments. IMDM was adjusted to pH8 prior to treatments to maximise construct and MTP40 solubility. Constructs were added to cell media at a working concentration of 2.5 μ M of either construct or control and incubated at 37°C for 24 hours with 5% CO₂. After 24 hours, cell media was transferred to 15ml falcon tubes and non-adherent cells were collected by centrifugation at 1000xg. Treatment media was stored at -20°C. Adherent cells were washed with 5ml PBS and incubated with 5ml PBS + 15mM EDTA for 5 minutes to detach. Cells were counted and proceeded to downstream analysis. The treatment conditions investigated for tsDC activation are shown in table 2.2.

Table 2-2: tsDC activation treatments

Sample	Treatment
A	tsDC in IMDM, no treatment
B	tsDC in IMDM + 2.5µM Streptavidin (neg control)
C	tsDC in IMDM + 2.5µM monomeric CD40R peptide (MTP40)
D	tsDC in IMDM + 2.5µM CD40R targeted streptavidin (Tet40)
E	tsDC in IMDM + 2.5µM untargeted nanoparticle control (UPN)
F	tsDC in IMDM + 2.5µM CD40R targeted nanoparticles (TPN40)
G	tsDC in IMDM + 10µg LPS (positive control)

Table 2.2 summarises the treatments added to cell culture flasks containing tsDC in complete culture media. Test treatments are highlighted in red.

2.12 DC co-culture with T cell lines

To determine the capacity of CD40R stimulated tsDC to initiate a priming response in T cell populations, activated tsDCs and naïve T cell lines were simultaneously cultured in a single flask. T cell outputs were investigated for three separate cell lines in response to co-culture, with six treatment conditions for each T cell line.

For co-culture experiments, 1×10^5 tsDC were seeded in T25 flasks as described in section 2.8.1 and left to adhere to the flasks overnight. This period allowed tsDC to adhere to the base of the flask (aiding separation from T cell lines, which remained in suspension) and provided opportunity for tsDC to enrich the culture media with stimulating cytokines required for T cell growth. After the initial 12 hours tsDC culture, treatment media containing 2.5µM of activating treatment in addition 1×10^6 cells from CTLL-2, RMA, or D10 cell lines to provide a 1:10 ratio of tsDC:T cells (as detailed in table 2.3). IMDM was adopted as the basic media for co-culture incubations as the T cell media required additional media supplementation to support growth, which may have altered the baseline activity of tsDCs. Co-culture flasks were incubated for 48 hours before harvest and analysis by FACS. This time frame was selected to allow time for cell-cell interactions to occur and tsDC to adhere to the base of T25 flasks while T cell lines formed non-adherent clusters. T cell cultures in suspension were removed *via* aspiration. tsDC were then washed once with fresh media to remove remaining T cells. Adherent cells assumed to be tsDC were detached for analysis by flow cytometry to confirm expression of tsDC markers.

Table 2-3: Co-culture activation experiment treatments

Sample	Treatment
A	tsDC in IMDM, no treatment
B	tsDC in IMDM + T cell line in IMDM, no treatment
C	tsDC in IMDM + T cell line + Streptavidin (-)
D	tsDC in IMDM + T cell line + MTP40 (-)
E	tsDC in IMDM + T cell line + Tet40
F	tsDC in IMDM + T cell line + UPN
G	tsDC in IMDM + T cell line + TPN40
H	tsDC in IMDM + T cell line + LPS (+)
I	tsDC in IMDM + T cell line + ID8 tumour lysate
J	tsDC in IMDM + T cell line + ID8 tumour lysate + Streptavidin (-)
K	tsDC in IMDM + T cell line + ID8 tumour lysate + MTP40
L	tsDC in IMDM + T cell line + ID8 tumour lysate + Tet40
M	tsDC in IMDM + T cell line + ID8 tumour lysate + UPN
N	tsDC in IMDM + T cell line + ID8 tumour lysate + TPN40
O	tsDC in IMDM + T cell line + ID8 tumour lysate + LPS (+)

Table 2.3 shows the treatment conditions and controls flasks prepared for co-culture experiments. The experimental layout was repeated three times, using either CTLL-2, D10, and RMA as the “T cell line”. For each experimental run, treatment flasks, negative controls, and untreated cells were run in parallel to minimise variation between runs. Test treatments are highlighted in red.

2.13 Fluorescence activated cell sorting

Fluorescence activated cell sorting (FACS) allows the measurement of internal and external characteristics of individual cells within a fluid suspension. The first fluorescence-based flow cytometer was developed by Wolfgang Ghorde at the University of Munster in 1968 (Thaer & Sernetz., 1973). The flow cytometer allows high-throughput automated quantification of cell populations and consists of three main components: the fluidics, optics, and electronics, which allow simultaneous measurement and analysis of multiple physical properties (figure 2.4).

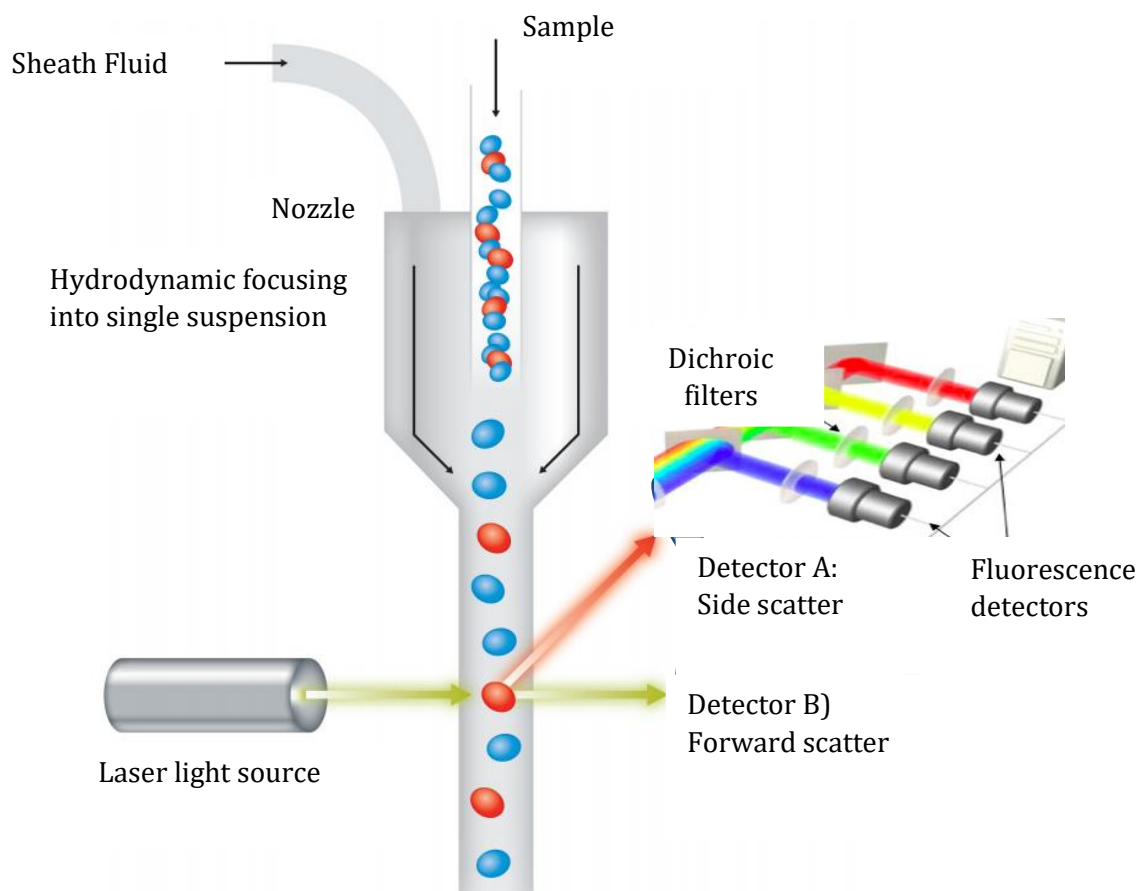


Figure 2.4: Fluidics system and optical components of the flow cytometer; adapted from BD website

The fluorescent light emitted by labelled cells travels along the same path as side scatter signals but is filtered by dichroic filters and mirrors which direct the correct wavelengths to the specific detectors.

The fluidics system applies hydro-dynamic force to produce a single cell suspension. When the single cell suspension passes through the laser light source at the interrogation point, the light is scattered by the cell, producing profiles of the cells size, granularity, and phenotype determined by fluorescent labels. The interrogation point is where the laser and sample intersect and optics collect the resulting scattered light and fluorescence. Forward and side scatter result from the physical size and complexity of a cell, respectively (figure 2.5). These optical signals are then converted to proportional electronic signals in the form of voltage pulses.

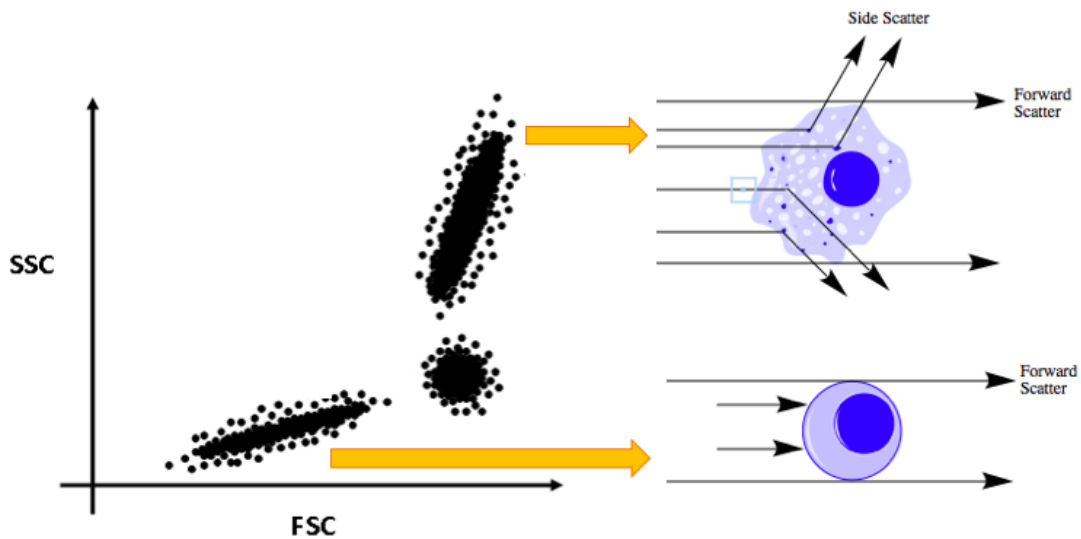


Figure 2.5: Forward and side scatter profiles produced by cell size and granularity

Forward scatter produced by a cell is directly proportional to the diameter of a cell and occurs primarily from light diffraction around the cell. Side scatter provides information relating to internal cell complexity as the interface between the laser and internal structures such as granules and the nucleus cause the light to refract. Authors own.

Fluorescence describes the excitation of a fluorophore by an external source of energy to a higher energy level, followed by the return of the fluorophore to its ground state, with the emission of light. The amount of emitted light is determined by how strongly the fluorophore is excited by a specific wavelength and colour. When laser light of the correct wavelength strikes the fluorophore, the fluorescent signal emitted is detected by the flow cytometer.

2.13.1 Surface receptor analysis *via* FACS

To investigate cell surface receptor expression levels, cells were washed three times with PBS before detaching from the flask using PBS + 15mM EDTA. Detached cells were counted with trypan blue and re-suspended to a working concentration of 1×10^5 cells in 100 μ L IMDM + 1% bovine serum albumin (BSA) in 1.5ml centrifuge microtubes. Samples were kept on ice throughout FACS preparation and analysis to slow cellular metabolism and thus minimise basal changes in receptor expression. All FACS antibodies were purchased from Biolegend and diluted as per the manufacturer's recommendations. Phycoerythrin (PE) or fluorescein (FITC) conjugated antibodies were added to samples as instructed and incubated in the dark for 1 hour at 4°C with rotation. Following incubation, the cells were collected by centrifugation at 1000xg for 5 minutes at 4°C and washed three times with

complete IMDM + 1% BSA to reduce non-specific labelling. Cells were fixed in 100µL PBS + 1% paraformaldehyde (BD Biosciences) for 15 minutes on ice before an additional three washes in PBS + 1% BSA. At the final wash step, cells were transferred to FACS tubes for acquisition on the cytometer. Unlabelled cells without antibody were washed and fixed alongside stained samples as a control for auto-fluorescence. Cells labelled with isotype control were prepared alongside samples as a negative control for non-specific immunoglobulin binding on the cell surface.

2.13.2 tsDC preparation for FACS saturation assay

A saturation curve was generated to determine the binding capacity of MTP40 for the CD40R by FACS. Flasks containing tsDC were cultured prepared as described in section 2.8.1. Aliquots containing 2×10^5 tsDC were incubated with FITC-labelled Tet40 or an equivalent concentration of NHS Dylight-488-labelled MTP40. The stock concentration of MTP40 and Tet40 were diluted 1.5 fold in IMDM + 1% BSA to produce a range of treatment concentrations ranging from 60-0.1µM for MTP40 and 17.6µM-0.1µM for Tet40 construct.

tsDC samples were incubated with Tet40 or MTP40 treatments diluted in 100µL binding media (IMDM supplemented with 10% FBS, 3% BSA, 100 units/ml Penicillin/Streptomycin, and 0.01% Tween-20) for 1 hour at 4°C over a 10-point concentration range. Unlabelled cells in complete binding media were used as negative controls for auto-fluorescence. After incubation, cells were collected by centrifugation at 200xg and the medium aspirated by p200 pipette. Samples were washed five times to remove unbound and non-specific labelling before being fixed in 1% PFA for 15 minutes on ice in the dark. Cells were analysed as described for receptor analysis using the FL1 FACS channel for detection of NHS Dylight-488.

2.13.3 FACS Analysis

Cells were acquired and analysed using a FACSCalibur Flow Cytometer with CellQuestPro Software (BD Biosciences). A minimum threshold of 1×10^4 cells was acquired from each sample. Forward scatter and side scatter plots were acquired to observe trends in the whole cell population and fluorescence from antibody labels was detected on either the FL1 or FL2 acquisition channel for FITC and PE labels, respectively.

Geometric mean of fluorescence intensity (GM) was used to analyse surface receptor expression under different treatment conditions. The GM value accounts for the log-normalised value of the data and is therefore less susceptible to skewing by anomalous signal from individual cells within a population. This value is useful when the behaviour of a whole heterogeneous population is of interest.

Samples containing 1×10^5 tsDC in $200 \mu\text{l}$ PBS + 1% BSA were transferred to FACS tubes. An unlabelled test tube was first acquired to determine acquisition forward scatter and side scatter laser intensity settings for the cell population of interest. A manual gate was defined to contain the major cell population excluding outlier populations resulting from cell debris or antibody clusters (figure 2.6).

The histograms of unlabelled tsDC and untreated tsDC labelled with anti-CD40R PE fluorophores were analysed at the start of each individual experiment to avoid erroneous results by re-aligning the GM value of the isotype control with previous experiments where necessary to account for fluctuations which may occur depending on the stage of the cell cycle during analysis (BD BioSciences Protocols).

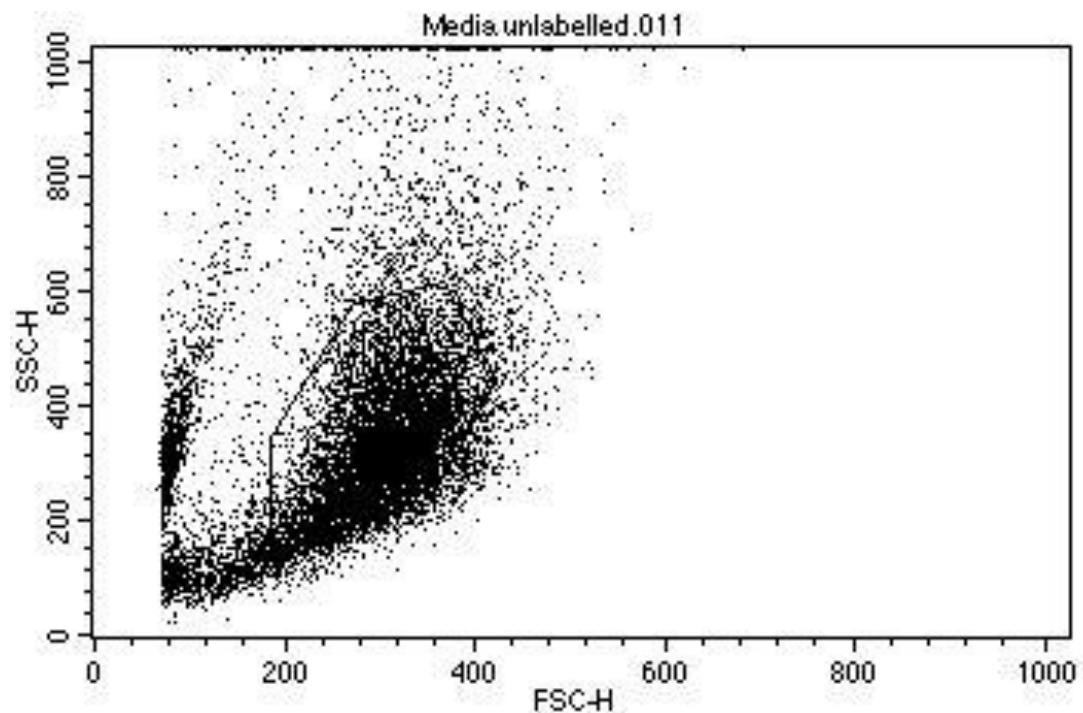


Figure 2.6: Gating populations of interest for analysis by flow cytometry

The representative scatter plot depicts the tsDC population following a 1-hour incubation with FITC-Tet40. A gated region was manually set to measure the population of interest and eliminate cellular debris.

2.14 Fluorescent microscopy of CD40R binding

Fluorescent microscopy was used to visualise binding of constructs to the tsDC surface. tsDC were seeded at 2×10^4 with 200 μ L IMDM complete media in 96 well plates and left to adhere overnight at 37°C+5% CO₂. After 12 hours of incubation, supernatants were removed and replaced with fresh media containing either 2.5 μ M FITC-Tet40 or 2.5 μ M FITC-streptavidin +5% BSA for blocking. Samples were incubated for 1 hour at 4°C in the dark before washing three times with 200 μ L complete IMDM warmed to 37°C. After an additional wash with 200 μ L PBS + 1% BSA, PBS without blocking reagent was added to each well for fluorescent imaging. Images were acquired using an Olympus IX 71 inverted microscope at 400x total magnification.

2.15 CD40R isolation by pull down assay

Pull down assays were conducted to confirm the binding capacity of MTP40 for CD40R. Streptavidin-coated magnetic Dynabeads were conjugated to BiotMTP40 and the resulting CD40R-targeted beads were incubated with whole tsDC lysate containing the CD40R (figure 2.7).

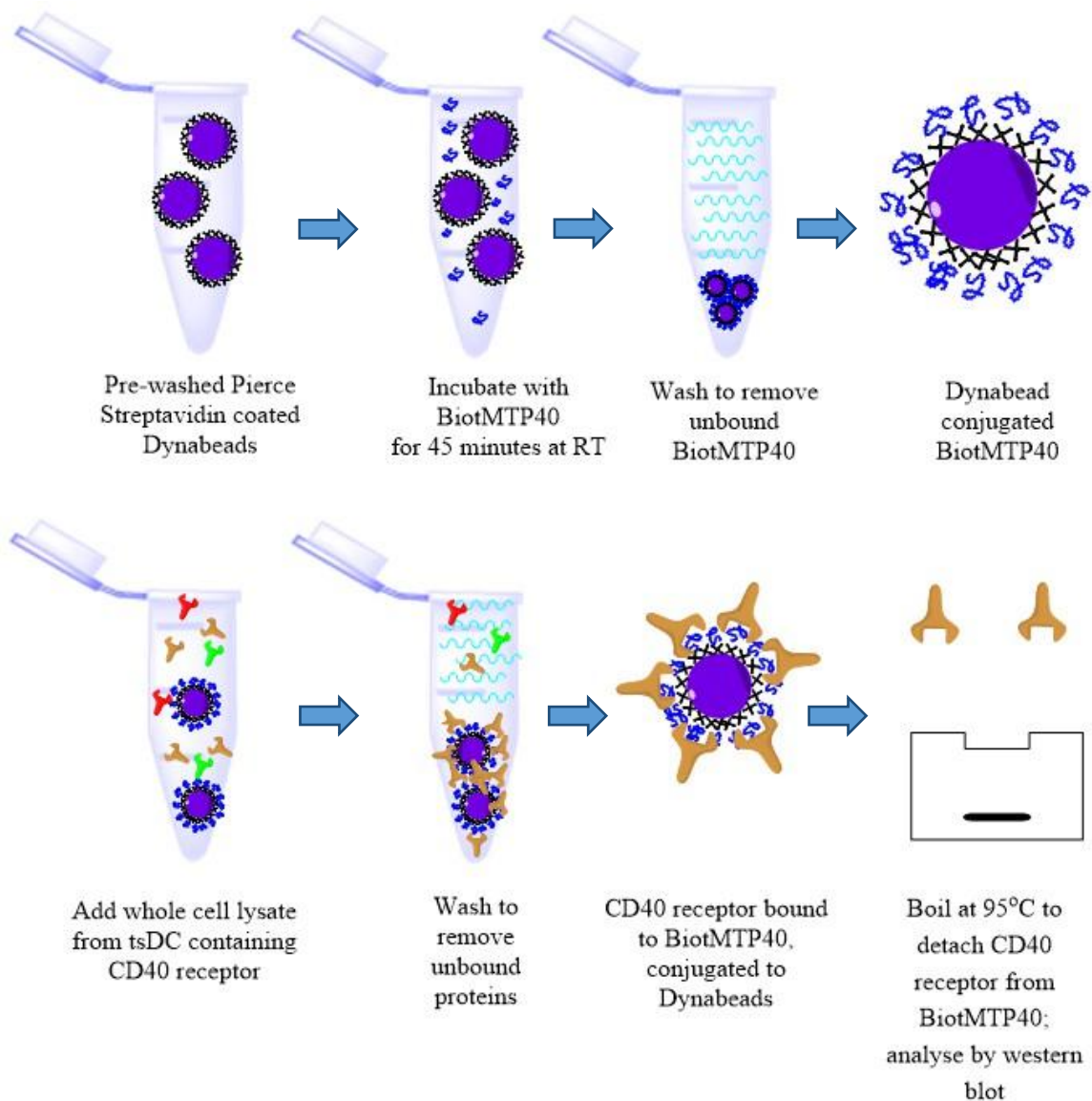


Figure 2.7: Stages of the CD40R-MTP40 pull down assay using Streptavidin Dynabeads

tsDCs seeded in T75 flasks at 2×10^5 cells per cm^2 were left to adhere overnight in 10ml IMDM. After 12 hours of incubation, flasks were treated with $10 \mu\text{g}/\text{ml}$ LPS for 24 hours to induce upregulation of the CD40R. Following activation, tsDC lysates were prepared (to be described in section 2.15.2) and protein concentration was determined by BCA. Lysates were kept on ice during the BCA assay to reduce degradation, before proceeding directly to the pull down protocol.

For the pull down assay, $200 \mu\text{l}$ $10 \text{mg}/\text{ml}$ streptavidin-labelled M-280 magnetic Dynabeads (Thermo Fisher Scientific) were transferred into a 1.5ml microtube and washed three times with $500 \mu\text{l}$ wash buffer (PBS + 0.1% BSA + 0.1% Tween-20) and re-suspended directly into $180 \mu\text{l}$ of $250 \mu\text{M}$ BiotMTP40. An excess of biotinylated MTP40 (biot-MTP40) was conjugated to pre-washed streptavidin-

coated magnetic Dynabeads (Thermo Fisher Scientific) to ensure saturation of the bead surface as mass spectrometry revealed incomplete biotinylation of the sample. The total reaction volume was adjusted to 500 μ L with wash buffer and incubated for 45 minutes at room temperature with rotation. After incubation, magnetic beads assumed to have bound biot-MTP40 were held against a neodymium earth magnet for 2 minutes until nanoparticles had visibly adhered to the side of the microtube before the supernatant was removed. The pellet was washed by re-suspension in a 500 μ l wash buffer and gentle pipetting up and down. This step was repeated four times to remove any unbound MTP40 from the solution.

Following the final wash, the magnetic beads were collected against the magnet for 2 minutes before removing the supernatant. The remaining beads were then re-suspended directly into 700 μ g of whole tsDC lysate (containing CD40R) and the sample volume was adjusted to 500 μ l with wash buffer. The sample was incubated for a further 45 minutes at room temperature with rotation. Following incubation, the beads were collected against the magnet for 2 minutes. Once the beads had cleared from the solution, the supernatant containing excess tsDC lysate (flow through) was aspirated and stored on ice to determine the presence of CD40R by western blot.

After removing the supernatant from the beads, the sample was washed an additional three times. After the final wash, the magnetic beads were re-suspended directly into 15 μ l PBS. The sample was added to an equal volume (15 μ l) pre-mixed sample buffer (Invitrogen) + 20% β -mercaptoethanol and boiled at 95 $^{\circ}$ C for 5 minutes on a hot plate to disassociate bound CD40R from the MTP40 and streptavidin beads. Dissociated samples were loaded into Sodium dodecyl sulphate polyacrylamide gel electrophoresis (SDS-PAGE) gels containing 10% acrylamide and subject to electrophoresis for 2 hours at 110V in a BioRad Mini Protean Electrophoresis tank. Running gels for increased time at lower voltage allowed for a higher resolution of protein bands with similar MWs as the epitope for CD40R is expected to visualise around 38kDa, while streptavidin bands is expected around 60kDa. Gels were then transferred to a polyvinylidene fluoride (PVDF) membrane for 1 hour at 100V with an ice pack positioned in the tank to maintain temperature. Following transfer, the membrane was probed with anti-CD40R (Abcam ab140043) as described for western blot in section 2.15.

After antibody probing, the PVDF membrane was incubated with a 15ml stripping buffer (Thermo-Fisher-Scientific) for 15 minutes at room temperature with agitation. After incubation with the stripping buffer, the PVDF membrane was saturated with ECL reagents and re-imaged to ensure no horseradish peroxidase (HRP)-bound antibodies remained on the membrane. Data were acquired using a Biorad Chemidoc imaging system.

2.16 Western Blot

Western blots allow identification of specific proteins of interest from a complicated mixture by separation based on MW and charge. In this method, proteins of various sizes and weights are migrated through a sodium-dodecyl-sulphate polyacrylamide gel matrix under the influence of electrophoresis (SDS-PAGE). Once proteins have migrated, the gel is placed on a PVDF membrane to transfer the proteins to a solid support and prevent uncontrolled protein movement. The membrane can then be probed with antibodies specific for the target of interest and visualised *via* secondary antibodies and detection reagents.

2.16.1 Gel casting and recipes

SDS-PAGE gels were cast in-house using the recipes described in table 2.2. Gels were cast in bulk and stored at 4°C for up to 4 weeks in PBS-soaked cloth before use. A Biorad gel casting apparatus was assembled as per the manufacturer's guidelines. Gel components for gel resolution and stacking were added to 15ml tubes, following the recipes outlined in table 2.1. Then, 10% ammonium persulphate (APS) and N,N,N',N'- Tetramethylethylenediamine (TEMED) solutions were added directly before transfer to 1mm plates to catalyse polymerisation. The resolving gel was added to the casting plate and overlaid with 300µl propanol to remove air bubbles. Resolving gels were left to set for half an hour before propanol was removed. APS and TEMED were then added to the stacking gel mixture to catalyse cross linking before immediate transfer into the casting plates and inserting well place holders into the plate.

SDS Gel components	<u>Volume per 5ml gel</u>		
	10% Resolving	15% Resolving	Stacking
H ₂ O	1.9	1.1	3.4
30% Acrylamide mix	1.7	2.5	0.83
1.5M Tris pH 8.8	1.3	1.3	-
0.5M Tris pH 6.8	-	-	0.63
10% SDS	0.05	0.05	0.05
10% APS	0.05	0.05	0.05
TEMED	0.002	0.002	0.005

Table 2-4: SDS gel recipes for 10% and 15% acrylamide gels

Standard SDS-PAGE gel recipes were taken from Cold Spring Harbour Protocols (Sambrook & Russell, 2006).

2.16.2 Lysate preparation

tsDCs were seeded at 2×10^6 cells in T75cm² flasks and cultured for approximately 7 days until 80% confluent. Flasks were washed with 4°C PBS before incubating for 10 minutes with 10ml PBS + 15mM EDTA. Cells were counted and collected by centrifugation at 1000xg for 5 minutes at room temperature before re-suspension of approximately 7×10^6 cells in 300µL lysis buffer (50mM Tris-HCl pH 7.4, 150mM NaCl, 100µl/ml Pierce protease and phosphatase inhibitors, 100µl 1% Triton x-100 (v/v)) using a p200 pipette. Samples were incubated in lysis buffer at 4°C for 2 hours with rotation. Cellular debris were separated from the lysate supernatant by centrifugation at 14,000xg for 15 minutes. Supernatants were transferred to a fresh 1.5ml centrifuge microtube for storage prior to quantification using a Pierce bicinchoninic acid (BCA) protein assay kit (Thermo Fisher Scientific) and absorbance values recorded using an EIX800 plate reader set to a wavelength of 562nm. Protein concentrations were calculated as per the BCA kit protocol.

2.16.3 Preparing heat-shocked ID8 cultures lysates

To induce upregulation of antigenic proteins within the ID8 cell line, cells were subjected to heat shock treatment prior to lysis. ID8 cells cultured to 70% confluence in T175 flasks were incubated for 30 minutes at 42°C in a pre-set water bath. Following heat shock treatment, the media were discarded from the flasks and replaced with fresh media before cells were returned to incubate at 37°C + 5% CO₂ for a further 24 hours to allow protein expression changes. Cells were then harvested by scraping from the base of the flask and prepared for BCA analysis using an EIX800 plate reader set to a wavelength of 562nm.

2.16.4 Protein quantification and gel loading

Protein lysate concentrations were quantified using the Thermo Fisher Scientific Pierce BCA Protein Assay for colorimetric detection and quantification of total protein. Plates containing 96 wells were incubated for 30 minutes at 37°C before absorbance was measured on an ELX800 microplate reader at 562nm. A standard curve was prepared by plotting the absorbance of the protein standard titration at 562nm *versus* concentration in µg/ml. The standard curve was used to calculate the protein concentration for each unknown sample based on linear regression. For detection of CD40R by western blot analysis, 60µg of whole cell lysate was loaded per well. Samples were mixed at a 1:1 ratio with sample loading buffer containing 20% β-mercaptoethanol and denatured by heating to 95°C for 5 minutes. Samples were loaded into 10 lane 1.0mm gels and run at 120V for 90 minutes in a Biorad Mini Protean gel electrophoresis tank. The gel was then assembled into a transfer cassette and run at 110V for 60 minutes to transfer to polyvinylidene fluoride PVDF membranes (Millipore, Livingston, UK).

2.16.5 Antibody probing

Following transfer, the PVDF membrane was blocked in TBST (Tris-Buffered Saline + 0.05% (v/v) Tween-20) with 5% BSA for 60 minutes at room temperature to reduce non-specific protein binding. After blocking, the membrane was washed three times with TBST and incubated overnight at 4°C with primary polyclonal antibodies against CD40R antibody (Abcam ab140043) diluted 1:1000 in TBS + 3% BSA.

After a minimum of 12 hours incubation, the primary antibody solution was removed and the membrane was washed three times with 20ml TBS + 3% BSA. Following these washes, HRP conjugated anti-rabbit secondary antibody (R&D) was added to the membrane for 1 hour at room temperature with shaking. Membranes were then washed a further three times before Pierce enhanced chemiluminescence (ECL) reagents were added (premixed at a 1:1 ratio immediately before visualisation). The membrane was visualised using a ChemiDoc XRS+ Molecular Imager (Bio-Rad, Hertfordshire, UK) and quantified using ImageJ software (National Institute of Health).

Following antibody probing for the protein of interest, blots were stripped of the original antibody by incubation with 15ml stripping buffer (Thermo-Fisher-

Scientific) for 15 minutes at room temperature with agitation. After incubation with stripping buffer, the PVDF membrane was saturated with ECL reagents and re-imaged to ensure no HRP-bound antibodies remained on the membrane. Clean membranes were stripped once more to remove ECL reagents, washed three times with TBST buffer before blocking for 1 hour with PBS + 1% BSA. Membranes were washed and re-probed with 15ml anti- β -actin (Cell Signalling) diluted at 1:1000 in PBS + 3% BSA overnight at 4°C with agitation. Following incubation with primary antibody, membranes were washed three times with PBS + 3% BSA and incubated with anti-rabbit secondary antibody for 1 hour at 4°C before repeating the wash, ECL and imaging steps to assess the consistency of well loading.

2.17 MTP40 peptide imaging by Coomassie Stain

MTP40 was incubated with UPN to produce TPN40 constructs, purified, and characterised as described in section 2.6.1. After removing unbound MTP40 by centrifugation and determining the concentration by absorbance, samples of UPN or TPN40 were added to sample buffer containing β -mercaptoethanol at a 1:1 ratio and boiled for 5 minutes at 95°C to reduce thiol bonds. Samples (maximum volume 60 μ l) and Novex Sharp Pre-stained protein ladder (Invitrogen) were loaded into wells of a 1mm SDS-PAGE containing 20% acrylamide and run for 1 hour at 100V.

Gels were removed from the running tanks and submerged in Coomassie Brilliant Blue staining solution (Thermo Fisher Scientific) consisting of 40% H₂O, 40% methanol, and 20% acetic acid with 0.1% coomassie dye for 1 hour at room temperature with agitation. Following staining, samples were transferred to de-staining solution (40% H₂O, 40% methanol, and 20% acetic acid, without coomassie dye) at room temperature overnight. Gels were rehydrated in H₂O for 1 hour and imaged on a BioRad Chemidoc.

2.18 Enzyme-linked immunosorbent assay

Enzyme-Linked ImmunoSorbent Assays (ELISA) are commonly used for the detection and analysis of soluble antigens including proteins, peptides, and cytokines thanks to its high sensitivity and specificity. Sandwich ELISA involves preparing the surface of a 96 well plate with a defined quantity of capture antibody and blocking any non-specific binding sites with BSA. The antigen of interest is then immobilised on the plate before adding primary antibodies specific to the protein of

interest, followed by secondary enzyme-linked antibodies which interact with the colorimetric substrate solution. This principle is outlined in figure 2.8.

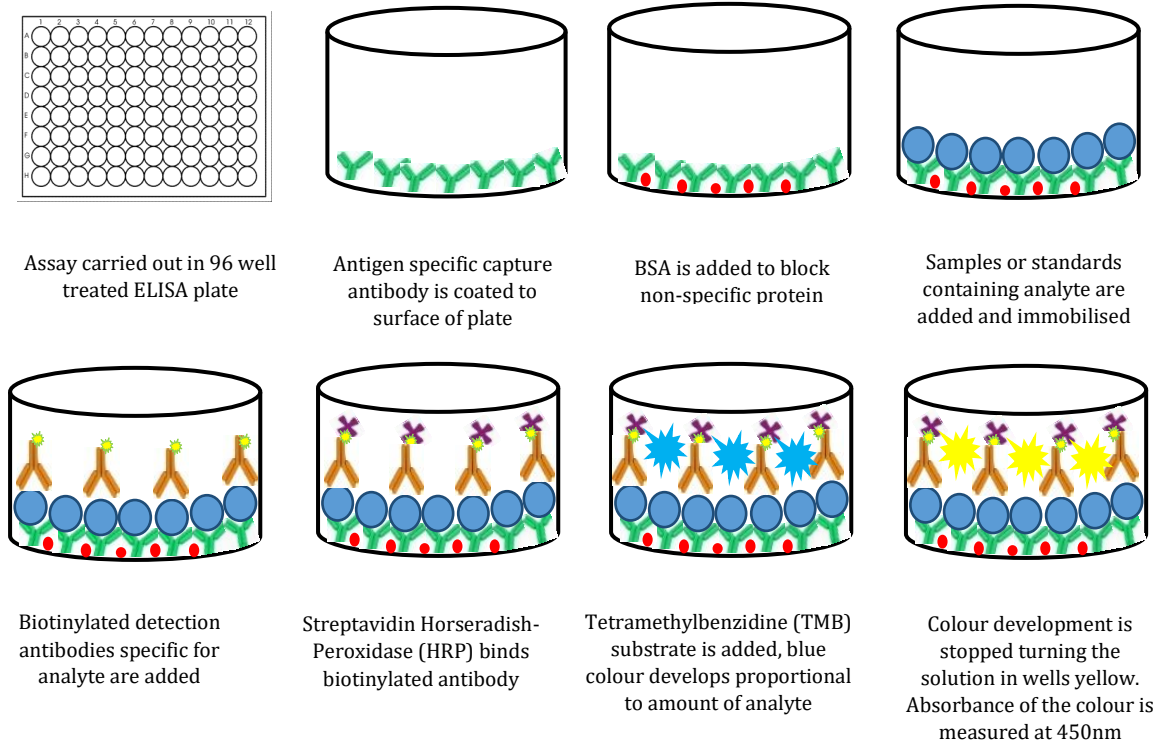


Figure 2.8 : Stages of the ELISA sandwich assay protocol

ELISA DuoSet assays from R&D biosystems were set up as described for analysis of IL-2, IL-10, IL-12 and IFN- γ production by DCs.

2.19 Cytokine analysis by ELISA assay

Following a 24-hour incubation with activation treatments as described in section 2.10, culture media were removed from tsDC samples. Non-adherent cells and debris were removed by centrifugation at 5000xg for 5 minutes at 4°C and the resulting supernatants were frozen at -20°C for 24 hours before transfer to -80°C for long-term storage until analysis to prevent sample degradation. Storing supernatants at -80°C minimises degradation to allow for simultaneous analysis of supernatants acquired on different dates to be analysed in parallel and minimises variation.

For murine IL-2, IL-10, and IL-12, ELISA DuoSet Development Systems from R&D Systems were used. Capture antibody was prepared by diluting to the working concentration in PBS as per the manufacturer's recommendations. Capture antibodies were added to 96 well ELISA plates at 100 μ l per well, sealed, and left to

incubate at room temperature overnight with agitation to ensure thorough coating of the plate surface.

Following overnight incubation, capture antibody was aspirated by multichannel pipette and the plate was washed three times with 200µL wash buffer (0.05% Tween 20 in PBS, pH 7.2-7.4). Wash buffer was discarded manually over the sink and the plate was blotted dry on fresh paper towels after the final wash to ensure liquid was completely removed. Plates were blocked for 90 minutes by adding 300µL blocking reagent (1% BSA in PBS, pH7.2-7.4 0.2µM filtered) with agitation. Aspiration and wash steps were repeated to prepare plates for samples.

Samples were diluted 1:1 with diluent (1% BSA in PBS, pH 7.2-7.4) before adding 100µl of unknown sample or pre-prepared standard to each well. Plates were re-sealed and incubated for 2 hours at room temperature with agitation. Samples were aspirated and washed with 200µl wash buffer before blotting dry. Detection antibodies were diluted as per the manufacturer's recommendations before adding 100µl to each well. Plates were sealed and left to incubate for a further 2 hours at room temperature. Following aspiration and washes, 100µl of streptavidin-HRP (diluted 1:40 in PBS) was added to each well and allowed to incubate for 20 minutes at room temperature. The wells were sealed with tinfoil to protect them from light.

Plates were aspirated and washed before 100µl of substrate solution containing a 1:1 mixture of Colour Reagent A (H₂O₂) and Colour Reagent B (Tetramethylbenzidine (TMB) was added to each well. Plates were incubated for 20 minutes at room temperature and sealed with tinfoil to protect them from light. TMB forms a blue-green liquid in solution when oxidised in the presence of peroxidase-labelled conjugate (HRP-bound antibody); 50µL of Stop Solution (2N H₂SO₄) was added directly into each well (without removal of colorimetric substrate solution) to provide the acidic conditions necessary to convert blue substrate solution to end-point yellow product to be determined by reading absorbance at 450nm. Wavelength correction was set to 540nm to correct for optical imperfections in the plate. A standard curve was produced by plotting the mean absorbance for each standard in triplicate on the y-axis against the concentration on the x-axis and a line of best fit was plotted through the data points. Sample concentrations were determined by taking the 450nm absorbance (corrected for

540nm) plus the intercept value of the standard curve divided by the graph coefficient.

For analysis of the T cell cytokine profile, 5×10^5 tsDC were seeded in T25 flasks and incubated with IMDM media containing activating treatments for co-culture experiments, as described in section 2.11. At the end of the incubation period, non-adherent T cells were collected by centrifugation at 1000xg for 5 minutes at room temperature and sample media were stored at -80°C until use. For IFN- γ , 96 well ELISA plates pre-coated with murine IFN- γ capture antibody were used as per the manufacturer's guidelines.

2.20 Nanoparticle imaging by Transmission Electron Microscopy

Transmission Electron Microscopy (TEM) was used to provide high resolution intracellular images for nanoparticle binding to tsDCs. tsDCs were cultured to 80% confluence and treated with UPN or TPNs as described in section 2.10. Detached cells were collected by centrifugation at 300xg in 1.5ml microtubes and transferred to the TEM unit. Briefly, cells underwent primary fixation in glutaraldehyde for 1 hour at room temperature followed by a 5 minute wash in cacodylate buffer (0.2M in H_2O) for 5 minutes. Samples were then additionally fixed in 1% osmium tetroxide in cacodylate buffer (2.5ml 2% osmium tetroxide stock in 2.5ml cacodylate buffer) overnight at 4°C in order to further crosslink cellular structures into a matrix to preserve cellular structure during treatments and electron scanning.

Samples were 4 washed four times (each 5 minutes) in cacodylate wash buffer, followed by 30 minutes incubation in 1% uranyl acetate (2ml 2.5% uranyl acetate filtered stock +2.5ml H_2O) to provide negative cell staining. The stained samples were then dehydrated *via* centrifugation and the pellet was re-suspended through a series of 3 washes in ethanol for 15 minutes with increasing concentration (30%, 50% and 70%, respectively) followed by overnight incubation in 70% ethanol. Following overnight incubation, samples were sub and re-suspended through further ethanol dilutions of 90% and 100% for 15 minutes, before embedding in propylene oxide (two cycles, 15 minutes each). Samples were then transferred to a 1:1 mixture of propylene oxide and full resin for 1 hour, before transferring to full resin for 60 minutes. Full resin was replaced fresh three times for 1 hour, before embedding in fresh araldite for 48 hours at 60°C . Samples were then removed from the oven and allowed to stand for a further 48 hours before sectioning. Sectioning was carried out

by Mrs Ann Lowry using a Leica EM UC6 ultramicrotome and imaged on JEOL 2010 High Resolution Transmission Electron Microscope.

2.21 Assessing antigen uptake using FITC-OVA model antigen

Antigen uptake capability was determined using FITC-labelled ovalbumin (FITC-Ova) as an established model antigen. tsDC were seeded in 1.2ml treatment media at 2×10^5 in 24 well plates and left to adhere overnight. Once adhered, well contents were aspirated before 800 μ l fresh media containing 2.5 μ M of activating treatments were added (as outlined in figure 2.4). Positive control wells were treated with 10 μ g/ml LPS. After 20 hours incubation at 37°C + 5% CO₂, FITC-Ova was added to all wells to a final concentration of 500 μ g/ml and incubated for a further 4 hours protected from light. For the final 10 minutes, PE-labelled CD86 (Biolegend) was added to each well to a final concentration of 4 μ g/ml and incubated at room temperature protected from light. After 10 minutes, labelling media was removed from the cells and four wash cycles were carried out with 1ml PBS + 0.05% Tween. Live cells were incubated in 800 μ l Fluorobrite media (Thermo Fisher Scientific) and imaged on the ImageXpress fluorescent microscope (Molecular Devices). Images were analysed using ImageJ analytical software.

2.21.1 Antigen uptake image analysis

NIH freeware ImageJ was used for the quantitative analysis of fluorescent images. JPEG images of each wavelength acquired were opened individually and converted to 8bit greyscale images. Colour overlays were added corresponding to fluorophore labels. CD86-labelled images were overlaid with FITC images using 40% transparency (figure 2.9).

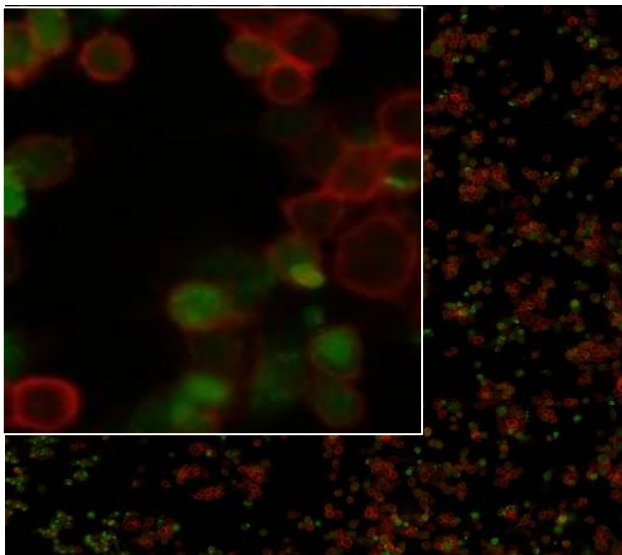


Figure 2.9: False colour overlay of MTP40 activated tsDC

tsDC FITC-Ova antigen uptake (green overlay) with PE-labelled CD86 (red) imaged under 100x and 400x total magnification.

2.22 Cell viability

Cellular viability was analysed in response to activation treatments for both tsDC and T cell lines. Activation experiments were set up as described in section 2.10 and 2.11, respectively. Following 24-hour incubation, activation media were aspirated and 100µl fresh IMDM media containing 2×10^4 T cells in suspension were added per well. DC were co-cultured with T cells at a 1:10 ratio for 24 hours before adding 20µl CellTiter Aqueous reagent (Promega) per well. Plates were incubated at 37°C and absorbance at 490nm resulting from formazan product formation was recorded at 6-hour, 8-hour, and 24-hour time points post reagent addition (figure 2.10). T cells stimulated with 10nM phorbol-12-myristate (PMA) + 2µM ionomycin were used as a non-specific positive control population to identify changes in T cell metabolism following DC-induced priming.

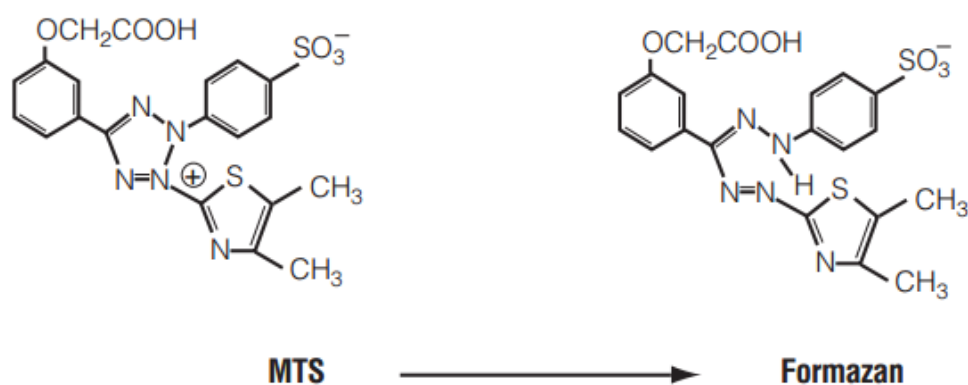


Figure 2.10 : MTS tetrazolium substrate conversion to formazan product

Reduction of the aqueous tetrazolium substrate during cellular metabolism results in the purple coloured formazan product detected at 490nm in the Promega CellTitre assay.

Chapter 3: Characterisation of a CD40R-targeting peptide (MTP40) and its conjugation to multivalent scaffolds

As discussed in section 1.2.2.2, CD40R stimulation has shown excellent potential to induce immune activation in the tumour environment of *in vitro* and *in vivo* models, but has as yet achieved limited translation into the clinic due to the limitations imposed by tolerance and cytotoxicity. Based on the potential for peptide therapies to provide improved therapeutic benefit compared to antibody based systems, the current chapter aims to investigate the capacity of a CD40R targeting peptide (MTP40) to induce outputs associated with activation in a the DC line tsDC.

Synthetic peptides are used in structure and function studies of biomimetic modelling and in the development of new drugs and vaccines. These peptides are involved in diverse aspects of human physiology from hormone function to anti-infective therapeutics, growth factor signalling, and ion channel binding. Peptide therapies are recognised for their high selectivity, and are commonly regarded as a safe and well-tolerated treatment option, with 140 clinical trials involving peptide therapeutics being launched in 2015 alone (Fosgerau & Hoffman, 2015).

The CD40R-targeting peptide used in the present research was based on previous work by Yu et al., 2013 in which the CD40L analogue (NP31) was developed by selective phage display. The original study demonstrated that the synthetic cyclic peptide NP31 could competitively inhibit binding of an enriched phage pool to human CD40R with an IC₅₀ of 440nM in a dose-dependent manner. Furthermore, the work by Yu et al., 2013, suggests that binding to the CD40R could be enhanced through multivalent presentation of NP31.

This chapter aims to address the following:

- Confirming the chemical composition of MTP40
- Determining the specificity of MTP40 for the CD40R
- Determining the dissociation constant and binding affinity of MTP40
- Demonstrating whether multivalent presentation of MTP40 alters its capacity for receptor binding

3.1 Theoretical sequence of MTP40

Building on the original work by Yu et al., 2013, NP31 was linearised by substituting one of the two cysteine residues for alanine to prevent intramolecular disulphide bridge formation while retaining similar hydrophobic properties. Based on the new linear sequence (illustrated schematically in figure 3.1), MTP40 had a theoretical mass of 2034Da.

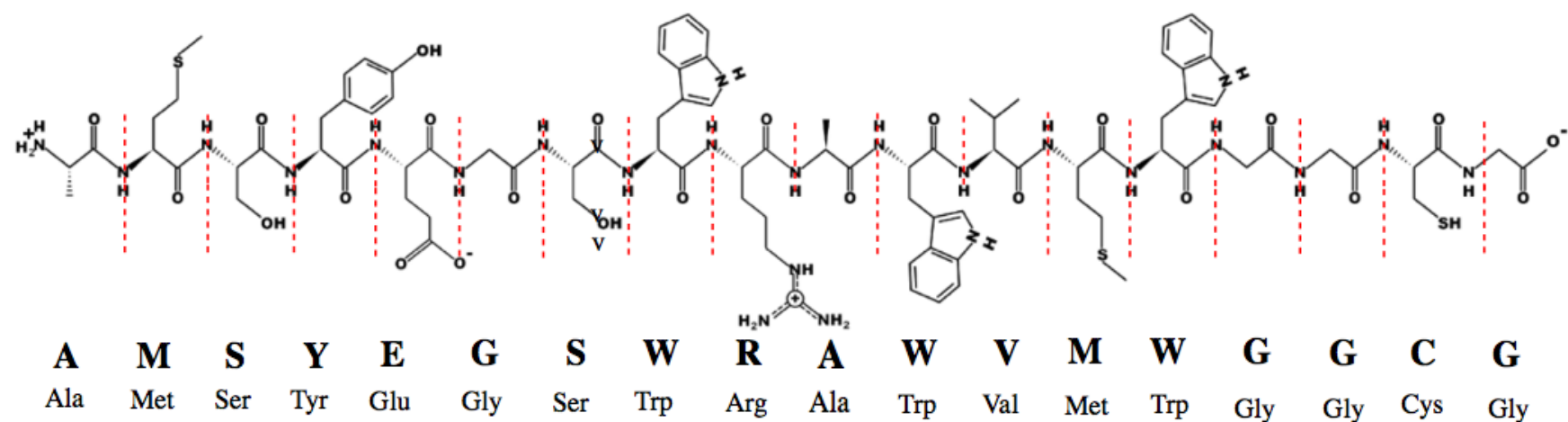


Figure 3-1: Hypothetical structure of MTP40 generated using the Tulane University Peptide Characterisation Tool

Expected characteristics of the MTP40 peptide included a predicted pI of 6.17, hydrophobicity of +11.06 Kcal and extinction coefficient of 17990M^{-1} . The amino acid sequence correlated with atomic structure $\text{C}_{91}\text{H}_{124}\text{N}_{24}\text{O}_{24}\text{S}_3$ and had an expected mass of 2034Da.

3.2 Chemical analysis of MTP40 via mass spectrometry

Chemical analysis was required to support the theoretical composition of MTP40. Mass spectrometry (MS) in proteomics enables the user to determine protein structure and interactions and identify specific proteins and peptides based on the mass of their fragments. As an analytical technique, MS ionises chemical species and sorts the ions based on a mass to charge ratio (m/z). Ionised fragments are analysed by the intensity of the current generated by ions deflected into the detector within a specific range. MS allows the user to accurately determine the purity of a sample, measure MW, and where appropriate, determine de novo characterisation of a peptide or protein (Chowdhury et al., 1990). The chromatogram for MTP40 was provided by Peptide Synthetics (figure 3.2).

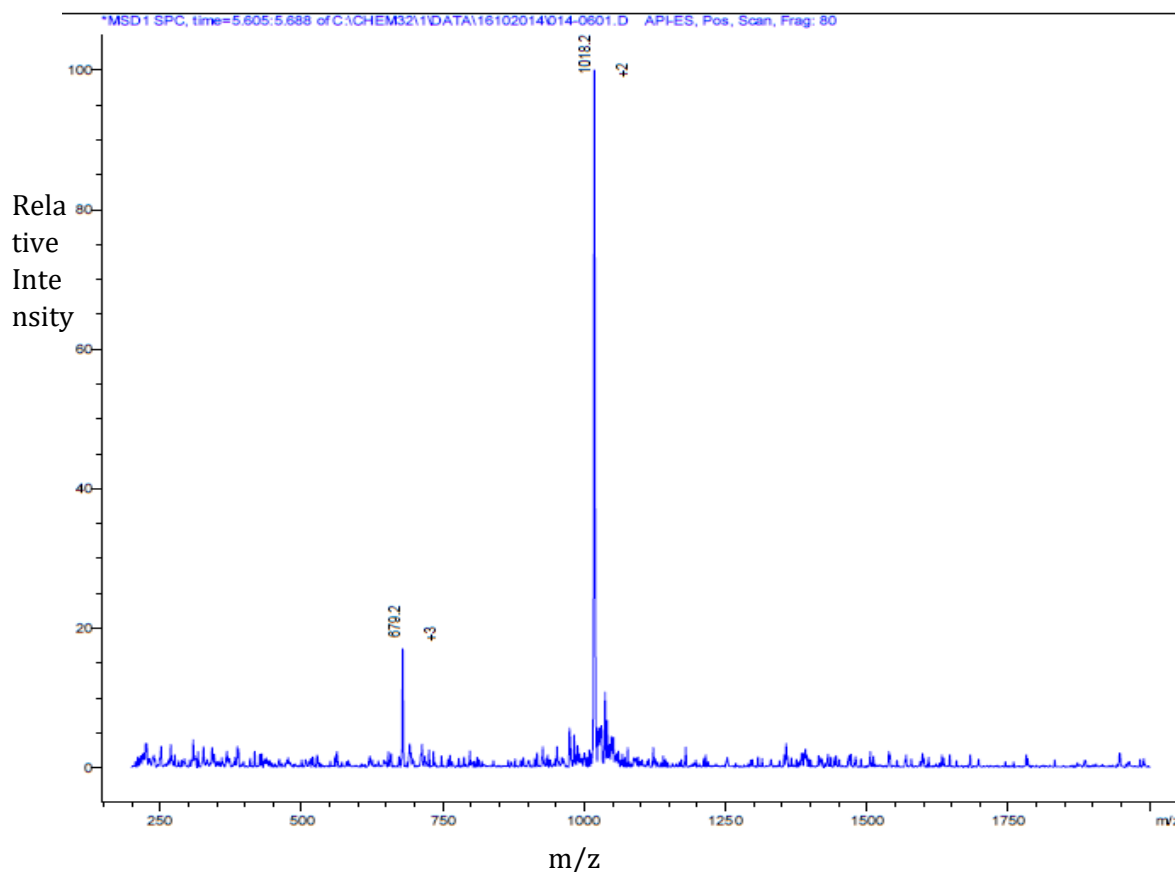


Figure 3-2: API-ES analysis of the MTP40 sample using a 130A 4.6x50mm column on 10-90% acetonitrile gradient for 8 minutes at 80°C

Two peaks were identified at 1018.2m/z and 679.2m/z during the chemical analysis of MTP40 by mass spectrophotometry.

The analysis from Peptide Synthetics revealed two characteristic peaks at 1018.2(⁺²) and 679.2(⁺³). For singly charged species, the observed mass should correspond to the expected monoisotopic mass of the analyte, which was expected to be 2034m/z for MTP40. Larger molecules have a greater chance of ion collisions in the mass spectrometer and as such, acquire multiple electrostatic charges per molecule. Doubly charged molecules presented a peak at 1018.2m/z, exactly half the mass of the singly charged molecular ion. The second peak represents fragments from the triply charged ion, equating to one third of the original peptide mass at 679.2m/z.

3.3 MTP40 specificity for the CD40R determined by *in vitro* pull down assay

As the original NP31 sequence was modified, an *in vitro* pull down assay was used to determine whether the MTP40 had retained the ability to bind to the CD40R. Pull down assays allow selective isolation of a certain protein or peptide from a complex solution and relies on specific protein-protein interactions. Pull down assays most commonly involve the use of protein-specific antibodies associated with a matrix material bead. Common pull down supports include avidin biotin matrices, glutathione-S-transferase (GST) tag systems, and histidine-tagged protein selection. Streptavidin matrices are a popular choice for pull down assays due to the high affinity of the interaction. To prepare MTP40 for analysis by pull down assay, MTP40 was biotinylated at the primary amine through N-hydroxysuccinimide (NHS) ester reaction and analysed by Kevin Welham from the University of Hull by MALDI-MS (figure 3.3).

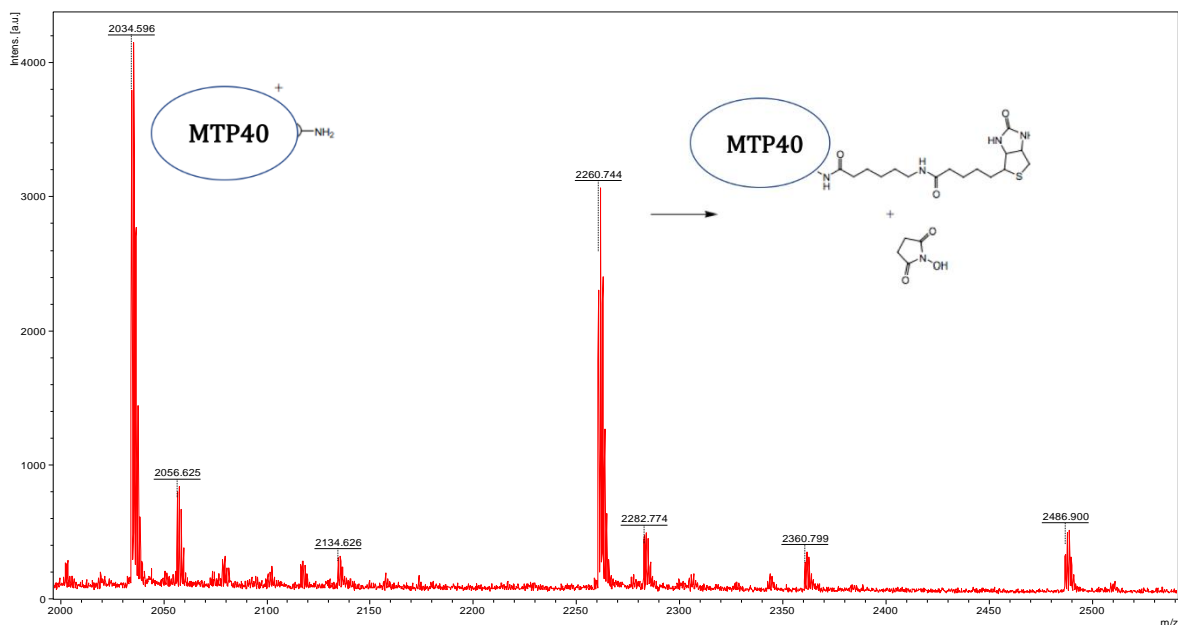


Figure 3-3: Low-resolution MALDI-MS chromatogram of biotinylated MTP40

Mass spectrometry of the biotinylated MTP40 revealed a major peak at 2034m/z and a second peak at 2260m/z.

Based on the MW of MTP40 (2034Da) plus EZ-Link NHS-Biotin (MW 341.38Da), the estimated mass of the reacted product was initially expected to occur at 2375.88m/z. Instead, a clear peak was observed at 2260m/z, which can be explained by the loss of the N-hydroxyl-succinimide (MW 115.09Da) from the biotin molecule during electron spray in the MS. Mass spectrometry findings suggest incomplete biotinylation because a substantial amount of the MTP40 was not bound to NHS-biotin, as demonstrated by the peak observed at 2034m/z.

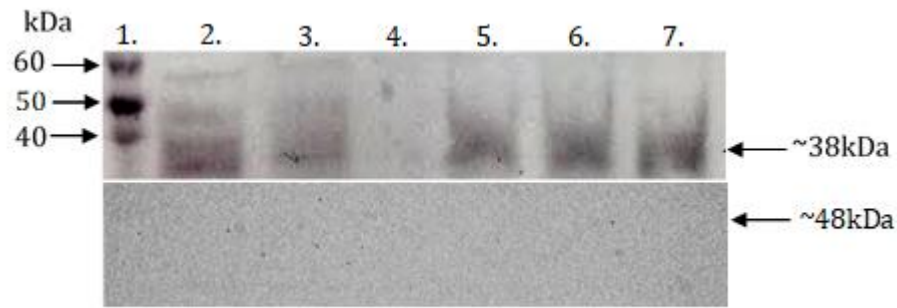


Figure 3-4: Pull down assay of the CD40R probed with Abcam anti-CD40R

Pull down assay of the CD40R from LPS-treated DC lysates incubated with 10 μ g/ml LPS for 24 hours at 37 $^{\circ}$ C + 5% CO₂. Lane contents from left to right: 1) Novex Sharp Pre-stained MW ladder; 2) CD40R pull down eluate n1; 3) CD40R pull down eluate n2; 4) Empty spacer well; 5) Flow through from CD40R pull down n1; 6) Flow through CD40R n2; 7) Whole cell extract. **Panel A)** Membrane probed with 1 μ g/ml Anti-CD40R from Abcam (ab140043) overnight at 4 $^{\circ}$ C in TBS + 3% BSA. Following three washes, membrane was incubated with secondary anti-rabbit HRP (1:10,000) for 1 hour at 4 $^{\circ}$ C. **Panel B)** Membrane re-probed with 1 μ g/ml anti- β -actin in TBS + 3% BSA overnight after stripping with Thermo Scientific stripping buffer for 15 minutes at room temperature.

When probed with anti-CD40R antibody from Abcam, bands at ~38kDa were detected, confirming the receptor had been successfully isolated from whole cell lysates. The CD40R from tsDC lysates was therefore assumed to have successfully bound to the Streptavidin Dynabeads coated with MTP40 peptide. The receptor must have remained bound through repeated wash steps. Bands were only observed when probed with anti-CD40R, and did not demonstrate a signal when the same membrane was subsequently incubated with stripping buffer and re-probed with anti-actin antibody (shown in panel B). This suggests that the protein band visualised by western blot was specific for CD40R as opposed to non-specific interaction between streptavidin or MTP40 and other proteins in the whole cell lysate. This observation confirmed that streptavidin beads successfully bound biotinylated MTP40, which in turn retained the capacity to specifically bind the CD40R from tsDC lysates. Bands were observed at the same MW in the flow through volume of both samples, which is likely to be caused by surplus CD40R remaining in the whole cell lysate after the MTP40 became saturated. These bands were expected as a high lysate volume was added from tsDC which had been pre-stimulated by 10 μ g LPS for 24 hours to upregulate CD40R expression, to ensure bead saturation. Lane 7 contained whole cell lysate from tsDC incubated with 10 μ g/ml LPS for 24

hours. This was included as a positive control to confirm presence of CD40R in the tsDC sample.

3.4 Characterising MTP40 bound to flexible multivalent scaffolds

3.4.1 Quantifying MTP40 conjugation to streptavidin

Peptides alone are often too small to elicit a sufficient immune response and may therefore be conjugated to a carrier scaffold molecule to elicit effective immune priming. Presentation of multiple peptide units per scaffold allows multiple receptors to be engaged synchronously, increasing the strength of interaction and therefore, the potentiation of downstream signals. The ability for multivalent delivery systems to specifically engage multiple receptors on the immune cell surface, has been demonstrated in vaccine therapies (Smith., 2010) and more recently, in tumour-specific vaccinations (Valkenberg., 2014; Oh et al., 2016).

Before investigating the biological activity of MTP40, it was essential to confirm that MTP40 could be quantifiably conjugated to a multivalent scaffold. In the original study by Yu et al., 2013, conjugation of NP31 peptide to tetrameric streptavidin molecules resulted in enhanced binding affinity. Yu et al demonstrated that while monomeric NP31 displayed an IC₅₀ of 84nmol/L, NP31 bound to tetrameric streptavidin construct demonstrated an IC₅₀ of 215nmol/L, equating to 2.5 fold higher affinity. Multimeric presentation is hypothesised to improve binding stability as interaction between CD40R and CD40L *in vivo* takes place in a trimeric conformation, and may therefore require multivalent presentation. Streptavidin also provides an attractive model system as the streptavidin-biotin complex is the strongest known non-covalent interaction between a protein and ligand ($K_D = 10^{-15}M$). The strength of the interaction renders it unaffected by fluctuations in pH, temperature, organic solvents, and other denaturing conditions. Consequently, streptavidin is well utilised across an array of immunological applications, including ELISA, immuno-histochemistry (IHC), western blotting, and cell surface labelling.

MTP40 binding to the streptavidin scaffold was quantified based on absorbance of streptavidin labelled with FITC fluorophore at 280nm and 493nm. Absorbance measurements were recorded in triplicate from both the stock streptavidin substrate and Tet40 product. FITC-labelled streptavidin was provided as a 19µM stock solution by Thermo Fisher Scientific. MTP40 was solubilised as described in

section 3.4.3 to 1mg/ml and incubated with FITC-labelled streptavidin to produce a Tet40 as detailed in section 2.6.2. Fresh Tet40 was synthesised prior to each experiment.

Following substrate reaction and purification, the absorbance of the Tet40 product was recorded at 280nm and 493nm. The concentration of streptavidin in the Tet40 product was calculated based on the observed absorbance of the product at 493nm. This approach provided a logical method to calculate streptavidin concentration in the reacted product because absorbance at 493nm could only result from the FITC-labelled streptavidin as no absorbance was observed from MTP40. Once the concentration of streptavidin molecules was determined for the sample, this value was then divided by four, to account for the four MTP40 molecules bound to each streptavidin scaffold. The method for calculating tetramer concentration is outlined in figure 3.5, overleaf.

Observed values:		Concentration (μM)	Observed A_{280}	Observed A_{493}
Stock MTP40		2465	0.46	0.02
Stock Streptavidin		19	15.75	5.83
Tetramer			12	4.08
Calculated values:				
A)	Streptavidin concentration in tetramer (μM)	13.30		
B)	Tetramer A_{280} resulting from streptavidin		11.02	
C)	Tetramer A_{280} resulting from peptide		0.98	
D)	Peptide concentration in tetramer (μM)	13.23		

=Tet A_{493} * Strep (μM)
Strep A_{493}

=Strep in tet(μM) * Strep A_{280}
Stock Strep (μM)

=Total Tet A_{280}
- A_{280} from strep

Tet A_{280} from MTP4C
 $4 * \text{MTP40 ExCo} * 10^6$

Figure 3-5: Excel file format for calculations determining the concentration of Tet40 reactions based on absorbance.

A) The theoretical concentration of streptavidin in the Tet40 was calculated by multiplying the stock concentration of streptavidin by the observed A_{493} of the Tet40 and divided by the observed A_{493} of the stock solution. B) The A_{280} of the Tet40, which resulted from streptavidin, was calculated based on concentration of streptavidin in the Tet40. This value was calculated by multiplying the Tet40 A_{280} from streptavidin by the A_{280} of stock streptavidin and divided by the stock concentration of streptavidin. C) The A_{280} of the Tet40, which resulted from MTP40, was calculated by subtracting the A_{280} produced by streptavidin stock from the observed A_{280} of the Tet40 product. D) Peptide A_{280} was converted into a molar concentration by dividing the remaining absorbance by the extinction co-efficient of MTP40 and multiplied by four to compensate for the tetrameric presentation of MTP40 molecules on each streptavidin backbone.

This calculation was generated in-house to provide a novel method of characterising the concentration of MTP40 solutions conjugated to a streptavidin backbone.

3.4.2 Characterising the binding affinity of MTP40 presented as monomer versus tetramer to CD40R

The pull down assay preliminarily confirmed binding of MTP40 to the CD40R and confirmed that MTP40 could successfully be conjugated to a streptavidin scaffold. The next question was whether this multivalent presentation had the potential to increase the binding affinity and specificity of MTP40 for the target CD40R. Flow cytometry allows internal and external characteristics of individual cells within a fluid suspension to be measured. This method also provides a tool for analysing the number of fluorescent particles bound to the cell surface.

Saturation assays allow the user to determine the affinity or dissociation constant (K_D) of a ligand to a receptor. The K_D is equal to the ligand concentration required to occupy 50% of available target receptors. Saturation assays are commonly used to determine and characterise protein-protein interactions (Pollard., 2010), while fluorescence-based ligands present a viable and accessible alternative for the use of radio ligands for protein-protein studies (Stoddart et al., 2016). Recent studies comparing the effect of multivalent presentation of folic acid on dendrimer scaffolds by SPR *versus* FACS analysis have revealed a close correlation between the two methods. Therefore FACS analysis was able to determine surface concentration in a range representative to that determined by SPR (Hong et al., 2007).

This approach allowed direct comparison of the binding efficacy monomeric MTP40 *versus* that of tetrameric Tet40 construct by treating samples with identical concentrations under the same conditions. Increasing concentrations of FITC-labelled MTP40 or FITC-labelled Tet40 were reacted for 1 hour until steady state conditions were reached. Once the population had been successfully gated on the flow cytometer to select the main cell population (eliminating cell debris or precipitated fluorescent conjugates), a histogram plot was set to include only fluorescent signal detected from cells in the gated population. At the setup of each new experiment, negative controls were adjusted to fall within the 10^0 and 10^{-1} boundary of the log scale. Once controls were set within an acceptable range, marker regions were applied to differentiate between negative and positive populations. Binding of fluorescent constructs to the cell surface caused the histogram to shift to the right as intensity increases. Notably, increased fluorescent labelling was observed in tsDC incubated with fluorescent MTP40 compared to

fluorescent Tet40 across the entire range of treatment concentrations (figures 3.6 and 3.7).

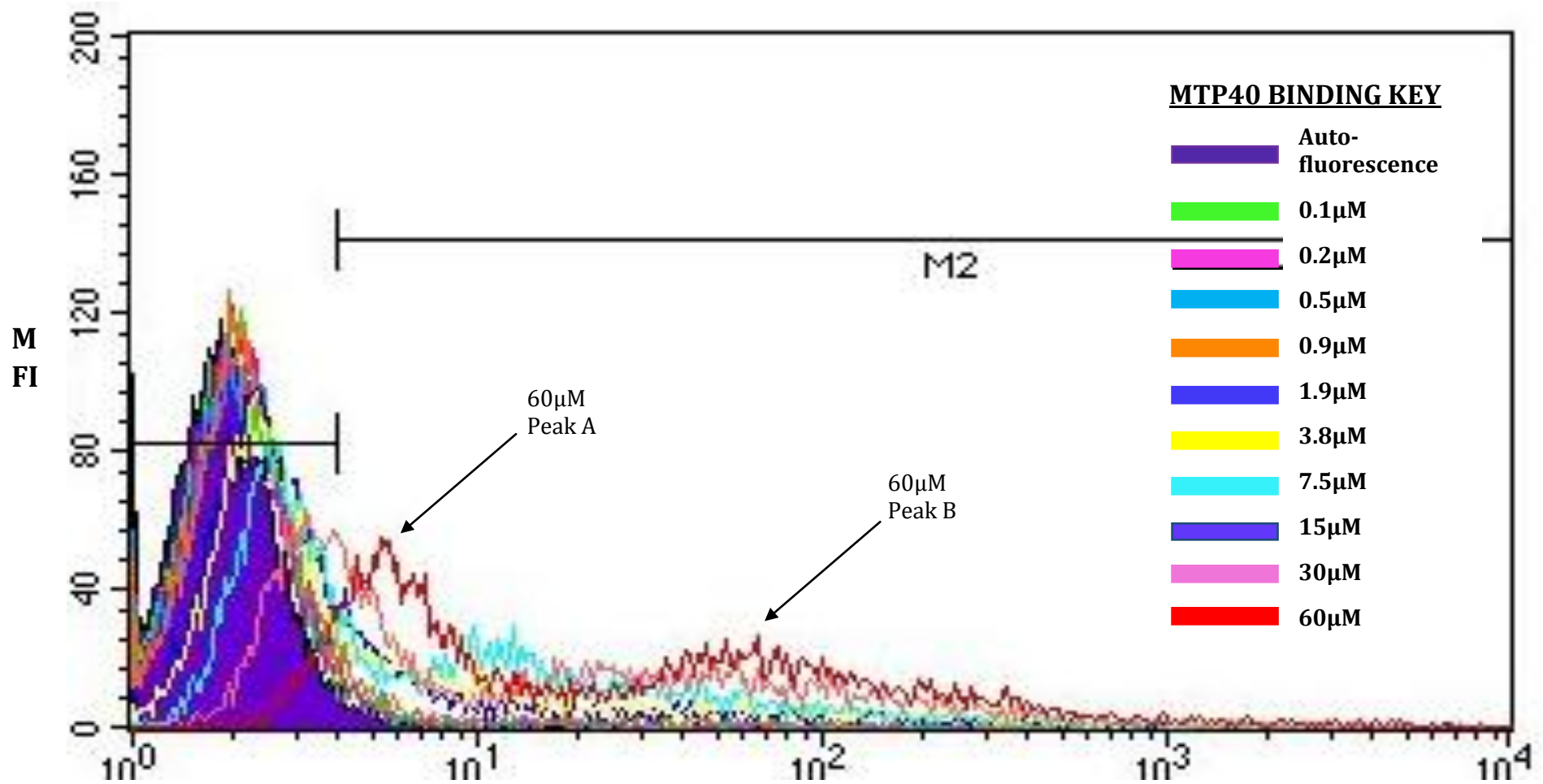


Figure 3-6: Histogram overlay of fluorescently labelled MTP40 titrations to CD40R on the tsDC surface

Wells containing 1×10^5 LPS activated tsDC were incubated with serial dilutions of MTP40 labelled with NHS-Dylight488 for 1 hour at 4°C . After gating the primary cell population, geometric means of individual sample histograms were taken to determine the geometric mean values of cells positive for fluorescence under FL1 excitation. Overlay of the geometric mean fluorescence (GMF) is provided to visually illustrate the shift in binding correlated with treatment concentration. Two fluorescent peaks were observed in response to monomer treatment at high concentrations, as indicated by arrows in the figure. Figure illustrates a representative histogram display chosen at random out of $n=5$ replicates.

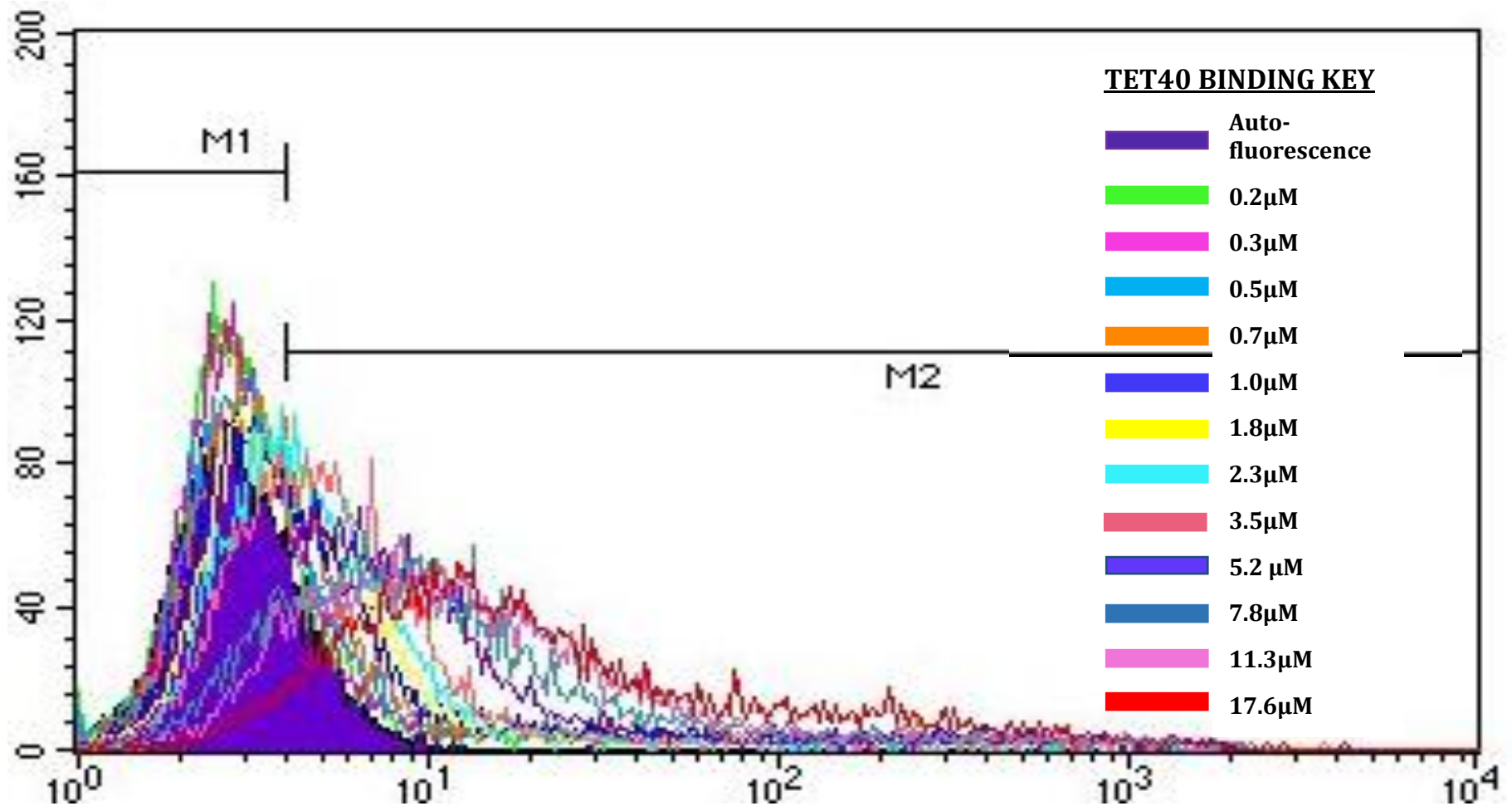


Figure 3-7: Histogram overlay of fluorescently labelled Tet40 titrations to CD40R on the tsDC surface

Wells containing 1×10^5 LPS activated DC were incubated with serial dilutions of Tet40 labelled with NHS-Dylight488 for 1 hour at 4°C . After gating the primary cell population, geometric means of individual sample histograms were taken to determine the geometric mean values of cells positive for fluorescence under FL1 excitation. Overlay of the geometric mean fluorescence (GMF) is provided to visually illustrate the shift in binding correlated with treatment concentration. Figure illustrates a representative histogram display chosen at random out of $n=3$ replicates.

Analysis of CD40R binding by FITC labelled MTP40 showed that two fluorescent peaks were observed in response to treatment with high concentrations of MTP40. This observation suggests that receptor binding by MTP40 was inconsistent because a large portion of the cell population displayed no fluorescent labelling, as indicated by the major peak overlaying the negative control for auto-fluorescence. A small number of cells from each sample exhibited a positive shift to the right, which may have resulted from MTP40 aggregation at the cell surface through disulphide bonds, or from heterogeneous expression patterns of the CD40R in the tsDC population following activation with LPS. In the latter case, tsDC expressing a high number of CD40R would need a greater concentration of MTP40 to saturate the cell surface in this subset of the tsDC population.

tsDC incubated with FITC labelled Tet40 revealed a single peak with decreased fluorescence compared to MTP40. This may result from Tet40 occupying multiple receptors simultaneously, meaning fewer fluorescent Tet40 molecules are required to saturate the equivalent number of receptors (1:4 binding) compared to monomeric presentation (1:1 binding).

The representative overlay in figure 3.8 demonstrates the shift in fluorescence peak between MTP40 and Tet40 binding across a range of concentrations. To illustrate this shift more clearly, figure 3.8 isolates the fluorescence peak observed in a representative image of DC incubated with MTP40 *versus* Tet40.

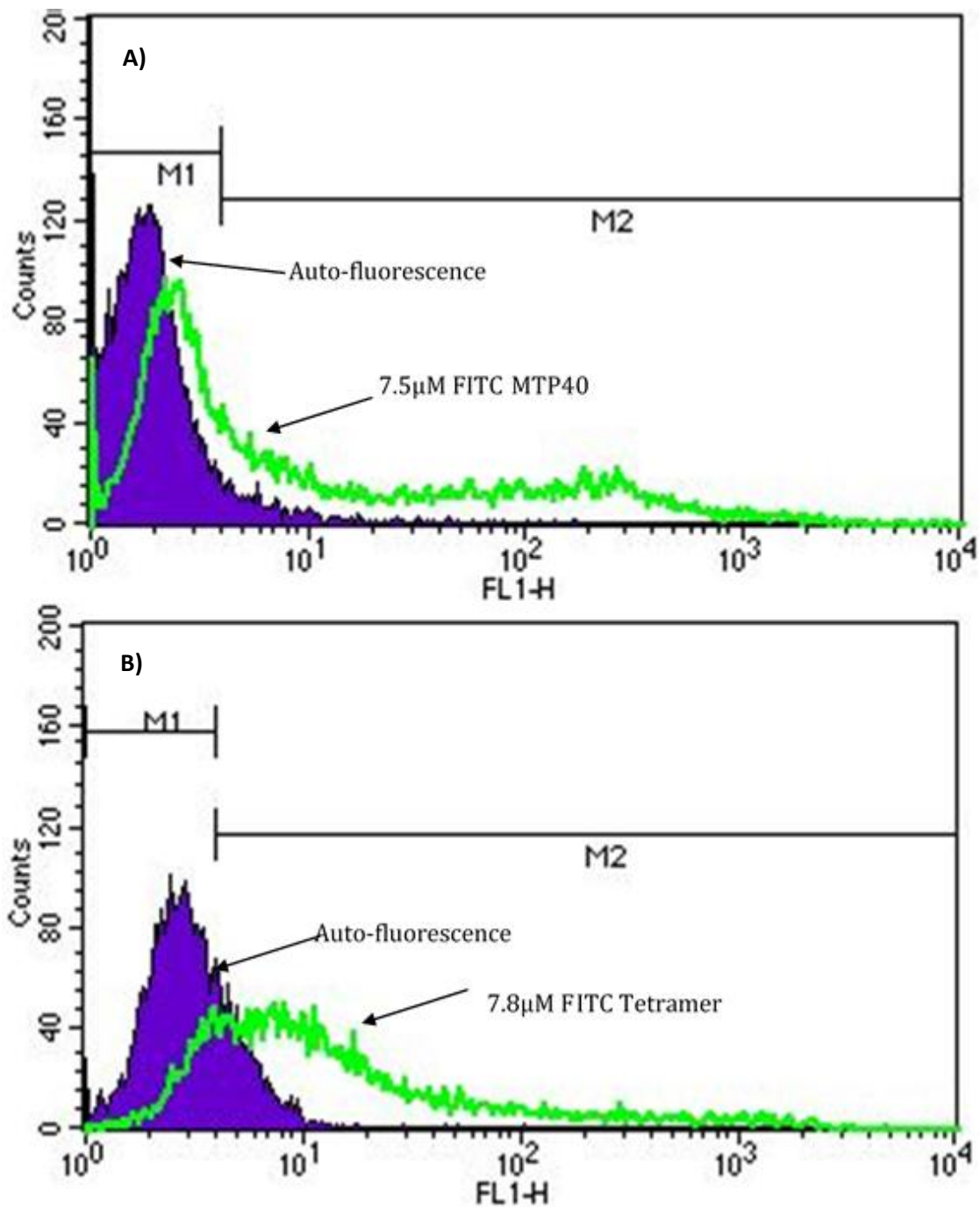


Figure 3-8: Comparison of MTP40 *versus* Tet40 binding patterns acquired by flow cytometry

Histograms illustrate the binding patterns of fluorescently labelled MTP40 *versus* Tet40 at comparable concentrations. Panel A) tsDC treated with $7.5\mu\text{M}$ FITC-MTP40. Panel B) tsDC treated with $7.8\mu\text{M}$ FITC-Tetramer.

Differential binding peaks were observed in DC treated with FITC-MTP40 *versus* FITC-Tet40. Aligning the histograms of comparable concentrations of MTP40 and Tet40 treatments highlights the differential fluorescent peaks between the two

treatments (figure 3.8). Treatment with fluorescently labelled MTP40 continued to show increased binding to the DC surface with treatment concentrations up to 60 μ M, while Tet40 treated cells demonstrated negligible shift in the fluorescent peak in populations treated with concentrations above 7.8 μ M.

This finding suggests that CD40Rs on the DC surface became saturated by Tet40 constructs at a lower concentration than the equivalent MTP40. Subsequently, the geometric mean values from n=3 replicates were transferred to Graphpad for quantitative analysis. Quantitative analysis demonstrated that the concentration required to reach the K_D with MTP40 (1.32 μ M) was significantly reduced when conjugated to the tetrameric streptavidin scaffold (0.07 μ M), showing increased affinity in the region of \log_{10}^2 (figure 3.9). For example, higher K_D values equate to a greater amount of substrates A and B being required to form the product AB and therefore, a lower binding affinity of the substrates. The significant reduction in K_D value of the Tet40 compared to MTP40 illustrates increased binding by multivalent presentation.

The original CD40R targeting peptide sequence extracted from the NP31 phage by Yu and colleagues in 2013 demonstrated micromolar affinity for the CD40R (0.44 μ M). The binding affinity of the original construct was initially reduced by modification by substituting cysteine residues to produce the linear sequence of MTP40 (K_D 1.32 μ M). In the present research however, the binding affinity was recovered and in fact improved through multivalent presentation on the streptavidin scaffold (K_D 0.07 μ M) , suggesting that tetrameric presentation of MTP40 increased binding affinity beyond that of the original targeting sequence.

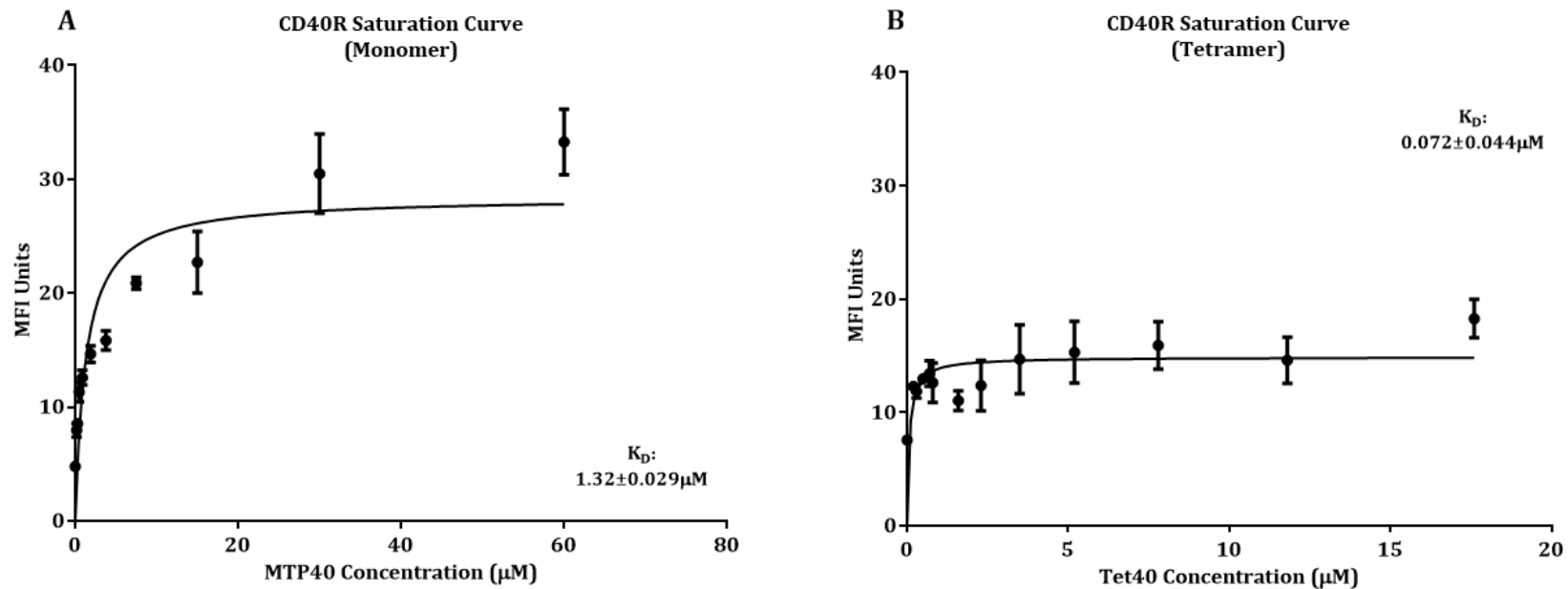


Figure 3-9 Kinetics of CD40R binding specificity of MTP40 and Tet40 analysed by flow cytometry

CD40R saturation data was acquired by flow cytometry across a range of concentrations. Panel A) The saturation curve of MTP40 binding to DCs. Panel B) The saturation curve of Tet40 binding to DCs. MTP40 labelled with Dylight 488. Data are representative of n=5 experiments. Tet40 containing FITC-labelled streptavidin data represent n=3 experiments. Data are depicted as Mean Fluorescence Intensity (MFI). Saturation curve was fit using a single-site model of receptor binding with Graphpad Prism version 5 software.

3.4.3 Visualisation of Tet40 binding to tsDC by fluorescent microscopy

Fluorescent microscopy was used to determine the extent of non-specific streptavidin binding *versus* specific Tet40 binding following incubation with tsDCs. tsDC treated with FITC-MTP40 or FITC-Tet40 were visualised by microscopy (figure 3.10).

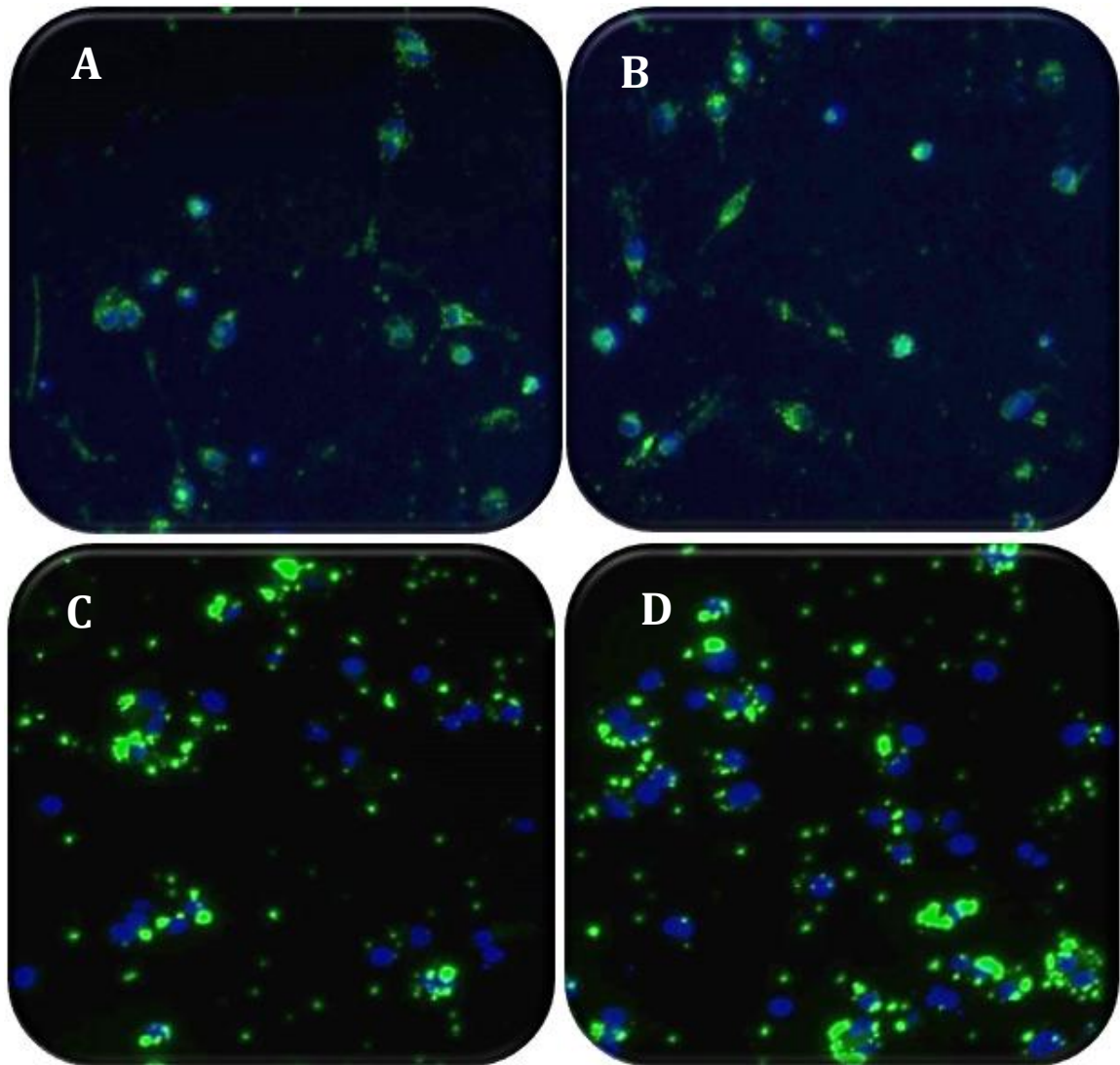


Figure 3-10: Fluorescent binding images of FITC-MTP40 and FITC-Tetramer to CD40R at the tsDC surface

Panels A & B) tsDC were treated with 2.5 μ M of FITC-labelled streptavidin (green) for 1 hour at 4°C. Panels C & D) tsDC were treated with 2.5 μ M of FITC-labelled tetramer (green) for 1 hour at 4°C. All wells were counterstained with NucBlue (blue) for 10 minutes at room temperature prior to image acquisition at 400x total magnification.

Panels A and B illustrate a cytosolic binding pattern which suggests streptavidin may have interacted with tsDCs non-specifically by phagocytosis. When bound to MTP40, non-specific binding was no longer apparent and was replaced by intense staining around the extracellular surface, suggesting that MTP40 bound to streptavidin as Tet40 prevented non-specific uptake of streptavidin by tsDCs due to a specific interaction with the CD40R at the cell surface.

3.5 Characterising MTP40 bound to rigid multivalent scaffolds

3.5.1 Quantification of MTP40 conjugation to gold nanoparticles by optical properties

Following the observation that tetrameric presentation of MTP40 resulted in significantly higher binding avidity for the CD40R, it was considered that increasing the number of ligands presented on the scaffold and the characteristics of the scaffold itself, may also impact the avidity and specificity of binding. Gold nanoparticles possess several unique characteristics which make them a strong candidate for drug delivery platforms, which are discussed in section 1.8. Therefore, **Untargeted Polyvalent gold Nanoparticles (UPNs)** were investigated as an additional multivalent platform to investigate how multivalent presentation affects the activating potential of MTP40.

Following incubation with 25nm UPN for 48 hours, MTP40 binding to the surface of gold dots was confirmed by absorbance at 280nm and total absorbance spectra. Also, following incubation with MTP40, a specific increase in absorbance was observed in targeted samples compared to untargeted controls. Total absorbance increased on average by 5nm, with a range between 4-6nm. UPN demonstrate peak absorbance around 520nm in the visible region, which is affected by particle size and therefore, MTP40 binding. As such, reactions demonstrating a shift in absorbance peak less than 4nm and greater than 6nm were discarded. As the particle diameter increased, the absorbance band visibly widened as illustrated in figure 3.11 likely to result from the increased light scattering associated with increased surface size and complexity.

The inherent interaction between the thiol side chain of cysteine residues and gold is commonly used to conjugate peptides to the surface of UPN, with incubation times varying from 30 minutes at room temperature to 72 hours at 4°C. Following incubation, samples are commonly purified by dialysis or centrifugation with

MWCO filter units suited to the application and size of the nanoparticles and peptide under investigation. Conjugation is almost universally confirmed based on a shift in the UV absorption spectra of UPN (Bastus et al., 2009; Parker et al., 2007). Additional confirmation is often provided by dynamic light scattering or raman spectroscopy profiles of the sample.

After separation by centrifugation at 12,000xg for 5 minutes, the UPN controls displayed absorbance at 280nm between 0.7 and 0.9 absorbance units (AU). This increases to between the range of 1.7-1.9 AU following MTP40 conjugation from tryptophan, tyrosine, and cysteine residues present in the amino acid sequence. A representative example of absorbance increase at 280nm following MTP40 conjugation is presented in figure 3.11. The specific shift in absorbance spectra and increased absorption at 280nm confirmed that the MTP40 had successfully adsorbed

surface of

Panel A)

Sample	Absorbance at 280nm (AU)
Non-targeted	0.785
Targeted	1.925

to the UPN.

Panel B)

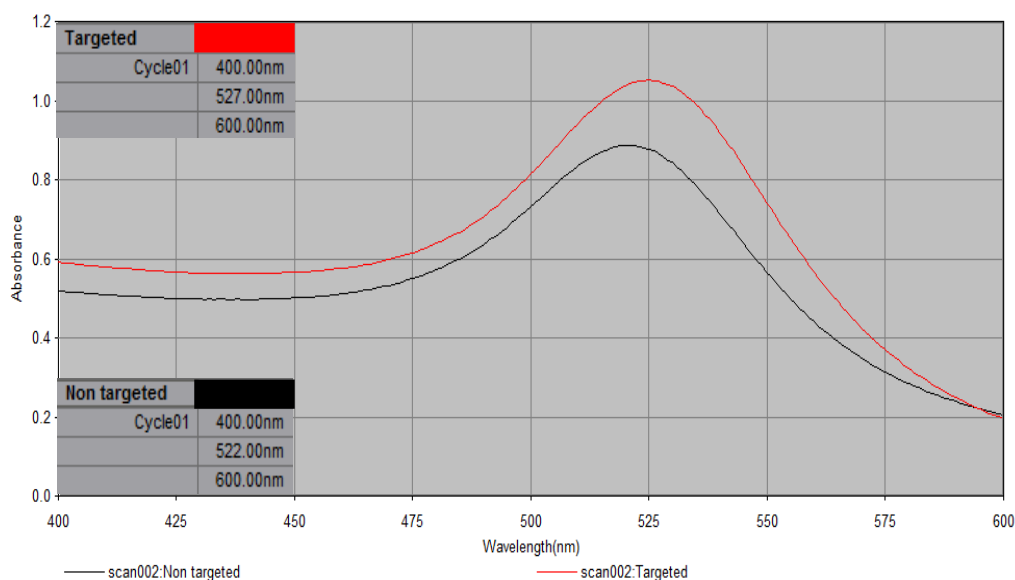


Figure 3-11: Characteristics of gold nanoparticles determined by absorbance

Panel A) Representative absorbance measurements of UPN and TPN40. **Panel B)** Absorbance spectra of UPN following MTP40 conjugation. A shift in absorbance was observed as a result of MTP40 conjugation to the surface of UPN. 500µl UPN (black

line) were incubated at 4°C with 50µl MTP40 for 48 hours with rotation to product TPN40 (red line). Reacted products were characterised by absorbance spectra immediately before cellular treatments, to ensure product quality.

3.5.2 Visualisation of MTP40 conjugation to gold nanoparticles by coomassie stain

Coomassie Brilliant Blue (Thermo Scientific) is commonly prepared in acidic solutions containing 25-50% methanol for the detection of proteins in gel electrophoresis. Acidic conditions permit the dye to bind basic amino acids, with the number of dye ligands being proportional to the number of positive charges found on the protein or peptide. This process allows direct visualisation of peptides and proteins in SDS-polyacrylamide gels, including MTP40 peptide conjugated to the surface of gold nanoparticles as TPN40, shown in figure 3.12.

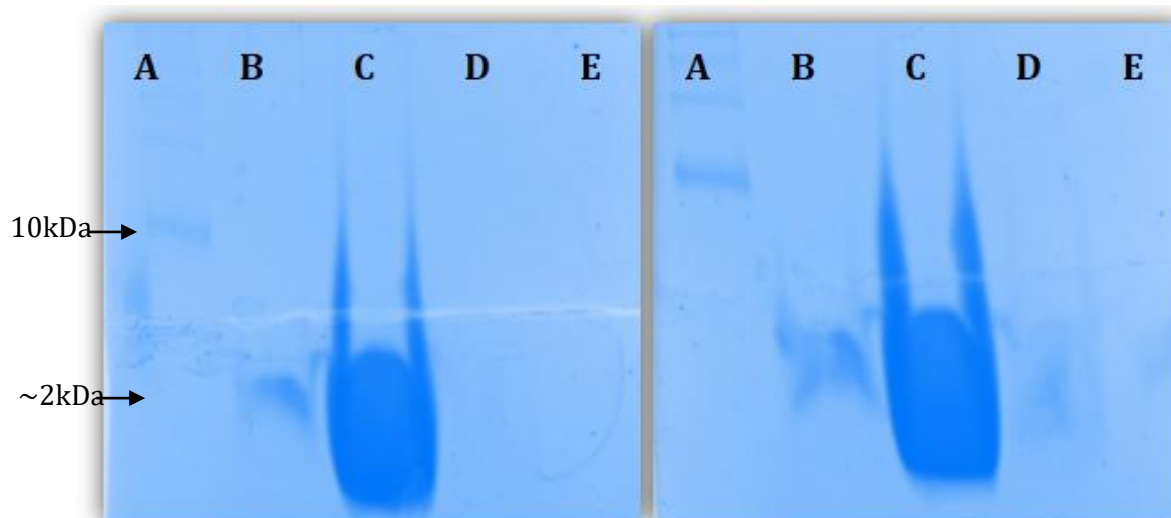


Figure 3-12: UPN and TPN40 incubated with Coomassie Brilliant Blue dye for visualisation on SDS-PAGE gels

Washed samples containing either UPN or TPN40 were mixed at a 1:1 ratio with loading buffer containing 20% β -mercaptoethanol. The samples were boiled for 5 minutes at 95°C to reduce thiol bonds and then 60µl was loaded into wells of 20% acrylamide SDS-PAGE gels for separation by gel electrophoresis. Well contents from left to right: A) Novex Sharp pre-stained MW ladder. B) Empty spacer well. C) TPN40. D) Empty spacer well. E) UPN.

To confirm that biotinylated MTP40 retained the ability to bind CD40R from tsDC when conjugated to streptavidin, it was possible to use streptavidin Dynabeads in place of the backbone to extract the receptor, dissociate by boiling under reducing conditions, and probe the product for anti-CD40R by western blot. To indicate whether the MTP40 was successfully bound to the surface of gold nanoparticles (*via*

innate interactions between cysteine and the gold surface), wells were loaded with UPN or TPN40, and probed with coomassie blue dye.

The maximum sample volume (60 μ l) was loaded into each well for coomassie staining because the characteristics of UPN in SDS gel electrophoresis were not well characterised, therefore high volumes were loaded to ensure a high enough volume of MTP40 would be present to be visualised in SDS gel. As shown in figure 3.12, wells containing MTP40-TPNs stained strongly with coomassie dye, whereas no staining was observed in the control well containing the UPN samples. Coomassie dye was expected to bind to the amino acids of TPN40 samples, while no direct interaction was expected between coomassie dye and the UPN gold nanoparticles. Gels were run for 1 hour at 100V due to the low MW (2034kDa) of linear MTP40 under reducing conditions. Novex-sharp pre-stained ladder was visible in the lane A of each gel, which indicates that the band was visualised around 2kDa. Visualisation of bands by coomassie staining indicate that MTP40 was successfully bound to TPN and retained following purification by centrifugation through Pall 10,000Da MWCO filter units.

3.6 General Discussion

Biotherapeutics including antibodies and peptides are attractive candidates for anti-cancer therapies because of their higher specificity and reduced toxicity compared to synthetic small molecules. Peptide therapies confer additional advantages over antibodies in terms of small size, potential for modification, and improved biocompatibility. As such, the main objective of the initial segment of this work was to establish that a MTP40 targeting the CD40R could bind the CD40R isolated from tsDC in culture.

To characterise MTP40, a variety of established methods were used. In summary, the data presented in the current chapter met the aim of confirming the chemical composition of MTP40 by mass spectrometry and hypothetical chemical structure. Mass spectrometry has been used as a definitive method of peptide characterisation, both for MW and amino acid sequence, for many decades (Carr et al., 1991). Here, mass spectrometry provided a reliable method to confirm the MW of MTP40. Furthermore, MTP40 was demonstrated to show specific binding for the CD40R, which was confirmed by multiple complementary methods. First, binding to CD40R

was indicated by anti-CD40R staining in pull down assay, which determined CD40R was present in wells containing MTP40. The ability of MTP40 to bind and retain CD40R from DC directly during in vitro pull down assay demonstrated a direct interaction between MTP40 and CD40R which is therefore not likely to be dependent on co-factors or interacting protein molecules.

Interactions between MTP40 and multivalent scaffolds were also assessed. Specific calculations were developed in house during this study to produce a theoretical method for quantifying the concentration of MTP40 present in a solution of Tet40 molecules. The second method used to infer binding used fluorescent microscopy to visualise the binding pattern of Tet40 to the surface of tsDC and therefore CD40R, which showed differential staining by Tet40 compared to fluorescent streptavidin control. Third, the saturation curve of MTP40 and Tet40 were produced via FACS, which confirmed that multivalent presentation via Tet40 lead to enhanced binding of CD40R, shown by a shift in KD from $1.32\mu\text{M}$ to $0.072\mu\text{M}$.

The specificity and strength of MTP40 binding to the CD40R was determined by saturation assay. The greater avidity of Tet40 for the CD40R of DCs versus affinity of MTP40 (KD $1.32 \pm 0.03\mu\text{M}$ versus KD $0.072 \pm 0.04\mu\text{M}$) suggests that enhanced receptor binding is induced in response to multivalent presentation of MTP40, which may optimise DC activation. The potential for CD40R targeted antibodies to induce anti-tumour immunity has been shown by many other research groups (Beatty et al., 2011; Vonderheide et al., 2007), however the doses required to produce clinical benefits also induce severe side effects (Nelson., 2012). Reducing the treatment concentration required to saturate CD40R at the DC surface has the potential to eliminate side effects associated with high-dose antibody treatments. Importantly, the data presented in this research indicate that the MTP40 used is indeed a potential ligand for the CD40R. Furthermore, the avidity of CD40R binding was improved by presentation on multivalent scaffolds.

The binding between MTP40 and gold nanoparticles was verified by a shift in absorbance spectra, respectively. Finally, MTP40 conjugation to GNP was confirmed by imaging on polyacrylamide gels, as the peptide was visualised by coomassie stain in wells containing TPN40, but not UPN alone. As nanoparticles continue to demonstrate potential as cancer therapies, characterising optical properties has been established as a standard method of characterising gold nanoparticles. The

changes in absorbance spectra observed in the present study were in line with observations made by other groups, based on the highly specific absorbance of gold nanoparticles at 520nm which results from particle size and surface complexity (Huang & Sayed., 2010).

Peptide drug conjugates offer select advantages compared to antibody therapies, including rapid distribution, reduced immunogenicity, ease and scalability of synthesis and affordable labelling (Reubi & Maecke., 2008). This represents some of the characteristics which make peptide drug conjugates an attractive modality for cancer immunotherapies. The data presented in this chapter outlines the conjugation of MTP40 peptide to two multivalent scaffolds, and supports the ability of MTP40 to bind CD40R from tsDC samples when presented in this manner. Successful production of multivalent targeting constructs able to bind CD40R presents a viable construct to induce and study the outputs of tsDC activation in response to CD40R stimulation.

Chapter 4: Analysis of tsDC outputs in response to CD40R Activation *via* a flexible multivalent construct

Data from the previous chapter demonstrated that MTP40 successfully bound to the surface of tsDC and that the kinetics of the interaction were vastly improved by tetrameric presentation compared to monovalent presentation. Specifically, saturation assay showed that the modified Tet40 showed improved affinity compared to the original NP31 sequence (Yu et al., 2013). Tet40 binding to CD40R showed significantly greater affinity than several of the monovalent antibodies currently involved in phase I and II clinical trials as immunotherapies, as outlined in chapter 1.5.4.

In light of the findings in the previous chapter, the work in the current chapter intended to determine whether the observed interaction between CD40R and the modified MTP40 peptide was capable of inducing phenotypic and functional changes associated with activation in the tsDC cell line.

Independent groups have shown CD40R signalling capable of triggering an immune cascade requires multivalent interactions between CD40R and CD40L at the DC surface (as discussed in section 1.6). As a result, we hypothesised activation of tsDC would produce more potent phenotypic changes when MTP40 molecules were presented *via* a multivalent scaffold than when presented as monomers, due to the ability to induce simultaneous binding of several CD40R proteins. Streptavidin presents a well-established scaffold for molecular, immunological, and cellular assays as its tetrameric structure can intensify staining detection of specific populations or interactions with, for example, low affinity T cell receptors (Wooldridge et al., 2009), and so was investigated as a model system for studying multivalent interactions, due to its innate ability to bind up to four biotinylated peptides.

Investigations in this chapter focus on identifying changes in well-known parameters associated with the DC maturation process. The innate DC function of antigen presentation relies on the DCs ability to process antigen, express co-stimulatory molecules at the cell surface required for T cell activation, and secrete co-stimulatory cytokines to shape the local environment. This rationale provided a framework to suggest outputs of tsDC which would be used to infer activation in response to CD40R targeted treatments.

The findings detailed in this chapter intend to address the following research aims:

- Characterising a positive response for tsDC activation using LPS to identify phenotypic changes induced in response to a known immune stimulating agent
- Analysing changes in tsDC receptor expression profiles following treatment with monomeric and tetrameric CD40R targeted treatments
- Assessing whether tsDC alter cytokine production in response to treatment with monomeric and tetrameric CD40R targeted treatments
- Evaluating the impact of CD40R targeting treatments on tsDC viability *in vitro*

4.1 Establishing a baseline for tsDC activation by activation using the known stimulator LPS

Before initiating DC treatments with activating compounds, a baseline for the expected changes in receptor expression following DC activation was established using LPS from the cell wall of *E. coli*. LPS was chosen as a model system to produce a known output as it is a potent, well-established immune stimulant. In its biological role, LPS is localised in the outer layer of cell membrane in gram negative bacteria, contributing to the integrity of the outer membrane and protecting the bacteria against degradation (Raetz & Whitfield, 2002). The structure of LPS consists of hydrophobic Lipid “A”, which contributes to the toxicity of the molecule alongside a core polysaccharide chain and an O-antigenic polysaccharide side chain.

To confirm that the DC population used for this work reacted to LPS in a similar manner as populations described in current literature, 2×10^4 tsDC were seeded in a 96 well flask and incubated with varying concentrations of LPS to establish whether LPS-induced changes in morphology and phenotype occurred. Changes in cell morphology observed by light microscopy provided a primary indicator of tsDC response to activating treatments (figure 4.1).

Changes in tsDC morphology were observed by light microscopy at 200x total

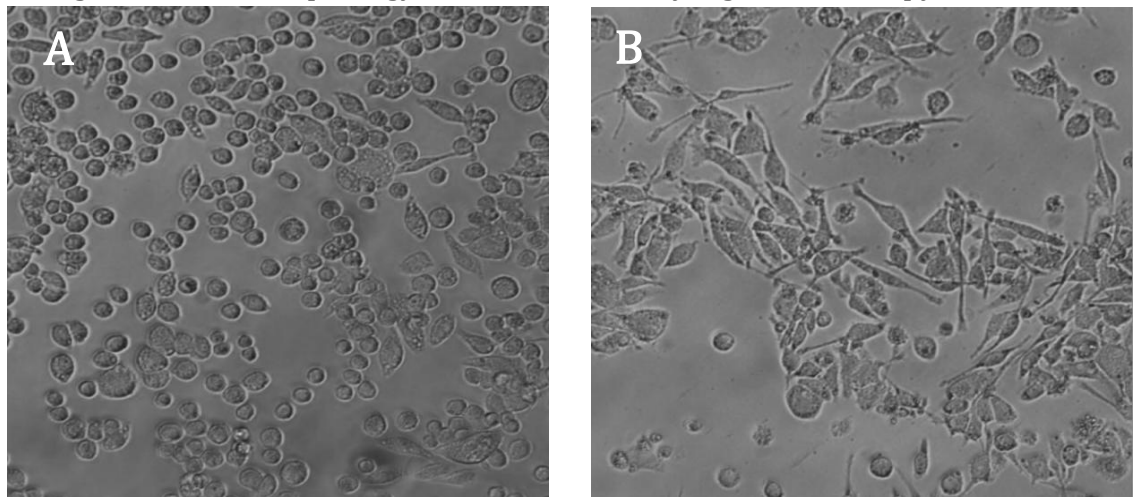


Figure 4-1: Morphology of tsDC following 24 hour activation with 10ug/ml LPS

magnification. Following 24 hour activation with LPS, activated DC samples were characterised by the development of spindle-like protrusions of the cell cytoplasm.

Following incubation with LPS for 24 hours, tsDC began to detach from the surface of the culture plate. The non-adherent cells retained viability when stained by trypan blue, suggesting changes in morphology occurred as a result of cellular activation rather than cell death. The proportion of tsDCs considered activated following 24-hour incubation with varying concentrations of LPS is detailed in figure 4.2. LPS induced activation was identified based on the appearance of the typical spindle-like projections of the tsDC cytoplasm. Rounded cells without spindle-like projections were considered non-activated. The percent activation calculated by microscopy was based on the adherent cell population only at this stage.

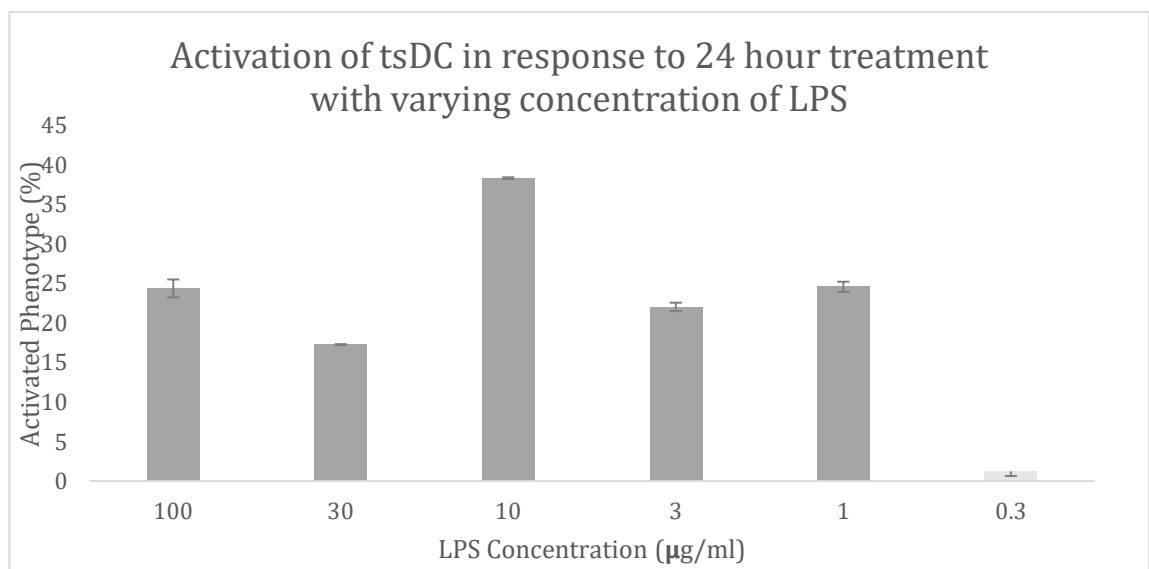


Figure 4-2: Percent activation of tsDC in response to LPS activation

Following activation with LPS across several concentrations, the highest proportion of tsDC demonstrating an “activated” morphology was observed following incubation with 10µg/ml LPS. Concentrations ranging 0.3-100µg/ml were tested, representative of n=2 individual experiments.

Figure 4.2 shows that the greatest percentage of cells demonstrating the “activated” phenotype (characterised by spindle-like projections) was observed in response to treatment with 10µg/ml LPS. Although it could be expected that higher concentrations would result in more efficient activation, at very high concentrations of 30 and 100µg/ml, cells in culture began to detach from the culture dish rapidly, showed dysmorphic cell membranes and appeared to be undergoing apoptotic. It may therefore be that high concentrations of LPS were too toxic and not well tolerated, therefore activated cells detached from the cell membrane and could not be counted. The concentration of 10µg/ml was selected

for experiments moving forward. Following the observation that incubation with 10µg/ml LPS for 24 hours induced the spindle-like phenotype associated with activation, it was next necessary to determine an optimal time point to investigate the outputs of tsDC activation. Therefore, tsDC were incubated with 10µg/ml over various time points before detaching with 15mM EDTA in PBS and analysing expression of CD40R by FACS. This process was carried out to determine which time point induced the greatest change in the expression of surface receptors associated with activation, illustrated in figure 4.3.

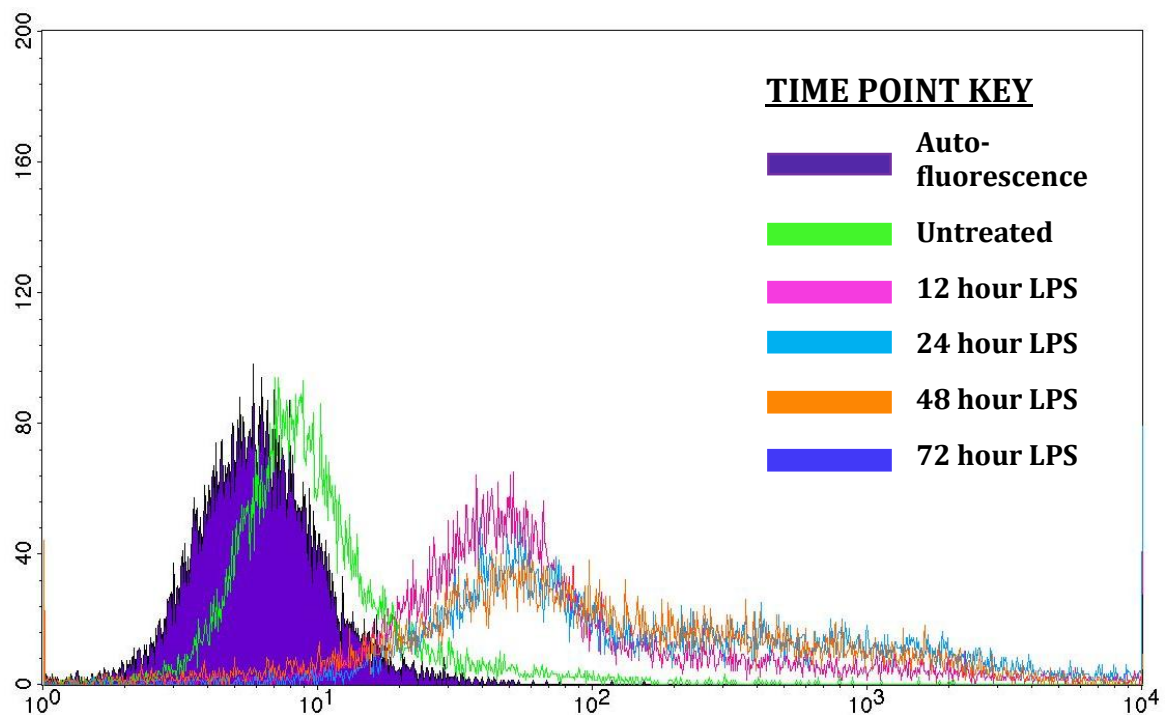


Figure 4-3: tsDC Expression of CD40R in response to time point activations with LPS

DC were seeded in 6 well plates at 1×10^6 cells/well. Cells were cultured for a total of 72 hours, and 10µg/ml LPS added to each well at the corresponding time point. Cells were harvested by EDTA and 1×10^6 cells were labelled with PE anti-CD40R antibody prior to fixation and analysis.

Following 24-hour incubation with 10ug/ml LPS, tsDC demonstrated identifiable changes in morphology, which could be observed by light microscopy. These changes corresponded with changes in CD40R expression at the cell surface, which the current literature indicates commonly serves as a marker of DC activation as discussed in section 1.6. As receptor expression profiles indicated an activated phenotype after 24 hours of stimulation, the DCs were incubated with activating treatments for 24 hours in all experiments. This approach was also taken because

some literature suggests that DCs become over-stimulated or “exhausted” between 24-48 hours exposure to LPS in the absence of co-stimulatory signals (Abdi et al., 2012). Exhausted DC populations maintain the capacity to respond to T cell populations through cytokine signalling but exhibit no further changes in response to re-challenge with LPS (Abdi et al., 2012).

Once a 24-hour time point had been established for effective DC activation based on cell morphology and CD40R expression, the receptor profile of tsDC was further characterised. Representative histograms of receptor expression patterns for a selection of receptors of interest following treatment with LPS are presented in figure 4.4.

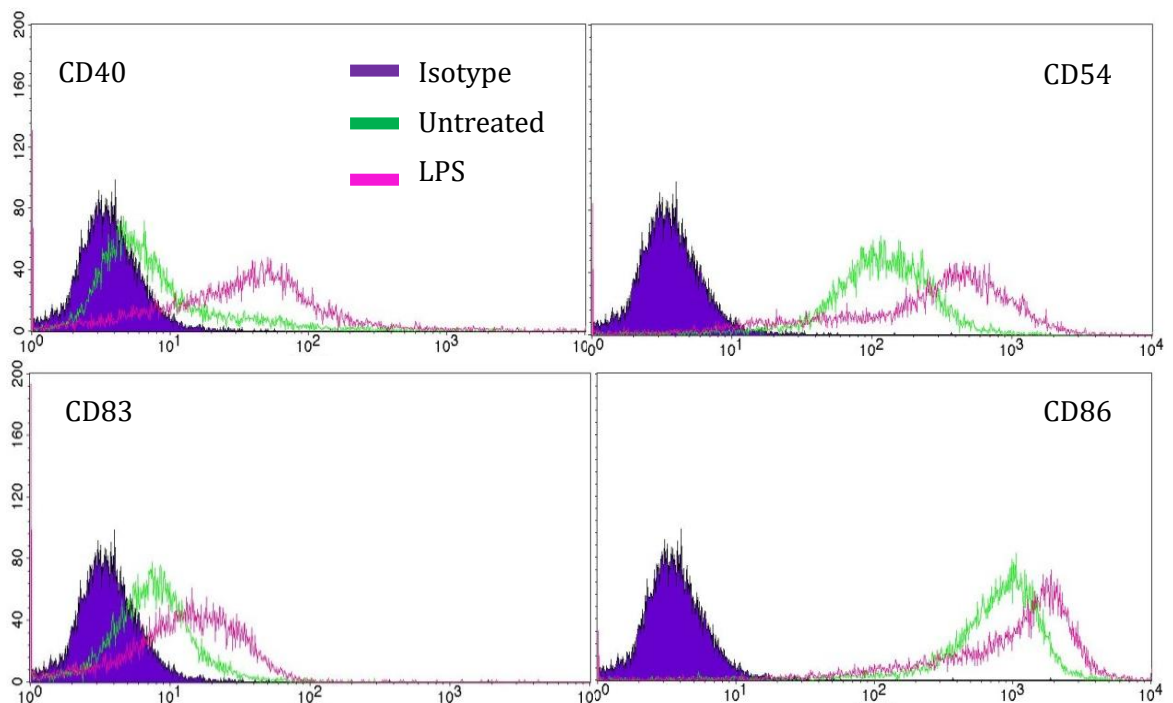


Figure 4-4: Histogram overlay of tsDC activation receptor changes in response to LPS activation. expression on DCs following 24 hour incubation period with 10µg/ml LPS at 37°C

After demonstrating that the tsDC cell line responded to LPS treatment by monitoring changes in the CD40R, tsDC surface receptors associated with activation were investigated following 24 hour activation with 10µg/ml LPS at 37°C. Analysis of receptor expression is illustrated in figures 4.5 and 4.6.

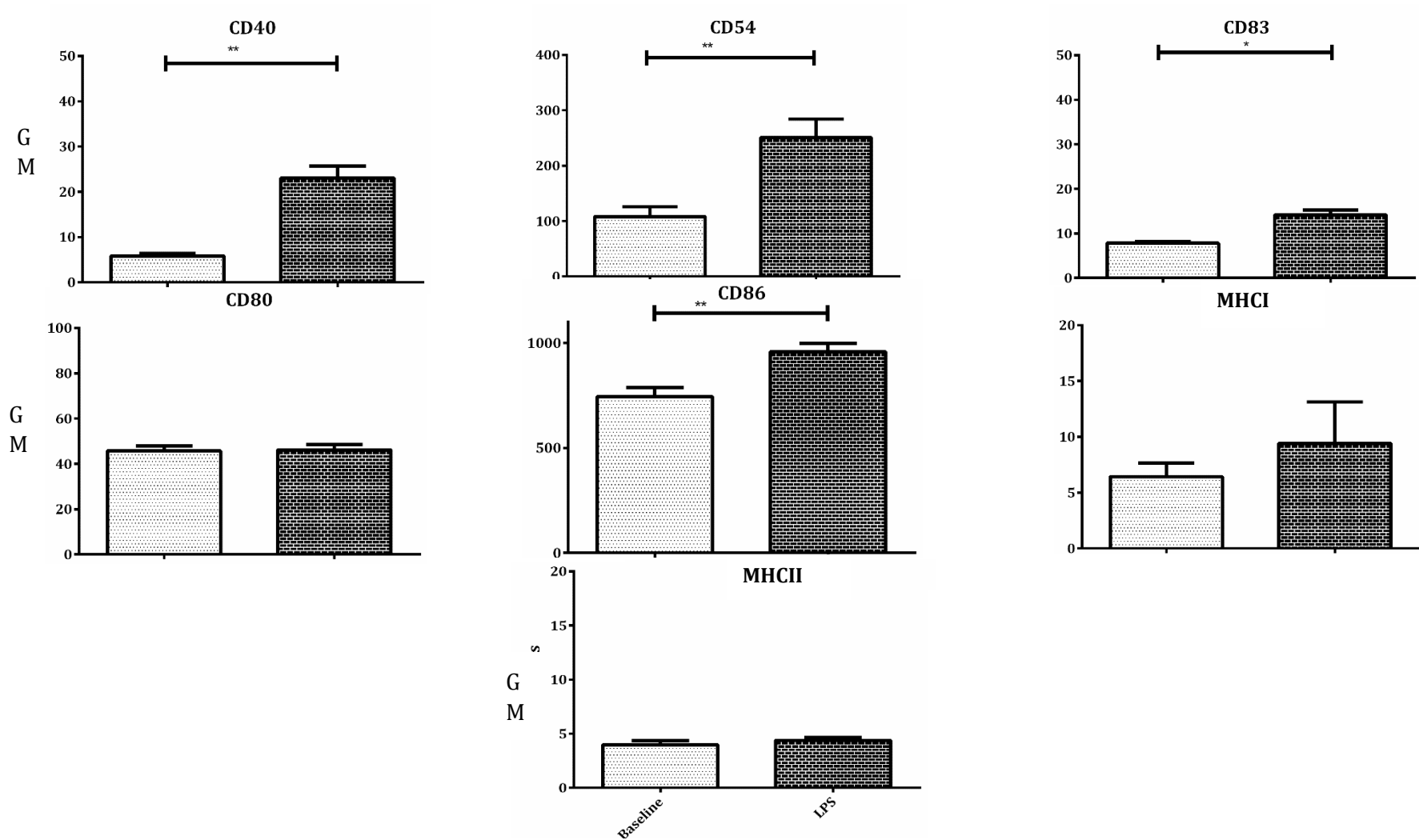


Figure 4-5: Expression changes in c-SMAC receptors at the tsDC surface in response to 24 hour treatment with 10µg/ml LPS.

Flasks containing 1×10^6 tsDC were incubated for 12 hours to allow cells to adhere to the flask prior to addition of 10µg/ml LPS treatment for 24 hours. Data are expressed as geometric mean of fluorescence intensity (GMF) \pm SD of three independent experiments. Statistical significance was determined by paired T test where * < 0.05 ** < 0.005 and *** < 0.001.

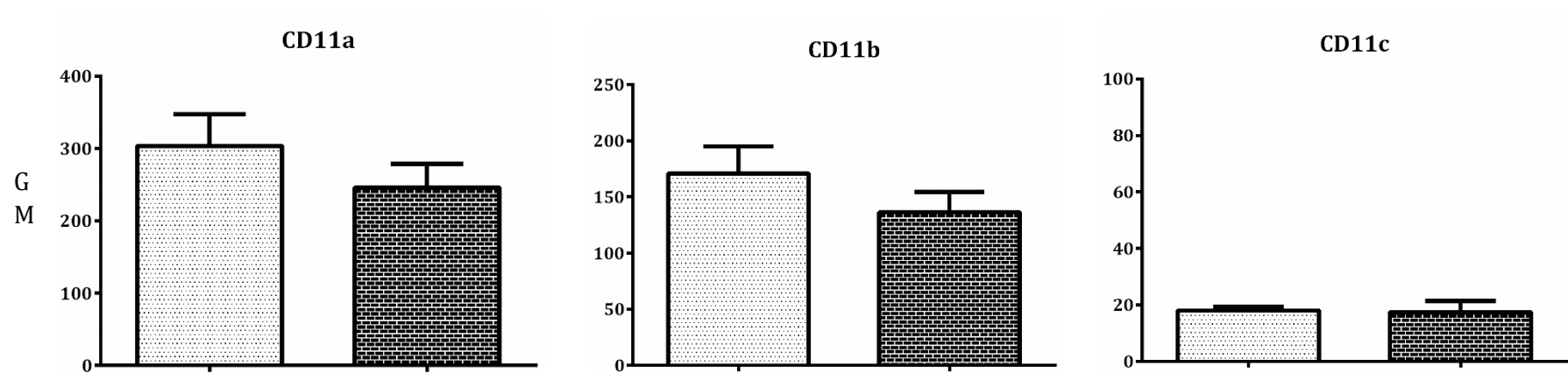


Figure 4-6: Expression changes in integrin receptors at the tsDC surface in response to treatment with 10µg/ml LPS for 24 hours

Flasks containing 1×10^6 tsDC were incubated for 12 hours to allow cells to adhere to the flask prior to addition of 10µg/ml LPS treatment for 24 hours. Data are expressed as geometric mean of fluorescence intensity (GMF) \pm SD of three independent experiments. Statistical significance was determined by paired T test where * <0.05 ** <0.005 and *** <0.001 .

Treatment with LPS induced changes in the expression of several tsDC surface receptors. Several markers associated with activation showed upregulation with statistical significance, in particular, CD40, CD54, CD83, and CD86 (figure 4.5). These observations determined that tsDC responded to stimulation by LPS as per the altered morphology and induced changes in the expression levels of receptors involved in maturation and activation at the cell surface.

These changes in receptor expression confirmed the capacity of the tsDC cell line to respond to a known inducer of activation, and provided phenotypic markers by which to identify tsDC activation. Cell phenotype was checked by light microscopy before each activation experiment to provide an initial indicator of general tsDC health and activation status.

4.2 Characterising the effect of CD40R targeted peptide on tsDC surface receptor expression when presented as a tetrameric conjugate

Following the observations that LPS activation induced changes in tsDC receptor profile, cell surface receptor expressions were analysed by flow cytometry, to determine whether stimulation with MTP40 or Tet40 had the potential to induce activation of tsDC. Flow cytometry which provides a rapid, low cost method of assessing direct changes in the DC phenotype and was therefore used as the primary means of detecting DC activation.

Receptors associated with c-SMAC interactions (as detailed in section 1.2.2.2) and therefore with DC activation were selected for analysis *via* flow cytometry, shown in figure 4.7. In addition, several receptors commonly expressed on the DC surface, but which are not typically associated with activation, were included to ensure that any changes could be rationally attributed to a specific activation response, shown in figure 4.8.

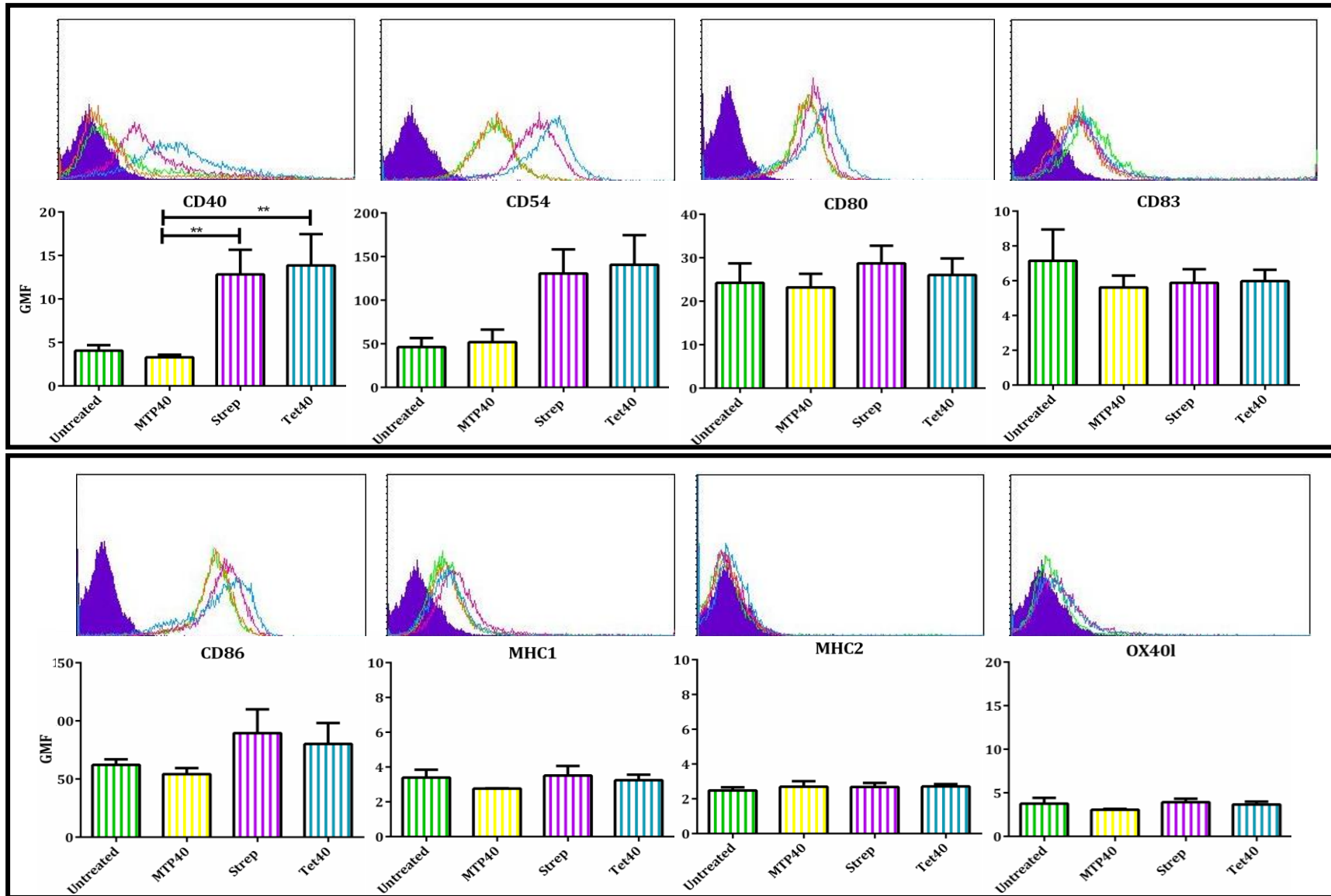


Figure 4-7: Expression of cSMAC associated proteins at the tsDC surface following 24-hour incubation with streptavidin-based activating treatments

To determine whether CD40R-targeted activation induced changes in the receptor expression profile of tsDCs, 1×10^6 DC were seeded in T25 flasks and incubated with $2.5 \mu\text{M}$ MTP40, Tet40 or streptavidin control for 24 hours at 37°C . For flow cytometry, washed cells were incubated for 1 hour at 4°C with PE-labelled antibodies for the cell surface proteins indicated. Samples were acquired using a BD FACSCalibur and analysed with GraphPad Prism software. Histograms depict fluorescence units while accompanying graphs present geometric mean of fluorescence intensity \pm SD of three independent experiments. Significant difference in receptor expression was identified by one-way ANOVA followed by Tukey post-hoc analysis, where $*p \leq 0.05$, $**p \leq 0.005$, or $***p \leq 0.001$.

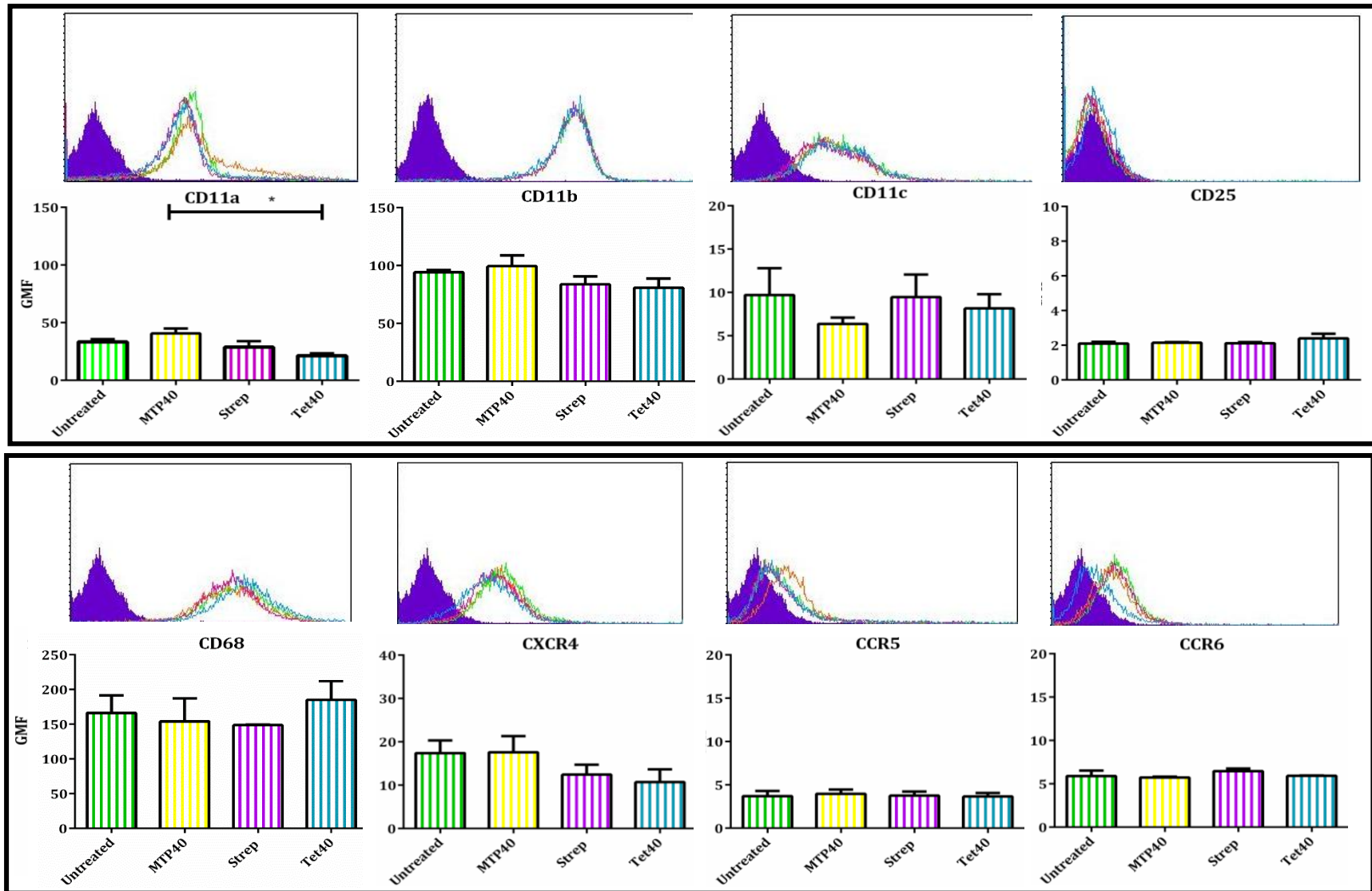


Figure 4-8 Expression of receptors not associated with activation at the tsDC surface following 24-hour incubation with streptavidin-based activating treatments

Treatment conditions and analysis methods used were identical to those described in figure 4.6.

The only treatment to induce a significant change in tsDC receptor expression was Tet40, to which statistically significant increases in CD11a and CD40R at the cell surface. Importantly, significant changes were not observed in any receptors following incubation with MTP40 compared to untreated cells. This finding suggests that MTP40 alone is not sufficient to stimulate effector outputs in the tsDC cell line, however this can be overcome by multivalent presentation of MTP40, which was sufficient to induce a stimulatory effect in some receptors.

A trend toward an activated profile was revealed by CD54, CD68, and CD86, which all displayed upregulated expression in response to Tet40, however the changes in these receptors failed to reach statistical significance. Other receptors, including CD11b and CXCR4, trended towards decreased expression following treatment with streptavidin or Tet40. The expression patterns of other receptors which were not specific to activation status of tsDC remained unchanged, suggesting that the responses observed occurred specifically in response to CD40R signalling. One receptor which did not conform to the expected changes associated with activation was CD83. This receptor showed slight, non-significant down regulation in all treatment samples, compared to the untreated control. However, this may not be representative of the true shift in expression in response to activation, as the untreated population shows greater standard deviation than the rest of the samples. This change may therefore be a result of anomalous data in the untreated population, suggesting this result dataset may need repeating to draw conclusions about the regulation of this receptor.

The changes observed by flow cytometry generally support the hypothesis that activating tsDCs *via* CD40R can induce phenotypic changes associated with DC maturation activation when presented in a multivalent manner. This is illustrated in the current section by observed changes in receptor expression which are associated with DC maturation.

4.3 Cytokine profile changes in response to Tet40, analysed by ELISA

Having established that multivalent Tet40 can induce specific changes in tsDC receptor expression, the next aim was to determine whether the observed changes translated to differences in the soluble cytokine profile of the tsDC population.

While receptor mediated cell surface interactions have a direct impact on neighbouring cells, cytokine changes more widely influence the cellular environment. Cytokine signalling varies depending on the different stages of DC development and maturation, and as such, is correlated with changes in production levels depending on the maturation status of DCs. To broadly categorise the cytokine milieu of tsDC in response to activation, a selection of pro-inflammatory and anti-inflammatory cytokines were investigated, shown in figure 4.9.

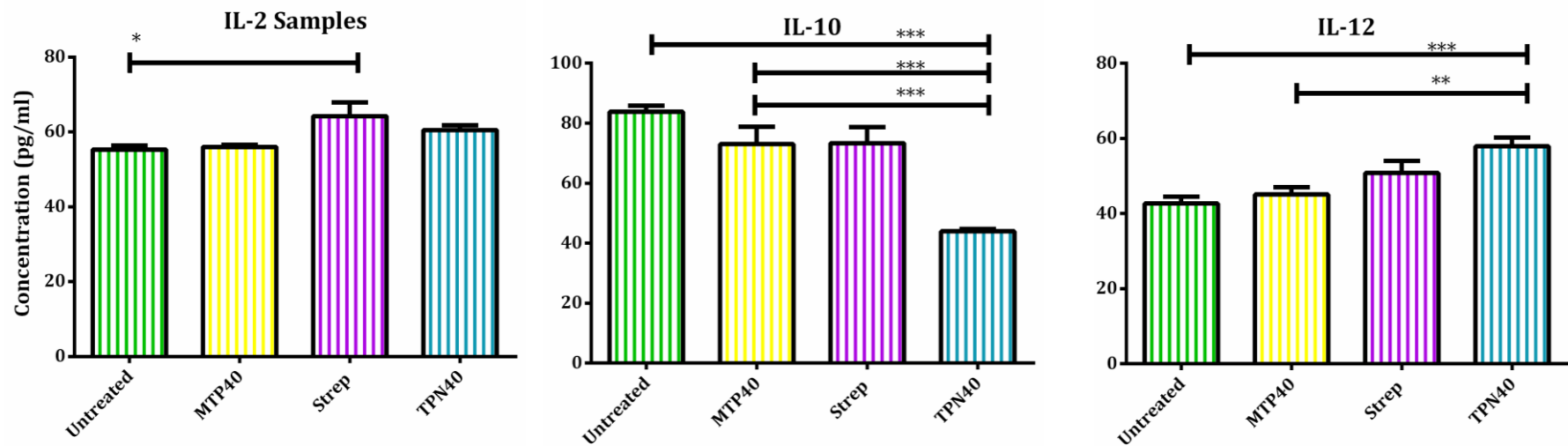


Figure 4-9: Cytokine changes observed by ELISA following 24-hour incubation with MTP40 presented on flexible multivalent scaffolds

To determine whether CD40R-targeted activation induced changes in cytokine production by tsDCs, 5×10^5 DC were seeded in T25 flasks and incubated with $2.5 \mu\text{M}$ MTP40, Tet40, or streptavidin control for 24 hours at 37°C . At the end of the incubation period, supernatants were transferred to a 15ml falcon tube and subject to centrifugation at $1000 \times g$ to remove cell debris before being transferred to -80°C for storage. ELISA plates and reagents were prepared as per the manufacturers recommendations (see section 2.17, ELISA DuoSet, R&D Systems). Immediately prior to analysis, samples were thawed on ice and diluted 1:1 with diluent. Absorbance was recorded on an EIX800 plate reader at 540nm with 450nm correction. These data represent the mean value of three independent experiments with samples tested in triplicate. Significant difference was identified by one-way ANOVA followed by Tukey post-hoc analysis, where $*p \leq 0.05$, $**p \leq 0.005$, or $***p \leq 0.001$.

Data revealed that incubation with CD40R targeting constructs influenced the cytokine profile of tsDCs (figure 4.8). tsDC response was characterised by a slight but significant increase in Th1 cytokines IL-2 and IL-12, and complementary downregulation of the Th2 type suppressive cytokine IL-10.

Treatment with MTP40 or Tet40 constructs resulted in slight changes in IL-2 production, however it is difficult to draw conclusions based on this data since the streptavidin control initiated a strong non-specific change in cytokine production. Analysis of IL-12 production demonstrated a small but highly reproducible change, where incubation with streptavidin control slightly affected IL-12 production, however the most significant upregulation was seen in response to Tet40 treatment, which increased production by 35.6%. Interestingly treatment with Tet40 downregulated IL-10 production by 47.6%, while streptavidin or MTP40 controls showed only modest changes (reductions of 12.5% and 12.9%, respectively).

In general, the changes induced in cytokine production following activation treatments were slight but with high reproducibility, suggesting cytokine production is more tightly regulated than surface receptor expression.

4.4 Analysis of streptavidin construct toxicity by MTS assay

Cell Titre from Promega was used to evaluate whether tsDC viability and proliferation were affected by exposure to MTP40, streptavidin, or Tet40. While proliferation is not a major output associated with DC maturation, it is necessary to determine a dose response curve for cytotoxicity for the construct to have potential to translate to *in vivo* applications, shown in figure 4.10.

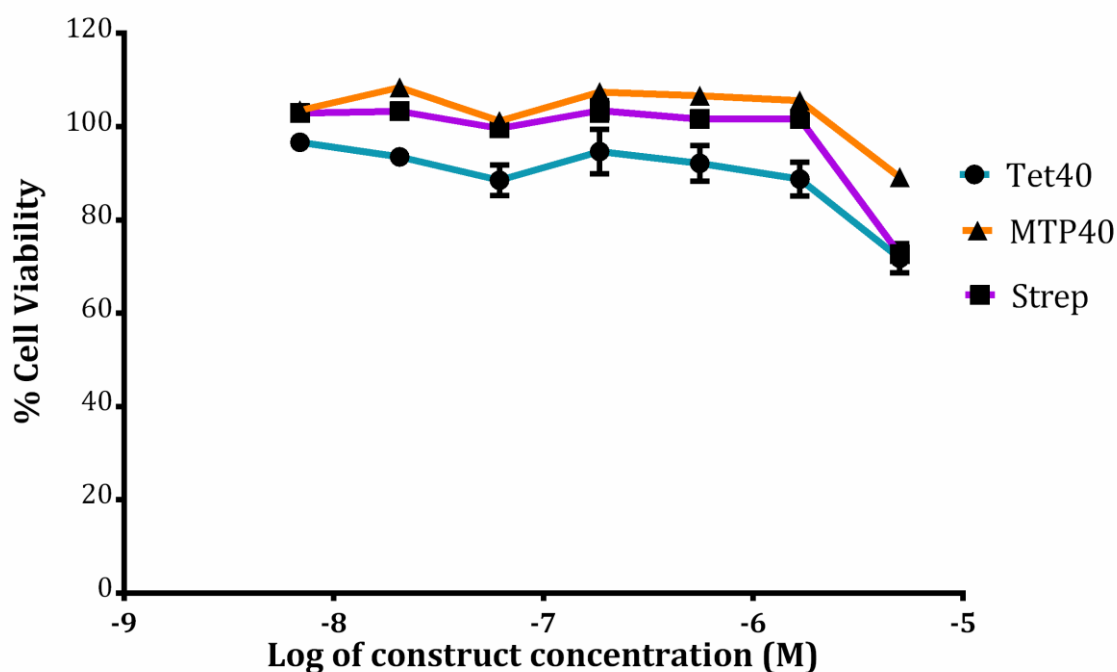


Figure 4-10: tsDC Viability assessed by MTS assay following activation with flexible multivalent scaffolds

tsDC were seeded in 96 well plates (2×10^4 cells per well) and incubated with varying concentrations of MTP40, strep or Tet40 for 72 hours at 37°C. Coloured product formation was detected by absorbance at 490nm wavelength. Data represents the mean values of n=3 individual repeats in triplicate, error bars represent \pm SD.

All treatments were well tolerated by tsDCs following 72 hours incubation and did not establish a lethal concentration (LD-50) capable of inducing 50% cell death after 72 hours incubation. These data suggest that MTP40 is well-tolerated as a biological molecule. At the end of the incubation period, cellular viability was 89% in samples treated with MTP40, suggesting that the MTP40 peptide alone was well tolerated. Treatment with streptavidin and Tet40 reduced viability to 72% and 73%, respectively, and was therefore less well tolerated. Treatment with either

streptavidin or Tet40 produced highly comparable survival curves, suggesting toxicity was more influenced by the incorporation of streptavidin than by MTP40.

4.5 General Discussion

In summary, the data presented in the current chapter met the specified aims. First, activation of tsDC by LPS demonstrated the ability of this cell line to show phenotypic changes in response to a known activation stimuli, as shown by phenotypic changes observed by light microscopy, and changes in receptor expression shown by FACS. This chapter also demonstrated that the tsDC line induce changes in surface receptor expression in response to multivalent stimulation of the surface receptor CD40R. When incubated with Tet40 treatment, tsDC induced statistically significant changes in CD40R and CD11a, analysed by FACS. Incubation with Tet40 also induced changes in cytokine production, causing down-regulation of IL-10 in favour of IL-12 analysed by ELISA. Finally, MTS assay confirmed that treatment with MTP40 and Tet40 were well tolerated *in vitro*, supporting further investigation.

By investigating the capacity of MTP40 to induce outputs associated with activation in the naïve tsDC population and examining how this capacity was affected by its presentation on a multivalent scaffold, it was revealed that multivalent presentation of MTP40 as tetrameric Tet40 induced greater changes in receptor expression and cytokine secretion than when delivered as linear monomer.

To ensure the changes observed were specific to multivalent presentation of MTP40, two controls were investigated: MTP40 to identify monomer-induced activation, and untargeted streptavidin to identify non-specific activation.

DC maturation is associated with expression of chemokine receptors which mediate DC migration from peripheral tissues to draining lymph nodes where they present antigenic peptides to specific T cells. This process also relies on expression of co-stimulatory molecules on the DC surface to promote cell-cell interaction and antigen presentation to T cells, capable of mounting an anti-tumour immune response.

Effective CD40R signalling is initiated by clustering of the CD40R in response to trimeric CD40L (Grassme et al., 2002), discussed in detail in section 1.5.2. It is therefore likely that multivalent presentation of CD40R-targeting molecules produces a signal more representative of the *in vivo* environment than delivery of

monomeric ligands, which may explain the increased changes induced by multivalent presentation. The data presented in the current research demonstrate a modest increase in CD40R following activation.

The data described in the current study support these findings of other groups who similarly observed changes in tsDC receptor expression associated with activation, in response to CD40R stimulation *via* multivalent targeting systems, as discussed in section 1.7.1. The upregulation of activating receptors at the tsDC surface reinforces the observations made by other groups, that multivalent receptor engagement optimises immune stimulation.

The results detailed in this chapter also demonstrate substantial upregulation of CD54 on the tsDC surface in response to Tet40. This is encouraging as observations by other groups have shown that CD54 has the potential to act as a surrogate marker for immune activation, and may potentiate an immune response in the absence of classical activation receptors as discussed in section 1.2.2.2, suggesting that Tet40 signalling prepared tsDCs for further activation.

The phenotypic changes observed in tsDC receptor expression provide preliminary data to support the activation of tsDCs *via* the CD40R pathway in response to Tet40 treatment. This was supported by the shift in cytokine profile toward a Th1 response, characterised primarily by downregulation of IL-10.

Finally, tsDC incubation with MTP40 and Tet40 constructs did not induce sufficient levels of cell death to determine a LD-50 concentration. Although some reduction in viability was determined across all activation treatments, this confirmed that CD40R targeting treatments were relatively well tolerated over a period of 72 hours.

Chapter 5: Analysis of tsDC outputs in response to CD40R Activation *via* a rigid multivalent construct

The previous chapter showed that presentation of MTP40 using a streptavidin scaffold to produce a tetrameric targeting molecule (Tet40) induced changes in tsDC outputs associated with activation. A potential limitation of this system was identified however, as the streptavidin backbone of the construct resulted in non-specific stimulation of the tsDC cell line both in receptor expression patterns and cytokine production. This intrinsic stimulation of the immune system may limit the potential of Tet40 as an immunotherapy due to off-target stimulation of DCs by streptavidin irrespective of antigen targeting, reducing the specificity of tsDC activation.

The strength and specificity of multivalent interactions are significantly influenced by the type of scaffold the biomolecule of interest is conjugated to. As streptavidin is a biologically active molecule derived from the surface of *Streptomyces avidinii*, it was unsurprising that the scaffold alone displayed some influence on tsDC activation outputs. The current chapter aimed to identify whether the stimulatory effects of multivalent MPT40 presentation could be preserved when conjugated to a different multivalent scaffold, and whether the use of an inorganic, biologically inert scaffold could reduce the extent of non-specific tsDC stimulation as was observed in response to streptavidin. UPN (**U**ntargeted **P**olyvalent gold **N**anoparticles) were selected as an alternative delivery scaffold due to the specific characteristics which make them attractive candidates for applications in tumour targeting, drug delivery and molecular imaging, as discussed in section 1.8. This system also provided additional benefits as it was possible to take advantage of the inherent high affinity binding between the thiol moieties of MTP40 with the surface of UPNs to produce multivalent TPN40 (**T**argeted **P**olyvalent gold **N**anoparticles for **CD40R**).

The findings detailed in this chapter are presented to address the following research aims:

- Determining whether multivalent binding of CD40R *via* biologically inert gold scaffolds could increase the potency and specificity of tsDC activation, compared to activation by streptavidin based (Tet40) platforms.

5.1 tsDC receptor changes in response to nanoparticle platform

MTP40 was conjugated to the surface of UPNs as described in section 3.2.2 based on the inherent cysteine bond formation between MTP40 and the UPN surface. TPN40 treatment and controls were incubated with tsDC following the same protocol as was used for streptavidin constructs to compare the effect of multivalent presentation on a rigid, biologically inert scaffold. Changes in surface receptor expression patterns following treatments were analysed as a primary indicator of activation. As was previously described for activation *via* flexible streptavidin scaffolds in section 4.2, surface receptors associated with tsDC activation and non-specific tsDC receptors were analysed (figures 5.1 and 5.2, respectively).

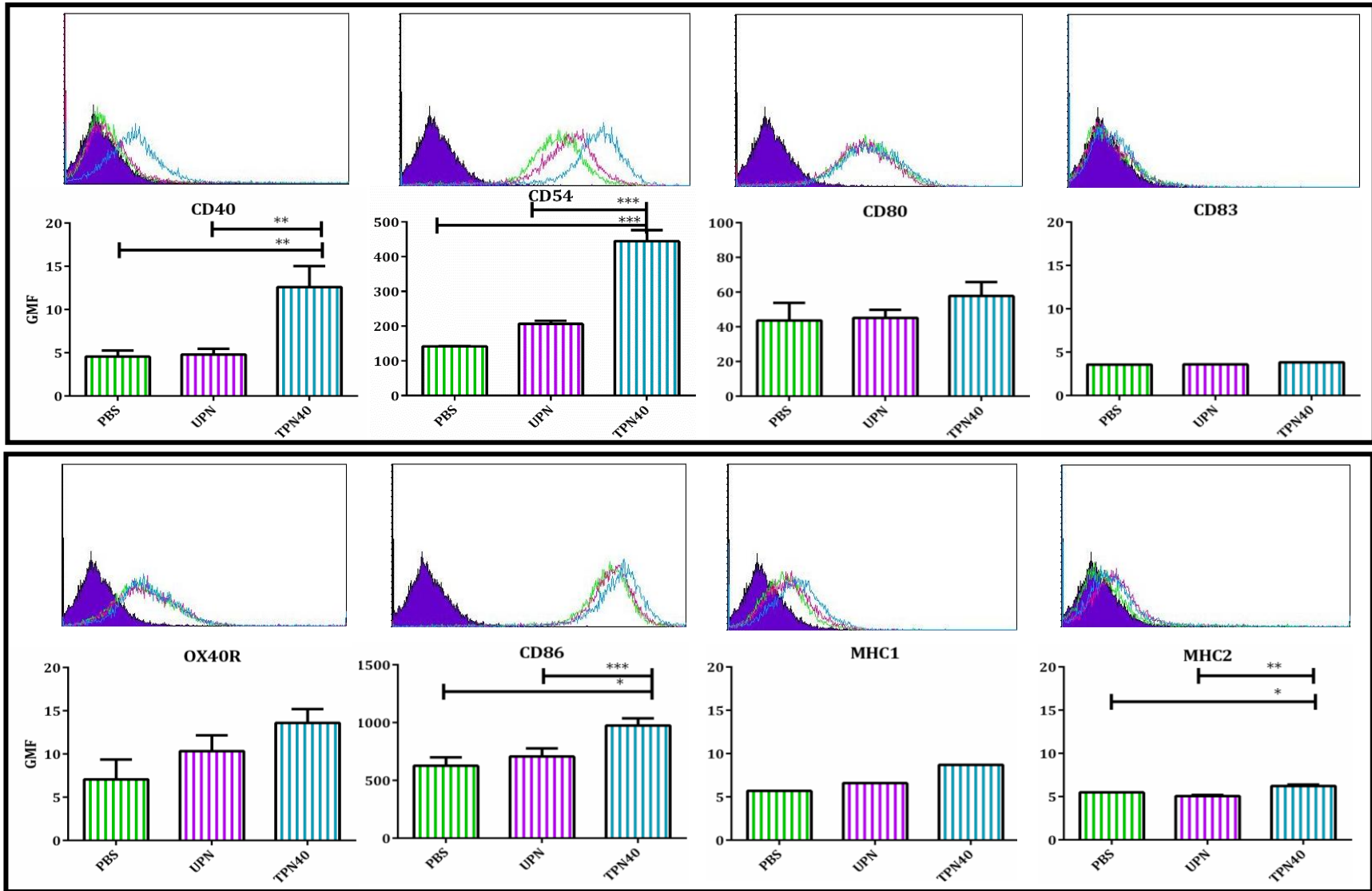


Figure 5-1 Expression of cSMAC associated proteins at the tsDC surface following 24-hour incubation with nanoparticle based activating treatments

To determine whether CD40R-targeted activation induced changes in the receptor expression profile of tsDCs, 1×10^6 tsDC were seeded in T25 flasks and incubated with $2.5 \mu\text{M}$ either TPN40 or UPN control for 24 hours at 37°C . For flow cytometry, washed cells were detached with EDTA for 10 minutes at 37°C before incubating for 1 hour at 4°C in PBS + 1% BSA containing the PE-labelled antibodies for the cell surface proteins indicated in figure 4.1. Samples were acquired using a BD FACSCalibur and analysed with GraphPad Prism software. Histograms depict fluorescence units while accompanying graphs present geometric mean \pm SD of three independent experiments. Significant difference in receptor expression was identified by one-way ANOVA followed by Tukey post-hoc analysis, where $*p \leq 0.05$, $**p \leq 0.005$, or $***p \leq 0.001$.

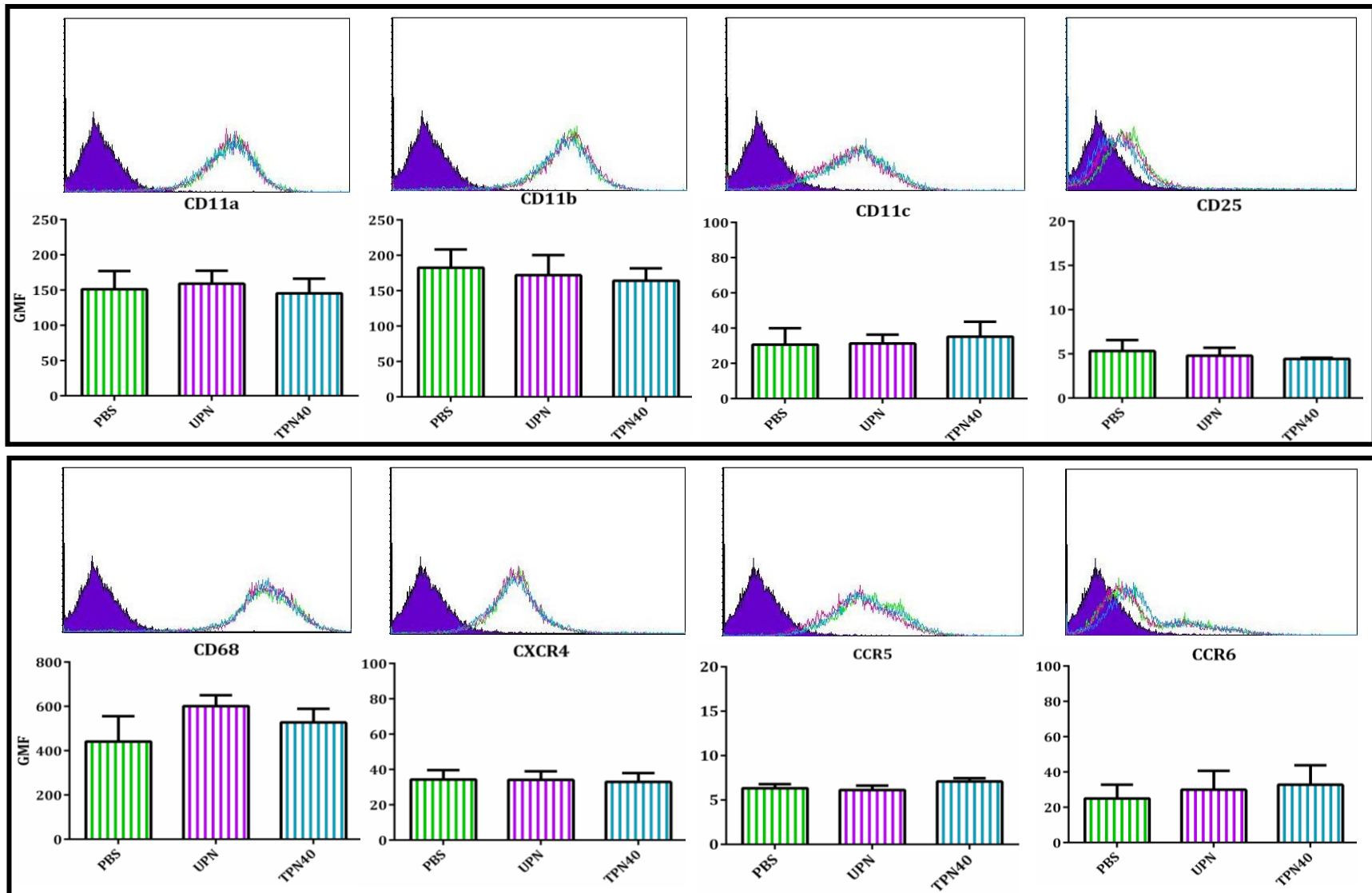


Figure 5-2: Expression of generic receptors not associated with activation at the tsDC surface following 24-hour incubation with nanoparticle-based activating treatments

Treatment conditions and analysis methods used were identical to those described in figure 5.1.

Identical treatment conditions were used to analyse tsDC receptor profile changes in response to TPN40 activation as had been used to analyse Tet40 activation. Similar trends were observed in surface receptor expression patterns when tsDCs were incubated with TPN40 as was observed following incubation with Tet40. Unlike the streptavidin platform, UPN-treated tsDCs displayed no significant changes in expression of any of the receptors analysed.

Statistically significant changes were observed in the expression of CD40R, CD54, CD86, and MHCII following incubation with TPN40, while minimal changes were observed in response to the untargeted UPN control. While the Tet40 platform also induced changes in CD40R, CD54, and CD86, this result could not be confidently attributed to CD40R signalling due to the significant changes observed when tsDC were incubated in streptavidin scaffold alone. This finding produces two important implications. First, the use of a biologically inert scaffold reduces non-specific activation of tsDC and second, transferring MTP40 onto an inert construct had no detrimental effect on the upregulation of activation receptors, suggesting that multivalent presentation is the key parameter to induce specific, potent activation through CD40R binding.

Incubation with TPN40 demonstrated expression changes in a greater number of tsDC surface receptors than was observed in response to Tet40 treatment. Also, UPN controls demonstrated lower immunogenicity than streptavidin control, determined by the absence of non-specific changes.

Significant changes in MHC expression at the tsDC surface were not induced following CD40R targeted activation. The capacity for mature DC to induce tumour regression and tumour-free survival through MHC interactions at the CTL surface was first established in murine models over two decades ago (Mayordomo et al., 1995). During the past 20 years, evidence has supported the theory efficient immune stimulation is dependent on several parameters in addition to interaction between the APC and T cell surfaces; including the cytokine environment and antigen expression at the cell surface (Duraishwamy et al., 2013). Considering that MHC plays a fundamental role in stimulating effective immunity, the activating treatments investigated in the current study did not induce the expected response in MHC expression. An explanation for this could be that the tsDC line has

previously been characterised to have weak T cell priming properties. Early work investigating tsDCs established that cell line was able to induce changes in surface markers associated with activation but were not able to prime activation of naïve T cells expressing a TCR variant specific for the serum protein C5 when presented with the model antigen (Volkman et al., 1996). In contrast, bone-marrow-derived DCs matured with GM-CSF have successfully presented C5 to naïve transgenic T cells (Volkman et al., 1996). Collectively, these data suggest that tsDC are able to induce various responses required to prime an immune response, but that these cells may not be as functionally robust as DCs matured in culture. This cell line therefore provided an adequate starting point to confirm the therapeutic potential of CD40R targeted activation *in vitro*, which provided a platform to generate reproducible conditions to confidently replicate activation experiments. Future research should therefore aim to investigate how the outputs here translate to an alternative cell line.

5.2 Cytokine profile changes in response to TPN40, analysed by ELISA

Considering that a greater number of changes were observed in tsDC receptor expression with lower non-specific changes using the TPN40 platform, the production of IL-2, IL-10, and IL-12 was therefore re-analysed following tsDC activation with TPN40 to determine whether a differential response could also be observed in cytokine production. Figure 5.3 illustrates the changes in cytokine production.

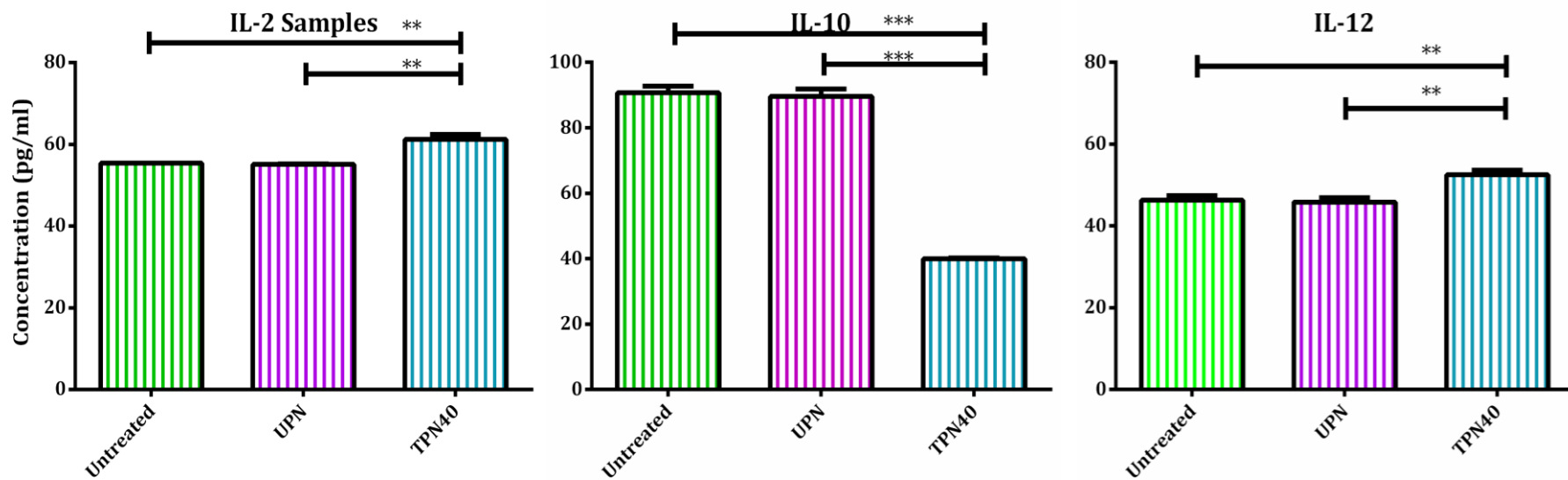


Figure 5-3: tsDC cytokine expression profile detected by ELISA following 24-hour incubation with MTP40 presented on rigid multivalent scaffolds.

Supernatants from treated DC were thawed on ice and diluted 1:1 with ELISA diluent before analysis as per the manufacturer’s recommendations. Data presented represent three independent experiments ran in triplicate \pm SD. Significant difference was identified by one-way ANOVA followed by Tukey post-hoc analysis, where * $p \leq 0.05$, ** $p = \leq 0.005$, or *** $p \leq 0.001$.

Stimulating CD40R activation using TPN40 resulted in a similar cytokine trends as was induced by Tet40. UPN treatments showed no significant change in any of the investigated cytokines in comparison to baseline levels produced by tsDC, and showed greater changes in IL-10 profile of tsDC, which was decreased by 56.0% following TPN40 treatment, whereas UPN treatment induced a negligible change of 1.2% reduction. This indicates much greater specificity than was observed in response to Tet40.

5.3 Analysis of nanoparticle construct toxicity by MTS assay

Following analysis of DC activation outputs by FACS and ELISA, cell viability assays were conducted to analyse the impact of UPN and TPN40, compared to MTP40 on tsDC proliferation and viability under identical conditions as was used for Tet40 analysis (described in section 4.4).

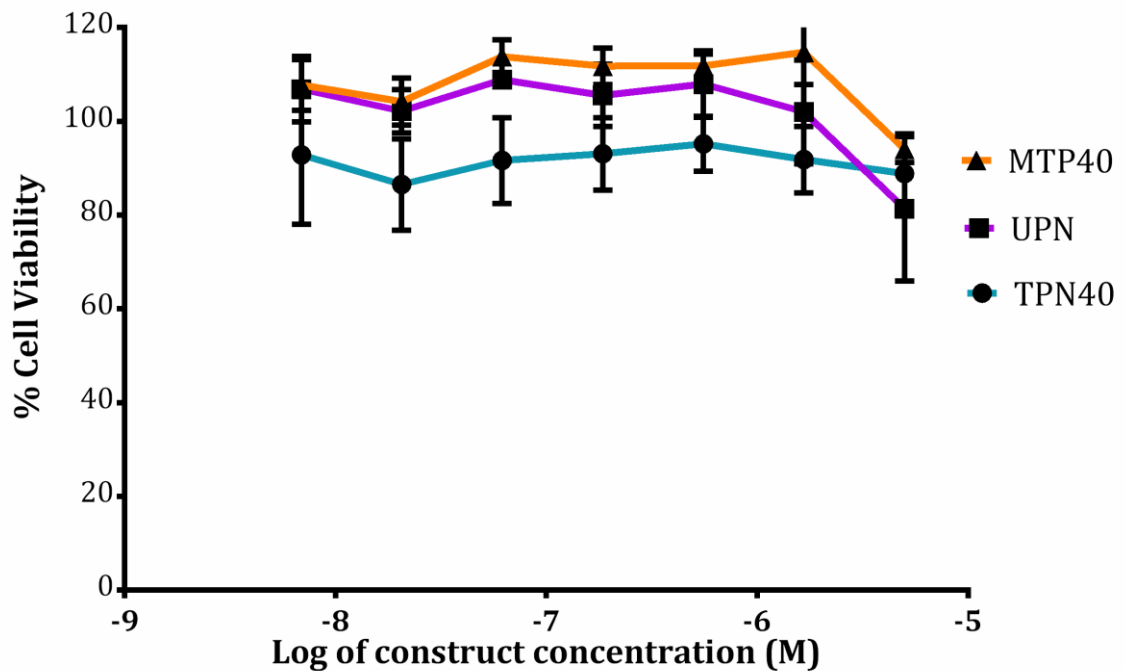


Figure 5-4: tsDC Viability assessed by MTS assay following activation with rigid multivalent scaffolds.

tsDC were seeded in 96 well plates (2×10^4 cells per well) and incubated with varying concentrations of MTP40, UPN or TPN40 for 72 hours at 37°C. Data represents the mean values of $n=3$ individual repeats, error bars represent \pm SD.

Nanoparticle treatments were well tolerated by tsDC following 72 hours in culture. At the highest concentration of 50 μ M, cellular viability following incubation with TPN-40 remained above 80%. Incubation with MTP40 and UPN controls was well tolerated throughout the concentration range. Treatment with nanoparticle conjugates induced greater variability in the datasets than was observed with streptavidin based conjugates. Based on this data, the 2.5 μ M concentration used throughout this work appears to be sufficiently well tolerated to allow *in vitro* analysis of tsDC activation, and supports the potential for TPN40 to be further investigated by *in vivo* methods in future.

5.4 Antigen uptake by tsDC

Because of the improved activation profiles of tsDC in response to treatment with MTP40 conjugated to the nanoparticle platform (as opposed to streptavidin conjugation), the next step was to determine whether this construct could induce antigen uptake in tsDCs. The ability to acquire antigen and present it on the cell surface is an essential function of DCs for eliciting an effective T cell response. It was therefore necessary to investigate this activity to fully characterise tsDC activation.

FITC-OVA is commonly used as a model system to detect antigen uptake by APCs. tsDCs were counterstained with CD86 in the present work to visualise the cell membrane, since this receptor is expressed at high levels in unstimulated tsDCs, and increased expression was also observed in response to activating treatments (as shown in figures 4.7 and 5.1). Outputs of tsDC response to model antigen are illustrated in figure 5.5.

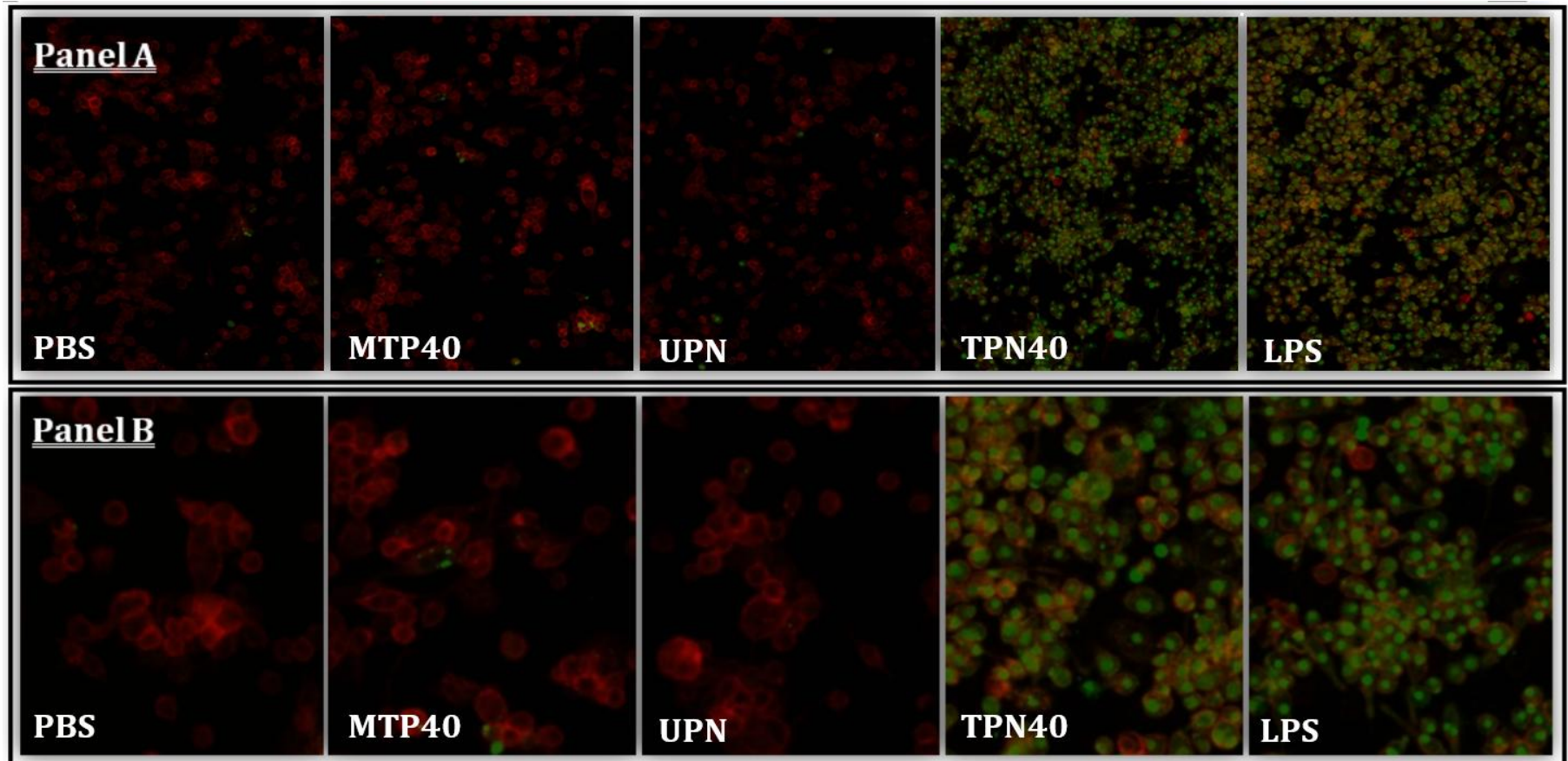


Figure 5-5: tsDC capacity for antigen uptake determined by phagocytosis of FITC-OVA post-activation.

tsDC were incubated for 20 hours with activating treatments (described in section 2.9). After 20 hours, 500 μ g/ml FITC-OVA (green) solubilised in PBS was added per well and returned to incubate at 37°C for a further 4 hours. Cells were counterstained for an additional 10 minutes with PE-labelled anti-CD86 (red). **Panel A**) tsDC under 100x total magnification. **Panel B**) tsDC under 400x total magnification.

tsDC cultures activated using either LPS or TPN40 displayed intense presentation of FITC-OVA (green) by fluorescent microscopy; there appears to be relatively homogenous uptake by all tsDC in response to these treatments. In contrast, PBS controls only showed anti-CD86 staining (red), which is highly expressed in tsDC regardless of maturation status. Thus, unstimulated tsDC do not appear to internalise FITC-OVA antigen. Cultures treated with MTP40 or UPN controls also demonstrated no uptake into cells. Effective antigen uptake was mediated by the positive LPS control as well as TPN40, suggesting that this change was induced specifically in response to activation.

5.5 Conclusions

The data presented in this chapter investigated the ability of MTP40 to induce outputs associated with tsDC activation when presented as a monomer versus multivalent presentation delivered on the surface of rigid gold nanoparticles (TPN40), compared to presentation on Tet40. In summary, the data presented in the current chapter met the aim of determining whether multivalent binding of CD40R via gold nanoparticle scaffolds could increase the potency and specificity of tsDC activation, compared to streptavidin based activation shown in chapter 4. During FACS analysis, a greater number of activation specific surface receptors showed significant changes in response to TPN40, including CD40, CD54, CD86 and MHCII. The cytokine profile of TPN40 activated tsDC remained similar to that of Tet40 activated tsDC when analysed by ELISA, and finally MTS assay showed that TPN40 treatments were better tolerated by tsDC than treatment with Tet40. TPN40 activated tsDC also showed enhanced antigen uptake potential compared to control treatments, shown by fluorescent microscopy.

Raw data initially suggested that similar changes were induced in receptor expression following presentation as Tet40 or TPN40, however activation in response to Tet40 was strongly influenced by non-specific activation by the streptavidin scaffold rather than by CD40R specific interaction. Of the receptors which demonstrated a significant change in expression, presentation as TPN40 induced changes in receptors specifically associated with activation (particularly c-SMAC associated receptors) compared to the streptavidin construct which induced non-specific changes in other receptors not associated with primary DC activation (for example changes in CD11 family receptors) which were not affected by TPN40. This could indicate that TPN40 induced an activation profile specific to CD40R activation since increased expression of c-SMAC associated receptors was observed (which as discussed in chapter 1.2.2.2 correlates with more efficient T cell priming). LPS and Tet40 treatments induced changes in a number of non-specific receptors, which may suggest this response occurred as a result of non-specific, phagocytic activation.

Although a Th1 skewed cytokine response was observed following treatment with each of the multivalent scaffolds, the streptavidin control again had significant influence on production levels, while treatment with UPN controls produced

negligible changes. The data in this chapter also suggest that tsDCs activated by TPN40 are capable of phagocytising antigen in a similar manner to cells which have been activated with LPS. This capacity was unique to activated cells, and was distinctly absent from cultures treated with negative controls. Although TPN40 was less well tolerated than Tet40, cell viability remained within an acceptable range, suggesting that TPN40 should be tolerated at therapeutic doses.

The work presented in the current chapter suggests the specificity of multivalent CD40R targeted activation was improved by presentation on rigid, biologically inert activators (TPN40), compared to flexible biologically active activators (Tet40), which induced non-specific changes in receptor display and cytokine production.

Chapter 6: Monitoring T cell effector outputs following incubation with TPN40-activated tsDCs

Data from chapters four and five demonstrate that multivalent presentation of MTP40 induces changes in tsDC associated with an activated phenotype. Increased expression of activation receptors and cytokine production by tsDC activated by Tet40 and TPN40 suggests that multivalent presentation optimises CD40R interactions compared to MTP40. The ability of both Tet40 and TPN40 constructs to induce similar changes in activation associated receptors and cytokine profiles suggest that the changes result from specific CD40R targeted stimulation rather than the supporting scaffold.

Furthermore, TPN40 induced more specific responses than Tet40. This could be accounted for by the fact UPN negative controls induced minimal non-specific activation; receptor expression, cytokine production, and antigen uptake remained unchanged in response to this treatment. Therefore, the current chapter aimed to investigate whether TPN40-activated tsDCs were capable of stimulating a downstream T cell priming response *in vitro*, and whether this could ultimately support tumour cell lysis.

In the current chapter, “activated” tsDCs stimulated by TPN40 were introduced to T cell cultures alongside simultaneous exposure to antigen (in the form of tumour lysates), aimed to provide activation stimuli to investigate T cell priming.

The findings detailed in this chapter are presented to address the following research aims:

- Evaluating whether changes in cytokine profiles are induced by T cell lines in response to stimulation with TPN40-tsDC
- Assessing the impact of TPN40-tsDC on T cell line viability
- Identifying whether TPN40-tsDC induces T cell cytotoxicity against an autologous tumour cell line (ID8)

6.1 Cytokine production induced by three T cell lines, following co-culture with TPN40 treated tsDC

Changes in T cell cytokine production is perhaps the most well known response to APC activation and is considered an essential step in to priming an effective immune response. Cell cultures from the three independent T cell lines were removed from their respective culture flasks and 2×10^7 cells were re-suspended in 2ml IMDM media in individual 15ml polypropylene tubes. Cells were transferred to IMDM media to prevent tsDC from becoming activated by the additional supplements required for T cell maintenance in culture. This aimed to provide an unbiased, comparable baseline between treatments. Following 24-hour incubation of tsDC with activating treatments, 200 μ l/well of media containing 2×10^6 T cells was added to each well. Cells were returned to the incubator for 48 hours.

At the end of incubation, cells were collected by centrifugation at 1000xg for 10 minutes at 4°C to clear the supernatant of debris. Treatment media (500 μ l) was collected from each well and transferred to 1.5ml microfuge tubes for storage at -20°C before analysing by ELISA. Samples were prepared as described in section 2.17. Figures 6.1-6.4 overleaf each illustrate the production of one cytokine, comparing production by the three T cell lines CTLL-2, RMA and D10.

Figure 6.1 illustrates the production of IL-2 of the three independent T cell lines, in response to incubation with activation treatments and controls (as shown in the figure key). The datasets shown here depict the production of IL-2 in response to treatment with MTP40, UPN, or TPN40. As a positive control for T cell activation, additional wells were treated with 10nM PMA + 2 μ M ionomycin, to determine a positive response to activation for each cell line. Each dataset (MTP40, UPN, TPN40 and PMA-IONO) have been normalised by subtracting the baseline levels of cytokine produced by tsDC+T cells+ID8 lysate, without treatment. Figures 6.2-6.4 represent identical experimental layouts, for the cytokines indicated in the figure title.

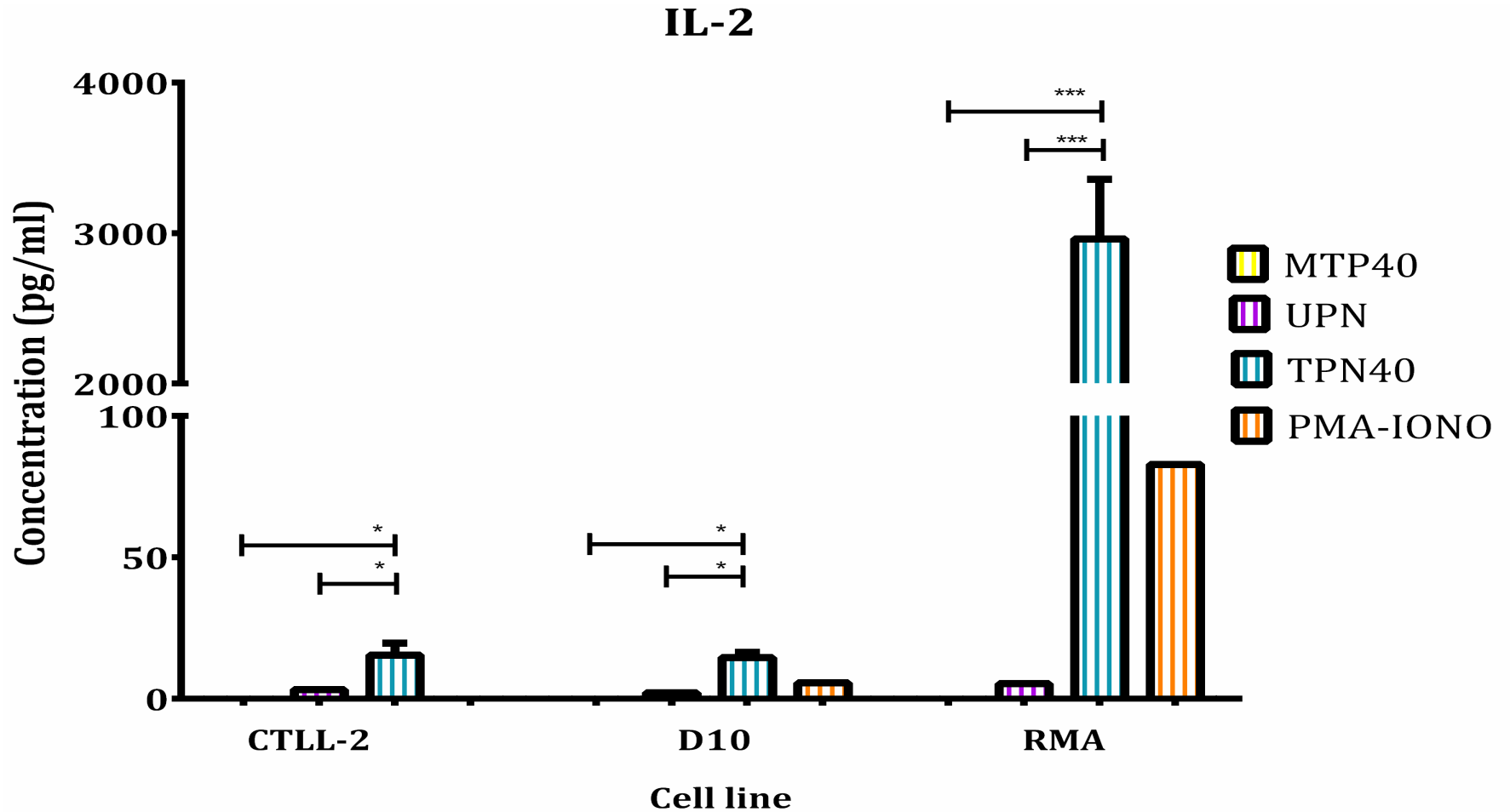


Figure 6-1: IL-2 production by T cell lines CTLL2, D10 and RMA following co-culture with “activated” tsDCs

tsDCs were incubated with activating treatments for 24 hours before adding T cell lines at a 1:10 ratio of DC:T cells for a further 48 hours before analysis. Each treatment value shown has been normalised by subtracting the baseline cytokine production by T cells incubated with untreated tsDC and 100µg/ml ID8 tumour lysates. Data represent two independent experiments containing samples ran in duplicate ± SD analysed by ANOVA with Tukey’s post-hoc test to define significance between samples

*=0.05, **=0.01, and ***=0.005. Treatment with 10nM PMA + 2 μ M ionomycin was used as a positive control to indicate the capacity of cell lines to respond to non-activation only and was therefore not subject to statistical analysis.

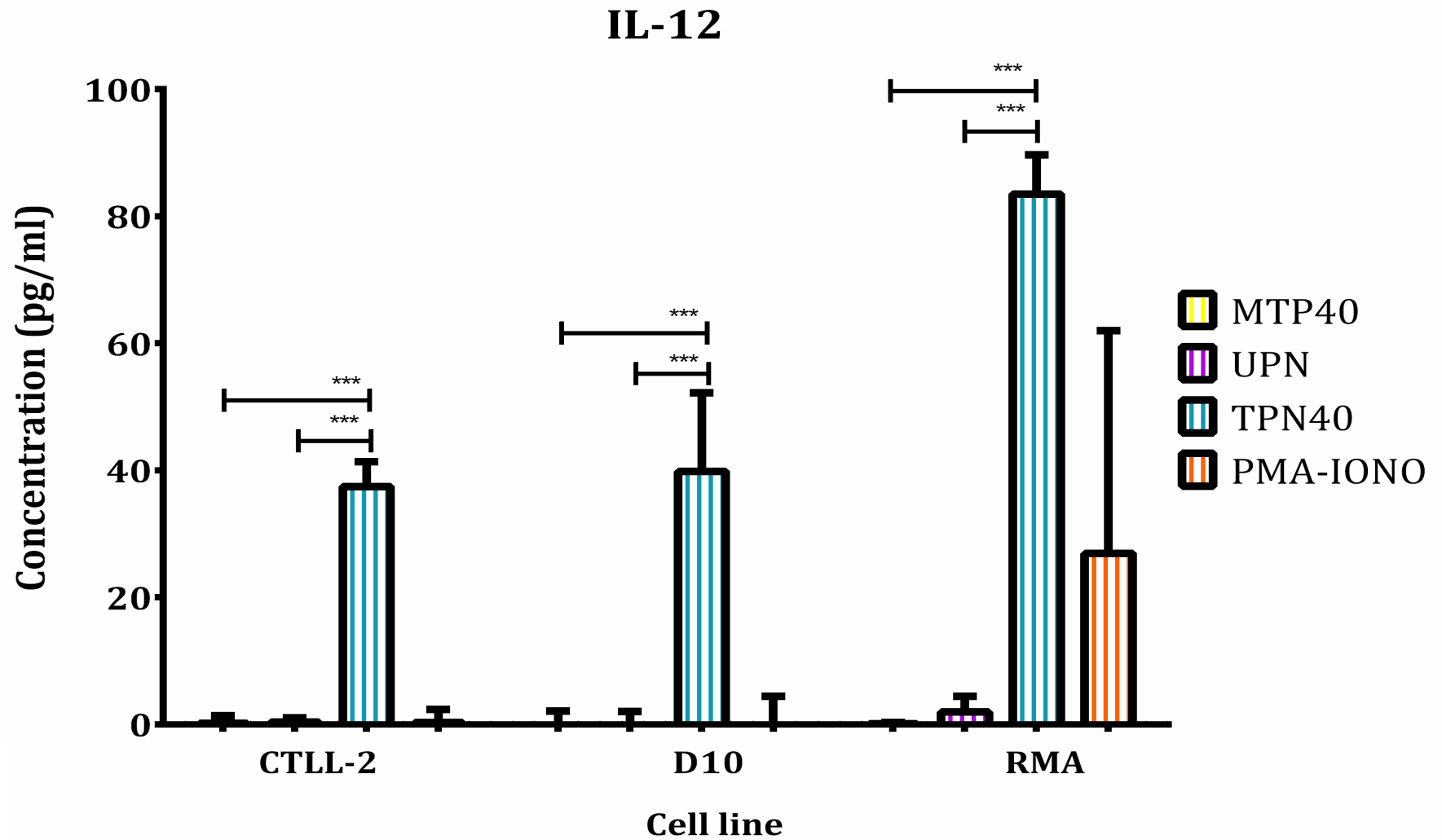


Figure 6-2: IL-12 production by T cell lines CTLL2, D10 and RMA following co-culture with “activated” tsDCs

Identical parameters were applied for the investigation of IL-12 as described for IL-2 analysis in figure 6.1

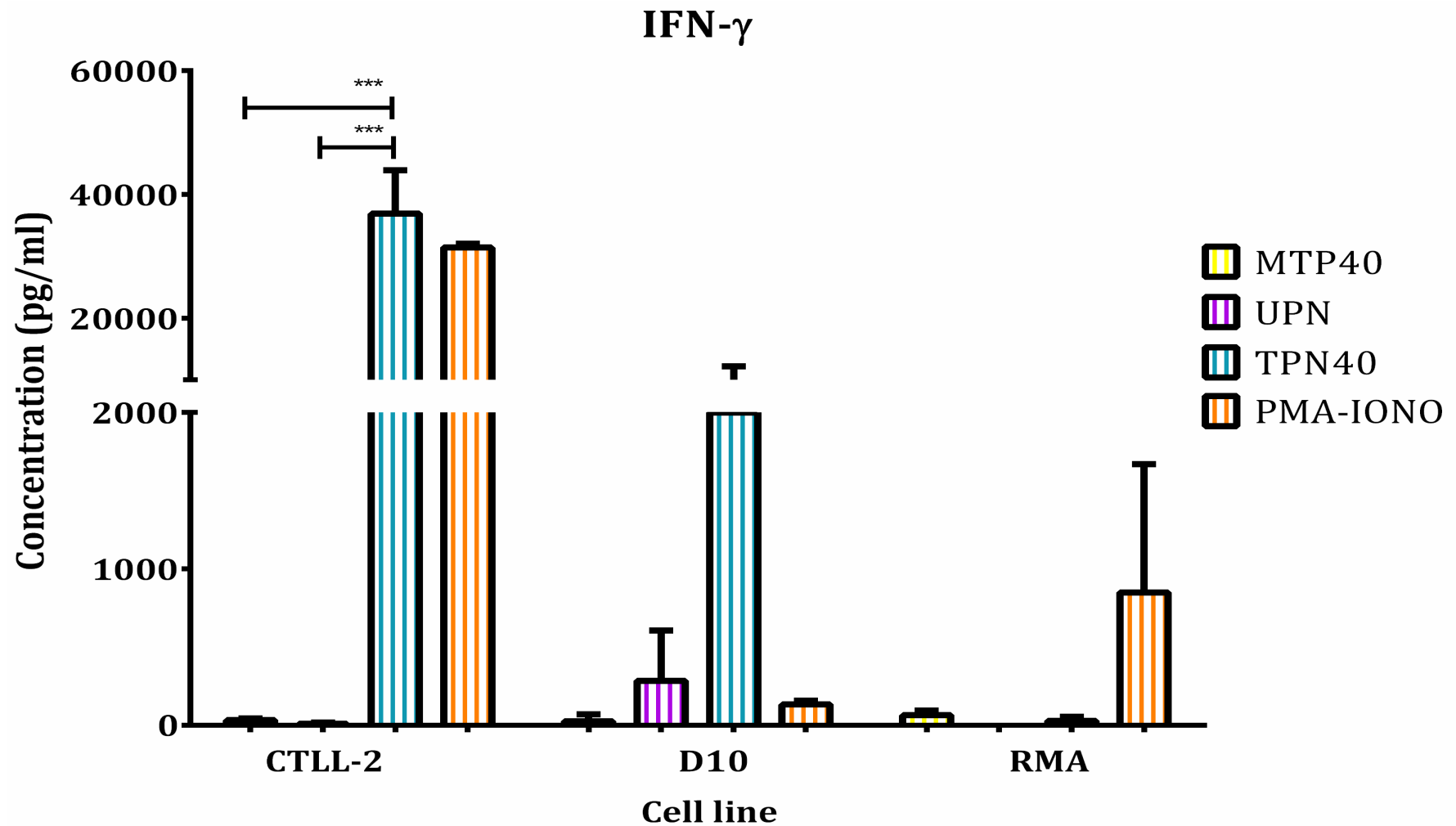


Figure 6-3: IFN- γ production by T cell lines CTLL2, D10 and RMA following co-culture with “activated” tsDCs

Identical parameters were applied for the investigation of IFN- γ as described for IL-2 analysis in figure 6.1

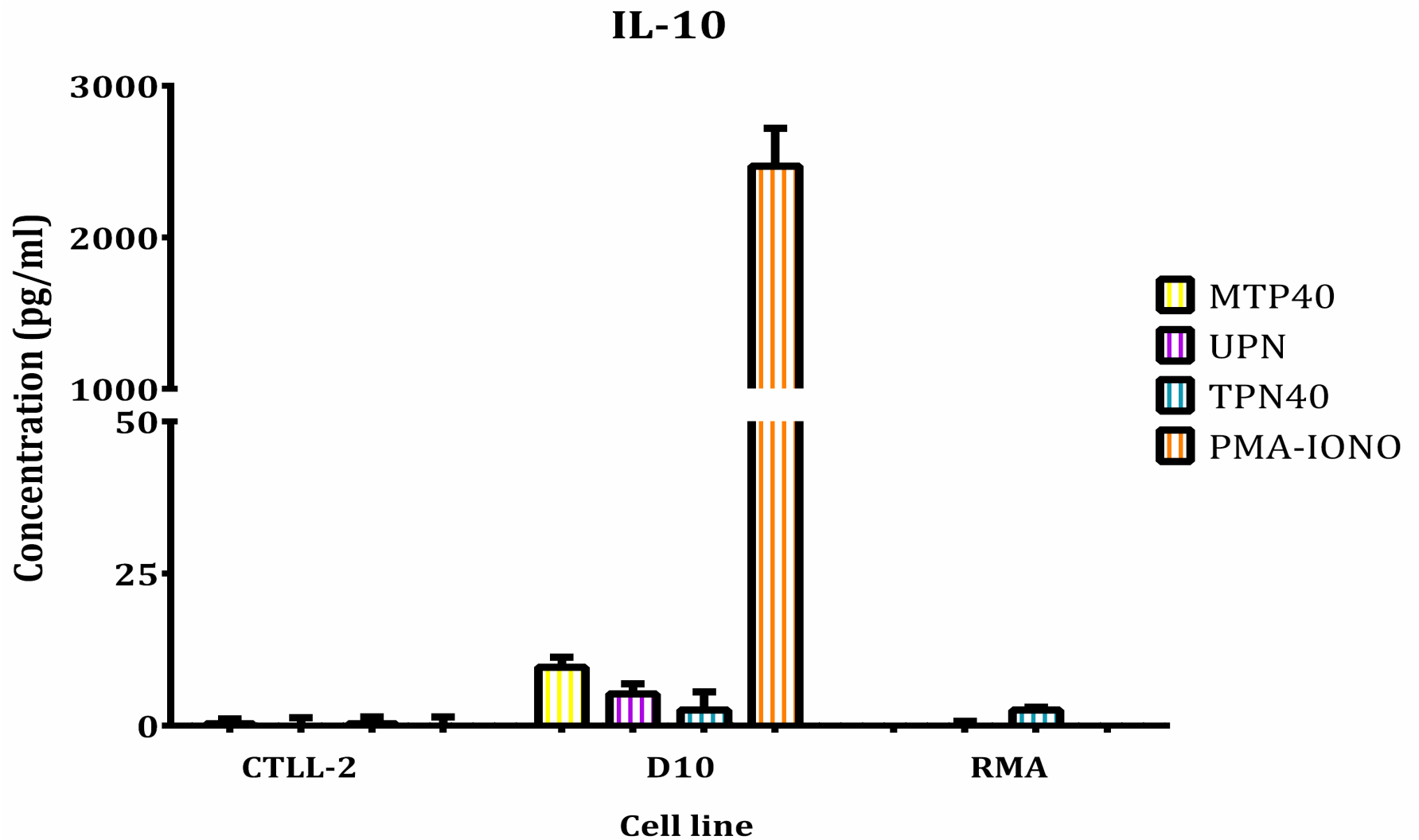


Figure 6-4: IL-10 production by T cell lines CTLL2, D10 and RMA following co-culture with “activated” tsDCs

Identical parameters were applied for the investigation of IL-10 as described for IL-2 analysis in figure 6.1

Table 6-1: Table summarising changes in cytokine production by T cell lines

	IL-2	IL-10	IL-12	IFN-γ
CTLL-2	*	-	***	***
D10-N4M	*	-	***	-
RMA	***	-	***	-

Table 6.1 summarises the statistically significant changes in cytokine production by CTLL-2, RMA, and D10 T cell lines in response to TPN-40 treatment compared to MTP40 or UPN controls. Tukey's post-hoc test was used to define significance between samples *=0.05, **=0.01, and ***=0.005.

6.1.1 CTLL-2 cell line induced IL-12 and IFN- γ production in response to TPN40-DCs

CTLL-2 is an established IL-2-dependent cell line derived from C57BL/6 mice and expresses markers for DC interaction, including B7 ligands, CD28, and the IL-2 receptor. This cell line was investigated to indicate whether TPN40-activated tsDCs produced IL-2 at sufficient levels to sustain T cell growth, and were able to elicit a cytokine response in CD8⁺ cytotoxic T cells.

In response to TPN40 activation, CTLL-2 displayed a statistically significant increase in IL-2, IL-12, and IFN- γ . Statistical significance was specifically observed in response to treatment with ID8 lysate and TPN40-DCs. This observation supports the hypothesis that antigen and co-stimulatory signals are required in parallel to induce T cell priming and cytokine production.

Investigation of the Th2 type cytokine IL-10 revealed negligible production with no statistical significance following any of the applied treatments. Data obtained with the CTLL-2 thus suggest that CD8⁺ cells can mount a Th1-skewed cytokine response to antigen following activation with TPN40 in the presence of an appropriate source of antigen.

6.1.2 D10 cell line induced IL-12 production in response to TPN40-DCs

D10-N4M is an IL-1-dependent cell line derived from AKR/J mice. In the present work, D10 cells were investigated to determine the response of Th2 cells to TPN40 DC targeting as these cells are known to produce IL-10, amongst other immunomodulatory cytokines including IL-4, IL-5, and IL-13 (Kupper et al., 1987; Kaye et al., 1984). D10 cells treated with TPN40-DC revealed significant upregulation of IL-2 and IL-12. The D10 cell line also displayed strong upregulation in IFN- γ in response to TPN40-DC. However this finding had poor reproducibility between replicates. No upregulation was observed in IL-10 production in response to TPN40 treatment,

Taken together, these data suggests TPN40-DCs induced negligible changes in Th2 cells in culture. In fact, treatment with TPN40-DC induced upregulation of Th1 type cytokines in this typically Th2 cell line; although, the levels of production were lower than in the Th1 and cytotoxic cell lines. Treatment with PMA and ionomycin as a positive control revealed a significant upregulation in IL-10, confirming that D10 cells can induce Th2 cytokines when non-specifically activated.

6.1.3 RMA cell line induced IL-2 and IL-12 production in response to TPN40-DCs

The RMA cell line derived from C57BL/6 mice T lymphoma which stably transfected to express B7 costimulatory molecules was used to investigate the response of Th1 CD4⁺ cells. The RMA cell line demonstrated the greatest upregulation in IL-2 compared with other cell lines, in agreement with the fundamental role of Th1 helper cell types, to induce and propagate effector cell responses through cytokine signalling. Statistically significant upregulation of IL-12 was also observed in this cell line. Notably, IFN- γ and IL-10 production were not altered in response to TPN40-DC incubation in this cell line.

The results from this section indicate that TPN40-DCs had the capacity to enhance cytokine signalling in both CD4⁺ and CD8⁺ subsets. CD4⁺ Th1 cells induced abundant production of IL-12 and IL-2, while the Th2 cell line D10 also induced IL-12 production. CD8⁺ cells responded to treatment by upregulating production of IL-12 and IFN- γ .

6.2 T cell viability following treatment with TPN40-DC co-culture

Following the observation that T cells cultured with TPN40-DC and ID8 lysates induced a significant upregulation in cytokines associated with enhanced proliferation and survival, the next step was to investigate the proliferation rates of T cell lines in response to treatment. The results of these analyses are presented in figures 6.5-6.7.

T cell lines were cultured in the presence of tsDC stimulated with TPN40 and ID8 tumour cell lysates, using the same treatments as outlined in table 2.3. This approach aimed to induce efficient T cell priming in the presence of activated tsDC, which are expected to induce expression of the co-stimulatory receptors and antigen presentation required for T cell interaction, as indicated by earlier data (see section 5.1 and 5.4). Identical conditions for activation were used as described for analysis of T cell cytokines, described in section 2.11. Heat shocked ID8 tumour cell lysates were additionally included to provide an appropriate source of antigen to generating a tumour specific T cell response.

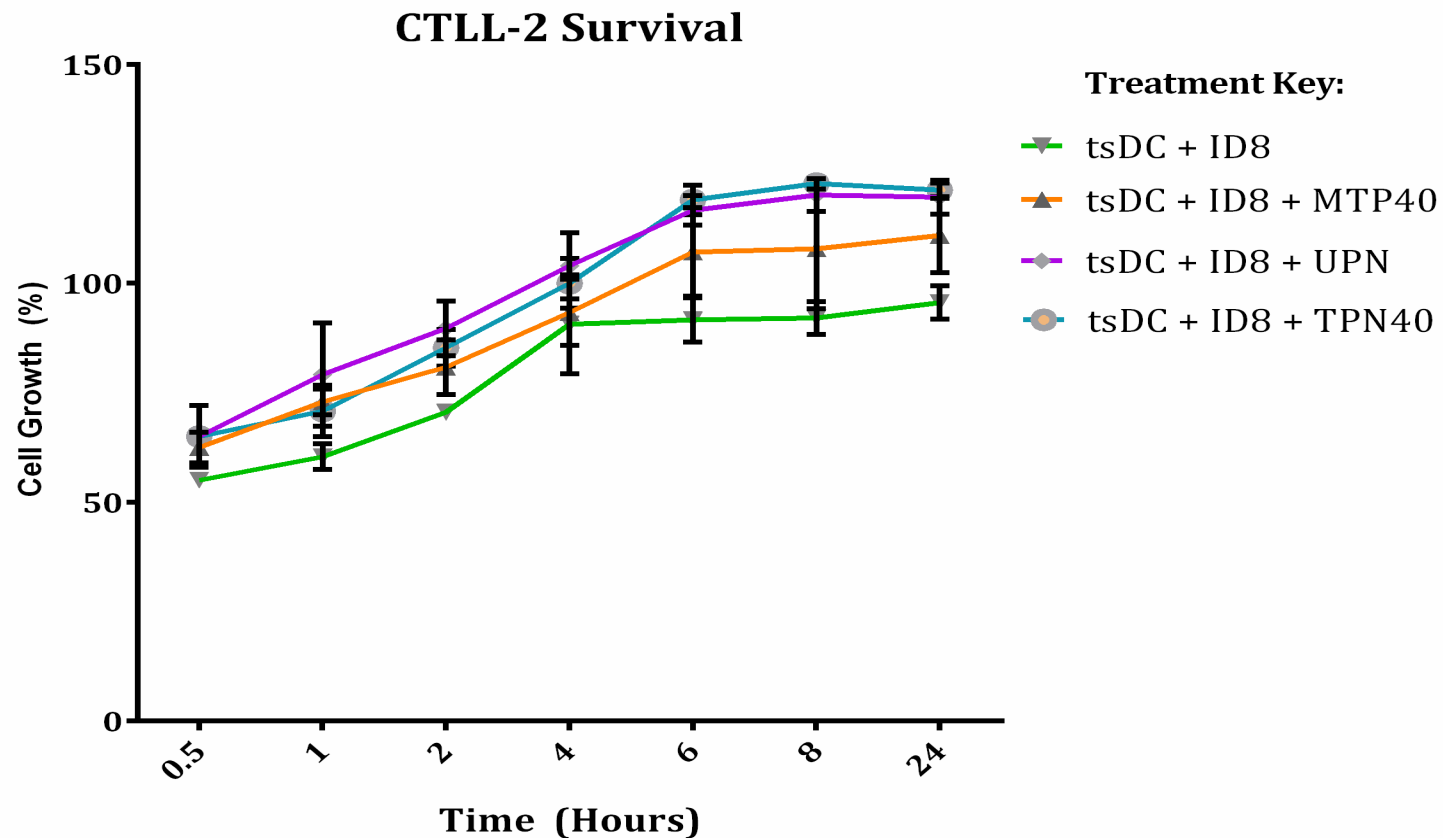


Figure 6-5: Cellular viability of the CD8⁺ T cell line CTLL2 following culture with TPN40-activated tsDC.

tsDC were seeded at 1×10^3 and incubated with activating treatments for 24 hours before adding T cell lines (indicated above) using a 1:10 ratio of DC:T cells. Mixed cell cultures were incubated for an additional 24 hours prior to the addition of MTS reagent. Production of formazan metabolite absorbance at 490nm was measured at various intervals up to 24 hours. Figures reveal per cent cell growth compared to the untreated DC:T cell co-culture as the baseline. Data represent two independent experiments containing samples ran in duplicate \pm SD.

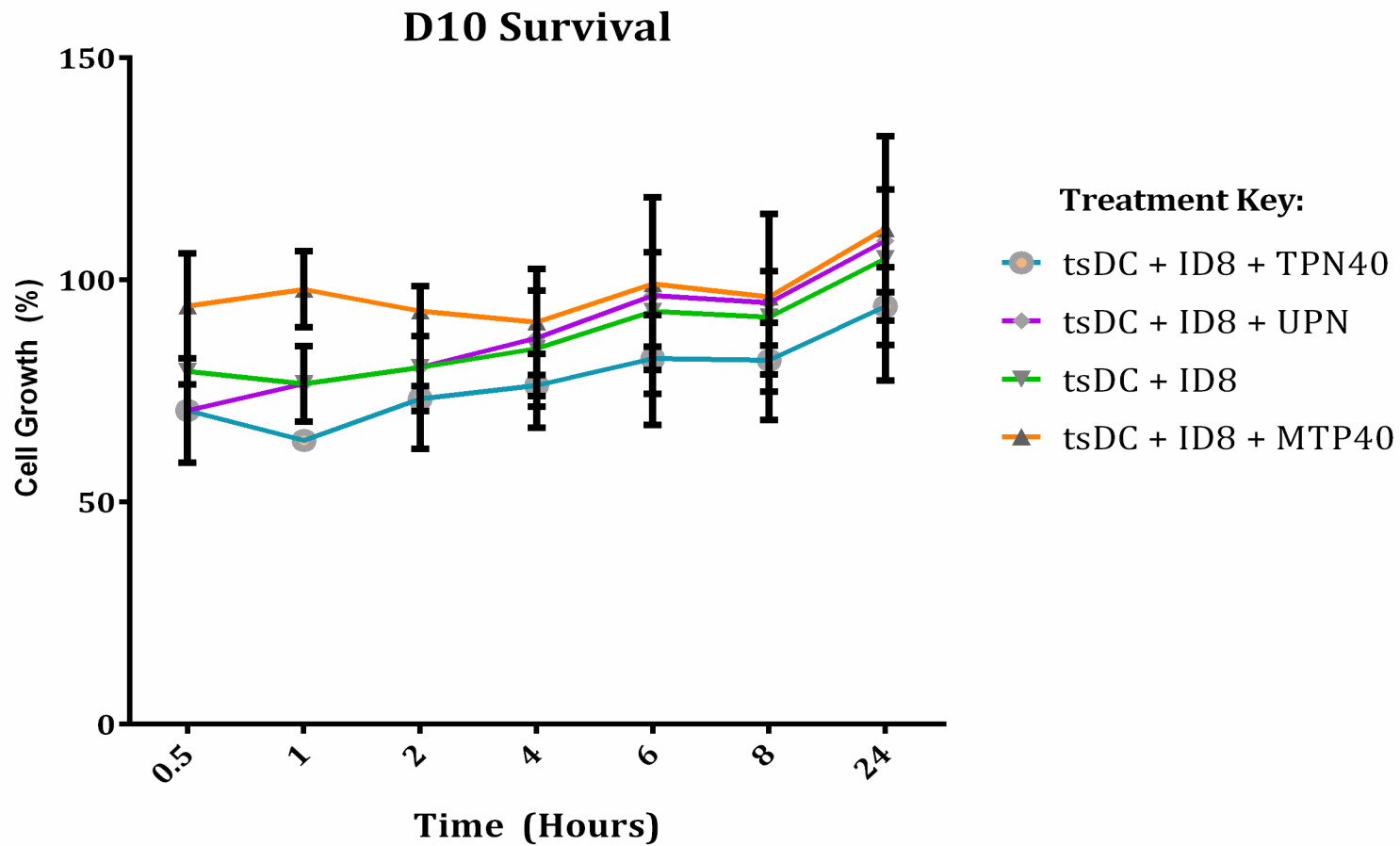


Figure 6-6: Cellular viability of the CD4⁺ Th2 cell line D10 following culture with TPN40-activated tsDC.

Identical treatment conditions and analysis methods were applied as described for figure 6.5.

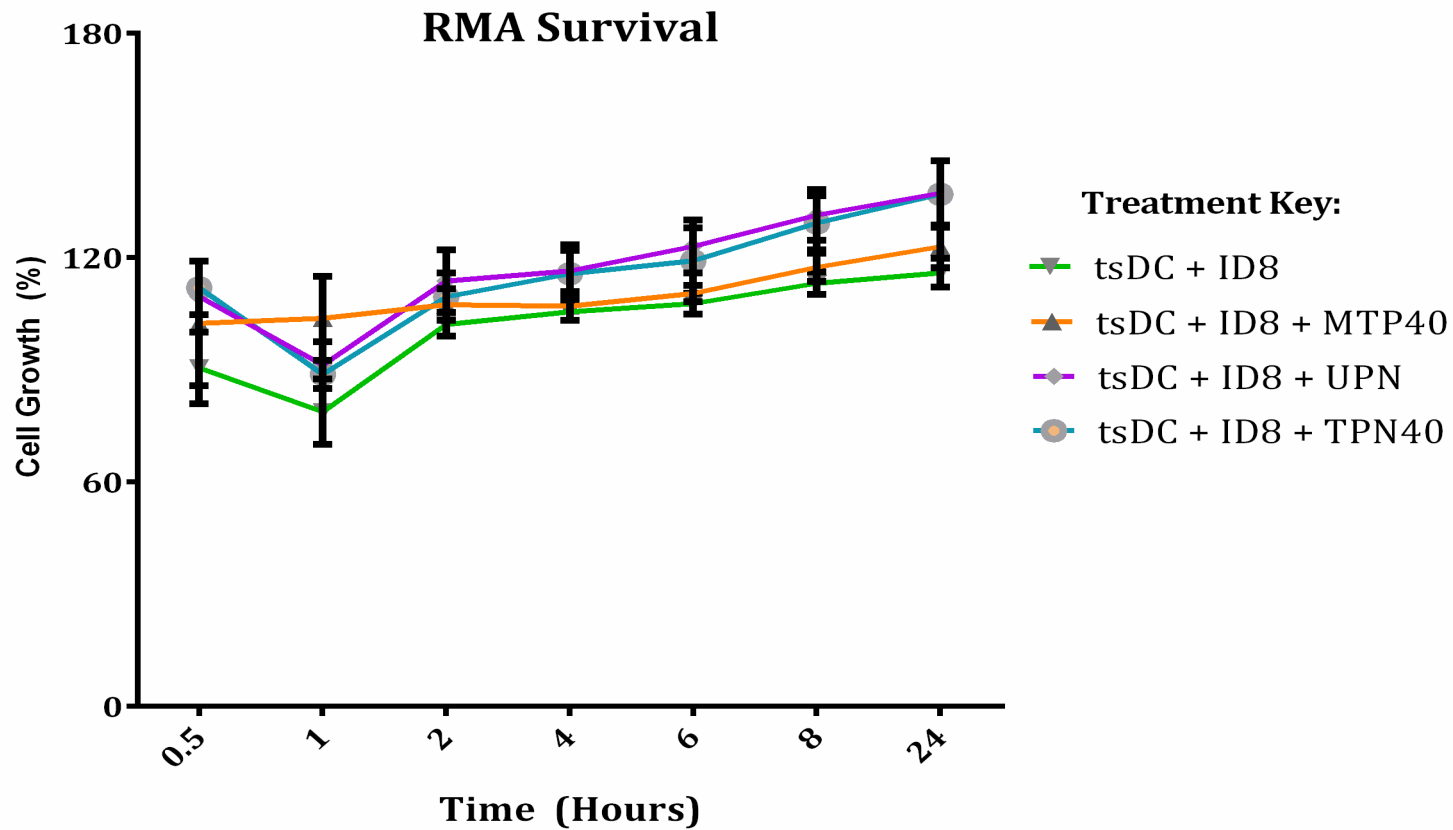


Figure 6-7: Cellular viability of the CD8⁺ T cell line CTLL2 following culture with TPN40-activated tsDC.

Identical treatment conditions and analysis methods were applied as described for figure 6.5.

Summary of T cell viability following activation treatments

Statistically significant changes were not observed in T cell lines in response to culture with TPN40-DC, although two interesting trends were observed. The changes in T cell proliferation in response to TNP40 is summarised in table 6.2 below.

Table 6-2: Summary of changes in T cell line viability in response to activation treatments

<u>Endpoint T cell proliferation (%)</u>			
<u>Treatment</u>	CTLL-2	D10	RMA
MTP40 	111	112	123
UPN 	96	123	116
TPN40 	92	98	120
ID8 Lysate 	96	105	116
ID8 + UPN 	120	109	137
ID8 + TPN40 	122	94	137

As summarised in table 6.2, the three T cell lines investigated responded differently to co-culture treatments. Interestingly, CTLL-2 and RMA cell lines (representative of CD8⁺ and Th1 effector cells, respectively) both showed a trend toward increased survival after 48 hour co-culture compared to the untreated baseline co-cultured with tsDC alone. Th1 helper and CD8⁺ effector cells both revealed a trend of increased survival following incubation with TPN40-DC compared to baseline, while the Th2 cell line D10 did not show increased survival following activation treatment. This finding suggests that TPN40-DC are well tolerated *in vitro*, and that further investigations using extended incubation periods will be required to determine whether this may have an effect on cellular proliferation as several treatments showed growth above 100%.

6.3 Determining the cytotoxic function of CTLL-2 cells in response to DC activation

Effector CD8⁺ cells induce direct cytotoxicity of target cells resulting in apoptosis, as discussed in section 1.2. The fluorescent dye used in the CellTox assay binds to the target cell DNA which is exposed following lysis, providing a direct measure of cytotoxicity. In this case, lysis buffer represents maximum cell lysis in response to treatment. The effects of TPN40-DC priming on the ability of CTLL-2 cells to initiate a cytotoxic response to target ID8 tumour cells is illustrated in figure 6.8.

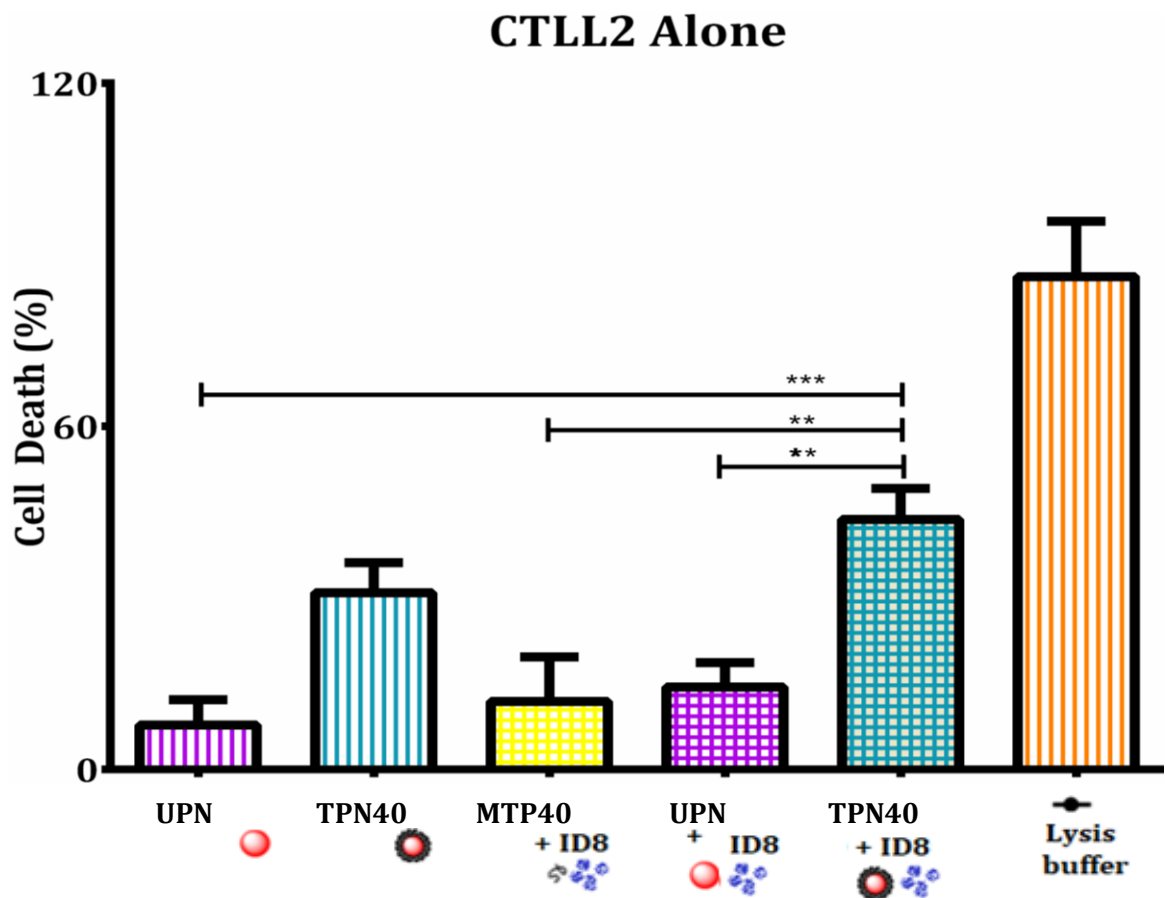


Figure 6-8: CTLL-2 induced cytotoxicity of ID8 murine tumour cells following incubation with TPN40 activated tsDCs

tsDC were seeded at 1×10^3 and incubated with activating treatments containing UPN, TPN40 or MTP40 with or without ID8 tumour cell lysates for 24 hours. After 24 hours, effector CTLL-2 CD8⁺ T cells were added at a 1:10 tsDC: CTLL2 cells. Mixed cell cultures were incubated for an additional 24 hours prior to addition of CellTox reagent. After CellTox label was added, wells were incubated for a further 48 hours before fluorescence was measured at 520nm. Figures show per cent cell death normalised by the untreated DC:T cell co-culture as baseline. Data represent three independent experiments containing samples ran in triplicate \pm SD analysed by ANOVA with Bonferoni post-test analyses. Lysis buffer supplied by the manufacturer supplemented with 0.05% Triton-X was used as a positive control representing maximum cell death, and was therefore not compared against treatments for statistical analysis. P values: *=0.05, **=0.01, and ***=0.005.

Figure 6.8 shows that TPN40-DC treatment increases the cytotoxic capacity of the CTLL-2 T cell line. CTLL-2 cell lines showed increased cytotoxicity against the ID8 tumour cell line following treatment with TPN40 alone compared to CTLL-2 cultures treated with UPN or MTP40 controls. This response was further enhanced by the inclusion of ID8 cell lysates,

This data suggests that MTP40 presented on multivalent scaffolds induced higher rates of cell death than untargeted control treatments, to a statistically significant level. The percent cytotoxicity was calculated based on the release of LDH from experimental test samples compared to maximum LDH release induced by lysis buffer. The results collected showed a substantial amount of variation, however this could be expected as the cells in assay was incubated for over 72 hours in total, whereas the CellTox assay is generally used for short term culture of less than 24 hours.

As discussed in section 1.2.1.2, efficient T cell priming in the *in vivo* environment requires input from Th1 helper T cells to induce effective activation. Because of this, the next experiment aimed to determine whether the effects of TPN40 activated tsDCs could be potentiated by inclusion of a Th1 cell line. Following the observation in section 6.1 that RMA cells produced significantly greater amounts of stimulatory Th1 associated cytokines in response to TPN40 activation, the cytotoxicity assay described in section in section 2.22 was therefore repeated in the presence of RMA cells. The current section aimed to determine whether including cells capable of Th1 cytokine production could potentiate ID8 cell killing by CTLL2 T cells.

CTLL2 + RMA

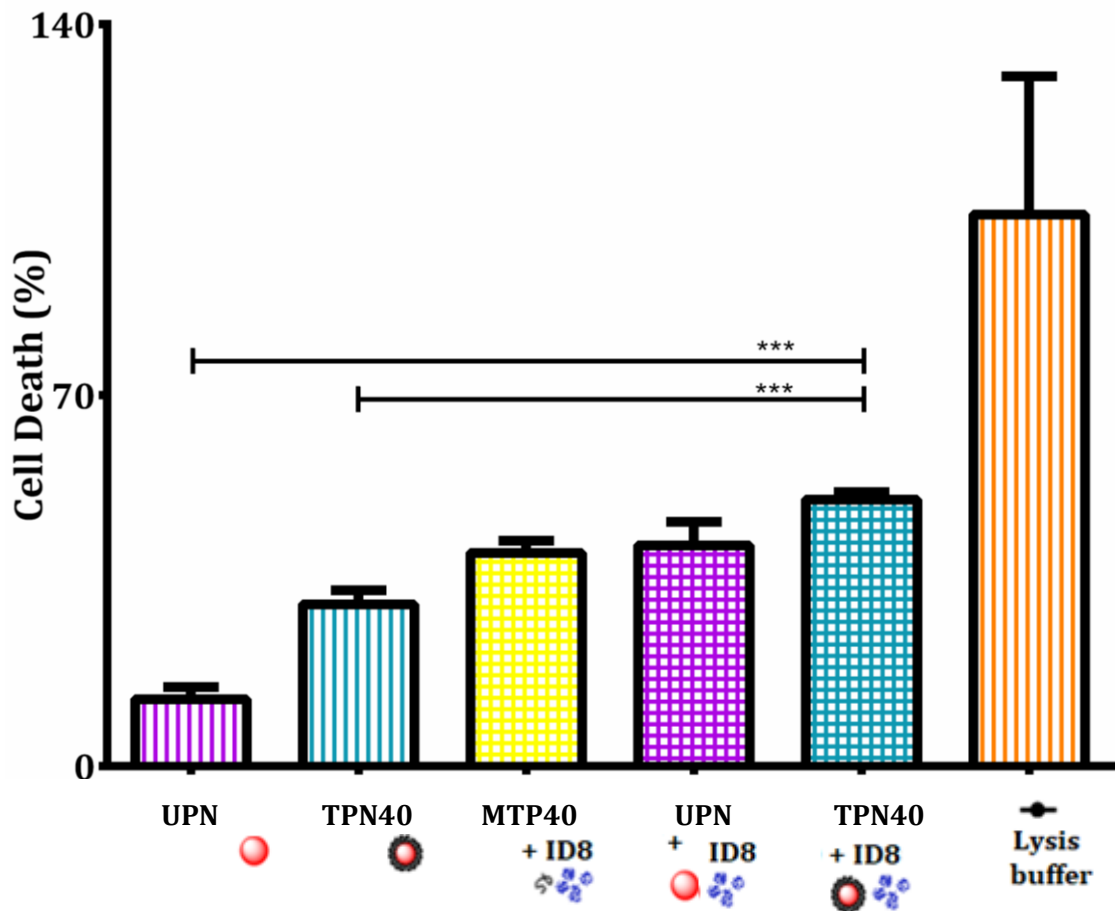


Figure 6-9: CTLL-2 induced cytotoxicity of ID8 murine tumour cells following incubation with TPN-40 activated tsDCs in the presence of the Th1 cell line RMA

DC were seeded at 1×10^3 and incubated with activating treatments containing UPN, TPN40 or MTP40 with or without ID8 tumour cell lysates for 24 hours. After 24 hours, effector CTLL-2 CD8⁺ T cells plus Th1 type RMA cells were added at a 1:1:10 ratio of tsDC:RMA:CTLL-2 cells. Mixed cell cultures were incubated for an additional 24 hours prior to addition of CellTox reagent. Fluorescence was measured at 520nm following an additional 48-hour incubation. Figures show per cent cell death compared to the untreated DC:T cell co-culture as baseline. Data represent three independent experiments containing samples ran in triplicate \pm SD analysed by ANOVA with Bonferoni post-test analyses. A Lysis buffer provided by the kit manufacturer (Promega) was included as a positive control for maximum cell death, and was therefore not compared against treatments for statistical analysis. P values: *=0.05, **=0.01, and ***=0.005.

The capacity of CTLL-2 cells to induce cytotoxicity in target cell populations was not improved by the inclusion of the T helper cell line RMA. The Th1 type helper cells

were included in co-culture experiments investigating ID8 cytotoxicity, to determine whether the additional cytokines produced by T helper cells could potentiate CTLL-2 cell cytotoxicity following priming by TPN40 activated tsDCs in the presence of ID8 lysates. CTLL-2 cytotoxicity was not significantly improved by the addition of Th1 type RMA cells.

The ability of CTLL-2 cells to induce cytotoxicity in the allogeneic murine tumour cell line ID8 supports the proof-of-principle concept that TPN40 activation of tsDCs can produce immune cascade. Ideally, future studies should investigate T cell survival over longer time frames (more than 72-hour to the end point of experiments) to determine whether the data observed here representing early changes in T cell outputs could result in effective clonal expansion during long term analysis.

6.4 Conclusions

The current research chapter addressed several aims. First, cytokine analysis by ELISA assay showed that T cell lines induced cytokine production in response to activating treatment with TPN40. All three T cell lines upregulated IL-2 and IL-12 in response to TPN40; CD8⁺ cell lines (but not CD4⁺ cell lines) induced IFN- γ , while IL-10 was not produced in response to TPN40. T cell cultures tolerated treatment with TPN40, however clonal expansion was not detected in any cell lines. The cytotoxic T cell line CTLL2 induced greater cell death in response to TPN40 than control treatments, however this did not show significant improvement when ID8 cell lysates were included in experimental setup as a source of antigen, and therefore was unlikely to indicate a tumour specific response.

Chapter 7: General discussion & limitations of the study

7.1 General Discussion

Utilising the power of the patient's immune response to produce specific tumour rejection is an ongoing goal in cancer therapy. The main goal of DC immunotherapies is to stimulate tumour antigen specific cytotoxic T cells to initiate an immune response directed specifically against the tumour, with minimum impact on surrounding host tissues. In this manner, immunotherapies aim to preserve and extend the quality of life in cancer patients.

The original research presented here shows that multivalent presentation significantly improved the binding capacity of MTP40. The modified sequence was conjugated to two multivalent scaffolds to investigate their tolerability and stimulatory capacity; Tet40 which is able to present four MTP40 ligands per structure, and TPN40 which are expected to display 2×10^3 binding sites per nanoparticle, representing a significant increase in binding epitopes compared to the two binding sites presented by IgG. This may also account for the improved binding affinity identified in the current study, compared to other work investigating CD40R targeted antibodies. As discussed in section 1.5.4, CD40R targeted antibodies currently being investigated in the clinic show varied affinities for the CD40R, ranging from 1×10^{-5} to 5×10^{-11} . Which correlates with the antibodies mechanism of interaction as immunotherapies. In comparison, the binding affinity of MTP40 showed baseline affinity of 1×10^{-6} when in the unmodified monomeric form, which was increased to 8×10^{-8} upon presentation as Tet40. As various earlier publications have suggested a role for multivalent engagement of the CD40R in initiating an effective downstream response, the improved binding affinity of MTP40 for CD40R when attached to multivalent scaffolds may account for the greater functional outputs observed, compared against monovalent targeting. Importantly, inducing potent immunity by multivalent targeting may enable more effective treatment and reduce systemic toxicity as lower doses were required to induce an equivalent output response compared to monomeric peptide treatment.

The current study investigated the impact of multivalent targeting systems on tsDC maturation at two levels: the phenotypic level (indicated by surface receptors) and the functional level (primarily antigen uptake and cytokine expression). Antigen

presentation by APC subsets activates helper T cells, stimulating them to express CD40L which, in turn, activates CD40⁺ DCs to prime effector T cells (Roy et al., 1993). The data presented in the current study suggests that multivalent receptor ligand interactions may potentiate the activation response associated with CD40R signalling by more efficiently engaging with the upregulated CD40R. Importantly, this work presents a novel method for delivering targeting peptides to the tumour microenvironment by determining the suitability of gold nanoparticles as scaffolds for multivalent immune targeting. This could present future potential in both targeted drug delivery, and improving traceability of treatment *in vivo* as gold nanoparticles have the capacity to be directly imaged *via* X-ray or CT imaging.

The current research suggests that stimulation of CD40R through multivalent surface receptor interactions induces greater functional responses in the tsDC cell line compared to its monomeric stimulation. This was supported as greater changes were observed in surface receptor expression, cytokine production, and antigen uptake capacity when MTP40 was presented either on Tet40 or TPN40 scaffolds. As such, changes in the tsDC outputs investigated here suggest that multivalent peptide presentation enhances immune stimulation at the DC level.

In this study, we optimised the sequence of an 18-residue peptide targeted toward the CD40R to produce a linear sequence for delivery *via* multivalent platforms. The findings presented are consistent with other groups investigating DC activation *via* CD40R antibodies and has further developed the field by investigating the use of alternative peptide therapies to confer advantages against the traditional antibody targeting method. First, peptides are commonly recognised as highly selective targeting compounds typically well tolerated *in vivo* (Slingluff et al., 2011). Peptides function as efficacious signalling molecules that bind specific cell surface receptors such as G protein coupled receptors, initiating intracellular events. Second, application of small molecules such as peptides leads to high penetration rates across leaky tumour vasculature (Fosgerau & Hoffmann., 2015). The multivalent constructs developed here are expected to possess a diameter of 10-15nm which equates to approximately half of the diameter compared to a typical IgG antibody with dimensions of 30 x 24nm (Saber et al., 2011). The reduction in size may improve potential for therapy to penetrate tumour vasculature and access target DCs specifically in the tumour where immunosuppressive phenotypes are observed.

Earlier work investigating the events required for efficient T cell priming has indicated that clustered presentation of CD40L at the T helper cell surface is a prerequisite for the formation of a functional immunological synapse and downstream signalling of the CD40R (Grassmé et al., 2002). As such, effective upregulation of the CD40R as was observed in response to multivalent CD40R activation presents great potential to induce a T cell response. Importantly, this finding is in line with recent results published by several other groups in which the activation of DCs using nanoparticles conjugated to agonistic antibodies for CD40, demonstrating upregulation of CD40R and CD86 on the DC surface, which induced down-stream priming of CD8⁺ T cells (Cruz et al., 2014; Rosalia et al., 2015), as described in sections 1.5.5 and 1.8. As discussed in section 1.2.2.2, substantial disparity has been reported in the upregulation of surface receptors in response to DC activation, depending on the DC subset involved (Gilliet et al., 2002; Lutz., 2012). The receptor profile affected in the current study may therefore be specific to the immortalised tsDC line, and so it would be interesting to investigate the activation potential in DCs extracted from patient blood samples to determine whether the changes are consistent.

Functionally, the cytokine profiles of tsDC showed slight shifts, however, this finding was not as significant as described by other groups, particularly in reference to IL-12, which is typically produced by APC populations in response to antigen exposure (Trinchieri., 1995; Demangel et al., 2001). This observation is contextually relevant because the DC data collected in the current study was produced to determine if DC outputs in response to CD40R ligation rather than in response to antigen exposure. It could therefore be argued that upregulated IL-12 production would be more likely to occur following combination treatments with targeting peptide alongside an appropriate source of antigen. Alternatively, the slight but tightly controlled upregulation of cytokines may be an encouraging finding because cytokine storm is one of the most common side effects of immunotherapy. Perhaps by utilising DCs mediators to launch a modest, highly specific immune response rather than stimulating T cells directly which may induce excessive immunity (*via* secretion of cytokines which are prone to inducing CRS as discussed in chapter 1.4.3), this side effect can be reduced.

Despite contrasting data regarding the ability of tsDC to induce changes associated with robust activation, the second major observation of the present research was that the tsDC line induced downstream changes in effector T cell lines, an output which was isolated to cultures activated by TPN40 in the presence of allogeneic tumour antigen. In terms of cytokine production, CD8⁺ T cells presenting exogenous pathogen *via* the MHCI pathway are characterised by production of IFN- γ , TGF- β and TNF- α . Th1 and Th2 subsets of CD4⁺ T cells are generally associated with IL-2 and IL-10, respectively (Murphy et al., 2001; Llopiz et al., 2017). Notably, the current study observed changes in cytokine production associated with CD8⁺ and CD4⁺ Th1 cell priming.

The results of this study provide strong indications that TPN40-DC were capable of interacting with T cells of both CD4⁺ and CD8⁺ subsets. This finding is interesting considering the complex interplay between multiple immune cells required to initiate effective immunity. *In vivo* studies are required to further characterise the repertoire of immune cell interactions involved in shaping DC maturation. As such, the data presented here demonstrate encouraging markers for DC activation but can only suggest limited applicability as a stand-alone, *ex-vivo* observation.

Analysis of tsDC receptor and cytokine profiles in response to TPN40 activation demonstrated greater changes associated with DC maturation than tsDC activated with Tet40. There was no indication of non-specific activation resulting from the nanoparticle scaffold, suggesting that this scaffold reduces non-specific reactivity of the treatments. Importantly, the specific responses elicited by TPN40 in comparison to Tet40 presented potential for TPN40 to meet the needs for highly specific targeting constructs.

The primary goal achieved by the present research was the production of a modified peptide and characterisation that the molecule successfully targeted the CD40R. The importance of this finding can be explained in the context that development of tumour progression coincides with a phenotypic switch in intra-tumoural DCs, whereby compromised maturation is observed and prevents effector T cell priming (Ma et al., 2012; Tran-Jancho et al., 2015). Interestingly, depleting resident DC populations in advanced stage tumours has revealed improved survival and delayed tumour progression (Ma et al., 2012), suggesting DCs adopt

immunosuppressive functions over time and that eliminating late-stage DCs alleviates immunosuppression.

The results presented in this section indicate that TPN40-activated tsDCs have the capacity to induce both upregulation of IFN- γ production in CD8⁺ T cell subsets and prompt IL-2 production in a Th1 cell line. The universal downregulation of tsDC produced IL-10 in response to both Tet40 and TPN40 targeted treatments is of particular interest, considering IL-10 is strongly correlated with the induction of Treg cells in the tumour microenvironment. This universal reduction in IL-10 suggests tsDC activation with multivalent CD40R targeted treatments may reduce production of immunosuppressive cytokines commonly observed in the tumour.

7.2 Limitations of the study

While the results of the current work indicate the potential for CD40R activation of tsDCs through multivalent peptide treatments, several protocols were additionally tested which did not yield successful results, and should be considered for further optimisations. Other experiments which could have provided further insights into the mechanism of action of MTP40 were unable to be carried out due to limited time and resources available. Areas of work that hold potential for future investigations are outlined in the following section.

7.3 Experiments requiring further optimisation

7.3.1 Collection and enrichment of DC precursors from human blood

In order to investigate the impact of CD40R activation on human DCs, cell enrichment was initially investigated using a MACS Cell Separation for magnetic cell isolation from patient blood samples. Patient samples were collected by centrifugation followed by buffy coat isolation, and aimed to isolate DCs based on retrieval of cells expressing CD14 which were then returned to culture under optimal media conditions. Unfortunately, low volume of patient sample resulted in very low cell yields which were not able to be maintained in culture.

7.3.2 Alternative outputs of DC activation

Migration capacity of DC serves as a marker of activation, as DCs alter surface receptor expression including ICAM1 in order to migrate to the draining lymph node following antigen exposure. This would be an interesting study to compare

whether the migratory capacity of tsDC changed following activation, but was not successfully optimised during the current work as tsDC line was highly affected by seeding density; seeding at too high volumes caused cells to detach from the base of the plate affecting the output, while seeding at too low density stunted cell growth and did not produce clear boundaries. Western blots were also conducted throughout the course of this study to investigate the activation of STAT3 and JAK3, which are phosphorylated following ligation of CD40R on the tsDC surface, however the membranes from these experiments were damaged and unable to be quantified. Downstream signalling cascades should therefore be investigated in future experiments to characterise the effects of CD40R ligation. Considering MHC expression did not show significant upregulation in response to any treatment in tsDC cultures, it may be necessary to repeat the current work with another DC line. A viable alternative may be to use the DC line D1, which other groups have used to demonstrate significant upregulation of MHCII, CD40R and CD86 (Trouche et al., 2007).

While the surface markers investigated in the current study provided an indication that TPN40 was capable of inducing changes associated with activation, it would be interesting to investigate the impact on a wider range of receptors, to further characterise the response. For example, CD70 and 41BB receptors were not included in the current work, and would provide interesting candidates for future research considering their proposed roles in tumour escape from immune detection (de Luca & Gommerman., 2012).

7.3.3 Protocol for T cell activation

Although there are many other avenues which could be explored to further characterise the impact of CD40R activation in tsDC, it may be more prevalent to focus on optimising the co-culture conditions between tsDC and T cell lines. In this case, a high number of variables likely to influence the level of activation, including whether DC are activated in the presence of tumour antigen alongside CD40R stimulation (and if so which treatment is applied first), how long to incubate for, the ratio of T cells to DC and whether the cell lines used here were optimal for this study. To provide the most robust data in this setting, it would be optimal to work with autologous cells of T, DC and tumour lineage from the same individual to increase the likelihood of TCR-MHC interactions. The use of autologous cell types

may optimise T cell activation outputs, particularly considering the universally low-level of MHC expression at the tsDC surface even after CD40R and tumour lysate activation, which may prevent this cell line from inducing effective T cell priming. Ideally, DC from healthy patient cohorts would be compared with DCs isolated from tumour samples, allowing characterisation of the response in healthy and immunosuppressed DCs.

7.4 Future directions

7.4.1 Alternative methods to assess T cell response

In the current work, T cell responses were investigated using routine cell lines, by relatively non-specific assays to provide an indication of T cell priming as part of a multi-step sequence of activation, from tsDC activation through to T cell priming. In order to characterise the specific nature of the T cell response more accurately, more specific techniques for T cell analysis could be used. One such example would be to perform flow cytometric analysis of intracellular T cell cytokine production. In this setting, T cells are treated with inhibitors of secretion such as monensin or brefeldin A, which cause cytokines to accumulate within the cytoplasm upon antigen activation. After fixation and permeabilization of the lymphocytes, intracellular cytokines can be quantified by cytometry, which would allow quantification of the number of T cells actively secreting the cytokine of interest, and the amount of cytokine produced per cell (Lechner et al., 2000). This could be further combined with cell surface markers to determine the phenotype of effector T cells, and would be most beneficial in combination with mixed patient samples, as opposed to homogenous cell lines.

7.4.2 Investigating efficacy of TPN40 in 3d models and *in vivo*

Initially, the work carried out here only investigated cell-cell interactions in routine cell culture. The current study investigated how tsDCs responded to activating treatments in 2D culture based on a murine cell line, and how this activation impacted the activity of T cell lines; providing a clear picture of direct cell-cell interactions. Currently, in drug discovery, the standard procedure of screening compounds starts with the 2D cell culture-based tests, followed by animal model tests, to clinical trials (DiMasi et al., 2007). Only about 10% of the compounds progress successfully through clinical development, largely due to lack of clinical

efficacy or unacceptable toxicity, which would ideally be eliminated before progressing to *in vivo* models.

Limitations of the current study are therefore associated with the animal model system used, and the *ex vivo* nature of experimental setup. Although animal cell cultures provide a controlled microenvironment to study cell-cell interactions in a homogenous population, providing clear advantages for routine characterisations and pharmacology studies, It would have been more relevant to investigate the impact of CD40R activation in a human model, before moving to *in vivo* work. This is particularly relevant due to the high specificity of interaction between peptides and their epitopes, which is unlikely to provide a representative response in an *ex vivo* mouse model system.

This becomes particularly complicated when studying tumour-immunology, where interactions occur at many levels. Epithelial ovarian cancer is characterized by periods of remission and relapse of sequentially shortening duration until chemoresistance occurs (Markman et al., 2004). Such patients are the best candidates for immunological studies, since T cells' presence can be utilized as markers for disease progress and can be evaluated at different stages of the disease (Schmielau & Finn., 2001). The progression of cancer in the peritoneal cavity and the frequent formation of ascites, which characterize advanced stages of ovarian cancer, mainly stage IV, make this tumor a model for the study of different lymphocytic populations. Furthermore, the composition of lymphocytic populations in blood, ascites and tumors is regulated by various cytokines and chemokines produced by the tumors or the components of the immune system; replicating this complex dynamic is beyond the scope of single cell monolayers. Since almost all cells in the *in vivo* environment are surrounded by other cells and extracellular matrix (ECM) in a three-dimensional (3D) fashion, 2D cell culture does not adequately take into account the natural 3D environment of cells (Birgersdotter et al., 2005).

Future work could consider the use of spheroid cultures before venturing into *in vivo* models. Spheroid matrices grow cells naturally in a 3D environment, allowing cells to interact with each other, the ECM, and their microenvironment. In turn, these interactions in such 3D spatial arrangement affect a range of cellular functions, including cell proliferation, differentiation, morphology, gene and protein

expression, and cellular responses to external stimuli (Rimann & Graf-Hausner., 2012). Spheroid studies therefore present an interesting future direction for the current research to provide a more robust investigation of the multi-level cell interactions observed in the tumour-immune dynamic.

In the current study, three T cell lines were investigated to demonstrate the T cell response to activated DCs in culture. Although this represented a broad spectrum of T cell subtypes within the limited scope available, this cannot compensate for the *in vivo* repertoire of T cell receptors and MHC combinations. In addition, co-culture overrides microanatomical factors that may constrain the probability of *in-vivo* contact between DCs and T cells within the T cell zones of lymphoid organs. For example, the majority of splenic CD11b⁺ cDCs are located outside the T cell zone in the steady state and would contact T cells only after Toll-like receptor (TLR)-dependent signals drive their relocation into the T cell zone, yet they may still present antigen to activate T cells *in vitro*, further illustrating the limitations of such studies. If *in vivo* investigations were able to be conducted, it would also be interesting to characterise the half-life of MTP40 as free peptide *versus* the half life of Tet40 and TPN40, which has implications for clearance and treatment regimens.

While the ID8 cell line provided a representative model to study ovarian cancer, this was utilised as an initial investigatory system based on the repertoire of literature suggesting DC activation is particularly dysregulated in this tumour type. This is not to say ovarian cancer provides the only or optimum setting for DC investigations, and it may be interesting to investigate other associated tumour models. For example, DC activation and function is also dysregulated in breast cancer and has been related to cell clustering in the draining lymph node (Chang et al., 2013), which may provide an alternative model system where treatment could be delivered through percutaneous injection to DCs localised in the lymph node directly.

The pro-inflammatory cytokine IL-12 is required to induce the upregulation of IFN- γ *in situ* immune response, and so the upregulation of IL-12 by both tsDC and T cell lines suggests T cell activation occurred, which is supported since activated T cells also demonstrated production of IFN- γ , which characteristically occurs following IL-12 stimulation. *In vivo*, this may induce recruitment of immune cells to the tumour

site, enhanced tumour surveillance, and regression across multiple tumour types *in vitro* and *in vivo* (Muranski et al., 2009; Castro et al., 2018).

Recent *in vitro* studies of the immune environment in breast cancer have demonstrated that naïve T cells develop into Treg phenotypes in the presence of plasmacytoid DC (pDC) alone and that this phenomenon is significantly greater when naïve T cells are exposed to pDCs in addition to tumour conditioned media (Su et al., 2017). Other groups have reported similar data *in vivo*, where DC activation by recombinant IL-33 have induced significant upregulation of surface CD40R and antigen cross-presentation, CD8⁺ expansion, and IFN- γ production in the tumour mass, demonstrating that DC function can be recovered in a malignancy to induce a tumour specific CD8⁺ response (Dominguez et al., 2017). The outputs of DC activation observed in the present study are therefore in line with those reported by other research groups. This finding suggests that the immunosuppressive phenotype of DCs in the tumour shapes the resulting effector lymphocyte response. Alleviating DC suppression has also been reported to lead to demonstrable improvements in T cell functions by other groups, which was similarly observed in the present work. DCs stimulated through the gold nanoparticle platform were able to induce priming in allogeneic T cell cultures, suggesting that multivalent interactions can propagate effective downstream signalling induction, which would be interesting to observe *in vivo*.

7.4.3 Prospects for *in vivo* delivery and imaging of TPN40

Considering the wider perspective, the outputs reported in this work are valuable when considering the repertoire of cancers which demonstrate deficiencies in DC phenotype or infiltration. In this respect, ovarian cancer presents a unique niche for therapeutic drug delivery *via* distribution to the intraperitoneal cavity. For example, direct administration into the peritoneal cavity *via* injection requires minimum time and trained expertise and could be administered in close proximity to the tumour. This treatment method has shown superior treatment efficacy for the delivery of cisplatin plus paclitaxel in ovarian cancer, although in this this case, the associated cost of increased risk of site-specific reactions was observed due to cytotoxicity of the chemotherapies involved (Gonzalez et al., 2011). As such, immunotherapies may be advantageous over chemotherapies in this setting, due to lower cytotoxicity to surrounding tissues when delivered in the local tumour environment.

Several studies have discussed the lack of immune infiltrates in various tumours, which could account for the disappointing results of targeted cancer vaccines to elicit an immune response in solid tumours, compared to their haematological counterparts. Lymphoid tumours have closer proximity for interaction with the circulation, which may provide an optimal setting for lymphocyte infiltration, explaining the more potent responses in haematological malignancies to date (as discussed in section 1.5.4). The application of TPN40 in *in vivo* studies would be particularly interesting due to the potential to directly visualise the localisation of gold nanoparticles X-ray or CT imaging or *via* TEM, which could provide insight into distribution and retention properties in a minimally invasive setting.

Considering the wider perspective, the outputs reported in this work suggest TPN40 could provide a viable therapeutic option for cancers demonstrating deficiencies in DC phenotype or infiltration. Ovarian cancer presents a unique niche for delivery of therapeutic agents by injection to the intraperitoneal (IP) cavity, particularly in the early stages of disease progression whereby the tumour has not spread to any distal metastatic sites. Direct administration in this manner requires minimum time and trained expertise and allows treatments to be delivered in close proximity to the tumour. IP administration has shown superior efficacy for the delivery of cisplatin plus paclitaxel in ovarian cancer, at the associated cost of increased risk of site-specific reactions which were observed due to cytotoxicity of the chemotherapeutic agents (Gonzalez et al., 2011). As such, immunotherapies such as TPN40 may be advantageous over chemotherapies in this setting, due to lower non-specific cytotoxicity to surrounding tissues when delivered to the local tumour environment.

Studies demonstrating that intra-tumoural delivery of IL-12 induces DC maturation *in vivo* (van Mierlo et al., 2004) support the theory that tumours prevent DC progression from the immature state, but also that the suppression can be reversed following direct administration of immunostimulatory agents at the tumour site. Other groups in parallel have demonstrated enhanced maturation of tumour-infiltrating DCs following dissociation from the tumour and transfer to *ex vivo* culture (Preynat-Seauve et al., 2006). Taken together, these findings strongly indicate that the impaired DC maturation observed in the tumour can be alleviated

by DC targeting, through direct delivery of targeting agents which have shown potential to reverse immunosuppression directly at the tumour site.

7.4.4 Combination prospects for TPN40 with other immunotherapies

As discussed in chapter 1.4.1.2, immunotherapies have shown encouraging results in some malignancies. Anti-CD40R antibodies alone have been described to have some efficacy as a single treatment against various tumors, however it is generally recognized that treatment with one immune modulating antibody or cytokine is not efficient (Liu et al., 2012). In relation to this, anti-CD40R in combination with IL-2 has recently been tested against tumors in murine models. In an *in vivo* study of mice with melanoma tumors, the group of Liu et al. showed that anti-CD40R in combination with IL-2 was able to enhance the expansion of adoptively transferred T cells in a 5–10-fold manner and increase their anti-tumor activity by various mechanisms, including increased secretion of IL-12 and a higher expression of costimulatory molecules (CD80 and CD86) on APCs (Liu et al., 2012). Combination therapy of TPN40 with IL-2 would therefore present a viable avenue for future investigation, and is particularly exciting considering treatment with recombinant human IL-2 is FDA approved for the treatment of renal cell carcinoma, lymphoma, and melanoma patients (Waldmann et al., 2003).

Alternatively, intra-tumoural delivery in combination with checkpoint inhibitors may enhance the synergistic potential of existing therapies. Future research should investigate the potential for combination regimens of TPN40 alongside checkpoint inhibitor therapies, particularly in respect to PD-1 or PD-L1 antagonists. This could lead to the development of new combination therapies with particular relevance for cancers with poor disease prognosis influenced by the immune climate. *In vivo* models of colorectal adenocarcinoma and melanoma have demonstrated PD-L1 is sufficient to suppress anti-tumour immunity, where both tumour and host derived PD-L1 influenced immunosuppression and reduced cytotoxicity (Juneja et al., 2017), and DC vaccines have shown durable long term responses in melanoma therapy (Alvarez-Dominguez et al., 2017). Scarlett and colleagues demonstrated significant upregulation of PD-L1 by DCs recovered from murine ovarian cancer tumours. Expression was associated with a switch toward an immunosuppressive phenotype and aggressive disease progression detected by palpable tumour development (Scarlett et al., 2009). Upregulated PD-L1 on the APC surface interacts with PD-1 on

the T cell surface, inducing inhibition of the CD28 kinase signalling pathway in the target cell, which prevents transcription of proteins essential for maintenance and growth (Dong et al., 1999).

Considering that PD-L1 is upregulated by immunosuppressed DCs, and that previous groups have shown encouraging data regarding the application of checkpoint blockade therapies in the ovarian cancer setting (Scarlett et al., 2009 discussed in chapter 1.5), an interesting direction for future studies would be to investigate whether combinations of TPN40 with checkpoint inhibitors could produce an enhanced tumour-immune response. It was not possible to investigate the potential for interactions in the current study due to time and funding limitations, but would be interesting for future studies to investigate checkpoint inhibitors for combination with therapies targeting CD40R, since the two pathways exert their effects at different stages of the immune response, allowing synergistic activation T cell stimulation and survival alongside enhanced tumour cell killing.

Future work should therefore investigate the potential for combination regimens of TPN40 alongside checkpoint inhibitor therapies, particularly in respect to PD-1 or PD-L1 antagonists. This direction could lead to the development of new combination therapies.

7.4.5 A role for FcYR studies in optimising TPN40 delivery

In the current literature, antibodies blocking inhibitory checkpoints on T cells have been a major advance in cancer treatment, while agonistic antibodies for CD40R have had less success due to toxicity concerns. As agonistic antibodies require FcR interactions, models carrying human CD40R and FcRs simultaneously may provide a more representative study of the toxicities observed *in vivo*, leading to more robust toxicology data and improved therapeutic success. The additional requirement for Fc engineering was unmanageable in the time scale of this project, however it would be an interesting avenue for future studies to investigate the efficacy of TPN40 in combination with FcY adjuvant therapies.

7.5 Concluding remarks

In conclusion, peptide targeting of the CD40R *via* a multivalent delivery system successfully initiated maturation responses in the tsDC population, which translated to functional changes in effector T cell populations. This work supports the use of

gold nanoparticles as a multivalent drug delivery platform for enhanced immune stimulation and reduced toxicities in the tumour microenvironment.

This result is significant, not only in the primary context of CD40R activation, but also on the wider scale of nanoparticulate drug delivery. The observation that both multivalent platforms investigated could produce much more robust DC activation, which translated to downstream priming in T cell cultures, presents a prospective mechanism of optimised targeted drug delivery in a broader context. Of the two potential platforms investigated, both have wide applicability. Delivery *via* gold nanoparticles holds particular advantages due to the robust prospects for peptide conjugation through the innate attraction between the thiol side chains in cysteine residues to the surface of gold, meaning this method of drug delivery could have potential to deliver a vast range of other bio-therapeutic drugs in other research areas.

The current research was concerned with producing a proof-of-principle system to demonstrate whether multivalent presentation of ligands targeted to the CD40R of tsDCs improved the dynamics of receptor binding, and whether this was able to optimise downstream binding and elicit T cell priming. The final data chapter of this study showed that T cells in culture successfully demonstrated functional changes including cytokine profile and cytotoxicity outputs, following culture with tsDCs treated with targeting peptides. T cell outputs were specifically induced in response to tsDCs which had been treated with CD40R targeted, multivalent stimulation, suggesting this provides a more durable cascade of activation than monomeric or control treatments.

Chapter 8: Reference list

- Abbas, A., Lichtman, A. & Pillai, S. (2017). *Cellular and Molecular Immunology*. 9th Edition, Chapter 2, Elsevier Publishing.
- Abdi, K., Singh, M. & Matzinger, P. (2012). Lipopolysaccharide-Activated Dendritic cells: "Exhausted" or Alert and Waiting? *The Journal of immunology*, **188**, 1-9.
- Adams, M. L., Lavasanifar, A. & Kwon, G. S. (2003). Amphiphilic block copolymers for drug delivery. *Journal of Pharmaceutical Sciences*, **92** (7) 1343-1355.
- Advani, R., Forero-Torres, A., Furman, R., Rosenblatt, J., Younes, A., Ren, H., Harrop, K. & Drachman, J. (2009). Phase I Study of the Humanized Anti-CD40 Monoclonal Antibody Dacetuzumab in Refractory or Recurrent Non-Hodgkin's Lymphoma. *Journal of Clinical Oncology*, **27** (26), 4371-4377.
- Agrawal, S., Reemtsma, K., Bagiella, E., Oluwole, S. & Braunstein, N. (2004). Role of TAP-1 and/or TAP-2 antigen presentation defects in tumorigenicity of mouse melanoma. *Cellular Immunology*, **228** (2), 130-137.
- Ahmad, S., Duke, S., Jena, R., Williams, M. & Burnet, N. (2012). Advances in radiotherapy. *British Medical Journal*, **345**, 1-8.
- Ahonen, C., Wasiuk, A., Fuse, S., Turk, M., Ernstoff, M., Suriawinata, A., Gorham, J., Kedl, R., Usherwood, E. & Noelle, R. (2008). Enhanced efficacy and reduced toxicity of multifactorial adjuvants compared with unitary adjuvants as cancer vaccines. *Blood*, **111**, (6), 3116-3125.
- AlDeghaither, D., Smaglo, B. & Weiner, L. (2015). Beyond Peptides and mAbs - Current Status and Future Perspectives for Biotherapeutics with Novel Constructs. *The Journal of Clinical Pharmacology*, **55** (S3), S4-S20.
- Algarra, I., Collado, A., Garrido, F. & Garrido, F. (1997). Altered MHC class I antigens in tumors. *International Journal of Clinical and Laboratory Research*, **27** (2), 95-102.
- Allen, T. (2002). Ligand-targeted therapeutics in anticancer therapy. *Nature Reviews Cancer*, **2** (10), 750-763.
- Alphonse, A. & Alahari, K. (2009). Stromal Cells and Integrins: Conforming to the Needs of the Tumor Microenvironment. *Neoplasia*, **11** (12), 1264-1271.
- Alvarez-Dominguez, C., Calderon-Gonzalez, R., Teran-Navarro, H., Salcines-Cuevas, D., Garcia-Castano, A., Freire, J., Gomez-Roman, J. & Rivera, F. (2017). Dendritic Cell Therapy in Melanoma. *Annals of Translational Medicine*. **5**, (19), 386.
- Amigorena, S. (2002). Fcy Receptors and Cross-Presentation in Dendritic Cells. *The Journal of Experimental Medicine*, **195** (1), f1-f3.

- An, H., Kim, Y., Song, D., Park, B., Kim, H., Lee, J. & Lee, H. (2011). Crystallographic and Mutational Analysis of the CD40-CD154 Complex and Its Implications for Receptor Activation. *The Journal of Biological Chemistry*, **286** (13).
- Anassi, E. & Ndefo, U. (2011). Sipuleucel-T (Provenge) Injection: The First Immunotherapy Agent (Vaccine) For Hormone-Refractory Prostate Cancer. *Pharmacy and Therapeutics*, **36** (4), 197-202.
- Anderson, D., Maraskovsky, E., Billingsley, W., Dougal, W., Tometsko, M., Roux, E. & Galibert, L. (1997). A homologue of the TNF receptor and its ligand enhance T-cell growth and dendritic-cell function. *Letters to nature*, **390**, 176-179.
- Aragon-Ching, J. & Zujewski, J. (2007). CNS Metastasis: An Old Problem in a New Guise. *Clinical Cancer Research*, **13**, 1644-1647.
- Armstrong, D. (2002). Relapsed Ovarian Cancer: Challenges and Management Strategies for a Chronic Disease. *The Oncologist*, **7** (e90005), 20-28.
- Ashrafi, G. & Perumal, D. (2015). Human Papillomavirus and Cancer - Immunological Consequences of MHC Class I Down-Regulation. *International Biological and Biomedical Journal*, **1** (1), 1-7.
- Aste-Amezaga, M., Ma, X., Sartori, A. & Trinchieri, G. (1998). Molecular Mechanisms of the Induction of IL-12 and Its Inhibition by IL-10. *The Journal of Immunology*, **160** (12), 5936.
- Attieh, Y., Clark, A., Grass, C., Richon, S., Pocard, M., Mariani, P. & Vignjevic, D. (2017). Cancer-associated fibroblasts lead tumor invasion through integrin-beta3-dependent fibronectin assembly. *The Journal of Cell Biology*, **216** (11), 3509-3520.
- Austyn, J., Steinman, R., Weinstein, D., Granelli-Piperno, A. & Palladino, M. (1983). Dendritic cells initiate a two stage mechanism for T lymphocyte proliferation. *Journal of Experimental Medicine*, **157**, 1101-1115.
- Autenrieth, S. & Autenrieth, I. (2008). Variable antigen uptake due to different expression of the macrophage mannose receptor by dendritic cells in various inbred mouse strains. *Immunology*, **127**, 523-529.
- Bakocevic, N., Worbs, T., Davalos-Miszlitz, A. & Forster, R. (2010). T Cell-Dendritic Cell interaction dynamics during the induction of respiratory tolerance and immunity. *Journal of Immunology*, **184**, 1317-1327.
- Balkow, S., Heinz, S., Schmidbauer, P., Kolanus, W., Holzmann, B., Grabbe, S. & Laschinger, M. (2010). LFA-1 activity state on dendritic cells regulates contact duration with T cells and promotes T-cell priming *Blood*, **116**, 1885-1894.
- Balkwill, F. R., Capasso, M. & Hagemann, T. (2012). The tumor microenvironment at a glance. *Journal of Cell Science*, **125** (23), 5591.

- Baltathakis, I., Alcantara, O. & Boldt, D. (2001). Expression of different NF-kappaB pathway genes in dendritic cells (DCs) or macrophages assessed by gene expression profiling. *Journal of Cellular Biochemistry*, **83**, (2), 281-290.
- Banchereau, J., de Paoli, P., Valle, A., Garcia, E. & Rousset, F. (1991). Long-term human B cell lines dependent on interleukin-4 and antibody to CD40. *Science*, **251** (4989), 70.
- Banchereau, J. & Steinman, R. (1998). Dendritic Cells and the control of Immunity. *Nature*, **392**, (6673), 245-252.
- Baskar, S., Kobrin, C. & Kwak, L. (2004). Autologous lymphoma vaccines induce human T cell responses against multiple, unique epitopes. *Journal of Clinical Investigations*, **113**, (10), 1498-1510.
- Bastús, N. G., Comenge, J. & Puentes, V. (2011). Kinetically Controlled Seeded Growth Synthesis of Citrate-Stabilized Gold Nanoparticles of up to 200 nm: Size Focusing versus Ostwald Ripening. *Langmuir*, **27** (17), 11098-11105.
- Bastús, N. G., Sánchez-Tilló, E., Pujals, S., Farrera, C., López, C., Giralt, E. & Puentes, V. (2009). Homogeneous Conjugation of Peptides onto Gold Nanoparticles Enhances Macrophage Response. *ACS Nano*, **3** (6), 1335-1344.
- Batrakova, E., Dorodnych, T., Klinskii, E., Kliushnenkova, E., Shemchukova, O., Goncharova, O. & Kabanov, A. (1996). Anthracycline antibiotics non-covalently incorporated into the block copolymer micelles: *in vivo* evaluation of anti-cancer activity. *British Journal of Cancer*, **74** (10), 1545-1552.
- Beatty, G., Chiorean, E., Fishman, M., Saboury, B., Teitelbaum, U., Sun, W. & Vonderheide, R. (2011). CD40 agonists alter tumor stroma and show efficacy against pancreatic carcinoma in mice and humans. *Science*, **331** (6024), 1612-1616.
- Beatty, G., Li, Y. & Long, K. (2016). Cancer immunotherapy: Activating innate and adaptive immunity through CD40 agonists. *Expert Review in Anticancer Therapy*, **17**, (2), 175-186.
- Beatty, G., Torigian, D., Chiorean, E., Saboury, B., Brothers, A., Alavi, A. & O'Dwyer, P. (2013). A phase I study of an agonist CD40 monoclonal antibody (CP-870,893) in combination with gemcitabine in patients with advanced pancreatic ductal adenocarcinoma. *Clinical Cancer Research*, **19** (22), 6286-6295.
- Beck, S. L. (2012). Effects of Aspirin on Colorectal Cancer Related to Lynch Syndrome. *Journal of the Advanced Practitioner in Oncology*, **3** (6), 395-398.
- Belkaid, Y. & Oldenhoe, G. (2008). Tuning Microenvironments: Induction of Regulatory T Cells by Dendritic Cells. *Immunity*, **29**, 362-371.
- Bellone, M., Camporeale, A. & Boni, A. (2004). Dendritic cell activation kinetics and cancer immunotherapy. *Journal of Immunology*, **172**, 2727-2728.

- Belz, G. (2008). Getting together: Dendritic cells, T cells, collaboration and fates. *Immunology and Cell Biology*, **86**, 310-311.
- Benencia, F., Sprague, L., McGinty, J., Pate, M. & Muccioli, M. (2012). Dendritic Cells The Tumor Microenvironment and the Challenges for an Effective Antitumor Vaccination *Journal of Biomedicine and Biotechnology*, **2012**, 1-15.
- Bennett, S., Carbone, F., Karamalis, F., Flavell, R., Miller, J. & Heath, W. (1998). Help for cytotoxic-T-cell responses is mediated by CD40 signalling. *Letters to Nature*, **393**, 478-480.
- Benvenuti, F. (2016). The Dendritic Cell Synapse: A Life Dedicated to T Cell Activation. *Frontiers in Immunology*, **7**, 70.
- Berenblum, I. (1944). Irritation and Carcinogenesis. *Archives of Pathology & Laboratory Medicine (Online)*, **38**, 233-244.
- Berken, A. & Benacerraf, B. (1966). Properties of Antibodies Cytophilic for Macrophages. *The Journal of Experimental Medicine*, **123** (1), 119-144.
- Bernatchez, P., Soker, S. & Sirois, M. (1999). Vascular Endothelial Growth Factor Effect on Endothelial Cell Proliferation, Migration, and Platelet-activating Factor Synthesis Is Flk-1-dependent. *Journal of Biological Chemistry*, **274** (43), 31047-31054.
- Bevan, M. (1976). Cross-priming for a secondary cytotoxic response to minor H antigens with H-2 congenic cells which do not cross-react in the cytotoxic assay. *The Journal of Experimental Medicine*, **185** (3), 1361-1366.
- Bhatt, R., de Vries, P., Tulinsky, J., Bellamy, G., Baker, B., Singer, J. W. & Klein, P. (2003). Synthesis and *in vivo* antitumor activity of poly(l-glutamic acid) conjugates of 20S-camptothecin. *Journal of Medicinal Chemistry*, **46** (1), 190-193.
- Bhattacharyya, S., Sen, P., Wallet, M., Long, B., Baldwin, A. Jr. & Tisch, R. (2004). Immunoregulation of dendritic cells by IL-10 is mediated through suppression of the PI3K/Akt pathway and of I κ B kinase activity. *Blood*, **104** (4), 1100-1109.
- Bijen, C., Bantema-Joppe, E., de Jong, R., Leffers, N., Mourits, M., Eggink, H., van der Zee, A., Hollema, H., Bock, G. & Nijman, H. (2010). The prognostic role of classical and nonclassical MHC class I expression in endometrial cancer. *International Journal of Cancer*, **126**, (6), 1417-1427.
- Birgersdotter, A., Sandberg, R. & Ernberg, I. (2005). Gene expression perturbation *in vitro* – a growing case for three-dimensional (3D) culture systems. *Seminars in Cancer Biology*, **15**, (5), 405-412.
- Blankenstein, T., Coulie, P., Gilboa, E. & Jaffee, E. (2012). The determinants of tumour immunogenicity, *Nature Reviews*, **12**, 307-313.

- Boehm, U., Klamp, T., Groot, M. & Howard, J. C., (1997). Cellular responses to interferon-gamma. *Annual Review of Immunology*, **15**, 749-795.
- Boon, T., Cerottini, J., Van den Eynde, B., van der Bruggen, P. & Van-Pel, A. (1994). Tumor antigens recognized by T lymphocytes. *Annual Review of Immunology*, **12**, 337-365.
- Bottcher, J., Bonavita, E., Chakravarty, P., Brees, H., Cabeza-Cabrero, M., Sammiceli, S., Rogers, N., Sahai, E., Zelenay, S. & Ries e Sousa, C. (2018). NK Cells Stimulate Recruitment of cDC1 into the Tumour Microenvironment Promoting Cancer Immune Control. *Cell*, **172**, (5), 1022-1037.
- Bose, T., Pham, Q., Jellison, E., Mouries, J., Ballantyne, C. & Lefrancois, L. (2013). CD11a Regulates Effector CD8 T Cell Differentiation and Central memory Development in Response to Infection with *Listeria monocytogenes* *Infection and Immunity*, **81**, 1140-1151.
- Bournazos, S., Woof, J., Hart, S. & Dransfield, I., (2009). Functional and clinical consequences of Fc receptor polymorphic and copy number variants. *Clinical and Experimental Immunology*, **157** (2), 244-254.
- Bouvard, V., Loomis, D., Guyton, K., Grosse, Y., Ghissassi, F., Benbrahim-Tallaa, L. & Straif, K. (2015). Carcinogenicity of consumption of red and processed meat. *The Lancet Oncology*, **16**(16), 1599-1600.
- Boyman, O. & Sprent, J. (2012). The role of interleukin-2 during homeostasis and activation of the immune system. *Nature Reviews Immunology*, **12** (3), 180-190.
- Bradley, J., & Pober, J. (2001). Tumor necrosis factor receptor-associated factors (TRAFs). *Oncogene*, **20** (44), 6428-6391.
- Braet, F. & Wisse, E. (2002). Structural and functional aspects of liver sinusoidal endothelial cell fenestrae: a review. *Comparative Hepatology*, **1**, 1-1.
- Brea, E., Oh, C., Manchado, E., Budhu, S., Gejman, R., Mo, G. & Scheinberg, D. (2016). Kinase regulation of Human MHC Class I Molecule Expression on Cancer Cells. *Cancer Immunology Research*, **4** (11), 936-947.
- Breckpot, K., Bonehill, A., Aerts, J. & Thielemans, K. (2007). Dendritic Cells, the Tumor Microenvironment and the Challenges for an Effective Antitumor Vaccination. *Science*, **1**, 1-42.
- Breslin, S. (2007). Cytokine-release syndrome: overview and nursing implications. *Clinical Journal of Oncology Nursing*, **11** (1), 37-42.
- Brimnes, M., Svane, I. & Johnsen, H. (2006). Impaired functionality and phenotypic profile of dendritic cells from patients with multiple myeloma, *Clinical and Experimental Immunology*, **144** (1) 76-84.

- Brown, K., Rumgay, H., Dunlop, C., Ryan, M., Quartly, F., Cox, A. & Parkin, D. (2018). The fraction of cancer attributable to modifiable risk factors in England, Wales, Scotland, Northern Ireland, and the United Kingdom in 2015. *British Journal of Cancer*, **118** (8), 1130-1141.
- Bruhns, P. (2012). Properties of mouse and human IgG receptors and their contribution to disease models, *Blood* **119** (24) 5640-5649.
- Bruno, T., Ebner, P., Moore, B., Squalls, O., Waugh, K., Eruslanov, E. & Slansky, J. (2017). Antigen-presenting tumor B cells impact the phenotype of CD4 tumor infiltrating T cells in lung cancer patients. *The Journal of Immunology*, **198** (1) 130.126.
- Bubenik, J. (2004). MHC class I down-regulation: tumour escape from immune surveillance? *International Journal of Oncology*, **25** (2), 487-491.
- Burington, B., Yue, P., Shi, X., Advani, R., Lau, J. T., Tan, J., Stinson, S., Stinson, J., Januario, T., de Vos, S., Ansell, S., Forero-Torres, A., Fedorowicz, G., Yang, T., Elkins, K., Du, C., Mohan, S., Yu, N., Modrusan, Z., Seshagiri, S., Yu, S., Pandita, A., Koeppe, H., French, A., Polson, A., Offringa, R., Whiting, N., Ebens, A. & Dornan, D. (2011). CD40 pathway activation status predicts response to CD40 therapy in diffuse large B cell lymphoma. *Science Translational Medicine*, **3** (74) 22-28.
- Burn, J., Gerdes, A.-M., Macrae, F., Mecklin, J.-P., Moeslein, G., Olschwang, S., Evans, D., Maher, E., Bertario, L., Bisgaard, M., Dunlop, M., Ho, J., Hodgson, S., Lindblom, A., Lubinski, J., Morrison, P., Murday, V., Ramesar, R., Side, L., Scott, R., Thomas, H., Vasen, H., Barker, G., Crawford, G., Elliott, F., Movahedi, M., Pylvanainen, K., Wijnen, J., Fodde, R., Lynch, H., Mathers, J. & Bishop, D. (2011). Long-term effect of aspirin on cancer risk in carriers of hereditary colorectal cancer: an analysis from the CAPP2 randomised controlled trial. *The Lancet*, **378** (9809), 2081-2087.
- Burton, D. (1985) Immunoglobulin G: functional sites. *Molecular Immunology*, **22** (3), 161-206.
- Butcher, D., Alliston, T. & Weaver, V. (2009). A tense situation: forcing tumour progression. *Nature Reviews Cancer*, **2** (9), 1-31.
- Böttcher, J., Bonavita, E., Chakravarty, P., Blees, H., Cabeza-Cabrerizo, M., Sammicheli, S. & Reis e Sousa, C. (2018). NK Cells Stimulate Recruitment of cDC1 into the Tumor Microenvironment Promoting Cancer Immune Control. *Cell*, **172** (5).
- Call, M. & Wucherpfennig, K. (2004). Molecular mechanisms for the assembly of the T cell receptor-CD3 complex. *Molecular Immunology*, **40** (18) 1295-1305.
- Carbognin, L., Pilotto, S., Milella, M., Vaccaro, V., Brunelli, M., Calio, A., Cuppone, F., Sperduti, I., Giannarelli, D., Chilosì, M., Bronte, V., Scarpa, A., Bria, E. & Tortola, G. (2015). Differential Activity of Nivolumab, Pembrolizumab and MPDOL3280 According to the Tumour Expression of Programmed Death

Ligand-1 (PD-L1): Sensitivity Analysis of Trials in Melanoma, Lung and Genitourinary Cancers. *PLoS ONE*, **10**, (6), e0130142.

- Caronni, N., Simoncello, F., Stafetta, F., Guarnaccia, C., Ruiz-Moreno, J. S., Opitz, B., Proux-Gillardeaux, V. & Benvenuti, F. (2018). Downregulation of Membrane Trafficking Proteins and Lactate Conditioning Determine Loss of Dendritic Cell Function in Lung Cancer. *Cancer Research*, **78** (7), 1685-1699.
- Carr, S., Hemling, M., Bean, M. & Roberts, D. (1991). Integration of mass spectrometry in analytical biotechnology. *Analytical Chemistry*, **63** (24), 2802-2824.
- Carrasco, C., Rigden, R., Schaffner, R., Gerber, H., Neuhaus, V., Inumaru, S. & Summerfield, A. (2001). Porcine dendritic cells generated *in vitro*: morphological, phenotypic and functional properties. *Immunology*, **104**, 175-184.
- Castiello, L., Sabatino, M., Jin, P., Clayberger, C., Marincola, F., Krensky, A. & Stroncek, D. (2011). Monocyte derived D maturation strategies and related pathways: a transcriptional view. *Cancer Immunology & Immunotherapy*, **60**, (4), 457-466.
- Castro, F., Cardoso, A., Goncalves, R., Serre, K. & Oliveira, M. (2018). Interferon-Gamma at the Crossroads of Tumour Immune Surveillance or Evasion. *Frontiers in Immunology; Spotlight*, (9), 847.
- Cauwels, A., Van Lint, S., Paul, F., Garcin, G., De Koker, S., Van Parys, A. & Tavernier, J. (2018). Delivering Type I Interferon to Dendritic Cells Empowers Tumor Eradication and Immune Combination Treatments. *Cancer Research*, **78** (2), 463.
- Caux, C., Ait-Yahia, S., Chemin, K., de Bouteiller, O., Dieu-Nosjean, M., Homey, B. & Vicari, A. (2000). Dendritic cell biology and regulation of dendritic cell trafficking by chemokines. *Seminars in Immunopathology*, **22**, 345-369.
- Caux, C., Massacrier, C., Vanbervliet, B., Dubois, B., Van Kooten, C., Durand, K. & Banchereau, J. (1994). Activation of human dendritic cells through CD40 cross-linking. *Journal of Experimental Medicine*, **180**, 1263-1272.
- Celluzzi, C., Mayordomo, J., Storkus, W., Lotze, M. & Falo, L. Jr. (1996). Peptide-pulsed dendritic cells induce antigen-specific CTL-mediated protective tumor immunity. *Journal of Experimental Medicine*, **183** (1), 283-287.
- Chang, A., Bhattacharya, N., Mu, J., Setiadi, A., Carcamo-Cavazos, V., Lee, G., Simons, D., Yagegarynia, S., Hemati, K., Kapelner, A., Ming, Z., Krag, D., Schwartz, E., Chen, D. & Lee, P. (2013). Spatial organisation of dendritic cells within tumour draining lymph nodes impacts clinical outcome in breast cancer patients. *Journal of Translational Medicine*, **2**, (11), 242-244.
- Chang, C. C., Wright, A. & Punnonen, J. (2000). Monocyte-derived CD1a+ and CD1a-dendritic cell subsets differ in their cytokine production profiles,

- susceptibilities to transfection, and capacities to direct Th cell differentiation. *Journal of Immunology*, **165** (7), 3584-3591.
- Chao, J., Lee, J. & Klempner, S. (2016). Moving molecular subtypes to the clinic in gastric cancer. *Translational Cancer Research*; **5** (1).
- Chittasupho, C., Siahaan, T., Vines, C. & Berckland, C. (2011). Autoimmune therapies targeting costimulation and emerging trends in multivalent therapeutics. *Therapeutic Delivery*, **2**, 873-889.
- Chowdhury, F., Johnson, P., Glennie, M. & Williams, A. (2014). Ex vivo assays of dendritic cell activation and cytokine profiles as predictors of *in vivo* effects in an anti-human CD40 monoclonal antibody ChiLob 7/4 phase I trial **2** (3) 229-240.
- Chowdhury, S., Katta, V., Beavis, R. & Chait, B. (1990). Origin and Removal of Adducts (Molecular Mass = 98 u) Attached to Peptide and Protein Ions in Electrospray Ionization Mass Spectra. *Journal of the American Society for Mass Spectrometry*, **1**, (5), 382-388.
- Clark, E. & Ledbetter, J. (1986). Activation of human B cells mediated through two distinct cell surface differentiation antigens, Bp35 and Bp50. *PNAS*, **83**, 4494-4498.
- Clatza, A., Bonifaz, L., Vignali, D. & Moreno, J. (2014). CD40-Induced Aggregation of MHC Class II and CD80 on the Cell Surface Leads to an early enhancement in antigen presentation. *Journal of Immunology*, **171**, 6478-6487.
- ClinicalTrials.gov [Internet]. Bethesda (MD): National Library of Medicine (US). https://clinicaltrials.gov/ct2/results?term=CART&Search=Apply&recrs=d&age_v=&gndr=&type=&rslt= Accessed January 2018.
- Colombo, M. (2017). On OX40 and PD-1 Combination: Why Should OX40 Be First in Sequence? *Clinical Cancer Research*, **23** (20), 5999.
- Conejo-Garcia, J., Benencia, F., Courreges, M., Kang, E., Mohamed-Hadley, A., Buckanovich, R., Holtz, D. & Coukos, G. (2004). Tumor-infiltrating dendritic cell precursors recruited by a beta-defensin contribute to vasculogenesis under the influence of Vegf-A. *Nature Medicine*, **10** (9), 950-8.
- Coulie, P., Van den Eynde, B., van der Bruggen, P. & Boon, T. (2014). Tumour antigens recognized by T lymphocytes: at the core of cancer immunotherapy. *Nature Cancer Reviews*, **12** (2) 135-146.
- Coussens, L. & Werb, Z. Inflammation and cancer (2002). *Nature*, **12**, **420**, 860-7.
- Cox, T., Bird, D., Baker, A., Barker, H., Ho, M., Lang, G. & Erler, J. (2013). LOX-mediated collagen crosslinking is responsible for fibrosis-enhanced metastasis. *Cancer Research*, **73** (6), 1721-1732.

- Croft, M., So, T., Duan, W. & Soroosh, P. (2009). The Significance of OX40 and OX40L to T cell Biology and Immune Disease. *Immunological Reviews*, **229** (1), 173-191.
- Cruz, L., Rosalia, R., Kleinovink, J., Rueda, F., Lowik, C. & Ossendorp, F. (2014). Targeting nanoparticles to CD40, DEC-205 or CD11c molecules on dendritic cells for efficient CD8(+) T cell response: a comparative study. *Journal of Controlled Release*, **192**, 209-18.
- Curiel, T., Coukos, G., Zou, L., Alvarez, X., Cheng, P., Mottram, P., Evdemon-Hogan, M. & Zou, W. (2004). Specific recruitment of regulatory T cells in ovarian carcinoma fosters immune privilege and predicts reduced survival. *Nature Medicine*, **10**, (9), 942-9.
- Curti, A., Ferri, E., Pandolfi, S., Isidori, A. & Lemoli, R. (2004). Dendritic cell differentiation. *Journal of Immunology*, **172**, 3-4.
- Dahan, R., Barnhart, B., Fubin, L., Yamnuik, A., Korman, A. & Ravetch, J. (2016). Therapeutic activity of agonistic, human anti-CD40 monoclonal antibodies requires selective FcγR engagement. *Cancer Cell*, **29**, (6), 820-831.
- Dalal, V., Kumar, R., Kumar, S., Sharma, A., Kumar, L., Sharma, J. & Vanamail, P. (2018). Biomarker potential of IL-6 and VEGF-A in ascitic fluid of epithelial ovarian cancer patients. *International Journal of Clinical Chemistry*, **482**, 27-32.
- Das, R., Verma, R., Sznol, M., Boddupalli, C., Gettinger, S., Kluger, H. & Dhodapkar, K. (2015). Combination therapy with anti-CTLA-4 and anti-PD-1 leads to distinct immunologic changes *in vivo*. *Journal of Immunology*, **194**, (3), 950-9.
- De Flora, S. & Bonanni, R. (2011). The prevention of infection associated cancers. *Carcinogenesis*, **32**, (6), 787-795.
- de Groot, J., Liang, J., Kong, L., Wei, J., Piao, Y., Fuller, G. & Heimberger, A. (2012). Modulating Antiangiogenic Resistance by Inhibiting the Signal Transducer and Activator of Transcription 3 Pathway in Glioblastoma. *Oncotarget*, **3**, (9), 1036-1048.
- Delaney, G., Jacob, S., Featherstone, C. & Barton, M. (2005). The Role of Radiotherapy in Cancer Treatment Estimating Optimal Utilization from a Review of Evidence-Based Clinical Guidelines. *Cancer*, **104**, 1129-1137.
- Demangel, C., Palendira, U., Feng, C., Heath, A., Bean, A. & Britton, W. (2001). Stimulation of Dendritic Cells *via* CD40 Enhances Immune Responses to Mycobacterium tuberculosis Infection. *Infection and Immunity*, **69** (4), 2456-2461.
- Deng, J., Pennati, A., Cohen, J., Wu, Y., Wu, J. & Galipeau, J. (2016). GIFT4 fusokine converts leukemic B cells into immune helper cells. *Journal of Translational Medicine*, **14**, 106.

- DeVita, V. & Chu, E. (2008). A history of cancer chemotherapy. *Cancer Research*, **68**, 8643-8653.
- Dey, N., De, P. & Brian, L. (2015). Evading anti-angiogenic therapy: resistance to anti-angiogenic therapy in solid tumors. *American Journal of Translational Research*, **7**, (10), 1675-1698.
- Dhodapkar, M. & Steinman, R. (2002). Antigen-bearing immature dendritic cells induce peptide-specific CD8(+) regulatory T cells *in vivo* in humans. *Blood*, **100**, (1), 174.
- Dilioglou, S., Cruse, J. & Lewis, R. (2003). Function of CD80 and CD86 on monocyte- and stem cell-derived dendritic cells. *Experimental and Molecular Pathology*, **75**, 217-227.
- DiMasi, J. & Grabowski, H. (2007). Economics of new oncology drug development. *Journal of Clinical Oncology*, **25**, (2), 209-216.
- Dissanayake, D., Murakami, K., Tran, M., Elford, A., Millar, D. & Ohashi, P. (2014). Peptide-Pulsed Dendritic Cells Have Superior Ability to Induce Immune-Mediated Tissue Destruction Compared to Peptide with Adjuvant. *PLoS ONE*, **9**, (3), e92380.
- Doll, R. & Peto, R. (1981). The causes of cancer: quantitative estimates of avoidable risks of cancer in the United States today. *Journal of the National Institute of Cancer*, **66**, (6), 1191-308.
- Dominguez, D., Ye, C., Geng, Z., Chen, S., Fan, J., Qin, L. & Zhang, B. (2017). Exogenous IL-33 Restores Dendritic Cell Activation and Maturation in Established Cancer. *The Journal of Immunology*, **198**, (3), 1365.
- Dong, H., Zhu, G., Tamada, K. & Chen, L. (1999). B7-H1, a third member of the B7 family, co-stimulates T-cell proliferation and interleukin-10 secretion. *Nature Medicine*, **5**, (12), 1365-1369.
- Dong, Y., Sun, Q., & Zhang, X. (2017). PD-1 and its ligands are important immune checkpoints in cancer. *Oncotarget*, **8**, (2), 2171-2186.
- Dotti, G., Gottschalk, S., Savoldo, B. & Brenner, M. (2014). Design and Development of Therapies using Chimeric Antigen Receptor-Expressing T Cells. *Immunology Reviews*. **257**, (1), 107-126.
- Duewell, P., Kisser, U., Heckelsmiller, K., Hoves, S., Stoitzner, P., Koernig, S., Morelli, A., Clausen, B., Dauer, M., Eigler, A., Anz, D., Bourguin, C., Maraskovsky, E., Endres, S. & Schnurr, M. (2011). ISCOMATRIX adjuvant combines immune activation with antigen delivery to dendritic cells *in vivo* leading to effective cross-priming of CD8+ T cells. *Journal of Immunology*, **187**, (1), 55-63.
- Dunn, G., Bruce, A., Ikeda, H., Old, L. & Schreiber, R. (2002). Cancer immunoediting: from immunosurveillance to tumor escape. *Nature Immunology*, **3**, (11) 991-998.

- Dunzendorfer, S., Lee, H., Soldau, K., & Tobias, P. (2004). TLR4 Is the Signaling but Not the Lipopolysaccharide Uptake Receptor. *The Journal of Immunology*, **173**, (2), 1166-1170.
- Duraiswamy, J., Kaluza, K., Freeman, G. & Coukos, G. (2013). Dual blockade of PD-1 and CTLA-4 combined with tumour vaccine effectively restores T cell rejection function in tumours. *Cancer Research*. **73**, (12), 3591-3603.
- Duray, A., Demoulin, S., Hubert, P., Delvenne, P., & Saussez, S. (2010). Immune Suppression in Head and Neck Cancers: A Review. *Clinical and Developmental Immunology*, **10**, 1-15.
- Dustin, M., Chakraborty, A. & Shaw, A. (2010). Understanding the Structure and Function of the Immunological Synapse. *Cold Spring Harbor Perspectives in Biology*, **2** (10), 127-129.
- Duenas-Gonzalez, A., Zarba, J., Patel, F., Alcedo, J., Beslija, S., Casanova, L., Pattaranutaporn, P., Hameed, S., Blair, J., Barraclough, H. & Orlando, M. (2011). Phase III, open-label, randomized study comparing concurrent gemcitabine plus cisplatin and radiation followed by adjuvant gemcitabine and cisplatin versus concurrent cisplatin and radiation in patients with stage IIB and IVA carcinoma of the cervix. *Journal of Clinical Oncology*, **29**, (13), 1678-1685.
- Dvorak, H., Weaver, V., Tlsty, T. & Gergers, G. (2011). Tumor Microenvironment and Progression. *Journal of surgical oncology*, **103**, (6), 468-474.
- Eakin, R., Snell, E. & Williams, R. (1941). The concentration and assay of avidin, the injury-producing protein in raw egg white. *Journal of Biological Chemistry*, **140**, 535-543.
- Ebert, E. (2004). Interleukin-12 up-regulates perforin- and Fas-mediated lymphokine-activated killer activity by intestinal intraepithelial lymphocytes. *Clinical Experimental Immunology*, **138**, (2), 259-265.
- Egen, J., & Allison, J. (2002). Cytotoxic T lymphocyte antigen-4 accumulation in the immunological synapse is regulated by TCR signal strength. *Immunity*, **16**, (1), 23-35.
- Elgueta, R., Benson, M., de Vries, V., Wasiuk, A., Guo, Y., & Noelle, R. (2009). Molecular mechanism and function of CD40/CD40L engagement in the immune system. *Immunological Reviews*, **229**, (1), 152-172.
- Ellmark, P., Andersson, H., Abayneh, S., Fenyö, E. M., & Borrebaeck, C. A. K. (2008). Identification of a Strongly Activating Human Anti-CD40 Antibody That Suppresses HIV Type 1 Infection. *AIDS Research and Human Retroviruses*, **24**, (3), 367-373.
- Emens, L., Ascierto, P., Darcy, P., Demaria, S., Eggermont, A., Redmond, W. & Marincola, F. (2017). Cancer immunotherapy: Opportunities and challenges

in the rapidly evolving clinical landscape. *European Journal of Cancer*, **81**, 116-129.

- Engelhardt, J., Boldajipour, B., Beemiller, P., Pandurangi, P., Sorensen, C., Werb, Z., Krummel, C. & Matthew F. (2012). Marginating Dendritic Cells of the Tumor Microenvironment Cross-Present Tumor Antigens and Stably Engage Tumor-Specific T Cells. *Cancer Cell*, **21**, (3), 402-417.
- Esquivel, F., Yewdell, J. & Bennink, J. (1992). RMA/S cells present endogenously synthesized cytosolic proteins to class I-restricted cytotoxic T lymphocytes. *The Journal of Experimental Medicine*, **175**, (1), 163.
- Evans, D., Prell, R., Thalhoffer, C., Hurwitz, A. & Weinberg, A. (2001). Engagement of OX40 enhances antigen-specific CD4(+) T cell mobilization/memory development and humoral immunity: comparison of alphaOX-40 with alphaCTLA-4. *Journal of Immunology*, **167**, (12), 6804-6811.
- Facciabene, A., Peng, X., Hagemann, I. S., Balint, K., Barchetti, A., Wang, L., Gimotty, P., Gilks, C., Lal, P., Zhang, L. & Coukos, G. (2011). Tumour hypoxia promotes tolerance and angiogenesis via CCL28 and Treg cells. *Nature*, **475**, (7355), 226-230.
- Feder-Mengus, C., Ghosh, S., Weber, W. P., Wyler, S., Zajac, P., Terracciano, L., Oertli, D., Heberer, M., Martin, I., Spagnoli, G. & Reschner, A. (2007). Multiple mechanisms underlie defective recognition of melanoma cells cultured in three-dimensional architectures by antigen-specific cytotoxic T lymphocytes. *British Journal of Cancer*, **96**, (7), 1072-1082.
- Fiegl, M., Mlineritsch, B., Hubalek, M., Bartsch, R., Pluschnig, U. & Steger, G. (2011). Single-agent pegylated liposomal doxorubicin (PLD) in the treatment of metastatic breast cancer: results of an Austrian observational trial. *BMC Cancer*, **11**, 373.
- Figdor, C., Vries, J., Lesterhuis, J. & Melief, C. (2004). Dendritic cell immunotherapy: mapping the way. *Nature Medicine*, **10**, (5), 475-480.
- Fleischer, J., Reiling, N., Grage-Griebenow, E., Flad, H. & Ernst, M. (1996). Differential expression and function of CD80 (B7-1) and CD86 (B7-2) on human peripheral blood monocytes. *Immunology*, **89**, (4), 592-598.
- Flenniken, M., Willits, D., Harmsen, A., Liepold, L., Harmsen, A., Young, M. & Douglas, T. (2006). Melanoma and lymphocyte cell-specific targeting incorporated into a heat shock protein cage architecture. *Chemistry & Biology*, **13**, (2), 161-170.
- Fogg, D., Sibon, C., Miled, C., Jung, S., Aucouturier, P., Littman, D., Cumano, A. & Giessmann, F. (2006). A Clonogenic Bone Marrow Progenitor Specific for Macrophages and Dendritic Cells. *Science*, **311**, (5757), 83-87.
- Fong, L. & Engleman, E. (2000). Dendritic Cells in Cancer Immunotherapy. *Annual Reviews in Immunology*, **18**, 245-273

- Fosgerau, K. & Hoffmann, T. (2015). Peptide therapeutics: current status and future directions. *Drug Discovery Today*, **20**, (1), 122-128.
- Fowler, J. Jr., Gottesman, J., Reid, C., Andriole, G. & Soloway, M. (2000). Safety and efficacy of an implantable leuprolide delivery system in patients with advanced prostate cancer. *Journal of Urology*, **164**, (3), 730-734.
- Francisco, J., Donaldson, K., Chace, D., Siegall, C. & Wahl, A. (2000). Agonistic properties and *in vivo* antitumor activity of the anti-CD40 antibody SGN-14. *Cancer Research*, **60**, (12), 3225-3231.
- Frantz, C., Stewart, K. & Weaver, V. (2010). The extracellular matrix at a glance. *Journal of Cell Science*, **24**, (11), 4195-4200.
- French, L., Huard, B., Wysocka, M., Shane, R., Contassot, E., Arrighi, J. & Rook, A. (2005). Impaired CD40L signaling is a cause of defective IL-12 and TNF- α production in Sézary syndrome: circumvention by hexameric soluble CD40L. *Blood*, **105**, (1), 219.
- French, R., Chan, H., Tutt, A. & Glennie, M. (1999). CD40 antibody evokes a cytotoxic T-cell response that eradicates lymphoma and bypasses T-cell help. *Nature Medicine*, **5**, (5), 548-553.
- Friedl, P., Th den Boer, A. & Gunzer, M. (2005). Tuning immune responses: diversity and adaptation of the immunological synapse. *Nature Reviews Immunology*, **5**, 532-545.
- Fry, T., Shah, N., Orentas, R., Stetler-Stevenson, M., Yuan, C., Ramakrishna, S., Wolters, P., Martin, S., Delbrook, C., Yates, B., Shalabi, H., Fountaine, T., Shern, J., Maizner, R., Stroncek, D., Sabatino, M., Feng, Y., Minitrov, D., Zhang, L., Nguyen, S., Qin, H., Dropulic, B., Lee, D. & Mackall, C. (2018). CD22-targeted CAR T cells induce remission in B-ALL that is naive or resistant to CD19-targeted CAR immunotherapy. *Nature Medicine*, **24**, (1), 20-28.
- Fujii, S., Liu, K., Smith, C., Bonito, A. & Steinman, R. (2004). The Linkage of Innate to Adaptive Immunity *via* Maturing Dendritic Cells *In Vivo* Requires CD40 Ligation in Addition to Antigen Presentation and CD80/CD86 Costimulation. *The Journal of Experimental Medicine*, **199**, (12), 1607-1618.
- Fukumura, D. & Jain, R. (2007). Tumor Microenvironment Abnormalities: Causes, Consequences, and Strategies to Normalize. *Journal of Cellular Biochemistry*, **101**, (4), 937-949.
- Galluzzi, L., Vitale, I., Eggermont, A., Fridman, W., Fucikova, J., Cremer, I., Galon, J., Tartour, E., Zitvogel, L., Kroemer, G. & Vacchelli, E., (2012). Trial watch: Dendritic cell-based interventions for cancer therapy. *Oncoimmunology*, **1**, (7), 1111-1134.
- Gao, D., Li, C., Xie, X., Zhao, P., Wei, X., Sun, W. & Li, J. (2014). Autologous Tumor Lysate-Pulsed Dendritic Cell Immunotherapy with Cytokine-Induced Killer

Cells Improves Survival in Gastric and Colorectal Cancer Patients. *PLoSone*, **9**, (4), 1-9.

Gardai, S., Epp, A., Linares, G., Westendorf, L., Sutherland, M., Neff-LaFord, H. & Law, C.-L. (2015). Abstract 2472: SEA-CD40, a sugar engineered non-fucosylated anti-CD40 antibody with improved immune activating capabilities. *Cancer Research*, **75**, (15 Supplement), 2472.

Gasparoto, T., de Souza Malaspina, T., Benevides, L., de Melo, E., Costa, M., Damante, J., Ikoma, M., Garlet, G., Cavassani, K., da Silva, J. & Campanelli, A. (2010). Patients with oral squamous cell carcinoma are characterized by increased frequency of suppressive regulatory T cells in the blood and tumor microenvironment. *Cancer Immunology and Immunotherapy*, **59**, (6), 919-828.

Gays, F., Unnikrishnan, M., Shrestha, S., Fraser, K., Brown, A., Tristram, C., Chraznowska-Lightowers, Z. & Brooks, C. (2000). The mouse tumour cell lines EL4 and RMA display mosaic expression of NK related and certain other surface molecules and appear to have a common origin. *Immunology*, **164**, (10), 5094-5102.

Gazda, M. & Coia, L. (2009). Principles of radiation therapy. *Radiation Therapy*, **14**, 1-19.

Geissmann, F., Man, M., Jung, S., Sieweke, M., Merad, M. & Ley, K. (2010). Development of Monocytes, Macrophages, and Dendritic Cells. *Science*, **327**, (5966), 656-661.

Gerlack, A., Steimle, A., Krampen, L., Wittmann, A., Gronbach, K., Geisel, J., Autenrieth, I. & Frick, J. (2012). Role of CD40 ligation in dendritic cell semimaturation. *BMC Immunology*. **13**, (22) 1-11.

Giannopoulos, A., Constantinides, C., Fokaeas, E., Stravodimos, C., Giannopoulou, M., Kyroudi, A. & Gounaris, A. (2003). The immunomodulating effect of interferon-gamma intravesical instillations in preventing bladder cancer recurrence. *Clinical Cancer Research*. **9**, (15), 5550-5558.

Gilliet, M., Boonstra, A., Paturel, C., Antonenko, S., Xu, X., Trinchieri, G. & Liu, Y. (2002). The Development of Murine Plasmacytoid Dendritic Cell Precursors Is Differentially Regulated by FLT3-ligand and Granulocyte/Macrophage Colony-Stimulating Factor. *The Journal of Experimental Medicine*, **195**, (7), 953-958.

Gillis, S. & Smith, K. A. (1977). Long term culture of tumour-specific cytotoxic T cells. *Nature*, **268**, 154-156.

Goede, V., Fischer, K., Busch, R., Engelke, A., Eichhorst, B., Wendtner, C., Chagorova, T., de la Serna, J., Filhuydy, M., Illmer, T., Opat, S., Owen, C., Samoylova, O., Kreuzer, K., Stilgenbauer, S., Dohner, H., Langerak, A., Ritgen, M., Kneba, M., Asikanius, E., Humphrey, K., Wenger, M. & Hallek, M. (2014). Obinutuzumab

plus chlorambucil in patients with CLL and coexisting conditions. *The New England Journal of Medicine*, **370**, 1101-1110.

- Goel, H. & Mercurio, A. (2014). VEGF targets the tumour cell. *Nature Reviews Cancer*, **13**, (12), 871-882.
- Goubran, H., Kotb, R., Stakiw, J., Emara, M. & Burnouf, T. (2014). Regulation of Tumor Growth and Metastasis: The Role of Tumor Microenvironment. *Cancer Growth Metastasis*, **2**, 9-18.
- Gradishar, W., Tjulandin, S., Davidson, N., Shaw, H., Desai, N., Bhar, P. & O'Shaughnessy, J. (2005). Phase III trial of nanoparticle albumin-bound paclitaxel compared with polyethylated castor oil-based paclitaxel in women with breast cancer. *Journal of Clinical Oncology*, **23**, (31), 7794-7803.
- Gramaglia, I., Weinberg, A., Lemon, M. & Croft, M. (1998). Ox-40 ligand: a potent costimulatory molecule for sustaining primary CD4 T cell responses. *Journal of Immunology*, **161**, (12), 6510-6517.
- Granucci, F., Feau, S., Zanoni, I, Pavelka, N., Vizzardelli, C., Raimondi, G. & Ricciardi-Castagnoli, P. (2003). The Immune Response Is Initiated by Dendritic Cells via Interaction with Microorganisms and Interleukin 2 Production. *Journal of Infectious Disease*, **15**, (187), 346-350.
- Granucci, F., Ferrero, E., Foti, M., Aggujaro, D., Vettoretto, K. & Ricciardi-Castagnoli, P. (1999). Early events in dendritic cell maturation induced by LPS. *Microbes and infection*, **1**, 1079-1084.
- Granucci, F., Vizzardelli, C., Pavelka, N., Feau, S., Persico, M., Virzi, E., Rescigno, M. & Ricciardi-Castagnoli, P. (2001). Inducible IL-2 production by dendritic cells revealed by global gene expression analysis. *Nature Immunology*, **2**, (9), 882-888.
- Granucci, F. & Zanoni, I. (2009). The dendritic cell life cycle. *Cell cycle*, **8**, 3816-3821.
- Grassme, H., Bock, J., Kun, J. & Gulbins, E. (2002). Clustering of CD40 ligand is required to form a functional contact with CD40. *The Journal of Biological Chemistry*, **277**, 30289-30299.
- Green, M., Manikhas, G., Orlov, S., Afanasyev, B., Makhson, A., Bhar, P. & Hawkins, M. (2006). Abraxane, a novel Cremophor-free, albumin-bound particle form of paclitaxel for the treatment of advanced non-small-cell lung cancer. *Annals of Oncology*, **17**, (8), 1263-1268.
- Gross, G., Waks, T. & Eshhar, Z. (1989). Expression of immunoglobulin-T-cell receptor chimeric molecules as functional receptors with antibody-type specificity. *Proceedings of the National Academy of Sciences USA*, **86**, (24), 10024-8.
- Grosso, J., Kelleher, C., Harris, T., Maris, C., Hipkiss, E., De Marzo, A., Anders, R., Netto, G., Getnet, D., Bruno, T., Goldberg, M., Pardoll, D. & Drake, C. (2007).

- LAG-3 regulates CD8+ T cell accumulation and effector function in murine self- and tumor-tolerance systems. *Journal of Clinical Investigations*, **117**, (11), 3383-3392.
- Groux, H. (2003). Type 1 T-regulatory cells: their role in the control of immune responses. *Transplantation*, **75**, (9), 8-12.
- Gu, L., Ruff, L., Qin, Z., Corr, M., Hedrick, S. & Sailor, M. (2012). Multivalent porous silicon nanoparticles enhance the immune activation potency of agonistic CD40 antibody. *Advanced Materials*, **24**, (29), 3981-3987.
- Gu, P., Fang Gao, J., D'Souza, C., Kowalczyk, A., Chou, K. & Zhang, L. (2012). Trogocytosis of CD80 and CD86 by induced regulatory T cells. *Cellular and Molecular Immunology*, **9**, (2), 136-146.
- Guo, W. & Giancotti, F. (2004). Integrin Signalling During Tumour Progression. *Nature Reviews Molecular Cell Biology*, **5**, (10), 816-826.
- Hainfeld, J., Slatkin, D. & Smilowitz, H. (2004). The use of gold nanoparticles to enhance radiotherapy in mice. *Physics in Medicine and Biology*, **49**, (18), 309-315.
- Hainfield, J., Smilowitz, H., O'Connor, M., Dilmanian, F. & Slatkin, D. (2013). Gold nanoparticle imaging and radiotherapy of brain tumours in mice. *Nanomedicine*, **8**, (10), 1601-1609.
- Hall, B. (2015). T Cells: Soldiers and Spies—The Surveillance and Control of Effector T Cells by Regulatory T Cells. *Clinical Journal of the American Society of Nephrology: CJASN*, **10**, (11), 2050-2064.
- Hamley, I. (2007). Peptide Fibrillization, *Angewanti Chemistry International Edition (English)*, **46**, (43), 8121-8147.
- Han, N., Zhang, Z., Liu, S., Ow, A., Ruan, M., Yang, W. & Zhang, C. (2017). Increased tumor-infiltrating plasmacytoid dendritic cells predicts poor prognosis in oral squamous cell carcinoma. *Archives of Oral Biology*, **78**, 129-134.
- Hanagiri, T., Shigematsu, Y., Shinohara, S., Takenaka, M., Oka, S., Chikaishi, Y., Nagata, Y., Iwata, T., Uramoto, H., So, T. & Tanaka, F. (2013). Clinical significance of the frequency of regulatory T cells in regional lymph node lymphocytes as a prognostic factor for non-small-cell lung cancer. *Lung Cancer*, **81**, (3), 475-479.
- Hanahan, D. & Coussens, L. (2012). Accessories to the crime: functions of cells recruited to the tumor microenvironment. *Cancer Cell*, **21**, (3), 309-22.
- Hanahan, D. & Weinberg, R. (2011). Hallmarks of Cancer: The Next Generation. *Cell*, **144**, (5), 646-674.

- Hangalapura, B., Timares, L., Oosterhoff, D., Scheper, R., Curiel, D. & de Gruijl, T. (2012). CD40 targeted adenoviral cancer vaccines: the long and winding road to the clinic. *The Journal of Gene Medicine*, **14**, (6), 416-427.
- Hanissian, S. & Geha, R. (1997). Jak3 is associated with CD40 and is critical for CD40 induction of gene expression in B cells. *Immunity*, **6**, (4), 379-387.
- Haque, A., Banik, N. & Ray, S. (2011). Chapter 5 - Molecular Alterations in Glioblastoma: Potential Targets for Immunotherapy. In S. Rahman (Ed.), *Progress in Molecular Biology and Translational Science*, **98**, 187-234.
- Hartkopf, A., Taran, F., Wallwiener, M., Walter, C., Krämer, B., Grischke, E. & Brucker, S. (2016). PD-1 and PD-L1 Immune Checkpoint Blockade to Treat Breast Cancer. *Breast Care*, **11**, (6), 385-390.
- Hartmann, J., Schussler-Lenz, M., Bondanza, A. & Buchholz, C. (2017). Clinical development of CAR T cells – challenges and opportunities in translating innovative treatment concepts. *EMBO Molecular Medicine*, **9**, (9), 1183-1197.
- Haswell, L., Glennie, M. & Al-Shamkhani, A. (2001). Analysis of the oligomeric requirement for signaling by CD40 using soluble multimeric forms of its ligand, CD154. *European Journal of Immunology*, **31**, (10), 3094-3100.
- Haworth, K., Leddon, J., Chen, C., Horwitz, E., Mackall, C. & Cripe, T. (2015). Going Back to Class I: MHC and Immunotherapies for Childhood Cancer. *Pediatric Blood & Cancer*, **62**, (4), 571-576.
- Hebb, J., Mosley, A., Vences-Catalán, F., Rajasekaran, N., Rosén, A., Ellmark, P. & Felsher, D. (2018). Administration of low-dose combination anti-CTLA4, anti-CD137, and anti-OX40 into murine tumor or proximal to the tumor draining lymph node induces systemic tumor regression. *Cancer Immunology, Immunotherapy*, **67**, (1), 47-60.
- He, L., Testa, J., Wasiuk, A., Jeffrey, W., Sisson, C., Vitale, L., O'Neill, T., Crocker, A., Widger, J., Goldstein, J., Marsh, H. & Keler, T. (2016). CDX-1140, a novel agonist CD40 antibody with potent anti-lymphoma activity. *Blood*, **128**, (22), 1848.
- Hee Han, T., Jin, P., Ren, J., Slezak, Marincola, F. & Stroncek, D. (2009). Evaluation of Three Clinical Dendritic Cell Maturation Protocols Containing Lipopolysaccharide and Interferon-gamma. *Journal of Immunotherapy*, **32**, (4), 399-407.
- Heinzerling, L., Burg, G., Dummer, R., Maier, T., Oberholzer, P., Schultz, J., Elzaouk, L., Pavlovic, J. & Moelling, K. (2005). Intratumoral injection of DNA encoding human interleukin 12 into patients with metastatic melanoma: clinical efficacy. *Human Gene Therapy*, **16**, (1), 35-48.
- Heinzerling, L., Ott, P., Hodi, F., Husain, A., Tajmir-Riahi, A., Tawbi, H., Pauschinger, M., Gajewski, T., Lipson, E. & Luke, J. (2016). Cardiotoxicity associated with

- CTLA4 and PD1 blocking immunotherapy. *Journal of Immunotherapy of Cancer*, **4**, (50), 16-22.
- Henry, J., Miller, M. & Pontarotti, P. (1999). Structure and evolution of the extended B7 family *Immunology Today*, **20**, (6), 285-289.
- Hernandez, M., Shen, L. & Rock, K. (2007). CD40-CD40 ligand interaction between dendritic cells and CD8+ T cells is needed to stimulate maximal T cell responses in the absence of CD4+ T cell help. *Journal of immunology*, **178**, (5), 2844-2852.
- Holler, N., Tardivel, A., Kovacsovics-Banhowski, M., Hertig, S., Gaide, O, Martinon, F., Tinel, A., Deperthes, D., Calderara, S., Schulthess, T., Engel, J., Schneider, P. & Tschopp, J. (2003). Two adjacent trimeric Fas ligands are required for Fas signaling and formation of a death-inducing signaling complex. *Molecular Cell Biology*, **23**, (4), 1428-1440.
- Hong, S., Leroueil, P., Majoros, I., Orr, B., Baker, J. & Banaszak Holl, M. (2007). The Binding Avidity of a Nanoparticle-Based Multivalent Targeted Drug Delivery Platform. *Chemistry & Biology*, **14**, (1), 107-115.
- Hong, S., Zhang, X., Chen, J., Zheng, Y. & Xu, C. (2013). Targeted gene silencing using a follicle-stimulating hormone peptide-conjugated nanoparticle system improves its specificity and efficacy in ovarian clear cell carcinoma *in vitro*. *Journal of Ovarian Research*, **6**, (80), 1-9.
- Howell, B. & Fan, D. (2010). Poly(amidoamine) dendrimer-supported organoplatinum antitumour agents. *Proceedings of the Royal Society A: Mathematical, Physical and Engineering Science*, **466**, (2117), 1515.
- Howler, J., Flanagan, M., Gleason, D., Klimberg, I., Gottesmann J. & Sharifi, R. (2000). Evaluation of an implant that delivers leuprolide for 1 year for the palliative treatment of prostate cancer. *Urology*, **55**, (5), 639-642.
- Hsu, C., Tsou, H., Lin, S., Wang, M., Yao, M., Hwang, W., Kao, W., Chiu, C., Lin, C., Lin, J., Chang, C., Tien, H., Liu, T., Chen, P. & Cheng, A. (2014). Chemotherapy-induced hepatitis B reactivation in lymphoma patients with resolved HBV infection: a prospective study. *Hepatology*, **59**, (6), 2092-2100.
- Huang, R., Eppolito, C., Lele, S., Shrikant, P., Matsuzaki, J. & Odinsu, K. (2015). LAG3 and PD1 co-inhibitory molecules collaborate to limit CD8+ T cell signalling and dampen antitumor immunity in a murine ovarian cancer model. *Oncotarget*, **6**, (29), 27359-27377.
- Huang, X., Chen, Y., Wu, J., Zhang, X., Wu, C., Zhang, C. & Chen, W. (2017). Aspirin and non-steroidal anti-inflammatory drugs use reduce gastric cancer risk: A dose-response meta-analysis. *Oncotarget*, **8**, (3), 4781-4795.
- Huang, X. & El-Sayed, M. (2010). Gold nanoparticles: Optical properties and implementations in cancer diagnosis and photothermal therapy. *Journal of Advanced Research*, **1**, (1), 13-28.

- Hunder, N., Wallen, H., Cao, J., Hendricks, D., Reilly, J., Rodmyre, R., Jungbluth, A., Gnjatic, S., Thompson, J. & Yee, C. (2008). Treatment of Metastatic Melanoma with Autologous CD4+ T Cells Against NY-ESO-1. *New England Journal of Medicine*. **358**, (25), 2698-2703.
- Hunter, T., Alsarraj, M., Gladue, R., Bedian, V. & Antonia, S. (2007). An Agonist Antibody Specific for CD40 Induces Dendritic Cell Maturation and Promotes Autologous Anti-tumour T-cell Responses in an *In vitro* Mixed Autologous Tumour Cell/Lymph Node Cell Model. *Scandinavian Journal of Immunology*, **65**, (5), 479-486.
- Hussain, K., Hargreaves, C., Roghanian, A., Oldham, R., Chan, H., Mockridge, C., Chowdhury, F., Frendeus, B., Harper, K., Strfford, J., Cragg, M., Glennie, M., Williams, A. & French, R. (2015). Upregulation of FcγRIIb on monocytes is necessary to promote the superagonist activity of TGN1412. *Blood*, **125**, (1), 102-110.
- Iikima, N., Yanagawa, Y., Iwabuchi, K. & Onoe, K. (2003). Selective regulation of CD40 expression in murine dendritic cells by thiol antioxidants. *Immunology*, **110**, (2), 197-205.
- Inoue, M., Arikawa, T., Chen, Y., Moriwaki, Y., Price, M., Brown, M. & Shinohara, M. (2014). T cells down-regulate macrophage TNF production by IRAK1-mediated IL-10 expression and control innate hyperinflammation. *Proceedings of the National Academy of Sciences*, **111**, (14), 5295.
- Inoue, M., Mimura, K., Izawa, S., Shiraishi, K., Inoue, A., Shiba, S. & Kono, K. (2012). Expression of MHC Class I on breast cancer cells correlates inversely with HER2 expression. *Oncoimmunology*, **1**, (7), 1104-1110.
- Irvine, D. (2011). One nanoparticle, one kill. *Drug Delivery*, **10**, (5), 342-343.
- Ishihara, J., Ishihara, A., Potin, L., Hosseinchi, P., Fukunaga, K., Damo, M., Gajewski, T., Swartz, M. & Hubbell, J. (2018). Improving efficacy and safety of agonistic anti-CD40 antibody through extracellular matrix affinity. *Molecular Cancer Therapeutics*. **17**, (11), 2399-2411.
- James, A., Richardson, V., Wang, J., Proctor, R. & Colditz, G. (2013). Systems intervention to promote colon cancer screening in safety net settings: protocol for a community-based participatory randomized controlled trial. *Implementation Science*. **8**, (58), 5908-18.
- Jemal, A., Thomas, A., Murray, T. & Thun, M. (2002). Cancer Statistics 2002. *CA: A Cancer journal for clinicians*, **52**, (1), 23-47.
- Jemal, A., Siegel, R., Ward, E., Hao, Y., Xu, J. & Thun, M. (2009). Cancer Statistics, 2009. *CA: A Cancer Journal for Clinicians*. **59**, (4), 225-249.
- Jiang, H., Muckersie, E., Robertson, M., Xu, H., Liversidge, J. & Forrester, J. (2002). Secretion of interleukin-10 or interleukin-12 by LPS-activated dendritic

cells is critically dependent on time of stimulus relative to initiation of purified DC culture. *Journal of Leukocyte Biology*, **72**, (5) 978-985.

- Johnson, P., Steven, N., Chowdhury, F., Dobbyn, J., Hall, E., Ashton-Key, M. & Glennie, M. (2010). A Cancer Research UK phase I study evaluating safety, tolerability, and biological effects of chimeric anti-CD40 monoclonal antibody (MAb), Chi Lob 7/4. *Journal of Clinical Oncology*, **28**, (15), 2507-2507.
- Ju, X., Silveira, P., Hsu, W., Elgundi, Z., Alingcastre, R., Verma, N., Fromm, P., Hsu, J., Bryant, C., Li, Z., Kupresanin, F., Lo, T., Clarke, C., Lee, K., McGuire, H., Fazekas de St Groth, B., Larsen, S., Gibson, J., Bradstock, K., Clark, G. & Hart, D. (2016). The Analysis of CD83 Expression on Human Immune Cells Identifies a Unique CD83+-Activated T Cell Population. *Journal of Immunology*, **197**, (12), 4613-4625.
- Juneja, V., McGuire, K., Manguso, R., LaFleur, M., Collins, N., Haining, N., Freeman, G. & Sharpe, A. (2017). PD-L1 on tumour cells is sufficient for immune evasion in immunogenic tumors and inhibits CD8 T cell cytotoxicity. *Journal of Experimental Medicine*. **214**, (4), 895-904.
- Jung, C., Kwon, J., Seol, J., Park, W., Hyun, J., Kim, E. & Lee, Y. (2004). Induction of Cytotoxic T Lymphocytes by Dendritic Cells Pulsed With Murine Leukemic Cell RNA. *American Journal of Haematology*, **75**, (3), 121-127.
- Kalergis, A. & Ravetch, J. (2002). Inducing Tumor Immunity through the Selective Engagement of Activating Fcγ Receptors on Dendritic Cells. *The Journal of Experimental Medicine*, **195**, (12), 1653-1659.
- Kalupahana, R., Mastroeni, P., Maskell, D. & Blacklaws, B. (2005). Activation of murine dendritic cells and macrophages induced by *Salmonella enterica* serovar Typhimurium. *Immunology*, **115**, (4), 462-472.
- Kantoff, P., Higanp, C., Shore, N., Bergerm R., Small, E., Penson, D., Redfern., Ferrari, A., Dreicer, R., Sims, R., Xu, Y., Frohlich, M. & Schellhammer, P. (2010). Sipuleucel-T immunotherapy for castration-resistant prostate cancer. *New England Journal of Medicine*, **363**, (5), 411-422.
- Karagiannis, G., Poutahidis, T., Erdman, S., Kirsch, R., Riddell, R. & Diamandis, E. (2012). Cancer-Associated Fibroblasts Drive the Progression of Metastasis through both Paracrine and Mechanical Pressure on Cancer Tissue. *Molecular Cancer Research*, **10**, (11), 1403.
- Karpusas, M., Hsu, Y., Wang, J., Thompson, J., Lederman, S., Leonard, C. & Thomas, D. (1995). 2 A crystal structure of an extracellular fragment of human CD40 ligand. **3**, (10), 1031-1039.
- Kaur, J. & Poole, J. Cancer Registration Statistics, England: 2015. (2017). *Office for National Statistics (ONS) Statistical Bulletin*, (1), 1-19.

- Kawabe, T., Matsushima, M., Hashimoto, N., Imaizumi, K. & Hasegawa, Y. (2011). CD40/CD40 ligand interactions in immune responses and pulmonary immunity. *Journal of Medicinal Science*, **73**, (3) 69-78.
- Kaye, J., Gillis, S., Mizel, S., Shevach, E., Malek, T., Dinarello, C., Lachman, L. & Janeway, C. (1984). Growth of a cloned helper T cell line induced by a monoclonal antibody specific for the antigen receptor: interleukin 1 is required for the expression of receptors for interleukin 2. *Journal of Immunology*, **133**, (3), 1339-1345.
- Kelsall, B., Stuber, E., Neurath, M. & Strober, W. (1996). Interleukin-12 production by dendritic cells. The role of CD40-CD40L interactions in Th1 T-cell responses. *Annals of the New York Academy of Sciences*. **31**, 795, 116-126.
- Kempf, M., Mandal, B., Jilek, S., Thiele, L., Voros, J., Textor, M., Merkle, H. & Walter, E. (2003). Improved stimulation of human dendritic cells by receptor engagement with surface-modified microparticles. *Journal of Drug Targeting*. **11**, (1), 11-18.
- Kennecke, H., Yerushalmi, R., Woods, R., Cheang, M., Voduc, D., Speers, C. & Gelmon, K. (2010). Metastatic Behavior of Breast Cancer Subtypes. *Journal of Clinical Oncology*, **28**, (20) 3271-3277.
- Kerkar, S. & Restifo, N. (2012). Cellular Constituents of Immune Escape within the Tumor Microenvironment. *Cancer Research*, **72**, (13), 3125.
- Khammari, A., Labarriere, N., Vignard, V., Vouven, J., Pandolfino, M., Knol, A., Quereux, G., Saiagh, S., Brocard, C., Jotereau, F. & Freno, B. (2009). Treatment of metastatic melanoma with autologous Melan-A/MART-1-specific cytotoxic T lymphocyte clones. *Journal of Investigative Dermatology*. **129**, (12), 2835-42.
- Kim, D., Oh, N., Kim, K., Lee, S., Pack, C., Park, J. & Park, Y. (2018). Label-free high-resolution 3-D imaging of gold nanoparticles inside live cells using optical diffraction tomography. *Methods*, **136**, (1), 160-167.
- Kim, T., Kim, D., Chung, J., Shin, S., Kim, S., Heo, D. & Bang, Y. (2004). Phase I and pharmacokinetic study of Genexol-PM, a cremophor-free, polymeric micelle-formulated paclitaxel, in patients with advanced malignancies. *Clinical Cancer Research*, **10**, (11), 3708-3716.
- Klausz, K., Cieker, M., Kellner, C., Oberg, H., Kabelitz, D., Valerius, T., Burger, R., Gramatzki, M. & Peipp, M. (2017). A novel Fc-engineered human ICAM-1/CD5 antibody with potent anti-myeloma activity developed by cellular panning of phage display libraries. *Oncotarget*, **8**, (44), 77552-77566.
- Klingemann, H. (2014). Are natural killer cells superior CAR drivers? *OncImmunology*, **3**, (4), e28147.
- Knudsen, L. (2010). Liraglutide: The therapeutic promise from animal models. *International Journal of Clinical Practise*, (167), 4-11.

- Kobayashi, T., Walsh, M. & Choi, Y. (2004). The role of TRAF6 in signal transduction and the immune response. *Microbes and Infection*, **6**, (14), 1333-1338.
- Koch, F., Stanzl, U., Jennewein, P., Janke, K., Heufler, C., Kämpgen, E. & Schuler, G. (1996). High level IL-12 production by murine dendritic cells: upregulation via MHC class II and CD40 molecules and downregulation by IL-4 and IL-10. *The Journal of Experimental Medicine*, **184**, (2), 741-746.
- Kong, Y., Fuchsberger, M., Plebanski, M. & Apostolopoulos, V. (2016). Alteration of early dendritic cell activation by cancer cell lines predisposes immunosuppression, which cannot be reversed by TLR4 stimulation. *Acta Biochimica et Biophysica Sinica*, **48**, (12), 1101-1111.
- Koorella, C., Nair, J., Murray, M., Carlson, L., Watkins, S. & Lee, K. (2014). Novel regulation of CD80/CD86-induced phosphatidylinositol 3-kinase signaling by NOTCH1 protein in interleukin-6 and indoleamine 2,3-dioxygenase production by dendritic cells. *Journal of Biological Chemistry*. **289**, (11), 7747-7762.
- Korman, A., Peggs, K. & Allison, J. (2006). Checkpoint blockade in cancer immunotherapy. *Advanced Immunology*, **90**, 297-339,
- Kornbluth, R., Stempniak, M. & Stone, G. (2012). Design of CD40 Agonists and Their Use in Growing B Cells for Cancer Immunotherapy. *International Reviews of Immunology*, **31**, (4), 279-288.
- Knorr, D., Dahan, R. & Ravetch, J. (2018). Toxicity of an Fc-engineered anti-CD40 antibody is abrogated by intratumoral injection and results in durable antitumor immunity. *Proceedings of the National Academy of Sciences of the United States of America*. **115**, (43), 11048-11053.
- Krempski, J., Karyampudi, L., Behrens, M., Erskine, C., Hartmann, L., Dong, H., Goode, E., Kalli, K. & Knutson, K. (2011). Tumor-infiltrating programmed death receptor-1+ dendritic cells mediate immune suppression in ovarian cancer. *Journal of Immunology*, **186**, (12), 6905-6913.
- Kumar, V., Sharma, N. & Maitra, S. (2015). *In vitro* and *in vivo* toxicity assessment of nanoparticles. *International Nanotechnology Letters*, **7**, (4), 243-256.
- Kupper, T., Horowitz, M., Lee, F., Robb, R. & Flood, P. (1987). Autocrine growth of T cells independent of interleukin 2: identification of interleukin 4 (IL 4, BSF-1) as an autocrine growth factor for a cloned antigen-specific helper T cell. *Journal of Immunology*, **138**, (12), 4280-4287.
- La Fuente, H., Mittelbrunn, M., Sanchez-Martin, Vicente-Manzanares, M., Lamana, A., Pardi, R. & Sanchez-Madrid, F. (2005). Synaptic Clusters of MHC Class II Molecules Induced on DCs by Adhesion Molecule-mediated Initial T-Cell Scanning. *Molecular Biology of the Cell*, **16**, (7), 3314-3322.

- Lapteva, N., Seethammagari, M., Hanks, B., Jiang, J., Levitt, J., Slawin, K. & Spencer, D. (2007). Enhanced activation of human dendritic cells by inducible CD40 and toll-like receptor-4 ligation. *Cancer Research*, **67**, (21), 10528-10537.
- Larsen, A., Escargueil, A. & Skladanowski, A. (2000). Resistance mechanisms associated with altered intracellular distribution of anticancer agents. *Pharmacology & Therapeutics*, **85**, (3), 217-229.
- Lasek, W., Zagozdzon, R. & Jakobisiak, M. (2014). Interleukin 12: still a promising candidate for tumor immunotherapy? *Cancer Immunology, Immunotherapy*, **63**, (5), 419-435.
- Laudicella, M., Walsh, B., Burns, E. & Smith, P. (2016). Cost of care for cancer patients in England: evidence from population-based patient-level data. *British Journal of Cancer*, **114**, (11), 1286-92.
- Lechner, M., Karimi, S., Barry-Hoson, K., Angell, T., Murphy, K., Church, C., Ohlfest, J., Hu, P. & Epstein, A. (2013). Immunogenicity of murine solid tumor models as a defining feature of *in vivo* behavior and response to immunotherapy. *Journal of Immunotherapy*, **36**, (9), 477-489.
- Lechner, F., Wong, D., Dunbarm O., Chapman, R., Chung, R., Dohrenwend, P., Robbins, G., Phillips, R., Klenerman, P. & Walker, B. (2000). Analysis of successful immune responses in persons infected with hepatitis C virus. *Journal of Experimental Medicine*, **191**, (9), 1499-1512.
- Lechtman, E., Mashouf, S., Chattopadhyay, N., Keller, B., Lai, P., Cai, Z., Reilly, R. & Pignol, J. (2013). A Monte Carlo-based model of gold nanoparticle radiosensitization accounting for increased radiobiological effectiveness. *Physics in Medicine and Biology*, **58**, (10), 3075.
- Lee, D., Kochenderfer, J., Stetler-Stevenson, M., Cui, Y., Delbrook, C., Feldan, S., Fry, T., Orentas, R., Sabatino, M., Shah, N., Steinberg, S., Stroncek, D., Tschernia, N., Yuan, C., Zhang, H., Zhang, L., Rosenberg, S., Wayne, A. & Mackall, C. (2014). T cells expressing CD19 chimeric antigen receptors for acute lymphoblastic leukemia in children and young adults: a phase 1 dose-escalation trial. *The Lancet*, **7**, (385), 517-528.
- Lee, E., Na, K. & Bae, Y. (2005). Doxorubicin loaded pH-sensitive polymeric micelles for reversal of resistant MCF-7 tumor. *Journal of Controlled Release*, **103**, (2), 405-418.
- Lee, G., Harnett, N., Zychla, L. & Dinniwell, R. (2012). Radiotherapy Treatment Review: A Prospective Evaluation of Concordance between Clinical Specialist Radiation Therapist and Radiation Oncologist in Patient Assessments. *Journal of medical imaging ad radiation sciences*, **43**, (1), 6-10.
- Lee, H., Dempsey, P., Parks, T., Zhu, X., Baltimore, D. & Cheng, G. (1999). Specificities of CD40 signaling: Involvement of TRAF2 in CD40-induced NF- κ B activation and intracellular adhesion molecule-1 up-regulation. *PNAS*, **96**, (4), 1421-1426.

- Lefrançois, L., Altman, J., Williams, K. & Olson, S. (2000). Soluble Antigen and CD40 Triggering Are Sufficient to Induce Primary and Memory Cytotoxic T Cells. *The Journal of Immunology*, **164**, (2), 725.
- Le-Naour, F., Hohenkirk, A., Grolleau, A., Misek, D., Lescure, P., Geiger, J., Hanash, S. & Beretta, L. (2001). Profiling changes in gene expression during differentiation and maturation of monocyte-derived dendritic cells using both oligonucleotide microarrays and proteomics. *Journal of Biological Chemistry*, **276**, (21), 17920-17921.
- Levin, M., Goldstein, H. & Gerhardt, P. (1950). Cancer and Tobacco Smoking; a Preliminary Report. *Journal of the American Medical Association*, **143**, (4), 336-338.
- Li, F. & Ravetch, J. (2011). Inhibitory Fcγ Receptor Engagement Drives Adjuvant and Anti-Tumor Activities of Agonistic CD40 Antibodies. *Science*, **333**, (6045), 1030-1034.
- Li, X., Hu, W., Zheng, X., Zhang, C., Du, P., Zheng, Z. & Wu, C. (2015). Emerging immune checkpoints for cancer therapy. *Acta Oncologica*, **54**, (10), 1706-1713.
- Li, Y., Zhao, H. & Ren, X. (2016). Relationship of VEGF/VEGFR with immune and cancer cells: staggering or forward? *Cancer Biology & Medicine*, **13**, (2), 206-214.
- Lie, W., Jian, W., Zhang, L., Liu, F., Yin, L., Zhang, M. & Yu, B. (2013). Novel Mechanism of Inhibition of Dendritic Cells Maturation by Mesenchymal Stem Cells *via* Interleukin-10 and the JAK1/STAT3 Signaling Pathway. *PLoSone*, **8**, (1), 1-13.
- Lim, T., Chew, V., Sieow, J., Goh, S., Yeong, J., Soon, A. & Ricciardi-Castagnoli, P. (2015). PD-1 expression on dendritic cells suppresses CD8(+) T cell function and antitumor immunity. *Oncoimmunology*, **5**, (3), e1085146.
- Lim, T., Goh, J., Mortellaro, A., Lim, C., Hammerling, G. & Ricciardi-Castagnoli, P. (2012). CD80 and CD86 Differentially Regulate Mechanical Interactions of T Cells with Antigen Presenting Dendritic Cells and B Cells. *PLoS ONE*, **7**, (9), e45185.
- Lin, P., Lin, S., Wang, P. & Sridhar, R. (2014). Techniques for physiochemical characterisation of nanoparticles. *Biotechnology Advances*, **32**, (4), 711-726.
- Linsley, P., Bradshaw, J., Greene, J., Peach, R., Bennett, K. & Mittler, R. (1996). Intracellular trafficking of CTLA-4 and focal localization towards sites of TCR engagement. *Immunity*, **4**, (6), 535-543.
- Lipscomb, M. & Masten, B. (2002). Dendritic Cells: Immune Regulators in Health and Disease. *Physiology Reviews*, **82**, (1), 97-130.

- Liu, C., Lewis, C., Lou, Y., Xu, C., Peng, W., Yang, Y., Gelbard, A., Lizee, G., Zhou, D., Overwijk, W. & Hwu, P. (2012). Agonistic antibody to CD40 boosts the antitumour activity of adoptively transferred T cells *in vivo*. *Journal of Immunotherapy*, **35**, (3), 276-282.
- Liu, J. & Cao, X. (2015). Regulatory dendritic cells in autoimmunity: A comprehensive review. *Journal of Autoimmunity*, **63**, 1-12.
- Llopiz, D., Aranda, F., Diaz-Valdes, N., Ruiz, M., Infante, S., Belsue, V. & Sarobe, P. (2016). Vaccine-induced but not tumor-derived Interleukin-10 dictates the efficacy of Interleukin-10 blockade in therapeutic vaccination. *Oncoimmunology*, **5**, (2), e1075113.
- Llopiz, D., Ruiz, M., Infante, S., Villanueva, L., Silva, L., Hervas-Stubbs, S. & Sarobe, P. (2017). IL-10 expression defines an immunosuppressive dendritic cell population induced by antitumor therapeutic vaccination. *Oncotarget*, **8**, (2), 2659-2671.
- Lotze, M., Chang, A., Seipp, C., Simpson, C., Vetto, J. & Rosenberg, S. (1986). High-dose recombinant interleukin 2 in the treatment of patients with disseminated cancer. Responses, treatment-related morbidity, and histologic findings. *JAMA*, **256**, (22), 3117-3124.
- Lotz, M., Frana, L., Sharrow, S., Robob, R. & Rosenberg, S. (1985). *In vivo* administration of purified human interleukin 2. I. Half-life and immunologic effects of the Jurkat cell line-derived interleukin 2. *Journal of Immunology*, **134**, (1), 157-166.
- Lowes, L. & Allan, A. (2018). Circulating Tumor Cells and Implications of the Epithelial-to-Mesenchymal Transition. *Advances in Clinical Chemistry*, (83), 121-181).
- Lopez, M., Pereda, C., Segal, G., Munzo, L., Aguilera, R., Gonzalez, F., Escobar, A., Ginesta, A., Reyes, D., Gonzalez, R., Mendoza-Naranjo, A., Larrondo, M., Compan, A., Ferrada, C. & Salazar-Onfray, F. (2009). Prolonged survival of dendritic cell vaccinated melanoma patients correlates with tumour specific delayed type IV hypersensitivity response and reduction of tumour growth factor beta-expressing T cells. *Journal of Clinical Oncology*, **27**, (6), 945-952.
- Lu, P., Weaver, V. & Werb, Z. (2013). The extracellular matrix: A dynamic niche in cancer progression. *Cell Biology*, **196**, (4), 395-406.
- Lucero, H., Ravid, K., Grimsby, L., Rich, C., Maki, J., Myllyharju, J. & Kagan, H. (2008). Lysyl Oxidase Oxidizes Cell Membrane Proteins and Enhances the Chemotactic Response of Vascular Smooth Muscle Cells. *Journal of Biological Chemistry*, **283**, (35), 24103-24117.
- Luheshi, N., Coates-Ulrichsen, J., Harper, J., Mullins, S., Sulikowski, M., Martin, P., Brown, J., Lewis, A., Davies, G., Morrow, M. & Wilkinson, R. (2016). Transformation of the tumour microenvironment by a CD40 agonist

antibody correlates with improved responses to PD-L1 blockade in a mouse orthotopic pancreatic tumour model. *Oncotarget*, **7**, (14), 18508-20.

Luster, A., Alon, R. & von Adrian, U. (2005). Immune cell migration in inflammation: present and future therapeutic targets. *Nature Immunology*, **6**, (12), 1182-1190.

Lutz, M. (2012). Therapeutic Potential of Semi-Mature Dendritic Cells for Tolerance Induction. *Frontiers in Immunology*, **3**, 123.

Ma, D. & Clark, E. (2009). The role of CD40 and CD40L in dendritic cells. *Seminars in Immunology*, **21**, (5), 265-272.

Ma, X., Yan, W., Zheng, H., Du, Q., Zhang, L., Ban, Y. & Wei, F. (2015). Regulation of IL-10 and IL-12 production and function in macrophages and dendritic cells. *F1000Research*, **4**, 1465.

Mach, F., Schonbeck, U., Sukhova, G., Atkinson, E. & Libby, P. (1998). Reduction of atherosclerosis in mice by inhibition of CD40 signalling. *Letters to Nature*, **394**, (6689), 200-203.

Mackey, M., Wang, Z., Eichelberg, K. & Germain, R. (2003). Distinct contributions of different CD40 TRAF binding sites to CD154-induced dendritic cell maturation and IL-12 secretion. *European Journal of Immunology*, **33**, (3), 779-789.

Madar, S., Goldstein, I. & Rotter, V. (2013). 'Cancer associated fibroblasts' – more than meets the eye. *Trends in Molecular Medicine*, **19**, (8), 447-453.

Maddams, J., Utley, M. & Møller, H. (2012). Projections of cancer prevalence in the United Kingdom, 2010–2040. *British Journal of Cancer*, **107**, (7), 1195–1202.

Mangsbo, S., Broos, S., Fletcher, E., Veitonmaki, N., Furebring, C., Dahlen, E., Norlen, P., Lindstedt, M., Totterman, T. & Ellmark, P. (2015). The human agonistic CD40 antibody ADC-1013 eradicates bladder tumors and generates T-cell-dependent tumor immunity. *Clinical Cancer Research*, **21**, (5), 1115-1126.

Manning, M., Chou, D., Murphy, B., Payne, R. & Katayama, D. (2010). Stability of protein pharmaceuticals: An update. *Pharmaceutical research*, **27**, (4), 544-575.

Mannino, M., Zhu, Z., Xiao, H., Bai, Q., Wakefield, M. & Fang, Y. (2015). The paradoxical role of IL-10 in immunity and cancer. *Cancer Letters*, **367**, (2), 103-107.

Mantovani, A., Sica, A., Sozzani, S., Allavena, P., Vecchi, A. & Locati, M. (2004). The chemokine system in diverse forms of macrophage activation and polarization. *Trends in Immunology*. **25**, (12), 677-686.

- Manz, M., Traver, D., Miyamoto, T., Weissman, U. & Akashi, K. (2011). Dendritic cell potentials of early lymphoid and myeloid progenitors, *Blood*, **97**, (11), 3333-41.
- Marigo, I., Zilio, S., Desantis, G., Mlecnik, B., Agnellini, Andrielly H. R., Ugel, S. & Bronte, V. (2016). T Cell Cancer Therapy Requires CD40-CD40L Activation of Tumor Necrosis Factor and Inducible Nitric-Oxide-Synthase-Producing Dendritic Cells. *Cancer Cell*, **30**, (3), 377-390.
- Markman, M. (2006). Pegylated liposomal doxorubicin in the treatment of cancers of the breast and ovary. *Expert Opinion on Pharmacotherapy*, **7**, (11), 1469-1474.
- Markman, M., Markman, J. & Webster, K. (2004). Duration of response to second-line, platinum based chemotherapy for ovarian cancer: implications for patient management and clinical trial design. *Journal of Clinical Oncology*, **22**, (15), 3120-3125.
- Marth, C., Windbichler, G., Hausmaninger, H., Petru, E., Estermann, K., Petzer, A. & Mueller-Holzner, E. (2006). Interferon-gamma in combination with carboplatin and paclitaxel as a safe and effective first-line treatment option for advanced ovarian cancer: results of a phase I/II study. *International Journal of Gynecological Cancer*. **16**, (4), 1522-1528.
- Martin, S., Agarwal, R., Murusaigan, G. & Saha, B. (2014). CD40 expression levels modulate regulatory T cells in Leishmania donovani infection. *The Journal of Immunology*, **185**, (1), 551-559.
- Martin-Fontecha, A., Baumjohann, D., Guarda, G., Reboldi, A., Hons, M., Lanzavecchia, A. & Sallusto, F. (2008). CD40L + CD4 + memory T cells migrate in a CD62P-dependent fashion into reactive lymph nodes and license dendritic cells for T cell priming. *Journal of Electronic Medicine*, **205**, (11), 2561-2574.
- Martini, M., Testi, M., Pasetto, M., Picchio, M., Innamorati, G., Mazzocco, M., Ugel, S., Cingarlini, S., Bronte, V., Zanovello, P., Krampera, M., Mosna, F., Cestari, T., Riviera, A., Brutti, N., Barbieri, O., Matera, L., Tridente, G., Colombatti, M. & Sartoris, S. (2010). IFN-gamma-mediated upmodulation of MHC class I expression activates tumor-specific immune response in a mouse model of prostate cancer. *Vaccine*, **28**, (20), 3548-3557.
- Mathur, D., Prakash, S., Anand, P., Kaur, H., Agrawal, P., Mehta, A., Kumar, R., Singh, S. & Raghava, G. (2016). PEPLife: A Repository of the Half-life of Peptides. *Scientific Reports*, **6**, 36617.
- Matsunaga, T., Ishida, T., Takekawa, M., Nishimura, S., Adachi, M. & Imai, K. (2002). Analysis of gene expression during maturation of immature dendritic cells derived from peripheral blood monocytes. *Scandinavian Journal of Immunology*, **56**, (6), 593-601.
- Maude, S., Teachey, D., Porter, D. & Grupp, S. (2015). CD19-targeted chimeric antigen receptor T cell therapy for acute lymphoblastic leukemia. *Blood*, **25**, (125), 4017-4023.

- Mayordomo, J., Zorina, T., Storkus, W., Zitvogel, L., Celluzzi, C., Falo, L., Melief, C., Iltstad, S., Martin-Kast, W., Delio, A. & Lotze, M. (1995). Bone marrow-derived dendritic cells pulsed with synthetic tumour peptides elicit protective and therapeutic antitumour immunity. *Nature Medicine*, **1**, 1297-1302.
- Mbeunkui, F. & Johann, D. (2009). Cancer and the tumor microenvironment: a review of an essential relationship. *Cancer Chemotherapy & Pharmacology*, **63**, (4), 571-582.
- McDermott, D., Lebbe, C., Hodi, F., Maio, M., Weber, J., Wolchok, J. & Balch, C. (2014). Durable benefit and the potential for long-term survival with immunotherapy in advanced melanoma. *Cancer Treatment Reviews*, **40**, (9), 1056-1064.
- McDonnell, A., Robinson, B. & Currie, A. (2010). Tumor Antigen Cross-Presentation and the Dendritic Cell: Where it All Begins? *Clinical and Developmental Immunology*, **2010**, e539519.
- Medina-Echeverez, J., Ma, C., Duffy, A., Kleiner, D. & Greten, T. (2014). Agonistic CD40 antibody induces immune-mediated liver damage and modulates tumor induced myeloid suppressive cells. *Journal for Immunotherapy of Cancer*, **2**, (3), 174.
- Mellman, I. & Steinman, R. (2001). Dendritic Cells: Specialized and Regulated Antigen Processing Machines *Cell*, **106**, (3), 255-258.
- Michielsen, A., Hogan, A., Marry, J., Tosetto, M., Cox, F., Hyland, J., Sheahan, K., O'Donoghue, D., Mulcahy, H., Ryan, E. & O'Sullivan, J. (2011). Tumour tissue microenvironment can inhibit dendritic cell maturation in colorectal cancer. *PLoSOne*, **6**, (11), e27944.
- Mihret, A., Mamo, G., Tafesse, M., Hailu, A. & Parida, S. (2011). Dendritic Cells Activate and Mature after Infection with Mycobacterium tuberculosis. *BMC Research Notes*, **4**, 247.
- Mills, E. & O'Neill, L. (2016). Reprogramming mitochondrial metabolism in macrophages as an anti-inflammatory signal. *European Journal of Immunology*, **46**, (1), 13-21.
- Mitchell, J., Burbach, B., Srivastava, R., Fife, B. & Shmizu, Y. (2013). Multistage T cell-dendritic cell interactions control optimal CD4 T cell activation through the ADAP-SKAP55-signaling module. *The Journal of Immunology*, **191**, (5), 2372-2383.
- Mittal, D., Gubin, M., Schreiber, R. & Smyth, M. (2014). New insights into cancer immunoediting and its three component phases — elimination, equilibrium and escape. *Current Opinion in Immunology*, **27**, 16-25.
- Moghimi, S., Hunter, A. & Murray, J. (2001). Long-circulating and target-specific nanoparticles: theory to practice. *Pharmacological Reviews*, **53**, (2), 283-318.

- Moghimi, S. & Szebeni, J. (2003). Stealth liposomes and long circulating nanoparticles: critical issues in pharmacokinetics, opsonization and protein-binding properties. *Progress in Lipid Research*, **42**, (6), 463-478.
- Mompo, S. & Gonzalez-Fernandez, A. (2018). Antigen specific human monoclonal antibodies from transgenic mice. *Human Monoclonal Antibodies*, **1060**, 245-276.
- Monks, C., Freiberg, B., Kupfer, H., Sciaky, N. & Kupfer, A. (1998). Three-dimensional segregation of supramolecular activation clusters in T cells. *Nature*, **395**, (6697), 82-6.
- Morgan, D., Ruscetti, F. & Gallo, R. (1976). Selective *in vitro* growth of T lymphocytes from normal human bone marrows. *Science*, **193**, (4257), 1007-1008.
- Morgillo, F. & Lee, Y. (2005). Resistance to epidermal growth factor receptor-targeted therapy. *Drug Resistance Updates*, **8**, (5), 298-310.
- Morris, N., Peters, C., Montler, R., Hu, H., Curti, B., Urba, W. & Weinberg, A. (2007). Development and characterization of recombinant human Fc:OX40L fusion protein linked *via* a coiled-coil trimerization domain. *Molecular Immunology*, **44**, (12), 3112-3121.
- Mullins, D. & Engelhard, V. (2006). Limited infiltration of exogenous dendritic cells and naive T cells restricts immune responses in peripheral lymph nodes. *Journal of Immunology*, **176**, (8), 4535-4542.
- Munz, C., Steinman, R. & Fujii, S. (2005). Dendritic cell maturation by innate lymphocytes: coordinated stimulation of innate and adaptive immunity. *Journal of Electronic Medicine*, **202**, (2), 203-207.
- Muranski, P. & Restifo, N. (2009). Adoptive immunotherapy of cancer using CD4(+) T cells. *Current Opinions in Immunotherapy*. **21**, (2), 200-208.
- Murphy, K., Travers, P., Walport, M. & Janeway, C. (2012). *Janeway's immunobiology*. (8th Edition), New York: Garland Science.
- Muthukkaruppan, V., Kubai, L. & Auerbach, R. (1982). Tumor-induced neovascularization in the mouse eye. *Journal of the National Cancer Institute*, **69**, (3), 699-708.
- Na, R., Zheng, S., Han, M., Yu, H., Jiang, D., Shah, S., Ewing, C., Zhang, L., Petkewicz, J., Gulukota, L., Helseth, D., Quinn, M., Humphries, E., Wiley, K., Isaacs, S., Wu, Y., Liu, X., Zhang, N., Wang, C., Khandekar, J., Hulick, P., Shevrin, D., Cooney, K., Shen, Z., Partin, A., Carter, H., Carducci, M., Eisenberger, S., Denmeade, S., McGuire, M., Walsh, P., Helfand, B., Brendler, C., Ding, Q., Xu, J. & Isaacs, W. (2017). Germline Mutations in ATM and BRCA1/2 Distinguish Risk for Lethal and Indolent Prostate Cancer and are Associated with Early Age at Death. *European Urology*, **71**, (5), 740-747.

- Nag, O. & Awasthi, V. (2013). Surface Engineering of Liposomes for Stealth Behavior. *Pharmaceutics*, **5**, (4), 542-569.
- Nagaraj, S., Youn, Je-In. & Gabrilovich, D. (2013). Reciprocal relationship between myeloid-derived suppressor cells and T cells. *The Journal of Immunology*, **191**, (1), 17-23.
- Nagarajan, N., Gonzalez, F. & Shastri, N. (2012). Non-classical MHC class Ib-restricted cytotoxic T cells monitor antigen processing in the endoplasmic reticulum. *Nature Immunology*, **13**, (6), 579-586.
- Nagorsen, D., Voigt, S., Berg, E., Stein, H., Theil, E. & Loddenkemper, C. (2007). Tumor-infiltrating macrophages and dendritic cells in human colorectal cancer: relation to local regulatory T cells, systemic T-cell response against tumor-associated antigens and survival. *Journal of Translational Medicine*, **5**, (1), 62-65.
- Naik, S. (2008). Demystifying the development of dendritic cell subtypes, a little. *Immunology and Cell Biology*, **86**, (5), 1-14.
- Naing, A., Papadopoulus, K., Autio, K., Ott, P., Patel, M., Wong, D., Falchook, G., Pant, S., Whiteside, M., Rasco, D., Mumm, J., Chan, I., Bendell, J., Bauer, T., Colen, R., Hong, D., Van Vlasselaer, k P., Tannir, N., Oft, M. & Infante, J. (2016). Safety, Antitumour Activity, and Immune Activation of Pegylated Recombinant Human Interleukin-10 (AM0010) in Patients with Advanced Solid Tumours. *Journal of Clinical Oncology*, **34**, (29), 3562-3569.
- Naismith, J. & Sprang, S. (1998). Modularity in the TNF-receptor family. *Trends in Biochemical Science*, **23**, (2), 74-79.
- Nelson, D. (2012). Turning the tumor microenvironment into a self vaccine site. *Oncoimmunology*, **1**, (6), 989-991.
- Nencioni, A., Grunebach, F., Schmidt, S., Muller, M., Boy, D., Patrone, F., Ballestrero, A. & Brossart, P. (2008). The use of dendritic cells in cancer immunotherapy. *Oncology Hematology*, **65**, (3), 191-199.
- Nguyen, L., Elford, A., Murakami, K., Garza, K., Schoenberger, S., Odermatt, B., Speiser, D. & Ohashi, P. (2002). Tumor Growth Enhances Cross-Presentation Leading to Limited T Cell Activation without Tolerance. *Journal of Experimental Medicine*, **195**, (4), 423-435.
- Ni, K., & O'Neill, H. (1997). The role of dendritic cells in T cell activation. *Immunology and Cell Biology*, **75**, (3), 223-230.
- Nieland, J., & Kruisbeek, (1995). T cell lymphoma can provide potent co-stimulatory effects to T cells that are not mediated by B7-1, B7-2, CD40, HSA or CD70. *International Immunology*, **7**, (11), 1927-1838.
- Nimanong, S., Ostroumov, D., Wingerath, J., Knocke, S., Woller, N., Gürlevik, E., Falk, C., Manns, M., Kuhnel, F. & Wirth, T. (2017). CD40 Signaling Drives Potent

Cellular Immune Responses in Heterologous Cancer Vaccinations. *Cancer Research*, **77** (8), 1918-1926.

- Nirschl, C. & Drake, C. (2013). Molecular pathways: coexpression of immune checkpoint molecules: signaling pathways and implications for cancer immunotherapy. *Clinical Cancer Research*, **19**, (18), 4917-4924.
- Nishida, N., Yano, H., Nishida, T., Kamura, T. & Kojiro, M. (2006). Angiogenesis in Cancer. *Vascular Health and Risk Management*, **2**, (3), 213-219.
- Novartis Pharmaceuticals Corporation Press Release; (August 2017). Kymriah (tisagenlecleucel) Prescribing information. East Hanover, New Jersey, USA.
- Novellino, L., Castelli, C. & Parmiani, G. (2005). A listing of human tumour antigens recognized by T cells: March 2004 update. *Cancer Immunology & Immunotherapy*, **54**, (3), 187-207.
- Oh, J. & Weiderpass, E. (2014). Infection and Cancer: Global Distribution and Burden of Diseases. *Annals of Global Health*, **80**, (5), 384-392.
- Ohshima, Y., Tanaka, Y., Tozawa, H., Takahashi, Y., Maliszewski, C., & Delespesse, G. (1997). Expression and function of OX40 ligand on human dendritic cells. *Journal of Immunology*, **159**, (8), 3838-3848.
- Okada, F. (2014). Inflammation-Related Carcinogenesis: Current Findings in Epidemiological Trends, Causes and Mechanisms. *Yonago Acta Medica*, **57**, (2), 65-72.
- Ophir, E., Bobisse, S., Coukos, G., Harari, A. & Kandalaft, L. (2016). Personalised approaches to activate immunotherapy in cancer. *Biochimica et Biophysica Acta*, **1865**, (1), 72-82.
- Oskarsson, T. (2013). Extracellular matrix components in breast cancer progression and metastasis. *Breast*, **22**, (2), 66-72.
- Ostman, A. & Augsten, M. (2009). Cancer-associated fibroblasts and tumor growth-bystanders turning into key players. *Current Opinion in Genetics & Development*, **171**, (76), 67-73.
- Ott, P., Hodi, S., Kaufman, H., Wigginton, J. & Wolchok. (2017). Combination immunotherapy: a road map. *Journal for the Immunotherapy of Cancer*. **5**, (16), 1-15.
- Palucka, K. & Banchereau, J. (2012). Cancer immunotherapy via dendritic cells. *Nature Reviews Cancer*, **12**, (4), 265-277.
- Palucka, K., Banchereau, J. & Mellman, I. (2010). Designing Vaccines Based on Biology of Human Dendritic Cell Subsets, *Cell Press*, **33**, (4), 464-479.
- Palucka, K. & Coussens, L. (2016). The Basis of Oncoimmunology. *Cell*, **10**, 164, (6), 1233-1247.

- Palucka, K., Taquet, N., Sanchez-Chapuis, F. & Gluckman, J. (1998). Dendritic cells as the terminal stage of monocyte differentiation. *Journal of Immunology*, **160**, (9), 4587-4595.
- Palucka, K., Ueno, H., Zurawski, G., Fay, J. & Banchereau, J. (2010). Building on dendritic cell subsets to improve cancer vaccines. *Current Opinion in Immunology*, **22**, (2) 258-263.
- Parker, C., Yang, Q., Yang, B., McCallen, J., Park, S. & Lai, S. (2017). Multivalent interactions between streptavidin-based pretargeting fusion proteins and cell receptors impede efficient internalization of biotinylated nanoparticles. *Acta Biomaterialia*, **63**, 181-189.
- Parry, R., Chemnitz, J., Frauwirth, K., Lanfranco, A., Lanfranco, A., Braunstein, I., Kobayashi, S., Kobayashi, S., Linsley, P., Thompson, C. & Riley, J. (2005). CTLA-4 and PD-1 receptors inhibit T-cell activation by distinct mechanisms. *Molecular Cell Biology*, **25**, (21), 9543-9553.
- Paszek, M., Boettiger, D., Weaver, V. & Hammer, D. (2009). Integrin Clustering is Driven by Mechanical Resistance from the Glycocalyx and the Substrate. *PLoS Computational Biology*, **5**, (12), 1-16.
- Paszek, M., Zahir, N., Johnson, K., Lakins, J., Rozenberg, G., Gefen, A. & Weaver, V. (2005). Tensional homeostasis and the malignant phenotype. *Cancer Cell*, **8**, (3), 241-254.
- Paul, S. & Lal, G. (2017). The Molecular Mechanism of Natural Killer Cells Function and Its Importance in Cancer Immunotherapy. *Frontiers in Immunology*, **13**, (8), 1124-1139.
- Paulson, K., Tegeder, A., Willmes, C., Iyer, J., Afanasiev, O., Schrama, D., Koba, S., Thibodeau, R., Nagase, K., Simonson, W., Seo, A., Koelle, D., Madeleine, M., Bhatia, S., Nakajima, H., Sano, S., Hardwich, J., Disis, M., Cleary, M., Becker, J. & Nghiem, P. (2014). Downregulation of MHC-I expression is prevalent but reversible in Merkel cell carcinoma. *Cancer Immunology Research*, **2**, (11), 1071-1079.
- Pearson, L., Castle, B. & Kehry, M. (2001). CD40-mediated signalling in monocytic cells: up-regulation of tumour necrosis factor receptor-associated mRNAs and activation of mitogen-activated protein kinase signalling pathways. *International Immunology*, **13**, (3), 273-283.
- Peggs, K., Quezada, S., Korman, A. & Allison, J. (2006). Principles and use of anti-CTLA4 antibody in human cancer immunotherapy. *Current Opinion in Immunotherapy*, **18**, (2), 206-213.
- Pegram, H., Lee, J., Hayman, E., Imperato, G. H., Tedder, T., Sadelain, M. & Brentjens, R. (2012). Tumor-targeted T cells modified to secrete IL-12 eradicate systemic tumors without need for prior conditioning. *Blood*, **119**, 18, 4133-41.

- Pelicano, H., Martin, D., Xu, R. & Huang, P. (2006). Glycolysis inhibition for anticancer treatment. *Oncogene*, **25**, (34), 4633-4646.
- Pentcheva-Hoang, T., Egen, J., Wojnoonski, K. & Allison, J. (2004). B7-1 and B7-2 selectively recruit CTLA-4 and CD28 to the immunological synapse. *Immunity*, **21**, (3), 401-413.
- Petit, V. & Thiery, J. (2000). Focal adhesions: structure and dynamics. *Biology of the Cell*, **92**, (7), 477-494.
- Petre, C. & Dittmer, D. (2007). Liposomal daunorubicin as treatment for Kaposi's sarcoma. *International Journal of Nanomedicine*, **2**, (3), 277-288.
- Philips, G. & Atkins, M. (2014). Therapeutic uses of anti-PD-1 and anti-PD-L1 antibodies. *International Immunology*, **27**, (1), 39-46.
- Pintaric, M., Gerner, W. & Saalmuller, A. (2008). Synergistic effects of IL-2, IL-12 and IL-18 on cytolytic activity, perforin expression and IFN-gamma production of porcine natural killer cells. *Vetinary Immunology & Immunopathology*. **121**, (2), 68-82.
- Pinzon-Charry, A., Maxwell, T. & Lopez, J. (2005). Dendritic cell dysfunction in cancer: a mechanism for immunosuppression. *Immunology & Cell Biology*, **83**, (5), 151-161.
- Platt, C. Ma, J. Chalouni, C., Ebersold, M., Bou-Reslan, H., Carano, R., Mellman, I. & Delamarre, L. (2010). Mature dendritic cells use endocytic receptors to capture and present antigens. *Proceedings of the National Academy of Sciences*, **107**, (9), 4287-4292.
- Pollard, T. (2010). A Guide to Simple and Informative Binding Assays. *Molecular Biology of the Cell*, **21**, (23), 4061-4067.
- Portillo, J, Greene, J., Schwartz, I., Subauste, M., Zarini, S., Bapputty, R., Kern, T., Gubitosi-Klug, R., Murphy, R., Subauste, C. & Subauste, C. (2015). Blockade of CD40-TRAF2,3 or CD40-TRAF6 is sufficient to inhibit pro-inflammatory responses in non-haematopoietic cells. *Immunology*, **144**, (1), 21-33.
- Portillo, J., Greene, J., Schwartz, I., Subauste, M. & Subuaste, C. (2015). Blockade of CD40-TRAF-2, 3 or CD40-TRAF-6 is sufficient to inhibit pro-inflammatory responses in non-haematopoietic cells. *Immunology*, **144**, (1), 21-33.
- Potente, M., Gerhardt, H. & Carmeliet, P. (2011). Basic and Therapeutic Aspects of Angiogenesis. *Cell*, **146**, (6), 873-887.
- Poudier, J. & Owens, T. (1994). CD54/intercellular adhesion molecule 1 and major histocompatibility complex II signalling induces B cells to express interleukin 2 receptors and complements help provided through CD40 ligation. *The Journal of Experimental Medicine*, **179**, (5), 1417-1427.

- Preynat-Seauve, O., Schuler, P., Contassot, E., Beermann, F., Huard, B. & French, L. (2006). Tumor-infiltrating dendritic cells are potent antigen-presenting cells able to activate T cells and mediate tumor rejection. *Journal of Immunology*, **176**, (1), 61-67.
- Pryczynicz, A., Cepowicz, D., Zaręba, K., Gryko, M., Hołody-Zaręba, J., Kędra, Kemon, A. & Guzińska-Ustymowicz, K. (2016). Dysfunctions in the Mature Dendritic Cells Are Associated with the Presence of Metastases of Colorectal Cancer in the Surrounding Lymph Nodes. *Gastroenterology Research and Practice*, **2016**, 2405437.
- Quezada, S., Peggs, K., Simpson, T., Shen, Y., Littman, D. & Allison, J. (2008). Limited tumor infiltration by activated T effector cells restricts the therapeutic activity of regulatory T cell depletion against established melanoma. *Journal of Experimental Medicine*, **205**, (9), 2125-2138.
- Raetz, C. & Whitfield, C. (2002). Lipopolysaccharide endotoxins. *Annual Reviews in Biochemistry*, **71**, 635-700.
- Ravetch, J. V. & Bolland, S. (2001). IgG Fc Receptors. *Annual Review of Immunology*, **19**, (1), 275-290.
- Reck, M., Rodriguez-Abreu, D., Robinson, A., Hui, R., Czoszi, T., Fulop, A., Gottfried, M., Peled, N., Tafreshi, A., Cuffe, S., O'Brien, M., Rao, S., Hotta, K., Leiby, M., Lubiniecki, G., Shentu, Y., Reshma, R. & Brahmer, J. (2016). Pembrolizumab versus Chemotherapy for PD-L1-Positive Non-Small-Cell Lung Cancer. *New England Journal of Medicine*, **375**, (19), 1823-1833.
- Remer, M., White, A., Glennie, M., Al-Shamkhani, A. & Johnson, P. (2017). The Use of Anti-CD40 mAb in Cancer. *Current Topics in Microbiology and Immunology*, **405**, 165-207.
- Reubi, J. & Maecke, H. (2008). Peptide-based probes for cancer imaging. *Journal of Nuclear Medicine*, **49**, (11), 1735-1738.
- Richman, L. & Vonderheide, R. (2014). Role of crosslinking for agonistic CD40 monoclonal antibodies as immune therapy of cancer. *Cancer Immunology Research*, **2**, (1), 19-26.
- Ridge, J., Di Rosa, F. & Matzinger, P. (1998). A conditioned dendritic cell can be a temporal bridge between a CD4+ T-helper cell and a T-killer cell. *Nature*, **393**, (6684), 474-478.
- Rimann, M. & Graf-Hausner, U. (2012). Synthetic 3D multicellular systems for drug development. *Current Opinions in Biotechnology*, **23**, (5), 803-809.
- Roby, K., Taylor, C., Sweetwood, J., Cheng, Y., Pace, J., Tawfik, O., Persons, D., Smith, P. & Terranova, P. (2000). Development of a syngeneic mouse model for events related to ovarian cancer. *Carcinogenesis*, **21**, (4), 585-591.

- Rogers, N., Jackson, I., Jordan, W., Lombardi, G., Delikouras, A. & Lechler, R. (2003). CD40 can costimulate human memory T cells and favors IL-10 secretion. *The European Journal of Immunology*, **33**, (2) 1094-1104.
- Rosalia, R., Cruz, L., van Duikeren, S., Tromp, A., Silva, A., Jiskoot, W., de Gruijl, T., Lowik, C., Oostendorp, J., Burg, S. & Ossendorp, F. (2015). CD40-targeted dendritic cell delivery of PLGA-nanoparticle vaccines induce potent anti-tumor responses. *Biomaterials*, **40**, 88-97.
- Rosenberg, S., Restifo, N., Yang, J., Morgan, R. & Dudley, M. (2008). Adoptive cell transfer: a clinical path to effective cancer immunotherapy *Nature Reviews*, **8**, (4), 299-308.
- Rosenberg, S. IL-2: the first effective immunotherapy for human cancer. (2014). *The Journal of Immunology*, **192**, (12), 5451-5458.
- Rosenthal, E., Poizot-Martin, I., Saint-Marc, T., Spano, J. & Cacoub, P. (2002). Phase IV study of liposomal daunorubicin (DaunoXome) in AIDS-related Kaposi sarcoma. *American Journal of Clinical Oncology*, **25**, (1), 57-59.
- Ruffell, B., Chang-Strachan, D., Chan, V., Rosenbusch, A., Ho, Pryer, N., Daniel, D., Hwang, S., Rugo, H. & Coussens, L. (2014). Macrophage IL-10 Blocks CD8+ T Cell-Dependent Responses to Chemotherapy by Suppressing IL-12 Expression in Intratumoral Dendritic Cells. *Cancer Cell*, **26**, (5), 623-637.
- Sabado, R. & Bhardwaj, N. (2010). Directing dendritic cell immunotherapy towards successful cancer treatment. *Immunotherapy*, **2**, (1), 37-56.
- Sabbatini, P., Aghajanian, C., Dizon, D., Anderson, S., Dupont, J., Brown, J., Peters, W., Jacobs, A., Mehdi, A., Rivkin, S., Eisenfeld, A. & Spriggs, D. (2004). Phase II study of CT-2103 in patients with recurrent epithelial ovarian, fallopian tube, or primary peritoneal carcinoma. *Journal of Clinical Oncology*, **22**, (22), 4523-4531.
- Saber, R., Sarkar, S., Gill, P., Nazari, B. & Faridani, F. (2011). High resolution imaging of IgG and IgM molecules by scanning tunneling microscopy in air condition. *Scientia Iranica*, **18**, (6), 1643-1646.
- Sahoo, S. & Labhasetwar, V. (2005). Enhanced antiproliferative activity of transferrin-conjugated paclitaxel-loaded nanoparticles is mediated via sustained intracellular drug retention. *Molecular Pharmaceuticals*, **2**, (5), 373-383.
- Saikh, K., Kahn, A., Kissner, A. & Ulrich, R. (2001). IL-15 induced conversion of monocytes to mature dendritic cells. *Clinical Experimental Immunology*, **126**, (3), 447-455.
- Sallusto, F., Palermo, B., Lenig, D., Miettinen, M., Matikainen, S., Jukunen, I., Forster, R., Burgstahler, R., Lipp, M. & Lanzavecchia, A. (1999). Distinct patterns and kinetics of chemokine production regulate dendritic cell function. *European Journal of Immunology*, **29**, 1617-1625.

- Sanchez-Paulete, A., Teijeira, A., Cueto, F., Garasa, S., Perez-Gracia, J., Sanchez-Arriaza, A., Sancho, D. & Melero, I. (2017). Antigen cross-presentation and T-cell cross-priming in cancer immunology and immunotherapy. *Annals of Oncology*, **28**, (12), 44-55.
- Sandin, L., Orlova, A., Gustafsson, E., Ellmark, P., Tolmachev, V., Totterman, T. & Mangsbo, S. (2014). Locally delivered CD40 agonist antibody accumulates in secondary lymphoid organs and eradicates experimental disseminated bladder cancer. *Cancer Immunology Research*, **2**, (1), 80-90.
- Sansom, D., Manzotti, C. & Zheng, Y. (2003). What's the difference between CD80 and CD86? *TRENDS in Immunology*, **24**, (6), 313-319.
- Sasaki, T., Hiroki, K. & Yamashita, Y. (2013). The Role of Epidermal Growth Factor Receptor in Cancer Metastasis and Microenvironment. *BioMed Research International*, **20**, (13), 1-8.
- Sato, T., Terai, M., Tamura, Y., Alexeev, Mastrangelo, M. & Selvan, S. (2011). Interleukin 10 in the tumor microenvironment: a target for anticancer immunotherapy, *Immunological Research*, **51**, (2), 170-182.
- Satpathy, A., Murphy, K. & Wumesh, K. (2011). Transcription Factor Networks in Dendritic Cell Development. *Seminars in Immunology*, **23**, (5), 388-397.
- Scarlett, U., Cubillos-Ruiz, J., Nesbeth, Y., Martinez, D., Engle, X., Gewirtz, T., Ahonen, C. & Conejo-Garcia, R. (2009). In Situ Stimulation Of CD40 And Toll-Like Receptor 3 Transforms Ovarian Cancer-Infiltrating Dendritic Cells from Immunosuppressive to Immunostimulatory Cells. *Cancer Research*, **69**, (18), 7329-7337.
- Schartz, E., Chaput, N., Taieb, J., Bonnaventure, P., Trebeden-Negre, H., Terme, M., Menard, C., Lebbe, C., Schimpl, A., Ardouin, P. & Zitvogel, L. (2005). IL-2 production by dendritic cells is not critical for the activation of cognate and innate effectors in draining lymph nodes. *European Journal of Immunology*, **35**, (10), 2840-2850.
- Schmidt, A., Oberle, N. & Krammer, P. (2012). Molecular Mechanisms of Treg-Mediated T Cell Suppression. *Frontiers in Immunology*, **21**, (3), 51.
- Schmielae, J. & Finn, J. (2001). Activated granulocytes and granulocyte-derived hydrogen peroxide are the underlying mechanism of suppression of T-cell function in advanced cancer patients. *Cancer Research*, **61**, (12), 4756-4760.
- Schneck, J., Slansky, J., O'Herrin, S. & Greten, T. (2001). Monitoring antigen-specific T cells using MHC-Ig dimers. *Current Protocols in Immunology*, **35**, (1), 17.
- Schnurr, M., Galambos, P., Scholz, C., Then, F., Dauer, M., Endres, S. & Eigler, A. (2001). Tumour cell lysate-pulsed human dendritic cells induce a T cell response against pancreatic carcinoma cells: an *in vitro* model for the assessment of tumour vaccines. *Cancer Research*, **61**, (17), 6445-6450.

- Sichien, D., Scott, C., Martens, L., Vanderkerken, M., Gassen, V., Plantinga, M., Joeris, R., De Prijck, S., Vanhoutte, L., Vanheerswynghels, M., Van Insterdael, G., Toussaint, W., Madeira, F., Vergote, K., Agace, W., Clausen, B., Hammad, H., Dalod, M., Saeys, Y., Lambrecht, B. & Guilliams, M. (2016). IRF8 Transcription Factor Controls Survival and Function of Terminally Differentiated Conventional and Plasmacytoid Dendritic Cells, Respectively. *Immunity*, **45**, (3), 626-640.
- Schoenberger, S., Toes, R., Van der Vooty, E., Ottringa, R. & Melief, C. (1998). T-cell help for cytotoxic T lymphocytes is mediated by CD40-CD40L interactions. *Letters to Nature*, **393**, (6684), 480-484.
- Schreiber, R., Old, L. & Smyth, (2011), Cancer immunoediting: integrating immunity's roles in cancer suppression and promotion, *Science*, **331**, (6024), 1565-70.
- Schulz, O., Edwards, A., Schito, M., Aliberti, J., Manickasingham, S., Sher, A. & Reis e Sousa, C. (2000). CD40 Triggering of Heterodimeric IL-12 p70 Production by Dendritic Cells *In Vivo* Requires a Microbial Priming Signal. *Immunity*, **13**, (4), 453-462.
- Schwaab, T., Weiss, J., Schned, A. & Barth, R. Jr. (2001). Dendritic cell infiltration in colon cancer. *Journal of Immunotherapy*, **24**, (2), 130-137.
- Schwartz, R. (1990). A cell culture model for T lymphocyte clonal anergy. *Science*, **248**, (4961), 1349-56.
- Schwiebs, A., Friesen, O., Katzy, E., Ferreirós, N., Pfeilschifter, J. & Radeke, H. (2016). Activation-Induced Cell Death of Dendritic Cells Is Dependent on Sphingosine Kinase 1. *Frontiers in Pharmacology*, **7**, 94.
- Seddiki, N., Santner-Nanan, B., Martinson, J., Zaunders, J., Sasson, S., Landay, A., Solomon, M., Selby, W., Alexander, S., Nanan, R., Kelleher, A. & Fazekas de St Groth, B. (2006). Expression of interleukin (IL)-2 and IL-7 receptors discriminates between human regulatory and activated T cells. *Journal of Experimental Medicine*, **203**, (7), 1693-1700.
- Segura, E. & Amigorena, S. (2013). Identification of human inflammatory dendritic cells. *Oncoimmunology*, **2**, (5), e23851.
- Seliger, B., Ritz, U., Abele, R., Bock, M., Tampe, R., Sutter, G., Drexler, I., Huber, C. & Ferrone, S. (2001). Immune escape of melanoma: first evidence of structural alterations in two distinct components of the MHC class I antigen processing pathway. *Cancer Research*, **61**, (24), 8647-50.
- Sellon, R., Tonkonogy, S., Schultz, M., Dieleman, L., Grenther, W., Balish, E., Rennick, D. & Sartor, R. (1998). Resident Enteric Bacteria Are Necessary for Development of Spontaneous Colitis and Immune System Activation in Interleukin-10 Deficient Mice. *Infection and Immunity*, **66**, (11), 5224-5231.

- Serkies, K., Węgrzynowicz, E. & Jassem, J. (2011). Paclitaxel and cisplatin chemotherapy for ovarian cancer during pregnancy: case report and review of the literature. *Archives of Gynecology and Obstetrics*, **283**, (Suppl 1), 97-100.
- Servais, C. & Erez, N. (2013) From sentinel cells to inflammatory culprits: cancer-associated fibroblasts in tumour-related inflammation. *Journal of Pathology*, **229**, (2), 198-207.
- Shachar, I. & Karin, N. (2013). The dual roles of inflammatory cytokines and chemokines in the regulation of autoimmune diseases and their clinical implications. *Journal of Leukocyte Biology*, **93**, (1), 51-61.
- Sheikh, N. & Jones, L. (2008). CD54 is a surrogate marker of antigen presenting cell activation. *Cancer Immunology & Immunotherapy*, **57**, (9), 1381-1390.
- Shevach, E. (2009). Mechanisms of foxp3+ T regulatory cell-mediated suppression. *Immunity*, **30**, (5), 636-645.
- Shi, V., Tran, K., Patel, F., Leventhal, J., Konia, T., Fung, M. A., Wilken, R., Garcia, M., Fitzmaurice, S., Joo, J., Monjazeb, A., Burrall, B., King, B., Martinez, S., Christensen, S. & Maverakis, E. (2015). 100% Complete response rate in patients with cutaneous metastatic melanoma treated with intralesional interleukin (IL)-2, imiquimod, and topical retinoid combination therapy: results of a case series. *Journal of the American Academy of Dermatology*, **73**, (4), 645-654.
- Shojaei, F., Zhong, C., Wu, X., Yu, L. & Ferrara, N. (2008). Role of myeloid cells in tumor angiogenesis and growth. *Trends in Cell Biology*, **18**, (8), 372-378.
- Shortman, K. (2000). Dendritic cells: Multiple subtypes, multiple origins, multiple functions. *Immunology and Cell Biology*, **78**, (2), 161-165.
- Shurin, M. (1996). Dendritic Cells Presenting Tumour Antigen. *Cancer Immunology and Immunotherapy*, **43**, (3), 158-164.
- Sichien, D., Scott, C., Martens, L., Vanderkerken, M., Van Gassen, S., Plantinga, M., Joeris, R., De Prijck, S., Vanhoutte, L., Vanheerswynghels, M., Van Isterdael, G., Toussaint, W., Madeira, F., Vergote, K., Agace, W., Clausen, B., Hammad, H., Dalod, M., Saeys, Y., Lambrecht, B. & Guilliams, M. (2016). IRF8 Transcription Factor Controls Survival and Function of Terminally Differentiated Conventional and Plasmacytoid Dendritic Cells, Respectively. *Immunity*, **45**, (3), 626-640.
- Siegel, R., Naishadham, D. & Jemal, (2012). Cancer Statistics, 2012. *CA: Cancer Journal for Clinicians*, **62**, (1), 10-29.
- Simpson, J., Al-Attar, A., Watson, N., Scholefield, J., Ilyas, M. & Durrant, L. (2010). Intratumoral T cell infiltration, MHC class I and STAT1 as biomarkers of good prognosis in colorectal cancer. *Gut*, **59**, (7), 926-933.

- Singh, J., Garber, E., Van Vlijmen, H., Karpusas, M., Hsu, Y., Zheng, Z., Naismith, J. & Thomas, D. (1998). The role of polar interactions in the molecular recognition of CD40L with its receptor CD40. *Protein Science: A Publication of the Protein Society*, **7**, (5), 1124-1135.
- Skehel, J. & Wiley, C. (2000). Receptor binding and membrane fusion in virus entry: the influenza hemagglutinin. *Annual Reviews in Biochemistry*, **69**, 531-569.
- Slingluff, C. (2011). The Present and Future of Peptide Vaccines for Cancer: Single or Multiple, Long or Short, Alone or in Combination? *Cancer Journal*, **17**, (5), 343-350.
- Slingluff, C., Petroni, G., Chianese-Bullock, K., Smolkin, M., Hibbitts, S., Murphy, C., Johansen, N., Grosh, W., Yamshchikov, G., Neese, P., Patterson, J., Fink, R. & Rehm, P. (2007). Immunologic and clinical outcomes of a randomized phase II trial of two multi-peptide vaccines for melanoma in the adjuvant setting. *Clinical Cancer Research*, **13**, (21), 6386-6395.
- Sluiter, B., van den Hout, M., Koster, B., van Leeuwen, P., Schneiders, F., van de Ven, R., Molenkamp, B., Vosslander, S., Verweij, C., van den Tol, M., van den Eertwegh, A., Scheper, R. & de Gruijl, T. (2015). Arming the Melanoma Sentinel Lymph Node through Local Administration of CpG-B and GM-CSF: Recruitment and Activation of BDCA3/CD141(+) Dendritic Cells and Enhanced Cross-Presentation. *Cancer Immunology Research*, **3**, (5), 495-505.
- Smith, K., Qiu, Z., Wong, R., Tam, V., Tam, B., Joea, D., Quach, A., Liu, X., Pold, M., Malyankar, U. & Bot, A. (2010). Multivalent immunity targeting tumor-associated antigens by intra-lymph node DNA-prime, peptide-boost vaccination. *Cancer Gene Therapy*, **18**, (1), 63-76.
- Smith, P., DiLillo, D., Bournazos, S., Li, F. & Ravetch, J. (2012). Mouse model recapitulating human Fcγ receptor structural and functional diversity. *Proceedings of the National Academy of Sciences of the USA*. **109**, (16), 6181-6186.
- Snyder, A., Makarov, V., Merghoub, T., Yuan, J., Zaretsky, J. M., Desrichard, A., Walsh, L., Postow, M., Wong, P., Ho, T., Hollman, T., Bruggeman, C., Kannan, K., Li, Y., Elipenahli, C., Liu, C., Harbison, C., Wang, L., Ribas, A., Wolchok, J. & Chan, T. (2014). Genetic basis for clinical response to CTLA-4 blockade in melanoma. *New England Journal of Medicine*, **371**, (23), 2189-2199.
- Sondermann, P., Pincetic, A., Maamary, J., Lammens, K. & Ravetch, J. (2013). General mechanism for modulating immunoglobulin effector function. *Proceedings of the National Academy of Sciences of the United States of America*, **110**, (24), 9868-9872.
- Song, K., Xu, P., Meng, Y., Geng, F., Li, J., Li, Z., Xing, J., Chen, J. & Kong, B. (2013). Smart gold nanoparticles enhance killing effect on cancer cells. *International Journal of Oncology*, **42**, (2), 597-608.
- Song, L., Lee, C. & Schindler, C. (2011). Deletion of the murine scavenger receptor CD68. *Journal of Lipid Research*, **52**, (8), 1542-1550.

- Song, Y. & Liu, S. (2015). A TLR9 agonist enhances the anti-tumour immunity of peptide and lipopeptide vaccines *via* different mechanisms. *Scientific Reports (Nature)*, **28**, (5), 12578.
- Sornasse, T., Flamand, V., De Becker, G., Bazin, H., Tielemans, F., Thielemans, K., Urbain, J., Leo, O. & Moser, M. (1992). Antigen pulsed dendritic cells can efficiently induce an antibody response *in vivo*. *Journal of Experimental Medicine*, **175**, (1), 15-21.
- Spaulding, C., Guo, W. & Effros, R. (1999). Resistance to apoptosis in human CD8+ T cells that reach replicative senescence after multiple rounds of antigen-specific proliferation. *Experimental Gerontology*, **34**, (5), 633-644.
- Sprokholt, J., Heineke, M., Kaptein, T., van Hamme, J. & Geijtenbeek, T. (2017). DCs facilitate B cell responses against microbial DNA *via* DC-SIGN. *PLoS ONE*, **12**, (10), e0185580.
- Stanculeanu, D., Daniela, Z., Lazescu, A., Bunghez, R. & Anghel, R. (2016). Development of new immunotherapy treatments in different cancer types. *Journal of Medicine and Life*, **9**, (3), 240-248.
- Stegner, D., Popp, M., Lorenz, V., Wax, J., Gessner, J. & Nieswandt, B. (2016). FcγRIIB on liver sinusoidal endothelial cells is essential for antibody-induced GPVI ectodomain shedding in mice. *Blood*, **128**, (6), 862-865.
- Steinman, R. & Banchereau, J. (2007). Taking dendritic cells into medicine. *Nature Reviews*, **449**, 419-426.
- Steinman, R. & Swanson, J. (1995). The endocytic activity of dendritic cells. *Journal of Experimental Medicine*, **182**, (2), 283-288.
- Stoddart, L., White, C., Nguyen, K., Hill, S. & Pflieger, K. (2016). Fluorescence- and bioluminescence-based approaches to study GPCR ligand binding. *British Journal of Pharmacology*, **173**, (20), 3028-3037.
- Stone, J. & Stern, L. (2006). CD8 T Cells, Like CD4 T Cells, Are Triggered by Multivalent Engagement of TCRs by MHC-Peptide Ligands but Not by Monovalent Engagement. *The Journal of Immunology*, **176**, (3), 1498.
- Stratikos, E. (2014). Modulating antigen processing for cancer immunotherapy. *Oncoimmunology*, **3**, e27568.
- Stuart, L. & Ezekowitz, R. (2005). Phagocytosis: Elegant Complexity. *Immunity*, **22**, (5), 539-550.
- Su, S., Liao, J., Liu, J., Huang, D., He, C., Chen, F., Yang, L., Wu, W., Chen, J., Lin, L., Zeng, Y., Ouyang, N., Cui, X., Yao, H., Su, F., Huang, J., Lieberman, J., Liu, O. & Song, E. (2017). Blocking the recruitment of naive CD4+ T cells reverses immunosuppression in breast cancer. *Cell Research*, **27**, (4), 461-482.

- Sudhakar, A. (2009). History of Cancer, Ancient and Modern Treatment Methods. *Journal of Cancer Science and Therapy*, **1**, (2), 1-4.
- Summers deLuca, L. & Gommerman, J. (2012). Fine-tuning of dendritic cell biology by the TNF superfamily. *Nature Reviews Immunology*, **12**, (5), 339-351.
- Suntharalingam, G. Perry, M., Ward, S., Brett, S., Castello-Cortes, A., Brunner, M. & Panoskaltsis, N. (2006). Cytokine storm in a phase 1 trial of the anti-CD28 monoclonal antibody TGN1412. *New England Journal of Medicine*, **355**, 1018-1028.
- Svenson, S. & Tomalia, D. A. (2005). Dendrimers in biomedical applications--reflections on the field. *Advanced Drug Delivery Reviews*, **57**, (15), 2106-2129.
- Swart, M., Verbrugge, I. & Beltman, J. (2016). Combination Approaches with Immune-Checkpoint Blockade in Cancer Therapy. *Frontiers in Oncology*, **1**, (6), 233.
- Swartz, M. & Lund, A. (2012). Lymphatic and interstitial flow in the tumour microenvironment: linking mechanobiology with immunity. *Nature Reviews Cancer*, **12**, (3), 210-219.
- Swerdlow, A. & Jones, M. (2005). Tamoxifen Treatment for Breast Cancer and Risk of Endometrial Cancer: A Case - Control Study. *Journal of the National Cancer Institute*, **97**, (5), 375-384.
- Swiecki, M. & Colonna, M. (2015). The multifaceted biology of plasmacytoid dendritic cells. *Nature Reviews Immunology*, **15**, (8), 471-485.
- Sznol, M. & Chen, L. (2013). Antagonist antibodies to PD-1 and B7-H1 (PD-L1) in the treatment of advanced human cancer. *Clinical Cancer Research*, **19**, (5), 1021-1034.
- Takahashi, T., Tagami, T., Tamazaki, S., Uede, T., Shimizu, J., Sakaguchi, N., Mak, T. & Sakaguchi, S. (2000). Immunologic self-tolerance maintained by CD25(+)CD4(+) regulatory T cells constitutively expressing cytotoxic T lymphocyte-associated antigen 4. *Journal of Experimental Medicine*, **192**, (2), 303-310.
- Tan, J. & O'Neill, H. (2005). Maturation requirements for dendritic cells in T cell stimulation leading to tolerance versus immunity. *Journal of Leukocyte Biology*, **78**, (2), 319-324.
- Tang, F. (2018). Tumor cells versus host immune cells: whose PD-L1 contributes to PD-1/PD-L1 blockade mediated cancer immunotherapy? *Cell & Bioscience*, **8**, (34), 1-8.
- Taube, J., Klein, A., Brahmer, J., Xu, H., Pan, X., Kim, J., Chen, L., Pardoll, D., Topalian, S. & Anders, R. (2014). Association of PD-1, PD-1 ligands, and other features of

the tumor immune microenvironment with response to anti-PD-1 therapy. *Clinical Cancer Research*, **20**, (19), 5064-5074.

- Tel, J., Van Der Leun, A., Figdor, C., Torensma, R. & De Vries, J. (2012). Harnessing human plasmacytoid dendritic cells as professional APCs. *Cancer Immunology and Immunotherapy*, **61**, (8), 1279-1288.
- ten Broeke, T., Wubbolts, R. & Stoorvogel, W. (2013). MHC Class II Antigen Presentation by Dendritic Cells Regulated through Endosomal Sorting. *Cold Spring Harbor Perspectives in Biology*, **5**, (12), a016873.
- Tesone, A., Rutkowski, M., Brencicova, E., Svoronos, N., Perales-Puchalt, A., Stephen, T., Allegranza, M., Payne, K., Nguyen, J., Wichramasinghe, J., Tchou, J., Borowsky, M., Rabinovich, G., Kossenkov, A. & Conejo-Garcia, J. (2016). Satb1 Overexpression Drives Tumor-Promoting Activities in Cancer-Associated Dendritic Cells. *Cell Reports*, **14**, (7), 1774-1786.
- Thaer, A. & Sernetz, M. (1973). Fluorescence Techniques in Cell Biology. *Fluorescence*, (1), 122-128.
- Thery, C. & Amigorena, S. (2001). The cell biology of antigen presentation in dendritic cells. *Current Opinions in Immunotherapy*, **13**, (1), 45-51.
- Theze, J., (2012) Therapeutic Drug Monitoring, *Immunology*, (3), 141-148.
- Thompson, E., Enriquez, H., Fu, Y. & Engelhard, V. (2010). Tumor masses support naive T cell infiltration, activation, and differentiation into effectors. *Journal of Experimental Medicine*, **207**, (8), 1791-1804.
- Thumann, P., Moe, I., Humrich, J., Berger, T., Schultz, E., Schuler, G. & Jenne, L. (2003). Antigen loading of dendritic cells with whole tumor cell preparations. *Journal of Immunological Methods*, **277**, (1), 1-16.
- Thèze, J. (1998). Interleukin 2 A2 - Delves, Peter J. In *Encyclopedia of Immunology (Second Edition)* (pp. 1436-1438). Oxford: Elsevier.
- Timmerman, J. & Levy, R. (1999). Dendritic Cell Vaccines for Cancer Immunotherapy. *Annual Reviews in Medicine*, **50**, 507-529.
- Tivol, E., Borriello, Schweitzer, A., Lynch, W., Bluestone, J. & Sharpe, A. (1995). Loss of CTLA-4 leads to massive lymphoproliferation and fatal multiorgan tissue destruction, revealing a critical negative regulatory role of CTLA-4. *Immunity*, **3**, (5), 541-547.
- Tolcher, A., Sugarman, S., Gelmon, K., Cohen, R., Saleh, M., Isaacs, C., Young, L., Healey, D., Onetto, N. & Slichenmyer, W. (1999). Randomized phase II study of BR96-doxorubicin conjugate in patients with metastatic breast cancer. *Journal of Clinical Oncology*, **17**, (2), 478-484.

- Topalian, S., Drake, C. & Pardoll, M. (2012). Targeting the PD-1/B7-H1(PD-L1) pathway to activate anti-tumor immunity. *Current Opinion in Immunology*, **24**, (2), 207-212.
- Tortorella, S. & Karagiannis, T. C. (2014). Transferrin receptor-mediated endocytosis: a useful target for cancer therapy. *The Journal of Membrane Biology* **247**, (4), 291-307.
- Tran-Janco, J., Lamichhane, P., Karyampudi, L. & Knutson, L. (2015). Tumor-Infiltrating Dendritic Cells in Cancer Pathogenesis. *The Journal of Immunology*, **194**, (7), 2985-2991.
- Trinchieri, G. & Scott, P. (1995). Interleukin-12: a proinflammatory cytokine with immunoregulatory functions that bridge innate resistance in antigen specific adaptive immunity. *Annual Reviews in Immunology*, **146**, (7), 521-576.
- Trouche, N., Wieckowski, S., Sun, W., Chaloin, O., Hoebeke, J., Fournel, S. & Guichard, G. (2007). Small multivalent architectures mimicking homotrimers of the TNF superfamily member CD40L: Delineating the relationship between structure and effector function. *Journal of the American Chemical Society*, **129**, (44), 13480-13492.
- Tuettenberg, A. Fondel, S., Steinbrink, K., Enk, A., & Jonuleit, H. (2010). CD40 signalling induces IL-10-producing, tolerogenic dendritic cells. *Experimental Dermatology*, **19**, (1), 44-53.
- Tzeng, A., Kauke, M., Zhu, E., Moynihan, K., Opel, C., Yang, N., Mehta, N., Kelly, R., Szeto, G., Overwijk, W., Irvine, D. & Wittrup, K. (2016). Temporally Programmed CD8alpha (+) DC Activation Enhances Combination Cancer Immunotherapy. *Cell Reports*, **17**, (10), 2503-2511.
- Ueno, H., Klechevsky, E., Schmitt, N., Ni, L., Flamar, A., Zurawski, S., Zurawski, G., Palucka, K., Banchereau, J. & Oh, S. (2011). Targeting human dendritic cell subsets for improved vaccines. *Seminars in Immunology*, **23**, (1), 21-27.
- Umansky, V. & Sevko, A. (2013). Tumor microenvironment and myeloid-derived suppressor cells. *Cancer Microenvironment*, **6**, (2), 169-177.
- Vaitaitis, G., Olmstead, M., Waid, D., Carter, J. & Wagner, D. (2014). A CD40-targeted peptide controls and reverses type 1 diabetes in NOD mice. *Diabetologia*, **57**, (11), 2366-2373.
- Valitutti, S., Müller, S., Salio, M. & Lanzavecchia, A. (1997). Degradation of T Cell Receptor (TCR)-CD3- ζ Complexes after Antigenic Stimulation. *The Journal of Experimental Medicine*, **185**, (10), 1859-1864.
- Valkenburg, S., Li, O., Mak, P., Mok, C., Nicholls, J., Guan, Y., Waldmann, T., Peiris, J., Perera, L. & Poon, L. (2014). IL-15 adjuvanted multivalent vaccinia-based universal influenza vaccine requires CD4+ T cells for heterosubtypic

- protection. *Proceedings of the National Academy of Sciences*, **111**, (15), 5676-5681.
- van der Merwe, P. & Dushek, O. Mechanisms for T cell receptor triggering. *Nature Reviews Immunology*, **11**, (1), 47-55.
- van Hall, T., van Bergen, J., van Veelen, P., Kraakman, M., Heukamp, L., Koning, F., Melief, C., Ossendorp, F. & Offringa, R. (2000). Identification of a Novel Tumor-Specific CTL Epitope Presented by RMA, EL-4, and MBL-2 Lymphomas Reveals Their Common Origin. *The Journal of Immunology*, **165**, (2), 869-877.
- van Kooten, C. & Banchereau, J. (2000). CD40-CD40 ligand. *Journal of Leukocyte Biology*, **67**, (1), 2-17.
- van Mierlo, G., Boonman, Z., Dunmortier, H., den Boer, A., Fransen, M., Nouta, J., van der Voort, E., Offringa, R., Toes, R. & Melief, C. (2004). Activation of dendritic cells that cross-present tumor-derived antigen licenses CD8+ CTL to cause tumor eradication. *Journal of Immunology*, **173**, (11), 6753-6759.
- Varga, G., Balkow, S., Wild, M., Stadtbaeumer, A., Krummer, M., Rothoef, T., Higuchi, T., Beissert, S., Wethmar, K., Scharffetter-Kochanek, K., Vestweber, D. & Grabbe, S. (2007). Active MAC-1 (CD11b/CD18) on DCs inhibits full T-cell activation. *Blood*, **109**, 661-669.
- Vazquez-Cintron, E., Monu, N. & Frey, A. (2010). Tumor-Induced Disruption of Proximal TCR-Mediated Signal Transduction in Tumor-Infiltrating CD8(+) Lymphocytes Inactivates Antitumor Effector Phase. *Journal of Immunology* **185**, (12), 7133-7140.
- Vergote, I., Amant, F., Kristensen, G., Ehlen, T., Reed, N. & Casado, A. (2011). Primary surgery or neoadjuvant chemotherapy followed by interval debulking surgery in advanced ovarian cancer. *European Journal of Cancer*, **47**, (3), 88-92.
- Veronese, F. & Mero, A. (2008). The impact of PEGylation on biological therapies. *BioDrugs*, **22**, (5), 315-329.
- Vitale, L., Thomas, L., He, L., O'Neill, T., Widger, J., Crocker, A., Sundarapandiyam, K., Storey, J., Forsberg, E., Weidlick, J., Baronas, A., Gergel, L., Boyer, J., Sisson, C., Goldstein, J., Marsh, H. & Keler, T. (2018). Development of CDX-1140, an agonist CD40 antibody for cancer immunotherapy. *Cancer Immunology, Immunotherapy*. **78**, (13), 3816.
- Vo, M., Lee, H., Kim, J., Hoang, M., Choi, N., Rhee, J., Lakshmanan, V., Shin, S. & Lee, J. (2015). Dendritic cell vaccination with a toll-like receptor agonist derived from mycobacteria enhances anti-tumor immunity. *Oncotarget*, **6**, (32), 33781-33790.
- Volkman, A., Neefjes, J. & Stockinger, B. (1996). A conditionally immortalized dendritic cell line which differentiates in contact with T cells or T

- cell-derived cytokines. *European Journal of Immunology*, **26**, (11), 2565-2572.
- Vonderheide, R. (2007). Prospect of Targeting the CD40 Pathway for Cancer Therapy. *Clinical Cancer Research*, **13**, (4), 1083-1088.
- Vonderheide, R., Burg, J., Mick, R., Trosko, J., Li, D., Shaik, M., Tolcher, A. & Hamid, O. (2013). Phase I study of the CD40 agonist antibody CD-870,893 combined with carboplatin and paclitaxel in patients with advanced solid tumours. *Oncoimmunology*, **2**, (1), e23033.
- Vonderheide, R., Flaherty, K., Khalil, M., Stumacher, M., Bajor, D., Hutnick, N. & Antonia, S. (2007). Clinical activity and immune modulation in cancer patients treated with CP-870,893, a novel CD40 agonist monoclonal antibody. *Journal of Clinical Oncology*, **25**, (7), 876-883.
- Vonherheide, R. & Glennie, M. (2013). Agonistic CD40 antibodies and cancer therapy. *Clinical Cancer Research*, **19**, (5), 1035-1043.
- Waldmann, T. (1989). The Multi-Subunit Interleukin-2 Receptor. *Annual Review of Biochemistry*, **58**, (1), 875-905.
- Wallet, M., Sen, P. & Tisch, R. (2005). Immunoregulation of dendritic cells. *Clinical Medicine and Research*, **3**, 166-175.
- Wang, E., Panelli, M. & Marincola, F. (2005). Understanding the Response to Immunotherapy in Humans. *Springer Seminars in Immunology*, **27**, (1), 105-117.
- Wang, L., Li, D., Yang, K., Hu, Y. & Zeng, Q. (2008). Toll-like receptor-4 and mitogen-activated protein kinase signal system are involved in activation of dendritic cells in patients with acute coronary syndrome. *Immunology*, **125**, (1), 122-130.
- Wantanabe, S., Kagamu, H., Yoshizawa, H., Fujita, N., Tanaka, H., Tanaka, J. & Gejyo, F. (2003). The duration of signalling through CD40 directs biological ability of dendritic cells to induce antitumour immunity. *The Journal of Immunology*, **171**, (11), 5828-5836.
- Watson, J. (1979). Continuous proliferation of murine antigen-specific helper T lymphocytes in culture. *The Journal of Experimental Medicine*, **150**, (6), 1510.
- Waugh, D. & Wilson, C. (2008). The Interleukin 8 Pathway in Cancer. *Clinical Cancer Research*, **14**, (21), 6735-6741.
- Webb, J., Milne, K., Kroeger, D. & Nelson, H. (2016). PD-L1 expression is associated with tumor-infiltrating T cells and favorable prognosis in high-grade serous ovarian cancer. *Gynaecological Oncology*, **141**, (2), 293-302.

- Weber, J., Postow, M., Lao, C. & Schadendorf, K. (2016). Management of Adverse Event Following Treatment with Anti-Programmed Death-1 Agents. *Oncologist*, **21**, (10), 1230-1240.
- Weiss, A. & Littman, D. (1994). Signal transduction by lymphocyte antigen receptors. *Cell*, **76**, (2), 263-274.
- Weiss, J., Gregory Alvord, W., Quiñones, A., Stauffer, J. & Wiltrout, R. (2014). CD40 expression in renal cell carcinoma is associated with tumor apoptosis, CD8+ T cell frequency and patient survival. *Human Immunology*, **75**, (7), 614-620.
- Werneburg, B., Zoog, S., Dang, T., Kehry, M. & Crute, J. (2001). Molecular characterization of CD40 signaling intermediates. *Journal of Biological Chemistry*, **276**, (46), 43334-43342.
- West, M. A., Wallin, R., Matthews, S., Svensson, H., Zaru, R., Ljunggren, G., Prescott, A. & Watts, C. (2004). Enhanced dendritic cell antigen capture *via* toll-like receptor-induced actin remodeling. *Science*, **305**, (5687), 1153-1157.
- Wherry, E. (2011). T cell exhaustion. *Nature Immunology*, **12**, 492-499.
- White, A., Beers, S. & Cragg, M. (2014). FcγRIIB as a Key Determinant of Agonistic Antibody Efficacy. *Current Topics in Microbial Immunology*, **382**, 355-371.
- White, A., Dou, L., Chan, H., Field, V., Mockridge, C., Moss, K., Williams, E., Booth, S., French, R., Potter, E., Butts, C., Al-Shamkhani, A., Cragg, M., Verbeek, J., Johnson, P., Glennie, M. & Beers, S. (2014). Fcγ Receptor Dependency of Agonistic CD40 Antibody in Lymphoma Therapy Can Be Overcome through Antibody Multimerization. *The Journal of Immunology*, **193**, (4), 1828-1835.
- White, A., Chan, H., French, R., Beers, S., Cragg, M., Johnson, P. & Glennie, M. (2013). FcγRIIB controls the potency of agonistic anti-TNFR mAbs. *Cancer Immunology and Immunotherapy*, **62**, (5), 941-948.
- White, A., Chan, H., French, R., Willoughby, J., Mockridge, C., Roghanian, A., Penfold, C., Booth, S., Dodhy, A., Polak, M., Potter, E., Ardern-Jones, M., Verbeek, J., Johnson, P., Al-Shamkhani, A., Cragg, M., Beers, S. & Glennie, M. (2015). Conformation of the Human Immunoglobulin G2 Hinge Imparts Superagonistic Properties to Immunostimulatory Anticancer Antibodies. *Cancer Cell*, **27**, (1), 138-148.
- White, A., Dou, L., Chan, H., Field, V., Mockridge, C., Moss, K., Williams, E., Booth, S., French, R., Potter, E., Butts, C., Al-Shamkhani, A., Cragg, M., Verbeek, J., Johnson, P., Glennie, M. & Beers, S. (2014). Fc gamma receptor dependency of agonistic CD40 antibody in lymphoma therapy can be overcome through antibody multimerization. *Journal of Immunology*, **193**, (4), 1828-1835.
- Whiteside, T. (2008). The tumour microenvironment and its role in promoting tumour growth. *Nature*, **27**, 5904-5912.

- Wilson, N., Young, L., Kupresanin, F., Naik, S., Vremec, D., Heath, W., Akira, S., Shortman, K., Boyle, J., Maraskovsky, E., Belz, G. & Villadangos, J. (2008). Normal proportion and expression of maturation markers in migratory dendritic cells in the absence of germs or Toll-like receptor signaling. *Immunology and Cell Biology*, **86**, (2), 200-205.
- Wilson, N., Yang, B., Yang, A., Loeser, S., Marsters, S., Lawrence, D., Li, Y., Pitti, R., Yee, S., Ross, S., Vernes, J., Lu, Y., Adams, C., Offringa, R., Kelley, B., Hymowitz, S., Daniel, D., Meng, G. & Ashkenazi, A. (2011). An Fc-gamma receptor-dependent mechanism drives antibody-mediated target-receptor signaling in cancer cells. *Cancer Cell*, **19**, (1), 101-113.
- Winzler, C., Rovere, P., Rescigno, M., Granucci, F., Penna, G., Adorini, L., Zimmermann, V., Davoust, J. & Ricciardi-Castagnoli, P. (1997). Maturation Stages of Mouse Dendritic Cells in Growth Factor-dependent Long-Term Cultures. *Journal of experimental medicine*, **185**, (2), 317-328.
- Wisse, E., Braet, F., Luo, D., De Zanger, R., Jans, D., Crabbe, E. & Vermoesen, A. (1996). Structure and function of sinusoidal lining cells in the liver. *Toxicologic & Pathology*, **24**, (1), 100-111.
- Won, S., Huang, W., Lai, Y. & Lin, M. (2000). Staphylococcal Enterotoxin A Acts through Nitric Oxide Synthase Mechanisms in Human Peripheral Blood Mononuclear Cells To Stimulate Synthesis of Pyrogenic Cytokines. *Infection and Immunity*, **68**, (4), 2003-2008.
- Wong, H., Bendayan, R., Rauth, A., Xue, H., Babakhanian, K. & Wu, X. (2006). A mechanistic study of enhanced doxorubicin uptake and retention in multidrug resistant breast cancer cells using a polymer-lipid hybrid nanoparticle system. *Journal of Pharmacology and Experimental Therapeutics*, **317**, (3), 1372-1381.
- Wooldridge, L., Lissina, A., Cole David, K., Van Den Berg Hugo, A., Price David, A. & Sewell Andrew, K. (2009). Tricks with tetramers: how to get the most from multimeric peptide-MHC. *Immunology*, **126**, (2), 147-164
- Wu, Q., Jinde, K., Endoh, M. & Sakai, H. (2004). Clinical significance of costimulatory molecules CD80/CD86 expression in IgA nephropathy. *Kidney International*, **65**, (3), 888-896.
- Xiao, X., Lao, X., Chen, M., Liu, R., Wei, Y., Ouyang, F., Chen, D., Zhao, X., Zhao, Q., Li, X., Zheng, L. & Kuang, D. (2016). PD-1 Hi Identifies a Novel Regulatory B-cell Population in Human Hepatoma that Promotes Disease Progression. *Cancer Discovery*, **6**, (5), 546-559.
- Xing, F., Wang, J., Hu, M., Yu, Y., Chen, G. & Liu, J. (2011). Comparison of immature and mature bone marrow-derived dendritic cells by atomic force microscopy. *Nanoscale research letters*, **6**, (1), 455.

- Xiong, J., Balcioglu, H. & Danen, E. (2013). Integrin signaling in control of tumor growth and progression. *The International Journal of Biochemistry & Cell Biology*, **45**, (5), 1012-1015.
- Xu, H. & Shaw, E. (2016). A Simple Model of Multivalent Adhesion and Its Application to Influenza Infection. *Biophysical Journal*, **110**, (1), 218-233.
- Xu, L., Pirolo, K., Tang, W., Rait, A. & Chang, E. (1999). Transferrin-liposome-mediated systemic p53 gene therapy in combination with radiation results in regression of human head and neck cancer xenografts. *Human Gene Therapy*, **10**, (18), 2941-2952
- Yadav, L., Puri, N., Rastogi, V., Satpute, P. & Sharma, V. (2015). Tumour Angiogenesis and Angiogenic Inhibitors: A Review. *Journal of Clinical and Diagnostic Research, JCDR*, **9**, (6), XE01-XE05.
- Yang, Z., Grote, D., Ziesmer, S., Niki, T., Hirashima, M., Novak, A., Witzig, T. & Ansell, S. (2012). IL-12 upregulates TIM-3 expression and induces T cell exhaustion in patients with follicular B cell non-Hodgkin lymphoma. *The Journal of Clinical Investigation*, **122**, (4), 1271-1282.
- Yatvin, M., Kreutz, W., Horwitz, B. & Shinitzky, M. (1980). pH-sensitive liposomes: possible clinical implications. *Science*, **210**, (4475), 1253-1255.
- Yeshchenko, O., Bondarchuk, I., Gurin, V., Dmitruk, I. & Kotko, A. (2013). Temperature dependence of the surface plasmon resonance in gold nanoparticles. *Surface Science*, **608**, 275-281.
- Yildirim, L., Thanh, N., Loizidou, M. & Seifalian, A. (2011). Toxicology and clinical potential of nanoparticles. *Nanotechnology Today*, **6**, (6), 585-607.
- Yin, W., Grovel, L., Zurawski, S., Li, D., Ni, L., Duluc, D., Upchurch, K., Kim, J., Gu, C., Ouedraogo, R., Wang, Z., Zue, Y., Joo, H., Grovel, J., Zurawski, G. & Oh, S. (2016). Functional Speciality of CD40 and Dendritic Cell Surface Lectins for Exogenous Antigen Presentation to CD8+ and CD4+ T cells. *EBioMedicine*, **5**, 46-58.
- Youssef, S., Mohammad, M. & Ezz-El-Arab, L. (2015). Clinical Significance of Serum IL-12 Level in Patients with Early Breast Carcinoma and Its Correlation with Other Tumor Markers. *Open Access Macedonian Journal of Medical Sciences*, **3**, (4), 640-644.
- Yoshihara, K., Tsunoda, T., Shigemizu, D., Fujiwara, H., Hatae, M., Masuzaki, H., Katabuchi, H., Kawakami, Y., Okamoto, A., Nogawa, T., Matsumura, N., Udagawa, Y., Saito, T., Itamochi, H., Takano, M., Miyagi, E., Sudo, T., Ushijima, K., Iwase, H., Seki, H., Terao, Y., Enomoto, T., Mikami, M., Akazawa, K., Tsuda, H., Moriya, T., Tajima, A., Inoue, I. & Tanaka, K. (2012). High risk ovarian cancer based on 126-gene expression signature is uniquely characterized by downregulation of antigen presentation pathway. *Clinical Cancer Research*, **18**, (5), 1374-1385.

- Yu, H., Segers, F., Sliedregy-Bol, K., Bot, I., Woltman, A., Boross, P., Verbeek, S., Overkleeft, H., van der Marel, G., van Kooten, C., van Berkel, T. & Biessen, E. (2013). Identification of a novel CD40 ligand for targeted imaging of inflammatory plaques by phage display. *FASEB Journal*, **27**, (10), 4136-4146.
- Yuan, F., Dellian, M., Fukumura, D., Leunig, M., Berk, D., Torchilin, V. & Jain, R. (1995). Vascular permeability in a human tumor xenograft: molecular size dependence and cutoff size. *Cancer Research*, **55**, (17), 3752-3756.
- Zakiryanova, G., Kustova, E., Urazalieva, N., Amirbekov, A., Baimuchametov, E., Nakisbekov, N. & Shurin, M. (2017). Alterations of oncogenes expression in NK cells in patients with cancer. *Immunity, Inflammation and Disease*, **5**, (4), 493-502.
- Zanoni, I., Ostuni, R., Capuano, G., Collini, M., Caccia, M., Ronchi, A., Rocchetti, M., Mingozi, F., Foti, M., Chirico, G., Costa, B., Zaza, A., Ricciardi-Castagnoli, P. & Granucci, F. (2009). CD14 regulates the dendritic cell life cycle after LPS exposure through NFAT activation. *Nature Letters*, **460**, (7252), 264-269.
- Zarek, P., Huang, C., Lutz, E., Kowalski, J., Horton, M., Linden, J., Drake, C. & Powell, J. (2008). A2A receptor signaling promotes peripheral tolerance by inducing T-cell anergy and the generation of adaptive regulatory T cells. *Blood*, **111**, (1), 251-259.
- Zavadova, E., Savary, C., Templin, S., Verschraegen, C., & Freedman, R. (2001). Maturation of dendritic cells from ovarian cancer patients. *Cancer Chemotherapy and Pharmacology*, **48**, (4), 289-296.
- Zelante, T., Fric, J., Wong, A., & Ricciardi-Castagnoli, P. (2012). Interleukin-2 Production by Dendritic Cells and its Immuno-Regulatory Functions. *Frontiers in Immunology*, **3**, 161.
- Zenewicz, L., Antov, A. & Flavell, R. (2009). CD4 T-cell differentiation and inflammatory bowel disease. *Trends in Molecular Medicine*, **15**, (5), 199-207.
- Zhang, D., Armstrong, A., Tam, S., McCarthy, S., Luo, J., Gilliland, G., & Chiu, M. (2017). Functional optimization of agonistic antibodies to OX40 receptor with novel Fc mutations to promote antibody multimerization. *mAbs*, **9**, (7), 1129-1142.
- Zhang, D., Goldberg, M. & Chiu, M. (2016). Fc Engineering Approaches to Enhance the Agonism and Effector Functions of an Anti-OX40 Antibody. *Journal of Biological Chemistry*, **291**, (53), 27134-27146.
- Zhang, D., Whitaker, B., Derebe, M., & Chiu, M. (2018). FcγRII-binding Centyrins mediate agonism and antibody-dependent cellular phagocytosis when fused to an anti-OX40 antibody. *mAbs*, **10**, (3), 463-475.
- Zhang, S., Liang, F., Li, W. & Wang, Q. (2017) Risk of treatment-related mortality in cancer patients treated with Ipilimumab: A systematic review and meta-analysis. *European Journal of Cancer*, **83**, (9), 71-79.

- Zhao, X., Rong, L., Zhao, X., Li, X., Liu, X., Deng, J., Wu, H., Xu, X., Erben, U., Qu, P., Syrbe, U., Sieper, J. & Qin, Z. (2012). TNF signaling drives myeloid-derived suppressor cell accumulation. *The Journal of Clinical Investigation*, **122**, (11), 4094-4104.
- Zheng, L. (2017). PD-L1 Expression in Pancreatic Cancer. *Journal of the National Cancer Institute*, **109**, (6), 304.
- Zhou, F. (2009). Molecular mechanisms of IFN-gamma to up-regulate MHC class I antigen processing and presentation. *International Reviews in Immunology*, **28**, (3), 239-260.
- Zhou, J., Shen, X., Hodes, R., Rosenberg, S. & Robbins, P. (2005). Telomere length of transferred lymphocytes correlates with in vivo persistence and tumour regression in melanoma patients receiving cell transfer therapy. *Journal of Immunology*, **175**, (10), 7046-7052.
- Zimmerman, M., Yang, D., Hu, X., Liu, F., Singh, N., Browning, D., Ganapathy, V., Choubey, D., Abrams, S. & Liu, K. (2010). IFN- γ Upregulates Survivin and Ifi202 Expression to Induce Survival and Proliferation of Tumor-Specific T Cells. *PLoS ONE*, **5**, (11).

8.1 Online Resources:

- Centers for Disease Control and Prevention (US) (2010). National Center for Chronic Disease Prevention and Health Promotion (US); Office on Smoking and Health (US). How Tobacco Smoke Causes Disease: The Biology and Behavioral Basis for Smoking-Attributable Disease: A Report of the Surgeon General. Atlanta; Online release. <https://www.ncbi.nlm.nih.gov/books/NBK53017/>. Accessed online September 2015
- ClinicalTrials.gov [Internet]. Bethesda (MD): National Library of Medicine (US). https://clinicaltrials.gov/ct2/results?term=CART&Search=Apply&recrs=d&age_v=&gndr=&type=&rslt=. Accessed January 2018.
- Transparency Market Research. (2012). Peptide Therapeutics Market: Global Industry Analysis, Size, Share, Growth, Trends and Forecast 2012-2018. (Press release). <https://www.transparencymarketresearch.com/peptide-therapeutics-market.html>. Transparency Market Research Database; accessed online November 2018.
- WHO Mortality Database, (2017). UK Cancer Mortality. https://www.who.int/healthinfo/mortality_data/en/. Database accessed online July 2017.